

University of Warwick institutional repository: <http://go.warwick.ac.uk/wrap>

A Thesis Submitted for the Degree of PhD at the University of Warwick

<http://go.warwick.ac.uk/wrap/873>

This thesis is made available online and is protected by original copyright.

Please scroll down to view the document itself.

Please refer to the repository record for this item for information to help you to cite it. Our policy information is available from the repository home page.

**Unravelling the Roles of Two Senescent Enhanced MYB
Transcription Factors in the Regulation of Anthocyanin
Biosynthesis in *Arabidopsis thaliana***

Nichola Maxine Warner

A thesis for the degree of Doctor of Philosophy.

Submitted to the University of Warwick

Conducted at Warwick HRI

October 2008

Table of Contents

List of Figures	xi
List of Tables	xv
Acknowledgements	xvii
Declaration	xvii
Summary	xviii
Abbreviations	xix
1 Introduction	1
1.1 Senescence	1
1.1.1 Structural Changes During Senescence	1
1.1.1.1 Senescence Associated Vacuoles	3
1.1.1.2 Transition of Peroxisomes into Glyoxysomes	4
1.1.2 Dismantling of Cellular Components	4
1.1.2.1 Lipid and Membrane Deterioration	5
1.1.2.2 Chlorophyll Degradation	8
1.1.2.3 Protein Degradation	9
1.1.2.4 Nucleic Acid Degradation	10
1.1.3 Regulation of Senescence	11
1.1.3.1 Internal Factors Regulating Senescence	11
1.1.3.1.1 Sugar Signalling	12
1.1.3.1.2 Hormones	13
1.1.3.1.2.1 Ethylene	13
1.1.3.1.2.2 Salicylic Acid	13
1.1.3.1.2.3 Methyl Jasmonate and Jasmonic Acid	14
1.1.3.1.2.4 Brassinosteroids	15
1.1.3.1.2.5 Cytokinin	15
1.1.3.1.2.6 Polyamines	16
1.1.3.1.2.7 Reactive Oxygen Species	16
1.1.3.2 Environmental Factors	17

1.1.3.3 Genetic Regulation	20
1.1.3.4 Different Types of Senescence	23
1.2 Photosynthesis	25
1.2.1 Photosynthetic Electron Transfer Reactions	26
1.2.2 Carbon Fixation Reactions	28
1.2.3 Photosynthesis During Senescence	29
1.3 Chlorophyll Fluorescence as a Measurement of Photosynthesis	
Activity	29
1.3.1 Background	29
1.3.2 Photosystem 2 Efficiency	30
1.3.2.1 The Maximum Quantum Efficiency of PS2 Primary Photochemistry (F_v/F_m)	31
1.3.2.2 The Operating Efficiency of PS2 ($F'_m - F'/F'_m$ or $F'q/F'_m$ or ϕ_{PS2})	31
1.3.2.3 Linear Electron Transport Rate (J)	31
1.3.3 Down Regulation of Chlorophyll Fluorescence	31
1.3.3.1 Photochemical Quenching (PQ, $(F'_m - F')/F_m - F_o$) or $F'q/F'_v$)	31
1.3.3.2 Non-Photochemical Quenching (NPQ or $F_m/(F'_m - 1)$)	32
1.3.3.2.1 Energy Dependent Quenching (qE)	34
1.3.3.2.2 Photoinhibitory Quenching (qI)	35
1.4 The Role of Anthocyanin Biosynthesis During Senescence	35
1.4.1 Anthocyanin and Flavonoid Biosynthesis	38
1.4.2 Regulation of Anthocyanin Biosynthesis	42
1.4.3 Resorption Protection	44
1.4.4 Direct Antioxidant Role of Anthocyanins	44
1.5 MYB90 and MYB75	47
1.5.1 Regulation of MYB90 and MYB75	49
1.5.2 Transcription Factor Interactions	50

1.6 Hypothesis and Aims	51
2 Materials and Methods	51
2.1 Materials	51
2.2 Plant Growth Experiments	51
2.2.1 Growth Room Conditions	51
2.2.2 Plant Growth	51
2.2.3 Leaf Tagging	51
2.2.4 Glass House Conditions	51
2.2.5 Low Nitrogen High Glucose Growth Plates	52
2.3 Gene Expression Studies	52
2.3.1 RNA Isolation	52
2.3.2 RNA Cleanup	52
2.3.2 RNA Quantification	53
2.3.4 Determination of RNA Quality	53
2.3.5 Gene Expression Analysis by Real Time PCR	53
2.3.5.1 DNase Treatment	53
2.3.5.2 First Strand cDNA Synthesis	53
2.3.5.3 Real Time PCR	53
2.3.6 Reverse Transcription PCR	54
2.3.7 Microarray Gene Expression Analysis	55
2.3.7.1 mRNA Amplification	55
2.3.7.2 Labelling aRNA	55
2.3.7.3 Purification of Labelled cDNA	55
2.3.7.4 Preparation of Labelled cDNA for Hybridisations	56
2.3.7.5 Microarray Prehybridisation	56
2.3.7.6 Microarray Hybridisation	56
2.3.7.7 Microarray Post-Hybridisation Washes	57
2.3.7.8 Microarray Data Analysis	57

2.4 Anthocyanin and Flavonoid Analysis	57
2.4.1 Anthocyanin and Flavonoid Extraction	57
2.4.1.1 UV-VIS Spectroscopy	57
2.4.1.2 HPLC Analysis of Anthocyanin/Flavonoid Extracts	58
2.5 Chlorophyll Fluorescence Measurements	58
2.6 Total Chlorophyll and Protein Analysis	60
2.6.1 Total Chlorophyll and Protein Extraction	60
2.6.1.1 Total Chlorophyll Content Measurement	60
2.6.1.2 Total Protein Content Measurement	61
2.7 Gateway Cloning	61
2.7.1 Entry Clones	61
2.7.1.1 PCR Amplification of <i>MYB90</i> and <i>MYB75</i> Promoters and <i>MYB90</i> Promoter Deletions	61
2.7.1.2 PCR Purification	62
2.7.1.3 BP Recombination Reaction	62
2.7.1.4 Identification of Entry Clones	63
2.7.2 Expression Clones	63
2.7.2.1 LR Recombination	63
2.7.3 Transformation of Expression Clones into Arabidopsis COL-0	63
2.7.3.1 Transformation into <i>Agrobacterium</i>	63
2.7.3.2 Floral Dipping	64
2.7.3.3 Selection of Homozygous Lines	64
2.8 Plasmid DNA Isolation from <i>Escherichia coli</i> (<i>E.coli</i>) clones	64
2.8.1 Mini Preparations	64
2.8.1.1 Glycerol Stocks	64
2.8.1.2 Sequencing	65
2.9 Analysis of Transgenic Plants Containing Promoter:GUS Fusions	65
2.9.1 Histochemical Staining	65

2.9.2 Quantification of GUS Activity	66
2.10 DNA Isolation	66
2.10.1 REDEExtract-N-Amp	66
2.10.2 Primers	67
2.11 Statistical Analysis	67
2.11.1 Student t-test	67
2.11.2 Standard error	67
3 The Role of <i>MYB90</i> During Leaf Development	68
3.1 Introduction	68
3.2 Plant Growth Experiments	69
3.2.1 Chlorophyll Measurements	69
3.2.2 Chlorophyll a/b Ratio	70
3.2.3 Protein Measurements	70
3.2.4 Chlorophyll Fluorescence Analysis	72
3.2.3.1 The Maximum PSII Efficiency	74
3.2.3.2 PSII Operating Efficiency	75
3.2.3.3 Photochemical Quenching (PQ	76
3.2.3.4 Non-Photochemical Quenching (NPQ)	77
3.2.3.5 Linear Electron Transport Rate (J)	78
3.2.3.6 Chlorophyll Fluorescence Analysis at 32 and 36 Days After Sowing	79
3.3 Gene Analysis	83
3.3.1 Analysis of Cluster1	83
3.3.1.1 Cluster 1 Promoter Analysis	85
3.3.2 Analysis of Other Differentially Expressed Anthocyanin Biosynthesis Genes	87
3.3.3 Analysis of Cluster 2	90
3.3.3.2 Promoter Analysis of Cluster 2 Genes	90

3.3.4 Analysis of Clusters Containing TT8	91
3.3.4.1 Analysis of Gene Ontologies	93
3.3.4.2 Promoter Analysis	94
3.3.5 Analysis of Differentially Expressed MYB Genes in the <i>MYB90</i> Knockout	95
3.3.6 Real Time PCR Analysis to Check Microarray Results	95
3.3.6.1 <i>MYB90</i>	96
3.3.6.2 <i>MYB75</i>	97
3.3.6.3 <i>Chalcone synthase (CHS)</i>	97
3.3.6.4 <i>SAG12</i>	97
3.4 Analysis of Anthocyanin Biosynthesis During Leaf Development	99
3.4.1 Anthocyanin Biosynthesis Plant Growth Experiment	99
3.4.2 Total Anthocyanin Content Measurements	99
3.4.3 Anthocyanin Composition	100
3.4.4 Quantification of Anthocyanin Components	103
3.5 Analysis of Flavonoid Content During Development	103
3.5.1 Flavonoid Composition	104
3.5.2 Total Flavonoid Content Measurement	107
3.6 Conclusions	108
3.6.1 Total Chlorophyll and Protein Levels During Development	108
3.6.2 Photosynthetic Performance	108
3.6.3 Gene Expression During Development	110
3.6.4 Anthocyanin Biosynthesis During Development	111
3.6.5 Flavonoid Biosynthesis During Development	112
3.6.6 Other Potential MYB Transcription Factors Involved in Anthocyanin Biosynthesis	113
3.7 Summary	113
4 The Role of <i>MYB90</i> During Plant Stress Responses	114

4.1 Introduction	114
4.2 High Light Stress	114
4.2.1 High Light Plant Growth Experiment	114
4.2.2 The Role of MYB90 in Anthocyanin Biosynthesis During High Light Exposure	116
4.2.2.1 Total Anthocyanin Content Measurements	117
4.2.2.2 Anthocyanin Profiles	118
4.2.2.3 Quantification of Anthocyanin Components	120
4.2.3 Role of MYB90 in Flavonoid Biosynthesis During High Light Exposure	121
4.2.3.1 Quantification of Total Flavonoid Content	121
4.3 High Light Time Course	121
4.3.1 High Light Time course Plant Growth Experiment	122
4.3.2 Chlorophyll Fluorescence Measurements	122
4.3.3 Role of MYB90 in Anthocyanin Biosynthesis During Different High Light Exposure Times	125
4.3.3.1 Total Anthocyanin Measurements After Different High Light Exposure Times	125
4.3.3.2 Anthocyanin Profiles After Different High Light Exposure Times	127
4.3.3.3 Quantification of Anthocyanin Components	129
4.3.4 Role of MYB90 in Flavonoid Biosynthesis During Different High Light Exposure Times	130
4.3.4.1 Flavonoid Profiles After Different High Light Exposure Times	130
4.3.4.2 Quantification of Total Flavonoid Content After Different High Light Exposure Times	131
4.3.4.3 Quantification of Flavonoid Components Following 48 h High Light Exposure	132
4.3.4.4 Analysis of the Main Flavonoid Component Following Different	

High Light Exposure Times	133
4.4 Conclusions	135
4.5 Summary	138
5 Functional Analysis of <i>MYB75</i>	140
5.1 Introduction	140
5.2 <i>MYB75</i> RNAi	140
5.3 The Role of <i>MYB75</i> During High Light Exposure	141
5.3.1 Chlorophyll Fluorescence Measurements	141
5.3.1.1 Maximum PSII Efficiency	143
5.3.1.2 Operating PSII Efficiency	144
5.3.1.3 Photochemical Quenching	145
5.3.1.4 Non-Photochemical Quenching	145
5.3.1.5 Linear Electron Transport Rate	146
5.3.2 Role of <i>MYB75</i> in Anthocyanin Biosynthesis During High Light Exposure	148
5.3.2.1 Total Anthocyanin Content Measurements	148
5.3.2.2 Anthocyanin Profile	149
5.3.2.3 Quantification of Anthocyanin Components	151
5.3.3 The Role of <i>MYB75</i> in Flavonoid Biosynthesis During High Light Exposure	152
5.3.3.1 Flavonoid Profiles	152
5.3.3.2 Quantification of Total Flavonoid Content	154
5.4 Conclusions	155
5.5 Summary	157
6 Analysis of <i>MYB90</i> and <i>MYB75</i> Expression Using a Reporter Gene	158
6.1 Introduction	158
6.2 Gateway Cloning of <i>MYB90</i> and <i>MYB75</i> Promoters	158
6.3 <i>MYB90</i> Promoter GUS Fusions Plant Growth Experiments	160

6.3.1 Analysis of GUS Activity During Senescence	160
6.3.2 Analysis of GUS Activity During Low Nitrogen/ High Glucose Stress	162
6.4 MYB75 Promoter GUS Fusions Plant Growth Experiments	163
6.4.1 Analysis of GUS Activity During Senescence	163
6.4.2 Analysis of GUS Activity During Low Nitrogen High Glucose Stress	166
6.4.3 Analysis of GUS Activity During High Light Exposure	166
6.5 Promoter Analysis	166
6.5.1 The Promoter Motifs Shared By Both <i>MYB90</i> and <i>MYB75</i>	167
6.5.2 <i>MYB90</i>	167
6.5.3 <i>MYB75</i>	168
6.6 MYB90 Promoter Deletions: GUS Fusion Plant Growth Experiment	171
6.7 Conclusion	175
6.7.1 <i>MYB90</i>	175
6.7.2 <i>MYB75</i>	176
6.8 Summary	178
7 General Discussion	179
7.1.1 <i>MYB90</i> Regulates Anthocyanin Biosynthesis Suring Senescence	179
7.1.2 <i>MYB90</i> and <i>MYB75</i> have a Role in Photo-oxidative Protection During High Light Stress	180
7.1.3 Regulation of <i>MYB90</i> and <i>MYB75</i> Promoter Activity	181
7.1.4 Identification of Potential Promoter Motifs Regulating <i>MYB90</i>	182
7.2 Summary	183
7.3 Future Work	183
8 Bibliography	184

List of Figures

Fig 1.1:	Changes in the ultra-structure of mesophyll cells during the autumn	3
Fig 1.2:	The structure of the chloroplast	26
Fig 1.3:	A diagram illustrating electron flow during the photosynthetic reactions in the thylakoid membrane.	29
Fig 1.4:	Chlorophyll Fluorescence measurement from an Arabidopsis leaf	33
Fig 1.5:	Schematic diagram of the flavonoid biosynthesis pathway	37
Fig 1.6:	The regulation of anthocyanin and proanthocyanidin biosynthesis by the interactions of transcription factors	41
Fig 1.7:	MYB75 over expression mutant and wild type COL-0	45
Fig 1.8:	Regulation of MYB90 and MYB75 during development	46
Fig 3.1:	WT and IM28 Leaf Seven Development	68
Fig 3.2:	The Total Chlorophyll Content, Chlorophyll a/b ratio and the Total Protein Content in the Seventh Rosette Leaf of WT and IM28 During Development	71
Fig 3.3:	Chlorophyll Fluorescence Images of WT Leaf 7 During Development	72
Fig 3.4:	Chlorophyll Fluorescence Images of IM28 Leaf 7 During Development	74
Fig 3.5:	The Maximum PSII Efficiency During Development	75
Fig 3.6:	PSII Operating Efficiency and Photochemical Quenching	77
Fig 3.7:	Non-photochemical Quenching and Linear Electron Transport Rate	79
Fig 3.8:	The Photosynthetic Performance in WT and IM28, 32 Days After Sowing	80
Fig 3.9:	The Photosynthetic Performance in WT and IM28, 36 Days After Sowing	82

Fig 3.10:	Clustering of Genes That Were Differentially Expressed During Development	84
Fig 3.11:	Analysis of Cluster 1	86
Fig 3.12:	Promoter Analysis of Cluster 1 Gene Promoters	87
Fig 3.13:	Analysis of Differentially Expressed Anthocyanin Biosynthesis Genes	89
Fig 3.14:	Analysis of Cluster 2 Genes	91
Fig 3.15:	Promoter Analysis of Cluster 2 Gene Promoters	92
Fig 3.16:	Analysis of TT8	93
Fig 3.17:	Promoter Analysis of Genes Clustered With TT8	95
Fig 3.18:	Analysis of MYB Genes Differentially Expressed in IM28	96
Fig 3.19:	The Relative Expression of MYB90, MYB75, CHS and SAG12 in the Seventh Rosette of WT and IM28 During Development	98
Fig 3.20:	Analysis of the Total Anthocyanin Content During Development of Leaf 8	100
Fig 3.21:	Anthocyanins in the eighth rosette leaf from WT during development	101
Fig 3.22:	Anthocyanins in the eighth rosette leaf from IM28 during development	102
Fig 3.23:	Quantitative Analysis of the Anthocyanin Composition	104
Fig 3.24:	Flavonoids in the eighth rosette leaf from WT during development	105
Fig 3.25:	Flavonoids in the eighth rosette leaf from IM28 during development	106
Fig 3.26:	Total Flavonoid Content in the Eighth Rosette Leaf From WT and IM28	107
Fig 4.1:	WT and IM28 High Light Plant Growth Experiment	115
Fig 4.2:	Total Anthocyanin Measurement	117
Fig 4.3:	Anthocyanin Profiles of WT and IM28 Following High Light	

	Exposure	118
Fig 4.4:	Quantification of Anthocyanin Components in Untreated and High Light Treated WT and IM28	120
Fig 4.5:	Quantification of the Total Flavonoid Content During High Light Exposure	121
Fig 4.6:	The Effect of High Light Exposure Times on the Maximum PS2 Efficiency (Fv/Fm)	123
Fig 4.7:	Total Anthocyanin Content Measurements	126
Fig 4.8:	Anthocyanin Profiles of WT and IM28 Following High Light Exposure	128
Fig 4.9:	Quantification of Anthocyanin Components Following 48 and 72h High Light Exposure	129
Fig 4.10:	Flavonoid Profiles of WT & IM28 Following High Light Exposure	131
Fig 4.11:	Quantification of the Total Flavonoid Content Following Different High Light Exposure Times	132
Fig 4.12:	Quantification of Flavonoid Components Following 48 and 72h High Light Exposure	133
Fig 4.13:	Analysis of the Main Flavonoid Component	134
Fig 5.1:	Selecting homozygous MYB75 RNAi Lines	141
Fig 5.2:	Maximum PS2 Efficiency Images Following 48h High Light Exposure	143
Fig 5.3:	Maximum PSII Efficiency (Fv/Fm) of WT and IM28 Plants Following High Light Exposure	144
Fig 5.4:	Measurements of Photosynthetic Parameters Following High Light Exposure	147
Fig 5.5:	Total Anthocyanin Content Measurement	148
Fig 5.6:	Anthocyanin Profiles of WT and MYB75 RNAi Following High Light Exposure	150

Fig 5.7:	Quantification of Anthocyanin Components in Untreated and 48h High Light Treated WT and MYB75 RNAi.	151
Fig 5.8:	Flavonoid Profiles of WT and MYB75 RNAi Following High Light Exposure	153
Fig 5.9:	Quantification of the Total Flavonoid Content of WT and MYB75 RNAi Plants Following High Light Exposure	154
Fig 6.1:	MYB90 and MYB75 Promoter Fragments	158
Fig 6.2:	Gateway BP Recombination Reaction	159
Fig 6.3:	Gateway LR Recombination Reaction	160
Fig 6.4:	Histochemical Staining of Transgenic Plants Containing the MYB90 Promoter GUS Fusions During Senescence	161
Fig 6.5:	The Quantification GUS Activity in MYB90 Promoter GUS Fusions During Development	162
Fig 6.6:	Effects of Low N High Glucose Stress on Transgenic Plants Carrying <i>MYB90</i> Promoter GUS Fusions	163
Fig 6.7:	Histochemical Staining of Transgenic Plants Containing <i>MYB75</i> Promoter GUS Fusions During Senescence	164
Fig 6.8:	The Quantification GUS Activity in <i>MYB75</i> Promoter GUS Fusions During Development	164
Fig 6.9:	Effects of Low N High Glucose Stress on Transgenic Plants Carrying <i>MYB75</i> Promoter GUS Fusions	165
Fig 6.10:	Histochemical Staining of Transgenic Plants Containing the MYB75 Promoter GUS Fusions Following High Light Stress	166
Fig 6.11:	MYB90 and MYB75 Promoter Motif Maps	170
Fig 6.12:	MYB90 Promoter Deletion: GUS Fusions	171
Fig 6.13:	Quantification GUS Activity in Transgenic Plants Containing MYB90 Promoter Deletion	173
Fig 6.14:	Cartoon representation of <i>MYB90</i> promoter activity in (A)	

senescent, low nitrogen high glucose treated, (B) mature green 174
and high light stressed plants

List of Tables

Table 1: Microarray analysis of MYB90 insertion mutant	47
Table 2: List of primers for real time PCR	54
Table 3: Light Curve 1	59
Table 4: Light Curve 2	59
Table 5: Dark Adaption Protocol	60
Table 6: List of Primers for Gateway Cloning	64
Table 7: List of Primers designed for Sequencing of Clones	67
Table 8: Primers used for PCR amplification and sequencing of the GST sequence in plants containing RNAi construct	67
Table 9: Significant GOs of Genes Clustered With TT8	94
Table 10: Web-Based Motif Analysis of MYB90 and MYB75 Promoters	169

Acknowledgements

I would like to thank my supervisor Dr. Vicky Buchanan-Wollaston for all the support, guidance and advise during my PHD. I am thankful to everyone in the senescence group for all their help, support and friendship over the last 4 years. I would also like to thank BBSRC for funding the project.

Declaration

The work referred to in this thesis is my own work and has not been submitted for a degree at another university.

Summary

MYB90 and MYB75 are two MYB transcription factors that regulate anthocyanin biosynthesis in Arabidopsis. Prior to this study a microarray experiment indicated that *MYB90* was required for senescence associated anthocyanin biosynthesis. The role of *MYB90* during senescence was investigated using a *MYB90* knockout insertion mutant, IM28. Gene expression studies at different time points during the development of the seventh rosette leaf showed that *MYB90* regulates anthocyanin biosynthesis genes and *MYB75* during senescence. The absence of *MYB90* expression reduced photosynthetic performance at two time points during development. Analysis of anthocyanin and flavonoid content showed that there was reduced anthocyanin biosynthesis in the absence of *MYB90* expression.

The role of *MYB90* and *MYB75* during high light stress was investigated by analysing the photosynthetic performance and anthocyanin content of high light treated IM28 and *MYB75* RNAi plants. *MYB90* is required for increased resistance during high light stress, which reflected anthocyanin levels. However, there was eventual compensation for the absence of *MYB90* expression in prolonged high light stress. *MYB75* was also required for increased resistance to high light stress, but this was not reflected in the anthocyanin levels.

The spatial and temporal regulation of *MYB90* and *MYB75* was investigated using transgenic plants containing promoter: GUS fusions. *MYB90* promoter activity was mainly localised to vascular tissue during senescence and low nitrogen/high glucose treatment. *MYB75* showed differential tissue specificity in different treatments. The transcriptional regulation of the *MYB90* promoter was analysed using promoter deletion GUS: fusions. A senescence specific activation region and a repressor region of the promoter were identified.

Abbreviations

AAT	Anthocyanin acyltransferase
ABA	Abscissic acid
ABRE	Abscissic acid response element
AGRIKOLA	Arabidopsis genomic RNAi knockout line analysis
AGT	Anthocyanidin 3-glucosyltransferase
AHP	Histidine phosphotransfer protein
AN	Anthocyanin
AN2	Anthocyanin 2
ANS	Anthocyanin synthase
AO	Antioxidant
APG	Autophagic gene
ARR	Response regulator protein
ATP	Adenosine triphosphate
B1	Booster 1
BAN	Banylus
bHLH	basic helix-loop-helix
BMV	Beta-amylase
BR	Brassinosteroids
b-ZIP	Basic region/ leucine zipper motif
C1	Colourless 1
C4H	Cinnamate 4-hydroxylase
CAB	Chlorophyll A-B binding protein
CATMA	A complete Arabidopsis transcriptome microarray
CHI	Chalcone isomerase
Chl	Chlorophyll
CHS	Chalcone synthase
COL-0	Columbia 0

DAD	Diode array ultra violet (UV) detector
DFR	Dihydroflavonol reductase
DNA	Deoxyribonucleic acid
DST	Delayed leaf senescence
E.coli	<i>Escherichia coli</i>
EDTA	Ethylenediaminetetracetic acid
EGL3	Enhanced glabrous 3
ERF	Ethylene response factor
F'	Light adapted fluorescence
F3'H	Flavonoid 3'hydroxylase
F3H	Flavonoid 3-hydroxylase
FCC	Fluorescent chlorophyll catabolites
Fd	Ferredoxin
FGT	Flavonol glycosyltransferase
FLS	Flavonol synthase
Fm	Maximum fluorescence
F'm	Light adapted maximum fluorescence
FNR	Ferredoxin-NADP ⁺ reductase
Fo	Fluorescence at ground state
F'o	Light adapted minimum fluorescence
FPS	Farnesyl diphosphate
F'q/F'm	Operating Photosystem II Efficiency
Fv	Maximum fluorescence minus the fluorescence at ground state
Fv/Fm	Maximum Photosystem II Efficiency
GFP	Green fluorescence protein
GL3	Glabrous 3
GO	Gene Ontology
GST	Glutathione S-transferase
GUS	β-glucuronidase

HPLC	High performance liquid chromatography
HXK	Hexokinase
HYS	Hypersenescence
IM28	Insertion mutant 28
IPT	Isopentenyl transferase
J	Linear electron transport rate
JA	Jasmonic acid
LDOX	Leucoanthocyanidin dioxygenase
LHC	Light harvesting complex
LiDs	Lithium dodecyl sulfate
MAPK	Mitogen activated protein kinase
MATE	Multidrug and toxic compound extrusion transporter
MOPS	3-(N-morpholino)propanesulfonic acid
MU	4-methylumbelliferone
MUG	4-methylumbelliferyl β -D-glucuronide
N	Nitrogen
Na	Sodium
NADP	Nicotinamide adenine dinucleotide phosphate
NASC	Nottingham Arabidopsis stock centre
NCCs	Non-fluorescent chlorophyll catabolites
NPQ	Non-photochemical quenching
OLD	Onset of Leaf death
P	Phosphorus
P680 ⁺	Chlorophyll monomer at centre of photosystem II
P700 ⁺	a dimer of Chlorophyll in photosystem I
PA	Proanthocyanidin
PAC	Pale aleurone colour
PAL	Phenylalanine ammonium lyase
PaO	Pheide a oxygenase

pC	Plastocyanin
PCR	Polymerase chain reaction
PD	Promoter deletion
pFCC	Primary fluorescent chlorophyll catabolites
PHY	Phytochrome
PI	Purple Leaf
PMSF	Phenylmethanesulphonylfluoride
PPFD	Photosynthetic photon flux density
PQ	Photochemical Quenching
PS1	Photosystem 1
PS2	Photosystem 2
Q	Plastoquinone
Q _A ⁻	a bound plastoquinone
qE	Energy dependent quenching
qI	Photoinhibitory quenching
qRT-PCR	Real time reverse transcription polymerase chain reaction
qT	State- transition quenching
R1	Red1
RBSCS	Ribulose-1, 5-bisphosphate carboxylase/ oxygenase
RCC	Red chlorophyll catabolite
RCCR	Red chlorophyll catabolite reductase
RNA	Ribonucleic acid
RNAi	RNA interference
ROS	Reactive oxygen species
SA	Salicylic acid
SAG	Senescence associated gene
SARK	Senescence associated receptor kinase
SAVs	Senescence associated vacuoles
SDS	Sodium dodecyl sulfate

SE	Standard error
SEN	Senescence
SOD	Superoxide dismutase
STDEV	Standard deviation
SV40	Simian virus 40
TAIR	The Arabidopsis information resource
TF	Transcription factor
TFA	Trifluoroacetic acid
TIP	Tonoplast intrinsic protein
TT	Transparent testa
TTG1	Transparent testa glabrous 1
TTP	Trehalose-6-phosphate
UV	Ultraviolet
WT	Wild Type

1 INTRODUCTION

1.1 Senescence

Senescence in plants is an active and highly regulated process of deterioration occurring during the later stages of development after cellular maturation and differentiation. The process is visible during autumn when leaves turn from green to yellow and red is followed by the death or the shedding of the leaf. The change in colour is due both to a loss of chlorophyll and the new synthesis of anthocyanins (red pigments). Trees prepare for winter during autumn by senescence followed by shedding the leaves and plants under stress will also show senescence leading to leaf shedding, for example plants shed leaves that have pathogen infection to prevent it spreading. Efficient senescence enhances the survival of the plant by recycling nutrients from unwanted regions and transferring them to growing regions of the plant. Nutrients are recycled by the catabolism of macromolecules such as proteins, lipids and nucleic acids (Gan, 2003). For example, approximately 90% of nitrogen from protein and nucleic acid breakdown is recycled (Himelblau & Amasino, 2001). The death of the leaf is delayed until completion of the nutrient recycling process. The process finally results in necrosis and cell death. The process of senescence can be divided into three stages: the initiation phase observes a dramatically reduced photosynthesis rate, resulting in the crossing of a metabolic threshold, which may be associated with the loss of chlorophyll or a change in sugar concentrations. Multiple signalling cascades control the process resulting in an altered redox state and a sink-source transition (Yoshida, 2003). The degeneration phase sees the degenerative and disassembly processes (Yoshida, 2003). The terminal phase observes the removal of the remaining metabolites, release of free radicals, and irreversible loss of cell integrity and viability and eventually cell death (Buchanan *et al.*, 2000, Yoshida, 2003).

1.1.1 Structural Changes During Senescence

In the degenerative/ reorganisation phase, highly ordered but reversible structural changes occur in the cell. Keskitalo *et al.* (2005) observed the changes in ultrastructure

of leaf cells and organelles during Aspen leaf senescence using transmission electron microscopy. Senescence was characterised by a loss of chlorophyll and the EM results showed the senescent stages (Fig 1.1).

a) Loss of 50% chlorophyll in a senescing leaf (Fig 1.1 A & B):

There were some cells unchanged. Some cells showed reduced definition of tonoplasts and a loss of chloroplast internal membrane structure.

b) Loss of 75 % chlorophyll in a senescing leaf (Fig 1.1 C & D):

There was a decline in the number of chloroplasts and mitochondria in a cell and an increase in the number of small vesicle structures present in the vacuole. There was a decline in electron dense material present in many cells. The chloroplasts present were deteriorating, there was a decline in starch granules, thylakoid membrane structure and an increase in the number and size of plastoglobuli.

c) <5% Chlorophyll in a senescing leaf (Fig 1.1 E & F):

The cell were less structured with the cytoplasm and plastids aggregating in the corners of some cells. Some of the mitochondria and nuclei still remained intact. Chloroplasts developed into swollen gerontoplast, which consisted mainly of plastoglobuli. Some of the plastoglobuli appeared to exude from the gerontoplasts.

d) Eventually the majority of cells appeared empty and dead.

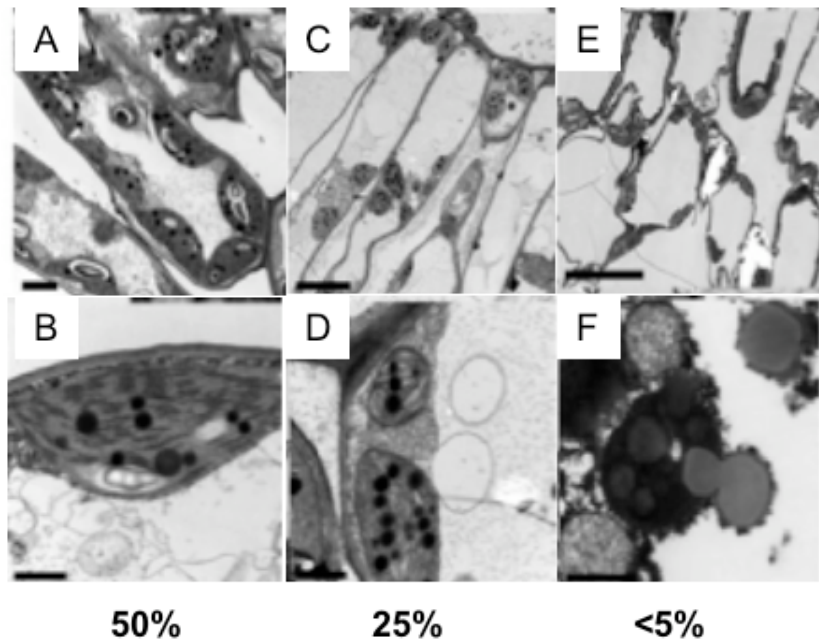


Fig 1.1: Changes in the ultra-structure of mesophyll cells during the autumn (Keskitalo *et al.*, 2005). Structural changes in cells (A, C, E) and chloroplasts (B, D, F) during autumn senescence of Aspen leaves, which is characterised by the chlorophyll content of the leaves (50%, 25% and <5% chlorophyll). Size bars correspond to 10 mm (E), 5 mm (C), 2 mm (A), 1 mm (B, D).

1.1.1.1 Senescence Associated Vacuoles

In a mature plant cell there is a large central vacuole, which contains a large number of different hydrolases, such as proteases, nucleases, phosphatases and glucosidases that have an acidic pH optimum. The vacuole may be involved in degradation of cellular components and nutrient recovery during senescence (Marty, 1999, Kim & Klionsky, 2000, Chiba *et al.*, 2003). Senescence associated vacuoles (SAVs) develop in the peripheral cytoplasm of mesophyll and guard cells. SAVs are small vacuoles, which differ from the central vacuole in content and composition. They are more acidic than the central vacuole and they lack the aquaporin γ -TIP (tonoplast intrinsic protein). *SAG12* expression occurs in cells containing SAVs in the leaf and the *SAG12* protein has been shown to be localised to the SAV. (Otegui *et al.*, 2005). The role of SAVs during senescence may be in the degradation of specific cellular components. SAVs may develop by autophagic mechanism, where cytosolic content and organelles are

internalised into vacuoles (Moriyasu and Hilmer, 2000). Usually autophagic mechanisms form double membrane vesicles that traffic different cytosol and organelles to the vacuole. There is increased expression of autophagic genes such as APG7, 8a, 8b, 8h and 9 during senescence (Buchanan-Wollaston *et al.*, 2005, Doelling *et al.*, 2002). The *apg7* and *apg9* mutants have accelerated senescence during nutrient deprivation, which indicates that controlled degradation via autophagic mechanisms is required for efficient senescence (Doelling *et al.*, 2002, Hanaoka *et al.*, 2002).

1.1.1.2 Transition of Peroxisomes into Glyoxysomes

Peroxisomes are subcellular organelles bound by a single membrane. In the leaf they are involved in photorespiration reactions. During senescence an increased number of peroxisomes and the transition of peroxisomes into glyoxysomes has been observed (Pastori & del Río, 1994, Pistelli *et al.*, 1996). Glyoxysomes contain enzymes involved in fatty acid β -oxidation and the glyoxylate cycle. There is a decline in the activity of enzymes involved in photorespiration and increased activity of glyoxylate enzymes as senescence progresses (Pastori & del Río, 1994, 1997). During senescence there is increased activity of the enzymes xanthine oxidase and urate oxidase, which indicated that peroxisomes/glyoxysomes may have a role in the catabolism of purines produced by the metabolism of nucleic acids (Corpas *et al.*, 1997, Pastori & del Río, 1994).

During senescence there was increased activity of the enzyme superoxide dismutase (SOD), which produces H_2O_2 and a decline in catalase activity (del Río *et al.*, 1998). This results in over-production of ROS, increased lipid peroxidation and increased H_2O_2 levels in the cytosol (Pastori & del Río, 1994, 1997).

1.1.2 Dismantling of Cellular Components During Senescence

1.1.2.1 Lipid and Membrane Deterioration

Lipids are a source of carbon and are metabolised during senescence to provide energy and also converted to sucrose for translocation in the phloem (Yoshida, 2003).

As senescence progresses there is a decline in function and structural integrity of cellular membranes as a result of accelerated metabolism of phospholipids, fatty acids and selective depletion of unsaturated fatty acids, which was shown to be associated with increased membrane leakiness (Borochoy *et al.*, 1982, Brown *et al.*, 1991, Thompson, 1988). The increased membrane permeability is due to changes in the composition and structure of the lipid bilayer. There is an increase in the sterol to fatty acid ratio that decreased lipid fluidity, lipid phase separations and this leads to packing imperfections and membrane leakiness (Barber & Thompson, 1980, 1983, Thompson, 1988). There was a loss of ionic gradients, changes in protein conformation, which reduced the function of membranes (Kirby and Green, 1980). The changes in the conformation of membrane proteins may cause them to protrude from the membrane and be targeted for proteolysis (Kirby and Green, 1980, Duxbury *et al.*, 1991a, 1991b).

There have been several lipid degrading enzymes identified as being associated with membranes of senescing tissues, including phospholipase D, phosphatidic acid phosphatase, lipolytic acyl hydrolase and lipoxygenase (Lynch & Thompson, 1984, Paliyath & Thompson, 1987). Phospholipase D mediates the first step in phospholipid degradation (Brown *et al.*, 1987). Diacylglycerols are membrane destabilising agents produced in a reaction catalysed by phosphatidic acid phosphatase (Allan *et al.*, 1976). These are degraded in a reaction catalysed by lipolytic acyl hydrolase to produce fatty acids, linoleic acid and linolenic acid, which are substrates for lipoxygenase (Galliard, 1980, Lynch & Thompson, 1984). Several senescence associated lipolytic acyl hydrolases were identified by Hong *et al.* (2000) and He & Gan, (2002). Transgenic plants over expressing lipolytic acyl hydrolases had precocious senescence and antisense suppression delayed senescence (He & Gan, 2002). This indicated that lipolytic acyl hydrolase activity is important for lipid metabolism and the initiation of senescence.

When an increased free fatty acid level occurs, the enzyme lipoxygenase induces lipid peroxidation (Grossman & Leshem, 1978, Lynch *et al.*, 1985). Lipid peroxidation produces reactive oxygen species such as the superoxide radical O_2^-

(Kappus, 1985, Duxbury *et al.*, 1991). The reaction is autocatalytic because the ROS can induce lipid peroxidation. The levels of antioxidant enzymes such as SOD and catalase regulate lipid peroxidation during development by controlling the ROS levels (Thompson *et al.*, 2000).

The thylakoid membranes contain a large source of carbon that is an important source of energy during senescence. The thylakoid membrane is composed mainly of galactolipids and the metabolism of these lipids appears to involve α -galactosidase, β -galactosidase and galactolipase (Woolhouse, 1984, Kim *et al.*, 2001, Lee *et al.* 2001). Lipid metabolism during senescence is associated with the increased expression of specific genes. In senescing *Arabidopsis* leaves, there was expression of lipases, acyl hydrolases, phospholipases, lipoxygenase and β -oxidation enzymes (Guo *et al.*, 2004). Buchanan-Wollaston *et al.*, (2005) found several genes involved in lipid catabolism were up-regulated during senescence, these included genes encoding lipases, α -dioxygenase, acyl-CoA dehydrogenase, ELIP protein and Rieske domain protein. Reduced expression of a senescence induced lipase delayed senescence in *Arabidopsis* (Thompson *et al.*, 2000).

The degradation of cellular membranes is a gradual process that occurs during senescence until all the membranes and organelles have disappeared (Kolodziejek *et al.*, 2003). Lipid catabolism produces membrane destabilising agents such as free fatty acids that cause phase separations in the lipid bilayer and form distinct domains. These domains were voided from the membrane, which may have acted to stabilise the membrane during nutrient recovery (Yao *et al.*, 1991a, 1991b, McKegney *et al.*, 1995, Hudak *et al.*, 1995). In the cytosol there have been lipid-protein particles identified that contain fatty acids, sterol esters, triacylglycerol, peroxidised lipids and catabolites of H^+ ATPase of plasma membrane origin (Hudak & Thompson, 1996, Yao *et al.*, 1991). In the chloroplast, plastoglobuli appear to be formed from degrading thylakoid membrane and voided into the stroma (Tevini *et al.*, 1985, Kaup *et al.*, 2002). In the stroma plastoglobuli are connected to each other and the membrane via a continuous lipid monolayer (Austin *et al.*, 2006). Isolated plastoglobuli contained galactolipids,

plastoquinone, α -tocopherol, triacylglycerol, carotenoids, free fatty acids and proteins, which indicated that they originated from the thylakoid membrane (Kaup *et al.*, 2002, Smith *et al.*, 2000). One protein found in plastoglobuli was the plastoglobular protein PAP, which was originally present on thylakoid membranes (Smith *et al.*, 2000, Rey *et al.*, 2000). PAP may be involved in the voiding of plastoglobuli from the membrane as the abundance of plastoglobuli increased when there was over expression of *PAP* (Rey *et al.*, 2000). PAP may also have a role in maintaining the structural integrity of the plastoglobuli (Rey *et al.*, 2000).

Senescence enhanced expression of genes involved in fatty acid β -oxidation, which is an important pathway when the carbohydrate supply has been depleted, has been shown (Graham and Eastmond 2002). In senescent barley, pumpkin fruit and detached cucumber organs fatty acid catabolism in the glyoxysomes produces acetyl Co A, which is used in respiration and synthesis of sugars via the glyoxylate pathway to produce phloem mobile sucrose (Gut & Matile, 1988; Graham, Leaver & Smith, 1992; Mc Laughlin & Smith, 1994 & Pistelli *et al.*, 1996). There is increased level of glyoxylate pathway enzymes such as isocitrate lyase and malate synthase. However in senescent Arabidopsis leaves the transcription of malate synthase and isocitrate lyase were not induced and the proteins were not detected (Charlton *et al.*, 2005 and Buchanan-Wollaston *et al.*, 2005). This indicates that acetyl Co A produced by β -oxidation is respired directly in Arabidopsis.

It is suggested that fatty acids may be mobilised from the membrane to the glyoxysomes by the particles voided from the membrane and there is some evidence that plastoglobuli may be exuded from the chloroplast envelope to the cytoplasm (Paramonova *et al.*, 2004).

1.1.2.2 Chlorophyll Degradation

Chlorophyll degradation is shown clearly by the yellowing of the leaf during senescence. Catabolism of chlorophyll is essential to maintain the cell viability during senescence, by detoxifying this reactive compound. This is not part of the nutrient

recycling process as it uses a lot of energy and no metabolites are recovered. The final products are non-fluorescent chlorophyll catabolites (NCCs) that are deposited in the vacuole (Hinder *et al.*, 1996). The accumulation of the phytotoxic chlorophyll products results in rapid cell death and reduces the efficiency of nutrient recycling.

The breakdown of chlorophyll involves five enzymatic reactions. In the chloroplast, chlorophyllase catalyses the removal of the phytol chain from chlorophyll, and produces chlorophyllide (Chlide) (Takamiya *et al.*, 2000, Tsuchiya *et al.*, 1999). The enzyme Mg dechelatase catalyses the removal of Mg from Chlide to produce pheophorbide (Pheide) (Suzuki & Shiou, 2002, Shioi *et al.*, 1996). The next step results in the loss of green colour, two reactions produces primary fluorescent chlorophyll catabolites (pFCC) from Pheide a. Pheide a oxygenase (PaO) opens the tetrapyrrole ring to produce red chlorophyll metabolites catabolites (RCC) (Hörtensteiner *et al.*, 1995). The *accelerated cell death 1 (ACD1)* gene was identified to encode Pao and antisense *ACD1* resulted in severe photo-oxidative damage from the accumulation of toxic pFCCs (Tanaka *et al.*, 2003). Recently the RCC forming factor (RFF) has been implicated in RCC formation along side PaO (Pruzinská *et al.*, 2005). pFCCs are released from RCC following a reduction catalysed by RCC reductase (RCCR) (Rodoni *et al.*, 1997). The *accelerated cell death2 (ACD2)* gene that encodes a defective RCCR, shows an accumulation of phytotoxic chlorophyll products, which induces rapid cell death (Vicentini *et al.*, 1998, Mach *et al.*, 2001, Pruzinská *et al.*, 2007).

The FCCs are exported from senescing chloroplasts (gerontoplast) by an ATP dependent transport system and imported into the vacuole by a tonoplast bound transport system (Hinder *et al.*, 1996). Finally the FCCs are converted to NCCs by two reactions. The first involves hydroxylation of an ethyl side chain of FCC possibly catalysed by a P450 dependent hydroxylase that may be located in the cytoplasm. The second reaction occurs in the vacuole where the change to an acidic pH converts FCC into NCC (Oberhuber *et al.*, 2001).

1.1.2.3 Protein Degradation

Proteins are degraded during senescence and there is increased expression of protease genes, the majority of which appear to be located in the vacuole. Approximately 75% of leaf protein is found in the chloroplast, but it has been very unclear how this protein is degraded during senescence since the majority of senescence-enhanced proteases are found in the vacuole of the cell and ubiquitin dependent proteolysis does not occur in the chloroplast. For example, the degradation of ribulose- 1, 5- biphosphate carboxylase/ oxygenase (RUBISCO) is not completed in isolated chloroplasts (Zhang *et al.*, 2007).

In the intact senescing chloroplast (gerontoplast), the stromal enzymes involved in carbon and nitrogen assimilation such as RUBISCO and glutamine synthetase are degraded early (Hörtensteiner & Feller, 2002). Degradation of the major stromal protein, RUBISCO may be initiated by increased reactive oxygen species (ROS). However, excess ROS are mainly produced by the degradation process and therefore occurred later in senescence. Prins *et al.*, (2008) showed that RUBISCO degradation may involve cysteine proteases and requires interaction with the cytosol. The degradation of RUBISCO was blocked in transgenic plants expressing the protease inhibitor oryzacystatin-1 (OC1). These plants had delayed decline of photosynthesis and RUBISCO, which is normally associated with senescence. Degradation of RUBISCO may occur in the vacuole. ATG dependent autophagic processes were shown to mobilise RUBISCO to the vacuole (Ishida *et al.*, 2007). The degradation of the stromal proteins appear to involve metalloendopeptidases and aminopeptidases (Roulin & Feller, 1998b, Feller & Fischer, 1994).

The thylakoid bound proteins are degraded in conjunction with the membrane and other membrane constituents, which suggested that the accessibility of the proteins determined degradation (Matile 1992). The light harvesting chlorophyll binding protein 2 (LHCP2) is an apoprotein tightly linked with chlorophyll in pigment-protein complexes. The degradation of apoproteins was closely associated with chlorophyll degradation (Tsuchiya *et al.*, 1999). For example proteolytic cleavage occurred only at

the protruding N-terminus of membrane bound LHCP2 and the degradation of the protein required the simultaneous loss of chlorophyll (Thomas & Donnison, 2000). Further evidence is a stay green mutant in which chlorophyll degradation was blocked during senescence. There was no degradation of chlorophyll and LHCP2 in this mutant but the stromal protein RUBISCO was still degraded (Bachmann *et al.*, 1994).

In the cytosol aminopeptidases and oligopeptidases may cleave oligopeptides into amino acids, and proteasomes and endoproteolytic enzymes may be involved in degradation of larger protein fragments (Brouquisse *et al.*, 2001). The vacuoles contain high levels of cysteine endopeptidases and carboxpeptidases (Buchanan-Wollaston, 1997) and they may not have a role in degradation until the final lytic stages when they are released from the vacuole (Buchanan-Wollaston *et al.*, 2003; Yoshida, 2003). RUBISCO and glutamine synthetase were identified in isolated SAVs, which indicates that SAVs are involved in the degradation of soluble photosynthetic proteins from the chloroplast (Martinez *et al.*, 2008).

The ubiquitin pathway may be involved in the degradation of non-chloroplast proteins during senescence. This was indicated by a delayed senescence mutant *ore9*, has a mutation in an F-box protein that is a component of the ubiquitin E3 ligase/SCF complex targeting proteins for degradation (Woo *et al.*, 2001). Buchanan-Wollaston *et al.*, 2005 found that there was increased expression of several genes involved in ubiquitin pathways such as F box proteins, C3HC4 type RING finger proteins, ASK1 protein and E2 conjugating enzymes. Also the polyubiquitin gene *SEN3* was up regulated during Arabidopsis leaf senescence (Park *et al.*, 1998). In general the mechanisms for protein degradation during senescence remain unresolved.

1.1.2.4 Nucleic Acid Degradation

Nucleic acids are a valuable source of phosphorus and nuclease activity increases during senescence. Buchanan-Wollaston *et al.*, 2005, observed an increased expression of genes encoding nucleases. During senescence, the nucleus is condensed but remains intact (Bhattacharya *et al.*, 1996, Inada *et al.*, 1998). The

nuclear and mitochondrial DNA is maintained or only partially degraded until a late stage of senescence (Makrides & Goldthwaite, 1981, Chang *et al.*, 1985). This is presumably so that there can be active transcription of genes encoding enzymes for example, which are required to accomplish the nutrient recycling process. The chloroplast DNA however is degraded at an early stage of senescence (Sodmergen *et al.*, 1989, 1991). Total RNA and some mRNA levels decrease rapidly as senescence progresses (Bate *et al.*, 1991).

1.1.3 Regulation of Senescence

Senescence is an age dependent process but can also be affected by endogenous and environmental factors. Therefore it is an adaptive process regulated by a complex network of signals. The endogenous developmental factors included age, hormones/growth regulators and developmental processes such as replication. The environmental factors includes nutrient deficiency, insufficient light, drought, pathogen infection, and extreme temperatures (He and Gan, 2003). The process of senescence improves the survival of the plant in unfavourable conditions, for example during pathogen infection, where the loss of an infected leaf could prevent the infection of the rest of the plant (Matthews, 1991). Premature senescence induced by stress can be reversed if the stress is removed before senescence enters the terminal stage (Vonshak & Richmond, 1975, Wittenhach, 1977).

1.1.3.1 Internal Factors Regulating Senescence

1.1.3.1.1 Sugar Signalling

In plants sugar signalling has a role in regulating plant development and growth in response or in combination with internal and environmental regulators. Sugar signalling has been reported to contribute to the regulation of leaf senescence. However the effect of low versus high sugar concentrations on senescence has been the subject of much debate (Hensel *et al.*, 1993, Quirino *et al.*, 2000, Stessman *et al.*, 2002, Masclaux *et al.*, 2000, Wingler *et al.*, 2006).

During senescence there is a decline in photosynthetic carbon assimilation, which would suggest a decline in sugar levels. However there was accumulation of glucose and fructose, which may be from the breakdown of starch (Wingler *et al.*, 1998).

A rapid decline in sugar levels may contribute to the induction of dark-induced senescence of individual leaves. This was indicated by repression of dark induced senescence upon the application of sucrose (Chung *et al.*, 1997). However, photosynthesis was enhanced by low sugar levels in green leaves and repressed by the accumulation of sucrose and glucose (Rolland *et al.*, 2002).

There is evidence that high concentration of sugars in combination with low nitrogen supply induce senescence. The changes in gene expression found were similar to that seen in developmental senescence with increased expression of the senescence specific gene, *SAG12* and nitrogen remobilisation gene encoding glutamine synthase (Wingler *et al.*, 2004, Pourtau *et al.*, 2006).

Sugar sensing is required for sugars to act as signalling molecules and hexokinase has been reported to influence signalling pathways by acting as a glucose sensor. Premature senescence was observed in transgenic plants over-expressing hexokinase and the over-expression of hexokinase in transgenic tomato resulted in an increased sensitivity to sugars and an accelerated senescence phenotype (Dai *et al.*, 1999, Moore *et al.*, 2003). The knockout mutant of hexokinase *hxx1* showed a delayed senescence phenotype in the presence of sugars and the nonsense mutation of the hexokinase-1 gene, *gin2-1* also had delayed senescence with no accumulation of hexoses in the senescing leaves (Moore *et al.*, 2003, Wingler *et al.*, 2006, Pourtau *et al.*, 2006). These results indicate that hexokinase may have a role in the regulation of senescence.

1.1.3.1.2 Hormones

Signalling molecules such as salicylic acid (SA), jasmonic acid (JA), ethylene, cytokinins and brassinosteroids have roles in regulating plant responses to environmental stresses such as drought, pathogen infection and salt also have a role in promoting, enhancing or inhibiting senescence in *Arabidopsis* (Pic *et al.*, 2002, Rivero *et al.*, 2007 Espinoza *et al.*, 2007, Ghanen *et al.*, 2008). In general these signalling molecules are not sufficient alone to promote senescence in *Arabidopsis* and there is considerable evidence to show that the signalling pathways interconnect to regulate gene expression (Brenner *et al.*, 2005).

1.1.3.1.2.1 Ethylene

Ethylene is a gaseous hormone that regulates plant growth and developmental processes such as fruit ripening, flowering and leaf senescence (Smalle & van der Straeten, 1997, Tanimoto *et al.*, 1995, Jones & Woodson, 1997, Tang & Woodson, 1996, Ogawara *et al.*, 2003). Ethylene induces senescence in an age dependent manner, the leaf has to reach a certain age before it is susceptible to ethylene (Jing *et al.*, 2005). Reduced expression of genes involved in ethylene biosynthesis such as *1-aminocyclopropane 1-carboxylic acid (ACC) synthase* and *ACC oxidase* delayed senescence in tomato, maize and tobacco (John *et al.*, 1995, Young *et al.*, 2004, Wi & Park, 2002). Ethylene regulated senescence through signal transduction pathways was indicated by the fact that the ethylene insensitive mutant *etr1-1* and the mutants in ethylene signalling pathway *ein2/ora3* had delayed senescence (Zacarias & Reid, 1990, Grbic and Bleeker 1995, Oh *et al.*, 1997). In these mutants senescence did occur and then progressed normally once in progress indicating that senescence was not dependent on ethylene.

1.1.3.1.2.2 Salicylic Acid

Salicylic acid is a phenolic compound that is a signal molecule involved in plant defence against pathogens by inducing ROS generation and cell death (Mur *et al.*,

1997, 2000). SA was also shown to play a role in senescence, indicated by four-fold increase in SA concentration in senescing leaves (Morris *et al.*, 2000). A delayed senescence phenotype was observed in transgenic plants NahG, which over-expressed an SA-degrading enzyme, which reduced the levels of SA compared to the wild type (Morris *et al.*, 2000, Buchanan-Wollaston *et al.*, 2005). *npr1* and *pad4* mutants defective in SA signalling also displayed a delayed senescence phenotype indicating that the signalling pathway was required for SA to promote senescence (Morris *et al.*, 2000). These SA deficient plants senesced normally, which suggested that SA is not essential for senescence. The senescence specific gene *SAG12* required the SA pathway for enhanced expression during senescence but was not induced in SA treated green leaves. These results indicated that the SA signalling pathway required an additional age dependent factor during senescence. Many senescence enhanced genes are dependent on SA for expression (Buchanan-Wollaston *et al.*, 2005).

1.1.3.1.2.3 Methyl Jasmonate and Jasmonic Acid

Jasmonic acid (JA) and methyl jasmonate are involved in response to wounding and induce genes such as proteinase inhibitors (Ryan, 1990, Penninckx *et al.*, 1998, Thomma *et al.*, 1998). During senescence a four-fold increase in the methyl jasmonate and JA levels was reported (He *et al.*, 2002). External application of JA induced premature senescence in *Arabidopsis* leaves, which was seen by chlorophyll breakdown and a decrease in RUBISCO (He *et al.*, 2002, Parthier, 1990). The JA signalling pathway is necessary for JA to promote senescence, since external application of JA on the JA insensitive mutant *coi1* did not induce accelerated senescence (He *et al.*, 2002).

However mutants defective in JA signalling or production of JA only exhibited delayed senescence, signifying that there may be cross over of signalling pathways and the JA signal was not required for senescence (He *et al.*, 2002).

1.1.3.1.2.4 Brassinosteroids

Brassinosteroids are steroid hormones that have a role in a wide range of developmental processes, including promoting leaf senescence (Clouse 2002). Evidence to suggest that BR promotes senescence included premature senescence after external application of BR in mung bean leaves and delayed senescence in a mutant deficient in BR synthesis (*det2*) (He *et al.*, 1996, Clouse *et al.*, 1998). BR regulated senescence through BR signalling pathway, the mutant *bri1*, deficient in BR signalling, had delayed senescence (Clouse *et al.*, 1998).

1.1.3.1.2.5 Cytokinin

Cytokinin has an inhibitory effect on senescence. Cytokinins such as kinetin, isopentenyl adenine and zeatins are involved in the majority of developmental stages including post mitotic senescence (Miller *et al.*, 1956, Binns, 1994). External treatment with cytokinin delayed leaf senescence (Richmond & Lang, 1957). The best evidence for the key importance of cytokinin in controlling senescence is an auto regulatory senescence inhibition system where the promoter of a senescence specific gene, *SAG12*, directs cytokinin biosynthesis by expressing isopentenyl transferase (IPT). Results showed that the increased biosynthesis of cytokinin during senescence delayed leaf senescence at an early stage with delayed chlorophyll and protein degradation, maintenance of photosynthetic activity and inhibition of *SAG12* expression. The longevity of the whole plant increased (Gan and Amasino, 1995, Wingler *et al.*, 1998). Delayed senescence was observed in petunia when a gene similar to IPT, *Sho* was over-expressed by activation tagging (Zubko *et al.*, 2002). Masferrer *et al.*, (2002) induced premature senescence in *Arabidopsis* by over expressing farnesyl diphosphate synthase (FPS), which is involved in the mevalonic pathway. This resulted in the reduction of substrates required for cytokinin synthesis.

Roitsch (2000) suggested that the role of cytokinins during development was in the regulation of source to sink transitions; in young leaves high levels of cytokinins increased the activity of apoplastic invertases, sugar transporters and

induced cell division and in senescing leaves, low cytokinin levels prevent growth. Werner *et al.*, (2003, 2008) observed delayed senescence in cytokinin deficient *Arabidopsis* plants and suggested that the altered sink-source relationship influences cytokinin regulation of senescence.

The cytokinin signalling pathway involves the phosphorylation of histidine phosphotransfer (AHP) proteins by a histidine protein kinase, which is then translocated to the nucleus (Ugeuchi *et al.*, 2001, Hwang & Sheen, 2001). The AHP protein then transfers a phosphoryl group to a response regulator protein (ARR), which then activates or represses cytokinin responsive genes (Suzuki *et al.*, 2001). There are three known cytokinin receptors in *Arabidopsis*, AHK2, AHK3 and AHK4 and it has been shown that cytokinin mediates leaf longevity through the cytokinin receptor AHK3, which phosphorylates the response regulator, ARR2 (Kim *et al.*, 2006).

1.1.3.1.2.6 Polyamines

Polyamines are ubiquitous cellular components that include putrescine, spermidine and spermine. They have roles in cell proliferation, growth and synthesis of proteins and nucleic acids (Jeevanandam & Petersen, 2001). The concentrations are high in actively dividing cells and low in cells that are not dividing (Kaur *et al.*, 1985). Senescence was retarded by exogenous application of polyamines, which resulted in inhibition of ribonuclease and protease activity. This prevented the loss of chlorophyll and membrane peroxidation (Evan and Malmberg, 1989). Polyamines share a common substrate with ethylene for biosynthesis, antisense technology blocking the ethylene biosynthesis channelled it to polyamine production (Wi & Park, 2002). The combination of increased concentrations of PA and the reduced concentration of ethylene may help to retard the senescence phenotype (Wi and Park, 2002).

1.1.3.1.2.7 Reactive Oxygen Species

Until recently reactive oxygen species (ROS) have been implicated only with oxidative stress. ROS include the superoxide radical, hydrogen peroxide and the hydroxyl

radical. High levels of ROS cause oxidative damage and trigger cell death. However there is evidence that indicates that they have a role in signalling throughout plant development, for example as secondary messengers in pathways such as mitosis, tropisms and cell death (Foyer & Noctor, 2005). Changes in the environment are signalled by ROS, For example, plants produce an oxidative burst of superoxide in the plant membrane to confer changes in the environment. Also, hydrogen peroxide causes up-regulation of transcription of small heat shock proteins during high light exposure (Doke *et al.*, 1994, Vanderauwera *et a.*, 2005). Antioxidant enzymes (AOs) such as glutathione reductase, ascorbate peroxidase and catalase have roles in elimination of ROS and in oxidative signalling, independently and by transmitting the ROS signal (Foyer & Noctor, 2005). An imbalance between ROS and AO's results in oxidative stress induced cell death. The catalase enzymes are scavengers of ROS and the catalase deficient mutants were sensitive to environmental stresses such as high light (Willekens *et al.*, 1997, Vanderauwera *et al.*, 2005).

During senescence there are increased levels of ROS and reduced antioxidant activity (Prochazkova *et al.*, 2001). The degradation of macromolecules during senescence causes increased levels of ROS (del Rio *et al.*, 1998). ROS also has a role in macromolecule degradation during senescence e.g. free radicals are involved in the degradation of polar lipids (Lin & Kao, 1998). ROS have also been shown to have a role in regulating senescence-associated genes (Navabpour *et al.*, 2003). There is good evidence to indicate that ROS signalling pathways interact with the signalling pathways of the hormones SA, JA and ethylene (del Río *et al.*, 2006, Clements and Atkins 2001).

1.1.3.2 Environmental Factors

Environmental factors contribute to the regulation of senescence and these factors include light quality and photoperiod, water, temperature and pathogen infection (He and Gan, 2003). When there are unfavourable environmental factors such as drought and nutrient deficiency the plant adapts to survive. Leaf senescence improves the

survival of the plant in unfavourable conditions by prematurely relocating accumulated nutrient to younger leaves or to flowers for reproduction. During pathogen infection the loss of an infected leaf can prevent the infection of the rest of the plant. Premature senescence induced by stress can be reversed if the stress is removed before senescence enters the terminal stage (Vonshak & Richmond, 1975, Wittenbach, 1977).

Light has an important role in the regulation of senescence, developmental senescence appears to be initiated by the photoperiod in Aspen leaves and is not influenced by other environmental signals, such as temperature (Keskitalo *et al.*, 2005). The length of exposure to light has a role in the regulation of senescence; *Arabidopsis* plants grown in long days senesced earlier than plants grown in short days (Nooden *et al.*, 1996). The light quality also has an effect on leaf senescence, it was reported that darkness induced highly localised senescence in individual leaves in an age dependent manner. Older leaves senesced more rapidly than younger leaves in dark induced senescence (Weaver and Amasino, 2001). The symptoms included protein and chlorophyll degradation, increased oxidative stress, a rapid decline in photosynthetic capacity, whilst the capacity for mitochondrial respiration was maintained and there was unequal degradation of organelles in different cell types (Weaver and Amasino, 2001, Causin *et al.*, 2006, Keech *et al.*, 2007). However, shading the whole plant delayed senescence, the photosynthesis capacity was maintained and the mitochondrial respiration decreased and organelles were retained in mesophyll and epidermal cells (Weaver and Amasino, 2001, Keech *et al.*, 2007). This suggested that the light quality exposure of the whole plant influenced senescence of individual leaves. Shading of leaves by other leaves reduced light intensity and changed the light quality and these leaves have occasionally been observed to yellow (Causin *et al.*, 2006). Senescence occurring in the shaded leaves is advantageous to the plant because the nutrients are transferred to the leaves with the higher photosynthetic capacity. Although dark induced senescence has many similarities to developmental senescence there were many differences in gene expression patterns that suggested alternative metabolic pathways and different signalling pathways (Buchanan-Wollaston

et al., 2005). For example, the salicylic pathway was important during developmental senescence but not dark-induced senescence (Buchanan-Wollaston *et al.*, 2005).

Higher light intensities have also been shown to promote senescence. Plants grown in a reduced light intensity of $180\mu\text{mol m}^{-2}\text{s}^{-1}$ lived longer than plants grown in higher light intensity of $300\mu\text{mol m}^{-2}\text{s}^{-1}$ (Nooden *et al.*, 1996). Senescence can be induced during chronic exposure to high light intensity because there is an increase in ROS, which results in photo-oxidative damage (Procházkará *et al.*, 2004).

Drought induced leaf senescence of older leaves is beneficial to the plant because the nutrients of the leaf are transferred to younger leaves and flowers. The abscission of the senescent leaf terminates the water consumption of the leaf, which is beneficial for water balance of the whole plant (Kozlowski 1976, Munné-Bosch and Alegre 2004). In several species that are adapted to grow in stressful conditions and reproduction is linked to whole plant senescence, drought accelerated the senescence process to help the plant survive and reach its full life span (Pic *et al.*, 2002). Unlike other stresses that induced senescence, drought induced senescence is a gradual process that increased in intensity over time and is characterised by leaf yellowing and changes in metabolism gene expression and cell ultrastructure (Munné-Bosch and Alegre, 2004). Rivero *et al.*, (2007) showed that drought induced senescence may be associated with increased levels of ROS. Tobacco plants expressing IPT driven by senescence associated receptor kinase (SARK) promoter, which is induced during stress and maturation were tolerant to drought stress. Senescence induction was suppressed in these plants, and there was increased activity of antioxidant enzymes and a reduced level of ROS.

Regulation of drought induced senescence by two hormones, ABA and cytokinin, was observed (Munné-Bosch & Alegre, 2004, Rivero *et al.*, 2007). In drought stressed rice and wheat increased ABA levels increased the relocation of carbon from the senescing leaves to grains (Ali *et al.*, 1999, Yang *et al.*, 2002). Cytokinins have a role in sink source transitions and delayed senescence whilst nutrients are recycled. During drought induced senescence, cytokinin levels declined and were positively

correlated with chlorophyll content and photosynthetic rate were negatively correlated with sucrose phosphate synthase activity. Reduced cytokinin levels accelerated leaf senescence and promoted plant survival during drought stress (Munné-Bosch and Alegre 2004).

1.1.3.3 Genetic Regulation

Genes that have a role in senescence have been identified by the discovery of mutants with altered senescence. Premature senescence was observed in early onset of leaf death mutants (*old1-3*) and the hypersenescence mutant (*hys1*) (Jing *et al.*, 2002, Yoshida *et al.*, 2002). *hys1* has an early induction of dark induced and age dependent senescence. The gene encodes a novel membrane protein that has a nuclear localisation signal (Yoshida *et al.*, 2002). Delayed senescence mutants include *ore-sara4* (*ore4*) that has delayed age dependent senescence but dark induced senescence is unaffected. The gene encodes a plastid ribosomal small subunit protein. Senescence is delayed in the mutant possibly because there is a reduced metabolic rate due to reduced photosystem 1 activity (Woo *et al.*, 2002). Evidence that senescence is an active process and under genetic control includes the identification of mutants that are defective in macromolecule degradation. Two mutants with late senescence phenotypes encode proteins involved in protein degradation. The *ore9* mutant encodes an F box protein that is a component of ubiquitin E3 ligase/SCF complex. Its role in the complex may be to target proteins that negatively regulate senescence for proteolysis (Woo *et al.*, 2001). The *delayed leaf senescence mutant* (*dst1*) encodes a R-transferase protein that is involved in the N-end rule proteolytic pathway. The mutant has delayed age and dark induced senescence, which suggests that senescence requires R transferase activity and proteolysis by the N end rule pathway (Yoshida *et al.*, 2002). The acyl hydrolase encoded by *SAG101* may be involved in lipid degradation. Antisense repression of *SAG101* reduced lipid degradation and resulted in delayed senescence and over-expression of the gene increased the symptoms of senescence (He *et al.*, 2002).

Another technique to identify genes involved in senescence has been the use of microarrays (Chen *et al.*, 2002, Buchanan-Wollaston *et al.*, 2005, Ma and Bohnert, 2007). This resulted in a considerable increase in the number and speed of genes identified as senescence associated genes (SAG). This technique has been used to identify genes, metabolic pathways and transcription factors involved in age dependent, dark-induced and stress induced senescence and to compare senescence mutants to the wild type (Chen *et al.*, 2002, B-Wollaston *et al.*, 2005, Ma and Bohnert, 2007, van der Graaff *et al.*, 2006). There are publicly available data sources such as the Arabidopsis information resource (TAIR), Genevestigator and the Nottingham Arabidopsis stock centre (NASC) that allow users to look at gene expression genome wide and investigate individual genes of interest during different treatments, in mutants and different tissues.

Analysis of gene expression confirms that senescence is genetically controlled rather than being a passive degenerative process. Specific sets of genes are up and down regulated. Genes that are up regulated during senescence are known as Senescence Associated Genes (SAG's). Senescence processes depend on the transcriptional activation of these genes by a network of signalling pathways. The mechanisms that regulated this process are not fully known and the identification of transcription factors that regulated the pathways downstream of the primary signal or signals is the subject of much research. During senescence, SAGs have to perform many roles, including the regulation of developmental aging, endogenous biological processes and cellular maintenance. There are SAGs that also respond to environmental factors since there is considerable overlap between age dependant senescence and senescence induced by environmental stresses (Lim *et al.*, 2003, Buchanan-Wollaston *et al.*, 2005). Senescence enhanced genes can be characterised into different categories: genes that direct developmental processes, genes that direct senescence as well as other endogenous processes, genes that respond to environmental factors and affect senescence, genes that up regulate senescence

associated activities or down regulate cellular maintenance activates and genes involved in executing the senescence process such as degradation and nutrient mobilisation (Lim *et al.*, 2003). Senescence enhanced genes were arranged into potential functional groups including regulation, degradation, transport, autophagy, secondary metabolism stress/defence etc. The genes involved with degradation processes encode many enzymes involved in the catabolism of macromolecules and mobilisation of their metabolites. These include genes encoding proteases (cysteine, serine and aspartyl proteases), nucleases and enzymes that degraded amino acids (lactoylglutathionelyase and proline oxidase) and chlorophyll (pheophorbide a oxygenase) (Buchanan-Wollaston *et al.*, 2005).

Many regulatory genes encoding transcription factors were found to be up regulated during senescence including MYB genes (e.g. *MYB2*), b-ZIP (e.g. *TBZF* and *TBZ17*) *ERF3*, zinc finger, ethylene response factor and several WRKY genes (*WRKY4*, *WRKY6*, *WRKY7* and *WRKY53*) (Chen *et al.*, 2002, Yang *et al.*, 2001, Robatzek and Somissich 2002, Miao *et al.*, 2004). *WRKY6* is involved in defence and senescence and positively regulates the *PR1* gene and a senescence specific receptor- like protein kinase SIKK (Robatzek and Somissich 2002). *WRKY53* is also involved in senescence, defence and wounding and regulates target genes such as SAGs, PR genes, stress related genes and transcription factors including other WRKY factors (*WRKY6* and *WRKY42*). *WRKY53* RNAi and knockout lines had delayed senescence phenotypes and over-expression of *WRKY53* showed accelerated senescence phenotype (Miao *et al.*, 2004). Interestingly *WRKY53* switched from leaf age dependent expression in six-week old plants to plant age dependent in 7 week old plants (Miao *et al.*, 2004).

Many other genes involved in signalling cascades are up-regulated during senescence. These include genes involved in protein modification such as kinase, receptor like kinases and phosphatases, indicating a role for kinase signalling cascades during senescence (van der Graaff *et al.*, 2006). Genes encoding calcium

and calmodulin binding proteins are up regulated, which indicates calcium signalling as part of the regulation of senescence (Buchanan-Wollaston *et al.*, 2005).

The senescing leaf recovers accumulated nutrients to transport to other tissues of the plant. There is an increased expression of many genes involved in transport, including ABC transporters, sugar, peptide, amino acid and cation transporters etc (Guo *et al.*, 2004, Buchanan-Wollaston *et al.*, 2005, van der Graaff *et al.*, 2006). There is down regulation of chloroplast localised transporters during senescence, which is associated with the decline of photosynthesis (van der Graaff *et al.*, 2006).

1.1.3.4 Different Types of Senescence

Buchanan-Wollaston *et al.*, (2005) compared natural leaf senescence with dark induced, and cell suspension senescence and van der Graaff *et al.*, (2006) compared natural leaf senescence with dark induced senescence in individual attached and detached leaves. There were similarities and differences between the transcript profiles.

There were differences in genes involved in nitrogen metabolism (Buchanan-Wollaston *et al.*, 2005):

- Three glutamine synthetase genes key to nitrogen mobilisation were not up regulated during dark induced senescence or in cell suspension senescence
- Two glutamate decarboxylase genes were only up regulated during natural senescence.
- There may be a novel pathway for asparagine production for exportation during dark induced and cell suspension senescence because there was up regulation of two genes encoding glutamate dehydrogenase, and genes encoding aspartate amino transferase and asparagine synthase, but not in natural leaf senescence.
- These results concur with the increased asparagines levels measured in dark treated leaves (Lin and Wu 2004).

Genes encoding transporters were up-regulated in normal leaf senescence and dark induced senescence of individually attached and detached leaves.

- During normal leaf senescence there was a higher fraction of amino acid and oligopeptide transporters (van der Graaff *et al.*, 2006).
- Transporters localised to the plasma membrane involved in secretory pathways were preferentially up regulated during natural leaf senescence and dark induced senescence of detached leaves.

During natural senescence there was a distinct set of genes up regulated involved in the flavonoid biosynthesis pathway (Buchanan-Wollaston *et al.*, 2005):

- There may be an alternative flavonoid biosynthetic pathway in dark-induced senescence. Since a different set of flavonoid biosynthetic pathway genes were up regulated during dark induced senescence compared to natural senescence.
- The cell suspension senescence did not up regulate the flavonoid pathway genes.

In dark induced senescence, the up regulation of certain genes may be to rectify the sugar imbalance:

- An alternative carbohydrate source may have been found by the up regulation of genes encoding trehalose-6-phosphate phosphatase (TPP) and genes involved in branched chain amino acid catabolism (Buchanan-Wollaston *et al.*, 2005).

The SA, JA and ethylene signalling pathways were found to be important during developmental senescence:

- The SA signalling pathway was found to be important specifically for developmental senescence by comparing different types of senescence in mutants deficient in hormones (Buchanan-Wollaston *et al.*, 2005).

- The majority of SA responsive genes were up-regulated during natural senescence but not induced in dark induced senescence in individual attached or detached leaves (van der Graaff *et al.*, 2006).
- The ethylene pathway was involved in dark induced and cell suspension senescence (Buchanan-Wollaston *et al.*, 2005).
- There was activation of different JA isoenzymes during natural leaf senescence and wounding (van der Graaff *et al.*, 2006).

There is considerable overlap between senescence and stress induced genes. Chen *et al.*, (2002) found common transcription factors induced during senescence and stress. Ma and Bohnert, (2007) analysed stress related profiles in Arabidopsis and identified 197 genes that represented a universal stress dependent expression profile, the majority of genes common to all plants, animals, and fungi. These included signalling pathways in protein degradation, mitogen activated protein kinases (MAPK), calcium, apoptosis, ROS and phospholipids. The genes specific to plants were associated with ABA and JA. The analysis of stress profiles showed that there were distinct responses to different stresses and the genes down regulated were usually regulated by development with tissue specific expression.

1.2 Photosynthesis

Photosynthesis is an extremely important process because nearly all life directly or indirectly depends on it. Photosynthesis occurs in higher plants, algae and cyanobacteria. Light energy is converted into chemical energy. Photosynthetic activity occurs in the thylakoids of chloroplasts. Chloroplasts are plastids that have three distinct membranes, the permeable outer membrane and the less permeable inner membrane that form the chloroplast envelope and the thylakoid membrane (Fig 1.2). Inside the chloroplast is the stroma that contains small circular DNA, ribosomes, thylakoids and proteins. They have their own genome and genetic system but many important proteins are nuclear encoded and transported into the chloroplast following translation (Martin *et al.*, 1998). The thylakoid membrane function and components in

chloroplasts of higher plants has been reviewed by Gounaris *et al.*, (1986). The thylakoids have a flattened disc like shape and are arranged in stacks called grana. Inside the thylakoid is the lumen, The thylakoid membrane system is unusual because its lipid composition is mainly glycosylglycerides rather than the usual phosphoglycerides. The protein complexes photosystem 2 (PS2), photosystem 1 (PS1), cytochrome b_6f and CF_0 - CF_1 are located in the membrane and are involved in energy generation (reviewed by Hankamer *et al.*, 1997, Herremann, 1996). This requires chlorophyll, electron transport chains and ATP synthase (Gounaris *et al.*, 1986).

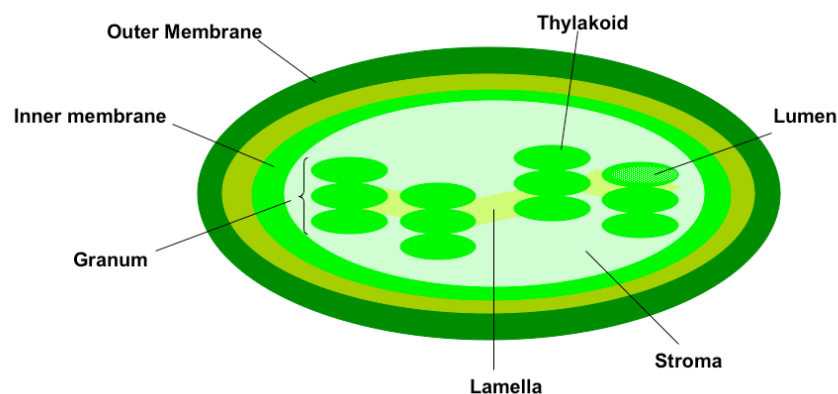


Fig 1.2: The structure of a chloroplast. The chloroplast is surrounded by the chloroplast envelope that consists of an outer and inner lipid bilayer membranes. Inside the chloroplast is the stroma, which contains small circular DNA, proteins and stacks of thylakoids known as grana. The thylakoid membrane contains protein complexes involved in photosynthetic reactions. Inside the thylakoid is the lumen.

There are two main processes involved in photosynthesis, photosynthetic electron transfer reactions and carbon fixation. These two processes are connected and controlled by feedback mechanisms.

1.2 1 Photosynthetic Electron Transfer Reactions (Fig 1.3)

Light capture involves the excitation of chlorophyll molecules, which then return to a more stable unexcited state following photosynthetic processes involving resonance

energy transfer whereby energy is transferred between chlorophyll molecules and an electron is transferred to an electron acceptor (Joliot & Joliot, 1983). Excess excitation energy is converted into less harmful heat and fluorescence to reduce oxidative damage (Krause & Weis, 1992, reviewed by Young *et al.*, 1997).

Energy is captured from light by photosynthetic electron transfer reactions. A photon of light excites a chlorophyll molecule in the antenna complex of photosystem II. The antenna complex consists of several distinct membrane protein complexes, known as the light harvesting complexes. These proteins are bound to chlorophyll molecules and accessory pigments such as carotenoids. Chlorophyll a is bound to the proteins psbB/D1 and psbC/D2 and associated with LHC2 proteins (Thornber & Barber, 1979, reviewed by Gounaris *et al.*, 1986). Resonance energy transfer channels the energy to a specific pair of chlorophyll a molecules in the reaction centre, P680.

The electron is immediately transferred to the primary electron acceptors, phaeophytin and Q_A and then passed along a chain of electron acceptors in the thylakoid membrane (Renger & Eckert, 1980, Joliot & Joliot, 1984). The cytochrome b_6f complex acts as a plastoquinol-plastocyanin oxidoreductase, catalysing the transport of electron carriers between PS2 and PS1 (Gounaris *et al.*, 1986, Malkin, 1992).

PS2 requires an external source of electrons to reduce oxidised chlorophyll molecules and therefore functions as a water-plastoquinone (PQ) oxidoreductase (Murata & Mugao, 1985). Two water molecules are oxidised, producing an oxygen molecule and four hydrogen ions as by-products. The hydrogen ions contribute to a proton gradient across the thylakoid membrane. The ATP synthase complex (CF_0 - CF_1) acts as a H^+ pump and produces an electrochemical proton gradient that drives the synthesis of ATP in the stroma (reviewed by Boyer, 1998, Turina *et al.*, 2003).

The role of PS1 in the electron transfer chain was reviewed by Shikani, (2007). PS1 is the final electron acceptor in the chain, it contains chlorophyll P700 in the reaction centre. A photon of light excites the electron and PS1 acts as a plastocyanin-ferredoxin reductase. The electron is passed down a chain of electron acceptors of

lowering energy to ferredoxin (Gounaris *et al.*, 1986), which uses the electron to reduce NADP^+ to produce NADPH.

1.2.2 Carbon fixation reaction

The carbon fixation reaction is also known as the Calvin-Benson-Bassham cycle (reviewed by Geiger & Servaites, 1994, Portis, 1992); it uses three molecules of ATP and two molecules of NADPH produced by the photosynthetic electron transfer reactions, to convert each CO_2 molecule into carbohydrate. The reaction begins in the stroma of the chloroplast and continues in the cytosol to produce sucrose.

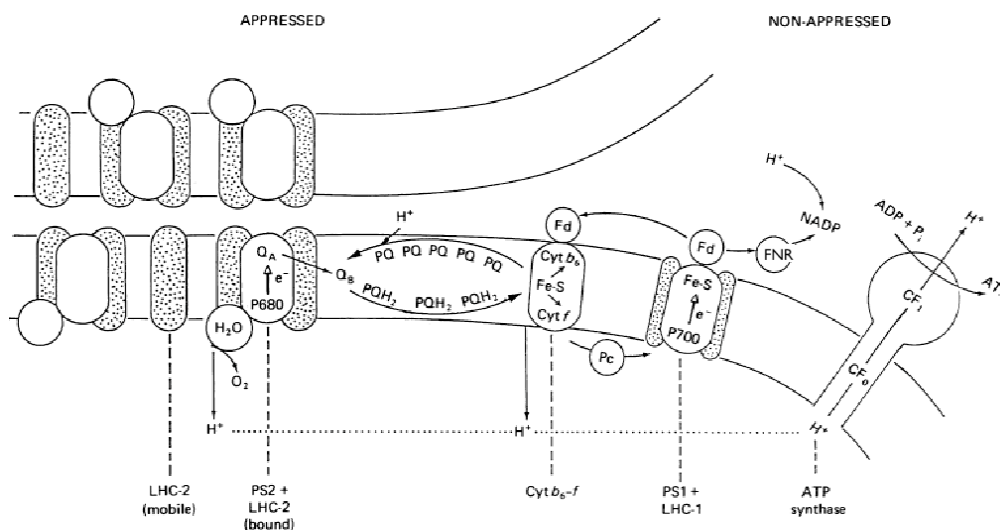


Fig 1.3: A diagram illustrating electron flow during the photosynthetic reactions in the thylakoid membrane (Gounaris *et al.*, 1986). There are four protein complexes shown, photosystem 2 (PS2), photosystem I (PSI), cytochrome b_6f and the ATP synthase ($\text{CF}_0\text{-CF}_1$). The PS2 complex is associated with light harvesting complex 2 (LHC2) and PS1 complex is associated with LHC1. An electron flows from the PS2 reaction centre chlorophyll P680 to the primary electron acceptor Q_A . Plastoquinones (PQ) and Plastocyanin (Pc) are electron carriers. The PS1 reaction centre chlorophyll P700 transfers an electron to Fe-S centres. Ferredoxin (Fd) passes electrons to NADP^+ and ferredoxin-NADP⁺ reductase (FNR) to generate NADPH. There is an electrochemical proton gradient between the stroma and thylakoid space created by the cytochrome b_6 complex accepting electrons from the plastoquinones, the ATP synthase complex pumping H^+ across the thylakoid membrane. H^+ is produced during oxidation of water in the thylakoid space and used during the formation of NADPH in the stroma.

1.2.3 Photosynthesis During Senescence

During senescence, there are complex processes occurring in the chloroplast since they are in the process of degradation whilst still maintaining photosynthesis (Keskitalo *et al.*, 2005). These processes must be highly regulated to reduce any disturbance to either process. The photosynthetic capacity of the leaf decreases as the chloroplasts are broken down and there is increase risk of photoinhibition because the breakdown of chloroplasts reduces the use of excitation energy used in photochemical processes. This results in an increase in the non-photochemical quenching to convert excess energy into heat and fluorescence.

1.3 Chlorophyll Fluorescence as a Measurement of Photosynthesis Activity

Chlorophyll fluorescence is a useful and non-invasive technique to assess the photosynthetic performance in leaves (Barbagallo *et al.*, 2003). Advances in technology and understanding of chlorophyll fluorometry have resulted in it being a more widely used technique, for example in screening programmes, to measure photosynthetic activity at cellular and sub-cellular levels in real time, and at low light levels. This technique has been used to measure the performance of mesophyll cells and stomatal guard cells (Lawson *et al.*, 2002) and also to investigate the heterogeneous pattern of performance in leaves after during stress such as sub-optimal temperature and drought (Haldimann *et al.*, 1996, Rong-Haul *et al.*, 2006).

1.3.1 Background

The energy from the light absorbed by a leaf is mainly used to power photosynthesis. However chlorophyll fluorescence and heat emission occur when there is excess light for photosynthesis. Light is absorbed for photosynthesis by the light harvesting pigment protein Complexes LHCs, and this results in the singlet excitation state of Chlorophyll a. If excitation occurs in a pigment other than Chl a, then the excitation is quickly transferred to Chl a. There are four routes for the excited Chl a to return to ground

state; the first is to transfer excitation to the reaction centre to drive photochemical reactions. Alternatively the energy in the excited Chl can be re-emitted as Chl fluorescence, or the Chl can be de-excited by thermal dissipation processes known as non-photochemical quenching or fourthly decay can occur via the triplet state. The triplet state generates a singlet state oxygen, which is a highly damaging ROS (Müller *et al.*, 2001).

During the excitation lifetime, the excitation energy can be transferred among all the Chls within the associated pigment matrix including the reaction centre Chl, which in PS2 is P680 and in PS1 is P700. One de-excitation pathway that occurs is via the formation of a radical pair, i.e. a Chl donor and a Quinone acceptor. When one or both of the components of this pair has a charge this is known as a closed reaction centre, both components then need to be taken back to a neutral state to generate an open reaction centre for further photochemistry to be possible. At PS2 the radical pair consists of $P680^+$ (a monomer of Chl a) and Q_A^- (a bound plastoquinone). Q_A^- transfers an electron to another electron carrier, Q_B . At PS1 the radical pair consists of $P700^+$ (a dimer of Chl a) and A_1^- (a bound quinone) (Oxborough, 2004). The functional difference between PS1 and PS2 is that a closed PS1 centre replaces photochemistry as a de-excitation route because $P700^+$ has a longer lifetime than A_1^- . At closed PS2 centres the photochemistry reactions are not replaced because the electron is transferred to $P680^+$ quicker than to Q_A^- and the increased fluorescence is due to the reduced number of electron acceptors. Therefore the chlorophyll fluorescence levels reflects PS2 performance and efficiency of photochemistry, not that of PSI (Oxborough, 2004).

1.3.2 PS2 Efficiency

Chl a fluorometry measures the fluorescence of Chl a when the system is in a known state and thus this assay can be utilized to investigate different parameters of PS2, such as the maximum possible PS2 efficiency, the operating PSII efficiency and the linear electron transport rate.

1.3.2.1 The Maximum Quantum Efficiency of PS2 Primary Photochemistry (F_v/F_m):

One parameter of photosynthesis that can be assessed by chlorophyll fluorescence is the maximum PS2 efficiency when all the reaction centres were open ($(F_m - F_o)/F_m$ or F_v/F_m). This is a measure of fluorescence in dark adapted material at a very low PPFD ($<1 \mu\text{mol m}^{-2} \text{s}^{-1}$) when all the reaction centres are open and the fluorescence is at ground state (F_o) and also during a pulse of highly saturating light when nearly all the reaction centres are closed and the fluorescence is raised to its maximum value (F_m). Q_A is the first electron acceptor of PS2 and is fully reduced. F_v is calculated as $F_m - F_o$. The maximum F_v/F_m value for a healthy plant is 0.8 and lower values indicate there is damage to the reaction centres (photoinhibition) (Björkman & Demmig, 1987).

1.3.2.2 The Operating Efficiency of PS2 ($(F'_m - F')/F'_m$ or F'_q/F'_m or ϕPS2):

The operating efficiency of PS2 reaction centres in the light at the point of measurement is related to the achieved PS2 efficiency (Baker *et al.*, 2001). This is estimated from the light adapted minimum and maximum fluorescence (F'_o and F'_m) and the measurement of the light adapted fluorescence signal (F'), which is a measurement that falls between F'_o and F'_m when a variable proportion of reaction centres are in the open state. F'_m is always lower than F_m . The operating efficiency of PS2 determines the proportion of the light absorbed by Chl that is used in photochemistry and has a strong linear relationship with efficiency of carbon fixation, unless the plant is under stress (Maxwell & Johnson, 2000).

1.3.2.3 Linear Electron Transport Rate (J):

The relative change in linear electron transport can be calculated from ϕPS2 , the incident light (PFDi , $\mu\text{mol photon m}^{-2} \text{s}^{-1}$) and a factor representing the energy sharing between PS2 and PS1 (0.5) by the following formula.

$$J = \phi\text{PS2} \times \text{PFDi} \times 0.5$$

A more accurate measurement of linear electron transport is to replace the incident light value with the absorbed light value (Maxwell & Johnson, 2000).

1.3.3 Down Regulation of Chlorophyll Fluorescence

The activity of some of the CO₂ fixation enzymes is light induced. Therefore upon application of constant illumination after dark adaption, the fluorescence yield increases because electron transport occurs milliseconds after illumination and reduces the electron acceptor Q_A. This results in a reduction of available electron acceptors in the photosynthetic pathway and the transient closure of reaction centres. There is no photochemistry at this point so the fluorescence yield increases. There is then a decrease in the fluorescence yield due to the activation of fluorescence quenching processes and it eventually reaches a steady state. The fluorescence quenching process involves the light activation of CO₂ fixation enzymes resulting in the increased rate of electron transport away from PS2, the opening of stomata and the increase in heat dissipation. The fluorescence yield can be used to assess the changes in photochemical quenching (PQ) and non-photochemical quenching (NPQ) because when the fluorescence yield is at its highest, photochemistry and NPQ are at their lowest.

1.3.3.1 Photochemical Quenching (PQ) $(F'_m - F') / (F_m - F_o)$ or F'_q / F'_v :

Photochemical quenching (PQ) reduces the yield of fluorescence by using the excitation energy to drive photochemistry and can be used as an estimate for the efficiency of photochemistry or the fraction of PS2 centres that are open. PQ relates the maximum PS2 efficiency to the operating PS2 efficiency and is non-linearly related to the proportion of PS2 in open state. At F'_m Q_A is fully reduced and the difference between F'_m and F' reflects the photochemical part of fluorescence quenching. A decrease in PQ indicates a reduction in the available electron acceptors and closure of reaction centres. (Maxwell & Johnson, 2000).

1.3.3.2 Non- Photochemical Quenching NPQ (F_m/F'_m-1):

Light harvesting needs to be regulated when the plants receives excess light, resulting in excess excitation energy. This leads to an increased level of fluorescence, which during de-excitation produces damaging ROS. Fluorescence yield can also be reduced by non-photochemical quenching NPQ that dissipates the excess excitation energy as thermal energy.

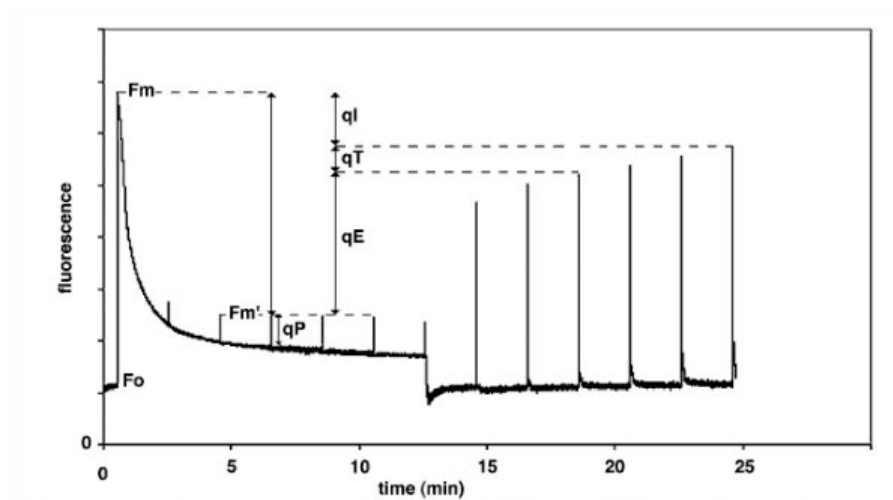


Fig 1.4: Chlorophyll fluorescence measurement from an Arabidopsis leaf (Muller *et al.*, 2001). In the presence of only weak measuring light the minimal fluorescence (F_o) is seen. When a saturating light pulse is given, the photosynthetic light reactions are saturated and fluorescence reaches a maximum level (F_m). Upon continuous illumination with moderately excess light ($750 \mu\text{mol photons m}^{-2} \text{sec}^{-1}$; growth light was $130 \mu\text{mol photons m}^{-2} \text{sec}^{-1}$), a combination of qP and NPQ lowered the fluorescence yield. NPQ ($qE + qT + qI$) can be seen as the difference between F_m and the measured maximal fluorescence after a saturating light pulse during illumination (F'_m). After switching off the light, recovery of F'_m within a few minutes reflected relaxation of the qE component of NPQ.

Estimations of NPQ are relative to the dark-adapted point F_m because it is not possible to inhibit heat dissipation. NPQ is a complex process linked to lumen acidification and the xanthophyll cycle. NPQ occurs when there is an increased photon irradiance or the supply of CO_2 is decreased. Mechanisms of NPQ (Fig 1.4) include the energy dependent quenching (qE), a major contributor that protects the reaction centres from light induced damage and involve a build up of a proton gradient, and the

light induced activation of the xanthophyll cycle. The state-transition quenching (qT) when the LHC is separated from PS2 by phosphorylation mediated migration of LHC between PS2 and PS1, is considered to be required for balancing the distribution of light between the two photosystems at low light (Harrison & Allen, 1992) and the photoinhibitory quenching (qI), is caused by protective processes and damage to the reaction centres.

1.3.3.2.1 Energy Dependent Quenching (qE):

Energy dependent quenching (qE) is the largest contributor to NPQ, and the most rapid component. qE protects against the short-term fluctuations in light intensity. Muller *et al.*, (2001) proposed a model, for qE. In limiting light the PS2 has efficient transfer of excitation energy to the reaction centre and qE is not induced. qE is triggered by high light, there is protonation of proteins in the LHC, which are most likely to be PsbS and at the same time the xanthophyll cycle is induced. The enzyme violaxanthin epoxidase that is associated with the thylakoid membrane is activated and the xanthophylls pigment violaxanthin is converted to zeaxanthin by de-epoxidation. The interconversion of violaxanthin is slower than the protonation of the proteins. Zeaxanthin binds to PsbS and forms a quenching complex and a conformational change of LHC. This results in the reduction of the Chl fluorescence lifetime. When there is a decrease in light, the decrease in pH causes a rapid de-protonation of the LHC proteins and disassembly of the quenching complex. Zeaxanthin is converted by epoxidation by the enzyme zeaxanthin epoxidase, this is slower than the de-protonation to allow for fluctuations in the light (Müller *et al.*, 2001).

1.3.3.2.2 Photoinhibitory Quenching (qI):

Photoinhibitory quenching is the least understood component of NPQ. It is long lasting and slowly reversible. qI may be a combination of photoprotection and damage. An example was in over wintering plants that had acclimatized to the cold by increasing the levels of xanthophylls, which is associated with qI (Müller *et al.*, 2001). An Fv/Fm

that is much lower than 0.8 indicates there is damage to the reaction centres due to photoinhibition. Photoinhibition can be estimated by comparing the F_v/F_m after a period of constant photon irradiance to the initial F_v/F_m . After the light is switched off the F_o and F_m approach but never reach the original dark-adapted levels. In dark-adapted state the energy dependent quenching qE decreases the F_o level in direct proportion to F_m by photo-protective quenching. Photoinhibition has increased levels of F_o because there is an increased fraction of reaction centres in a photo inactivated state resulting in a reduced PSII photochemical capacity and there is a decrease in F_m indicating an increase in NPQ (Oxborough, 2004).

1.4 The Role of Anthocyanins During Senescence

Anthocyanins are red-purple pigments that are present in leaves at specific developmental stages and are often produced in response to environmental stresses. They are famously associated with senescence, and are clearly visible during autumn when leaves turn from green to yellow and red. They are also produced during pathogen attack and wounding, as well as temperature and nutrient stress, for example during phosphorus (P) and nitrogen (N) deficiency (Lillo *et al.*, 2008).

1.4.1 Anthocyanin and Flavonoid Biosynthesis

Anthocyanins are secondary metabolites that are produced by a branch of the flavonoid pathway. The anthocyanins are red to purple pigments that are synthesised in the vegetative part of the plant. The other metabolites produced by this pathway are flavonols and proanthocyanidins. Flavonols are colourless to pale yellow pigments and are synthesised in vegetative part of the plant and in the seed coat. Proanthocyanidins (PA, also known as condensed tannins) are colourless pigments that turn brown and are synthesised in the seed coat (Nesi *et al.*, 2001).

The shikimate pathway provides phenylalanine for synthesis of anthocyanins, flavonoids and proanthocyanidins as well as for protein synthesis and other secondary metabolites. The pathway for synthesis of flavonoid components is shown in Figure

1.5. The enzyme phenylalanine ammonium lyase is the first step in the phenylpropanoid biosynthesis pathway. There are four different genes encoding this enzyme in *Arabidopsis*. The hydroxylation of cinnamic acid into p-coumaric acid is catalysed by cinnamate 4-hydroxylase (C4H). There are four genes that encode proteins with C4H activity in *Arabidopsis*.

The synthesis of naringenin chalcone by chalcone synthase (CHS) is the first committed step in biosynthesis for all the flavonoid subpathways (Fig 1.5). There is only one gene that encodes CHS in *Arabidopsis*. Naringenin chalcone is rapidly isomerised into the flavanone naringenin by chalcone isomerase (CHI). The hydroxylation of naringenin to give dihydrokaempferol is catalysed by the enzyme flavonoid 3-hydroxylase (F3H). The 3'-hydroxylation of flavonoids is catalysed by flavonoid 3'-hydroxylase (F3'H). The synthesis of flavonols from dihydrokaempferol and dihydroquercetin is catalysed by flavonol synthases. Leucoanthocyanidins are synthesised in a reaction catalysed by dihydroflavonol reductase (DFR). PA monomers are synthesised from leucoanthocyanidins by the enzyme encoded by banylus (*BAN*) gene (Nesi *et al.*, 2001).

The mutants of several flavonoid or anthocyanin biosynthesis genes have a transparent testa phenotype, CHS (*tt4*), CHI (*tt5*), F3H (*tt6*), F3'H (*tt7*), DFR (*tt3*) and glutathione S-transferase (GST) (*tt19*) (Shirley *et al.*, 1995, Wiseman *et al.* 1998, Schoebohm *et al.*, 2000). The transparent testa phenotype has been a good marker to detect mutants in the pathway and is one of the reasons that this pathway is so well described in *Arabidopsis*.

Anthocyanins are synthesised in the cytoplasm where all the enzymes in the flavonoid pathway are located, with the exception of F3'H. This enzyme is found in the endoplasmic reticulum, where it may aid anthocyanin synthesis by anchoring a large enzyme complex (Burbulis & Winkel-Shirley, 1999). Anthocyanins are transported and accumulated in the cell vacuoles. PAs interact with proteins more strongly than the anthocyanin monomers, so PA synthesis is likely to occur in the vacuoles instead of the cytoplasm (Abraham *et al.*, 2003).

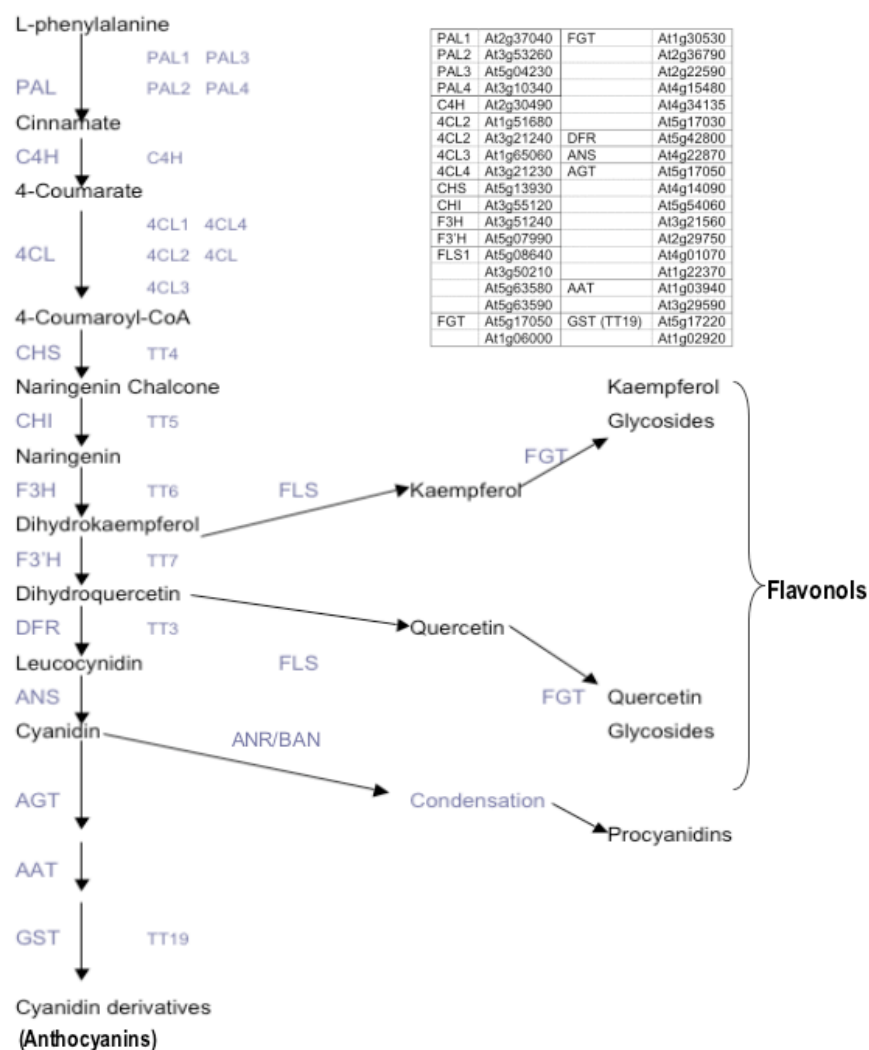


Fig 1.5: Schematic of the flavonoid biosynthesis pathway starting with phenylpropanoid metabolism and diverging into anthocyanin, flavonol and proanthocyanidin pathways. Enzyme names are abbreviated as follows: phenylalanine ammonia lyase (PAL), cinnamate 4-hydroxylase (C4H), 4-coumarate-CoA ligase (4CL), chalcone synthase (CHS), chalcone isomerase (CHI), flavanone 3-hydroxylase (F3H), flavonol synthase (FLS), flavonol glycosyltransferase (FGT), flavonoid 3'-hydroxylase (F3'H), dihydroflavonol 4-reductase (DFR), anthocyanin synthase/ leucoanthocyanidin dioxygenase (ANS), anthocyanidin reductase/ banylus (ANR/BAN), anthocyanidin 3-glucosyltransferase (AGT), anthocyanin acyltransferase (AAT), glutathione S-transferase (GST) and unknown condensing enzyme(s).

The translocation of anthocyanins may involve glutathione S transferase (GST/TT19) and the Arabidopsis gene *transparent testa12* (TT12), which codes for a multidrug and toxic compound extrusion (MATE) transporter specifically involved in PA transport

(Abrahams *et al.*, 2003). The vacuole has a glutathione (GS-X) pump activity, and the addition of glutathione to anthocyanins by GST action may tag them for transport (Mol *et al.*, 1998).

1.4.2 Regulation of Anthocyanin Biosynthesis

A network of regulatory proteins controls the anthocyanin biosynthesis pathway. A comprehensive study of the regulation of anthocyanin biosynthesis showed the importance of MYB genes. The first evidence that they are involved was via maize mutants in *COLOURLESS1 (C1)* and *PURPLE LEAF (Pl)* (Goff *et al.*, 1992). These genes encode R2R3 MYB proteins. C1 for example has an amino terminus similar to the DNA binding domain of MYB oncoproteins and has a region rich in acidic amino acids that shares homology with acidic transcriptional activation domains found in many regulatory proteins (Goff *et al.*, 1992). MYB proteins are involved in nuclear translocation and DNA binding activity and protein- protein interactions and have conserved residues required for binding to a specific DNA motif in the R3 repeat (Nesi *et al.*, 2001). Different MYB transcription factors may have some structural homology but have different DNA binding specificities and affinities.

C1 and Pl both have a role in the light regulation of anthocyanin biosynthesis but in different tissues and control many steps from chalcone synthase onwards. C1 is specific to seed tissues and Pl is specific to vegetative tissues (Martin and Paz-Ares, 1997).

C1 requires an interaction with bHLH proteins from the RED (R1) /BOOSTER (B1) family of proteins for transcriptional activation of anthocyanin biosynthesis genes (Goff *et al.*, 1992). The MYB domain of C1 directly interacts with the N-terminus of B1, which may induce a conformational change in C1 or both the proteins to produce a functional DNA binding complex. Mammalian bHLH proteins are involved in DNA binding and interactions between proteins to form dimers (Murre *et al.*, 1989, Ferré-D'Ameré *et al.*, 1994). The basic domain is responsible for DNA binding and the HLH domain is responsible for dimerisation (Goff *et al.*, 1992).

The C1 protein provides a transcriptional activation domain specific for anthocyanin biosynthesis genes (Goff *et al.*, 1992). The bHLH transcription factors R1 and B1 control pigmentation in different organs or tissue. R1 mainly regulates the pigmentation of the kernel, embryo and plant tissue whereas B1 regulates anthocyanin accumulation in the vegetative parts of the plant.

Studies in other plant species have also indicated the requirement for the MYB/bHLH protein interaction for anthocyanin and flavonoid biosynthesis. In strawberry the MYB1 protein was shown to interact with the maize bHLH protein, RED1 (R1) (Aharoni *et al.*, 2001) and in *Petunia hybrida* the MYB protein ANTHOCYANIN2 (AN2) interacts with the bHLH proteins JAF13 and AN1 and regulates anthocyanin biosynthesis in flower petals (Fig 1.6) (Davies and Schwinn, 2003, Quattrochio *et al.*, 1999).

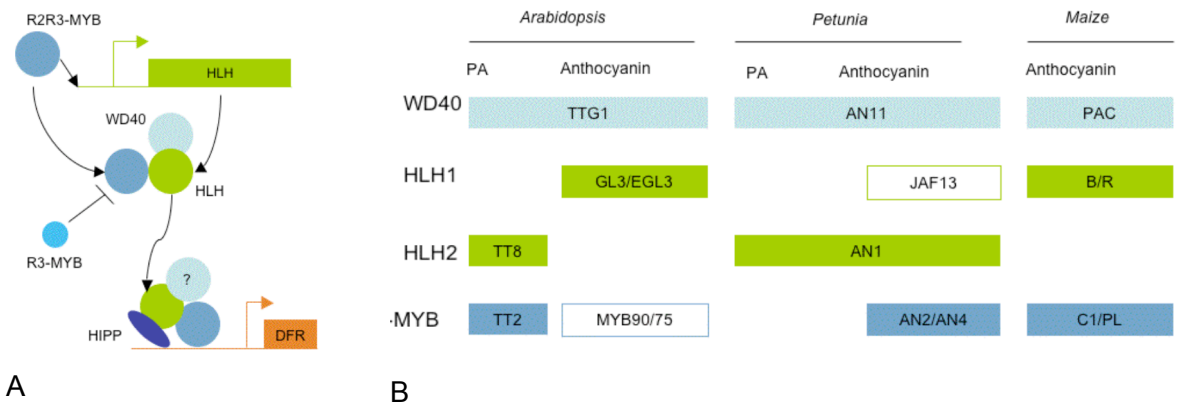
In *Arabidopsis thaliana* the ectopic expression of two transcription factors, MYB90 and MYB75 resulted in the transcriptional activation of a set of anthocyanin biosynthesis genes and accumulation of anthocyanins. This was visible by the purple pigmentation of leaves, stem and petals (Borevitz *et al.*, 2000). Both MYB90 and MYB75 have sequence homology to the AN2 MYB transcription factor of Petunia and to the C1/PI MYB transcription factors of maize that both have roles in the regulation of the flavonoid pathway. Therefore, these may be the Arabidopsis homologues of these two MYB genes.

The regulation of anthocyanin biosynthesis in Arabidopsis also involves bHLH factors (Fig 1.6). The over expression of two bHLH proteins, GLABROUS 3 (GL3) and ENHANCED GLABROUS 3 (EGL3) resulted in the activation of anthocyanin biosynthesis (Ramsay *et al.*, 2003). These proteins were shown to physically interact with MYB90 and MYB75 and strongly activated transcription of DFR (Zimmermann *et al.*, 2004a). The bHLH proteins are involved in overlapping networks including trichome development, anthocyanin, and proanthocyanidin and mucilage biosynthesis. The bHLH proteins each enhanced anthocyanin production but were functionally

homologous. Another bHLH protein is TRANSPARENT TESTA8 (TT8). This protein is required for seed coat pigmentation, and has an activity similar to the maize R protein (Zhang *et al.*, 2003). The mutant *tt8* did not produce proanthocyanidins and the seed coat pigmentation was altered.

There is another higher level of regulation of anthocyanin biosynthesis. GL3, EGL3 and TT8 interact with a WD repeat protein TTG1 (Fig 1.6) (Zhang *et al.*, 2003). A number of developmental and biochemical networks are dependent on TTG1 including anthocyanin biosynthesis, production of seed mucilage and hair formation. *ttg1* is a transparent testa mutant that has no seed pigmentation, and only the triple mutant *gl3 egl3 tt8* was indistinguishable from *ttg1* (Zhang *et al.*, 2003). The role of TTG1 in the complex may be to increase the activity of MYB/bHLH.

The regulation of proanthocyanidin biosynthesis in the seed coat by TTG1 was investigated in detail (Walker *et al.*, 1999, Baudry *et al.*, 2004, 2006, Zimmermann *et al.*, 2004a). The interaction of TTG1 with TT8 and TT2 (MYB123) was shown to increase the activity of the MYB: bHLH protein complex during the induction of *BANYLUS* (*BAN*) and *DIHYDROFLAVANOL REDUCTASE* (*DFR*), the collective action increased the accumulation of proanthocyanidins in the seed coat (Baudry *et al.*, 2004, 2006; Zimmermann *et al.*, 2004a). The level and specificity of expression of these genes may be due to the developmental control of *TT2*, *TT8* and *TTG1* expression levels (Baudry *et al.*, 2004). *ttg1* showed an altered *TT8* expression level indicating that TTG1 has a role in regulating TT8. *TT8* expression was also altered by over expression of *MYB75* and *TT2* (*MYB123*) (Fig 1.6A) (Nesi *et al.*, 2001, Baudry *et al.*, 2006). Also *in vivo* TT2, MYB75, GL3 and EGL3 have been shown to bind to the *TT8* promoter in combination with the simultaneous expression of *TT8*, indicating that *TT8* regulated its own expression (Baudry *et al.*, 2006). Anthocyanin, flavonoid and proanthocyanidins biosynthesis is not dependent on individual bHLH factors, for example TT8 was replaced by other bHLH factors GL3 and EGL3 in the transcription of *BAN*. However the MYB genes may be more specific, *TT2* was the only MYB gene able to activate the transcription of *BAN* (Baudry *et al.*, 2004).



A **B**

Fig 1.6: The regulation of anthocyanin and proanthocyanidins biosynthesis by the interaction of transcription factors. (A) A model of the interactions between the MYB, bHLH and WD40 proteins in the regulation of transcriptional activation of *DIHYDROFLAVANOL REDUCTASE* (*DFR*) (Koes *et al.*, 2005). The proteins interact and form a complex, the MYB proteins bind to the promoter and the bHLH proteins may bind through interaction with a bHLH INTERACTING PROTEIN (HIP) and it was unclear if the WD40 protein in the complex on the promoter. Some of these proteins also have a role in regulating some bHLH factors such as TT8. There may be a small R3-MYB protein that acts as an inhibitor through interaction with bHLH proteins. (B) The different WD40, bHLH and MYB protein regulating anthocyanin and proanthocyanidins (PA) biosynthesis in *Arabidopsis*, *petunia* and *maize* (Koes *et al.*, 2005). The *Arabidopsis* genes are *TRANSPARENT TESTA GLABROUS1* (*TTG1*) At5g24520, *TRANSPARENT TESTA8* (*TT8*) At4g09820, *GLABROUS3* (*GL3*) At5g41315, *ENHANCED GLABROUS3* (*EGL3*) At1g63650, *MYB123/TRANSPARENT TESTA2* (*TT2*) At5g35550, *MYB90* (At1g66390) and *MYB75* (At1g56650). The *petunia* genes are *ANTHOCYANIN11* (*AN11*), *JAF13*, *ANTHOCYANIN1* (*AN1*) *ANTHOCYANIN2* (*AN2*) and *ANTHOCYANIN4* (*AN4*). The *maize* genes are *PALE ALEURONE COLOUR* (*PAC*), *BOOSTER* (*B*), *RED* (*R*), *COLOURLESS1* (*C1*) and *PURPLE LEAF* (*P*).

There is a homologous protein to TTG1 in *Petunia hybrida* AN11 (Fig 1.6) that also regulates anthocyanin biosynthesis and it is distantly homologous to β subunits of heterotrimeric G proteins that have a role in signal transduction (Walker *et al.*, 1999).

The MYB transcription factor MYB12 independently regulates several genes of the flavonoid biosynthesis pathway including *CHS*, *CHI*, *FLS* and *F3H*. The MYB domain of the protein has a high structural similarity to the maize gene *P1*. MYB12

does not regulate *DFR* and therefore does not regulate anthocyanin biosynthesis (Mehrtens *et al.*, 2005).

There are other potential regulators of the flavonoid and anthocyanin biosynthesis pathways. Two genes that may act upstream of *TT2* in regulating the biosynthesis of proanthocyanidins in the seed coat are *TRANSPARENT TESTA1* (*TT1*, zinc finger protein) and *TRANSPARENT TESTA16* (*TT16*, MADS box transcription factor) (Sagasser *et al.*, 2002, Nesi *et al.*, 2002).

Anthocyanin biosynthesis is also regulated by Phytochrome A in response to light (Shin *et al.*, 2007). Phytochromes are red/far red light receptors that regulates various light responses by interacting with signalling components. Phytochromes interact with PIF3, a bHLH factor that has a complex role in light signalling (Kim *et al.*, 2003). PHYA mediates the induction of anthocyanin biosynthesis by interacting with PIF3, which collaboratively and positively regulates the pathway in far red light with HY5 (Shin *et al.*, 2007) by transcriptional activation of all anthocyanin biosynthesis genes including, *CHS*, *CHI*, *F3H*, *F'3H*, *LDOX* and *DFR* by binding to specific motifs in the promoters.

1.4.3 Resorption Protection

It has been suggested that anthocyanins can provide protection against photo-oxidative damage in senescing cells and reduce the photo-inhibition of photosystems under light stress by reducing excitation pressure during periods when there is an imbalance of light capture, CO₂ assimilation and carbohydrate utilisation (Steyn *et al.*, 2002). The red anthocyanins that are present in vegetative tissues absorb green and UV light but have lower absorbance of blue light and very little of red light (McClure, 1975). This modifies the quantity and quality of the light available to chlorophyll and occurs in proportion to the anthocyanin concentration (Neill & Gould, 1999), which reduces the excitation pressure.

Hoch *et al.*, (2003) proposed that anthocyanins provide resorption protection during senescence and acts by shading the photosynthetic apparatus to protect it from

high light levels. This allows photosynthesis to be maintained. The protective role of anthocyanins has been investigated in several studies. The effect of anthocyanin accumulation on reducing photoinhibition was tested by Feild *et al.*, (2001) in red and yellow senescing leaves of red-osier dogwood where the red leaves showed reduced photoinhibition compared to the yellow leaves. Also red pods of *Bauhinia variegata* had a higher tolerance to high blue-green and white light intensities than green pods (Smillie & Hetherington, 1999). Evidence from anthocyanin deficient mutants in three senescent deciduous tree species showed that absence of anthocyanin resulted in signs of irreversible photodamage and lower level of nitrogen resorption compared to the wild type (Hoch *et al.*, 2003). Keskitalo *et al.*, (2005) observed that once anthocyanin biosynthesis was initiated in senescing Apsen leaves the accumulation of anthocyanins was dependent on light levels.

Anthocyanins accumulate in the peripheral tissues that are exposed to high irradiance and are produced in tissues that are susceptible to stress, such as during early development when young leaves are expanding and during late development when leaves are senescing. The leaves are susceptible to photooxidative stress at these stages of development because they have a lower potential to use the absorbed light energy (Steyn *et al.*, 2002).

Nitrogen limitation reduces photosynthetic capacity of leaves, which increases the susceptibility to excessive light induced photo-oxidative stress. Anthocyanin accumulation is associated with low nitrogen conditions and acts as a protective screen by absorbing light and reducing the excitation energy (Scheible *et al.*, 2004). Nitrogen limitation induces genes involved in anthocyanin biosynthesis and protein degradation and down regulates genes involved in photosynthesis and synthesis of proteins, amino acids and nucleotides (Peng *et al.*, 2007). The *nitrogen limitation adaption mutant (nla)* has increased expression of anthocyanin biosynthesis genes in low nitrogen conditions but at a lower level than the WT (Peng *et al.*, 2007). The *nla* plants adapted to the stress by increased expression of genes involved in oxygen and radical detoxification (Peng *et al.*, 2007).

1.4.4 Direct Antioxidant Role of Anthocyanins

Flavonoids and anthocyanins also have direct antioxidant (AO) properties, however in vegetative tissue the anthocyanins are stored in the vacuole away from the chloroplast, limiting their AO effectiveness. Flavonols can directly scavenge ROS and anthocyanins function as electron donors for the peroxidase reaction, in a similar manner to ascorbate and glutathione (Yamasaki *et al.*, 1997). During severe stress, ROS are released from the chloroplast and mitochondria, H₂O₂ can diffuse across membranes so may enter the vacuole that contains the anthocyanins and peroxidase (Yamaski *et al.*, 1997, Gould *et al.*, 2002, Hatier, 2008). Evidence to suggest that anthocyanins have an AO role was found in anthocyanin mutants exposed to UVB light, where there was a 60% higher level of lipid peroxidation (Landry *et al.*, 1995).

1.5 **MYB90 and MYB75**

MYB90 and MYB75 are two MYB transcription factors involved in the regulation of anthocyanin biosynthesis in *Arabidopsis* along with other transcription factors. They were identified by Borevitz *et al.*, (2000) who identified an enhancer trap line overexpressing *MYB75* that showed massive activation of anthocyanin biosynthesis genes such as *CHS*, *DFR*, *GST* and *PAL*. *MYB75* over expression resulted in increased anthocyanin accumulation and was visible by the purple colouration of the whole plant, including the rosette leaves, cauline leaves, stem, sepals, anthers, carpels and roots (Fig 1.7). *MYB90* over expression was then tested transgenically and this showed anthocyanin accumulation in the rosette leaves and stems. This suggested that the two genes both regulated anthocyanin biosynthesis but might show differential effects.



Fig 1.7: *MYB75* over expression mutant and wild type COL 0. The wild type was green in appearance and transgenic plants enhancing *MYB75* expression had purple pigmentation in the whole plant (from Borevitz et al., 2000).

Recently metabolomics and transcriptomics were integrated to analyse *Arabidopsis* plants over-expressing *MYB75* (Tohge *et al*, 2005). The flavonoid biosynthesis was analysed and results found that there was an accumulation of cyanidin and quercetin derivatives and eight novel anthocyanins were identified. The flavonol F1 accumulation was repressed in the *MYB75* over-expressing plants. Known genes involved in anthocyanin production and also genes of unknown function, including glycosyltransferase, acyltransferase, glutathione S-transferase, sugar transporters and transcription factors were induced by *MYB75*.

Using publicly available microarray data from Genevestigator, comparison of the expression of the two MYB genes during development showed that *MYB75* was expressed throughout development, whereas *MYB90* was expressed at a low level in early development and highly expressed during senescence (Fig 1.8). This suggested that *MYB90* may be responsible for the massive induction of anthocyanin biosynthesis during senescence.

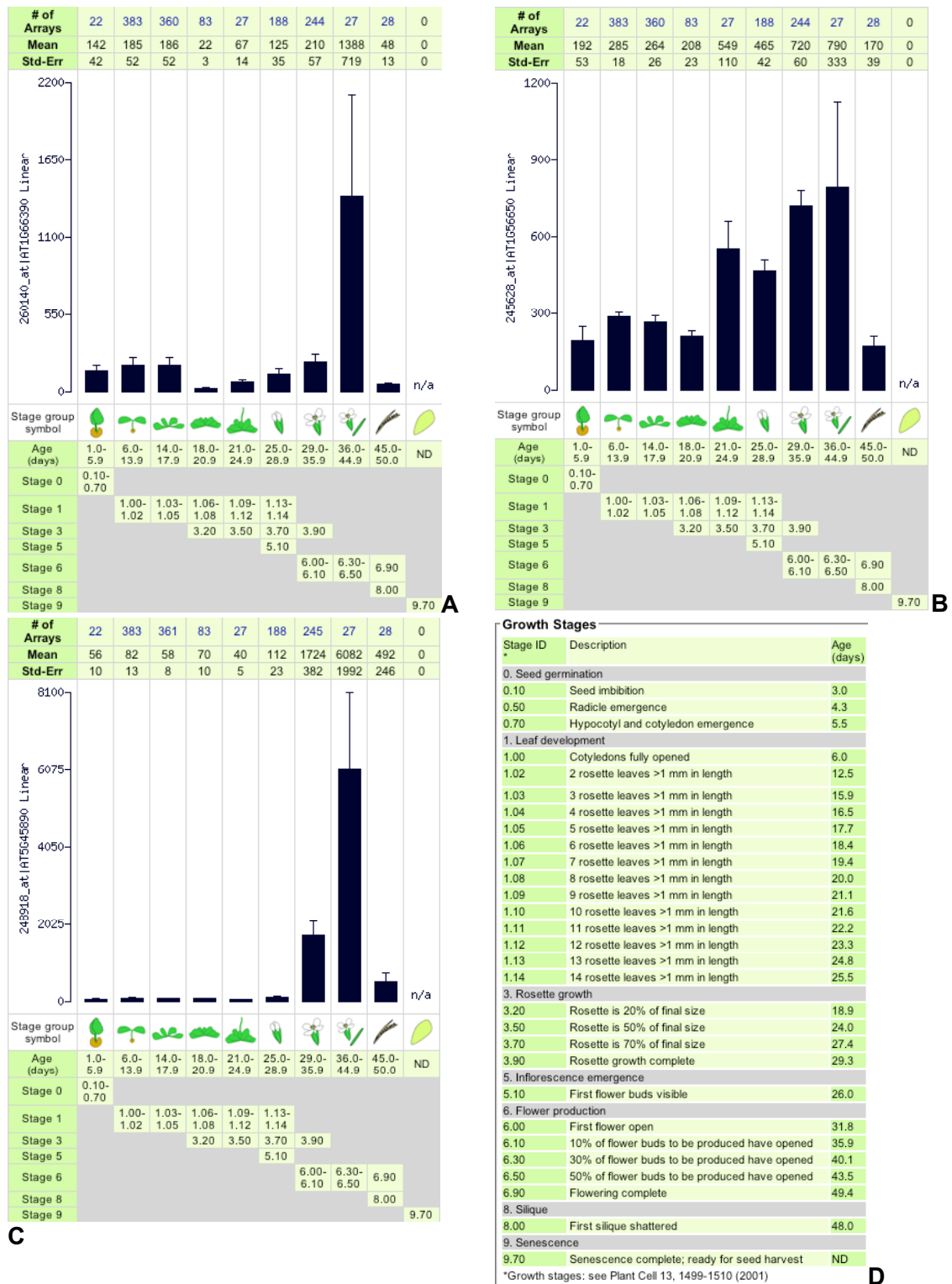


Fig 1.8: Microarray analysis of *MYB90* (A), *MYB75* (B), *SAG12* (C) expression levels at different stages of development and (D) showed the development description of each stage by Geninvestigator 'Gene Chronologer' (Zimmermann *et al.*, 2004b).

Previously, in the Warwick lab, a study of gene expression in WT (COL-0) and a *MYB90* knockout insertion mutant (obtained from SALK) in mature green and senescent *Arabidopsis* leaves showed the expression of a few genes was down-

regulated in this mutant (Table 1). This included *MYB90*, *MYB75* and several genes of the flavonoid biosynthesis pathway. This result implicated *MYB90* as being important for flavonoid biosynthesis during senescence.

	Ratio	p-value
Myb-related protein MYB75	0.29	0.035337
Anthocyanin 5-aromatic acyltransferase	0.21	0.024254
Dihydroflavonol 4-reductase	0.14	0.004616
Phenylalanine ammonia lyase (PAL1)	0.12	0.013438
Flavonol 3-O-glucosyltransferase	0.11	7.84E-04
UDP-glycosyltransferase family	0.10	0.008284
Glutathione transferase	0.10	0.020367
Myb-related transcription factor MYB90	0.09	0.045915
Naringenin-chalcone synthase tt4 protein	0.08	0.010762
Flavanone 3-hydroxylase (FH3)	0.03	0.010869

Table 1: Microarray analysis of MYB90 insertion mutant showing genes that were down regulated. Normalised data was obtained using Genespring analysis. Ratio indicated the extent of down regulation (mutant/wild type). P values (n=4) indicate significance from ratio of 1.

1.5.1 Regulation of MYB90 and MYB75

MYB75 and several anthocyanin biosynthesis genes were reported to show circadian regulation (Harmer *et al.*, 2000). However there was no suggestion in the literature that *MYB90* shows circadian regulation. Circadian regulation allows genes to anticipate changes to the environment such as dawn and dusk and is a biochemical oscillator controlling the rhythmic changes of gene expression. Circadian regulated genes continued to oscillate for 24 hours in a constant environment of light or dark (Davies and Miller, 2001). Phenylpropanoid genes such as chalcone synthase and dihydroflavonol reductase are coordinated to have low expression in the afternoons, peak before dawn and a high expression early morning (Deikman and Hammer, 1995).

Some MYB genes that regulated the phenylpropanoid biosynthesis pathway are seen to have a phase and wave form similar to the pathway, examples of such MYB gene are *AN2* of petunia and *MYB75* of Arabidopsis (Harmer *et al.*, 2000). The extent of *MYB75* co-regulation with the pathway indicated a role as a key regulator of circadian controlled expression (Harmer *et al.*, 2000).

The two MYB genes were found to have a role in regulating anthocyanin biosynthesis in response to stress, the purple colouration was more intense when the plants were under stress, such as high light (Borevitz *et al.*, 2000). This was also shown by Vanderauwera *et al.*, (2005) who found *MYB90* and *MYB75* to be clustered with anthocyanin biosynthesis genes following high light treatment. *MYB90* was also implicated with anthocyanin biosynthesis in response to phosphate starvation. Following over expression of a gene involved in response to phosphate starvation, *AtSPX1*, there was an increased transcript levels of *MYB90* (Duan *et al.*, 2008).

Nitrogen limitation reduces the plants photosynthetic capacity and therefore an increased susceptibility to excess light. Anthocyanin biosynthesis increased in response to nitrogen deficiency, which also involved increased transcriptional activation of anthocyanin biosynthesis genes, *MYB90* and *MYB75* (Scheible *et al.*, 2004, Peng *et al.*, 2007). *MYB90* was more highly induced than *MYB75* under nitrogen deficiency (Lillo *et al.*, 2008, Peng *et al.*, 2007). Diaz *et al.* (2006) found that the quantitative trait loci (QTL) associated with anthocyanin associated redness during low nitrogen conditions is linked to the whole plant age and nutrient limitation and is genetically independent of senescence associated leaf yellowing QTL.

Sugars have a role in the signalling during plant development and in the regulation of senescence and anthocyanin biosynthesis (Bleeker and Patterson, 1997). There was evidence that shows different sugars have different regulatory roles and sucrose was the most effective inducer of anthocyanin biosynthesis, accompanied by the induction of *MYB75* and *MYB90* (Teng *et al.*, 2005, Lillo *et al.*, 2008). In older leaves, *MYB90* expression was induced in low nitrogen and high glucose conditions (Pourtau *et al.*, 2006).

H₂O₂ has a role in the regulation of *MYB90*, *MYB75* and anthocyanin biosynthesis genes. Vanderauwera *et al.*, (2005) reported that the normal increased transcriptional activation of these genes during high light stress was deregulated by H₂O₂.

1.5.2 Transcription Factor Interactions

As discussed earlier the MYB transcription factors can interact synergistically with bHLH transcription factors and form a complex with a WD repeat transcription factor resulting in induced expression of anthocyanin biosynthesis genes (Fig 1.6) (Koes *et al.*, 2005). The WD repeat transcription factor TTG1 is essential for anthocyanin biosynthesis and proanthocyanidins biosynthesis (Zhang *et al.*, 2003). In the seed coat, TTG1 forms a complex with MYB transcription factor TT2 and the bHLH transcription factor TT8 (Baudry *et al.*, 2006). TTG1 regulates EGL3 and GL3 that interacted with MYB90 and MYB75 to achieve transcriptional activation of anthocyanin biosynthesis genes (Zimmermann *et al.*, 2004). However unlike *MYB90* and *MYB75*, *TTG1* expression was not effected by nutrient deficiency and therefore not responsible for stress induced anthocyanin biosynthesis (Lillo *et al.*, 2008). Tohge *et al.*, (2005) also found that over expression of *MYB75* increased the transcript levels of two transcription factors involved in proanthocyanidins biosynthesis, *TT8* and *TRANSPARENT TESTA GLABROUS2 TTG2* (WRKY protein) and a transcription factor involved in ethylene mediated signalling, *AP2* (At5g61600).

1.6 HYPOTHESIS AND AIMS

Previous experiments in this lab and in others indicated that the two MYB genes, *MYB75* and *MYB90* may both function in controlling the anthocyanin and/ or flavonoid biosynthesis pathway but were regulated differently. The hypothesis was that the expression of the flavonoid pathway during senescence depends on the transcription factor *MYB90*. The aims of this project were:

To identify the role of *MYB90* in senescence:

- Analysing the effects of insertions into *MYB90* on the phenotype, photosynthetic parameters and anthocyanin components of senescing leaves.
- Identifying the genes that are the downstream targets of *MYB90*.

To identify the role of *MYB90* and *MYB75* during stress:

- Analysing the effects of insertions into *MYB90* on the phenotype, photosynthetic parameters and anthocyanin components of stressed leaves.
- Analysing the effects of *MYB75* RNAi on the phenotype, photosynthetic parameters and anthocyanin components of stressed leaves.

To investigate the upstream signals regulating the expression of *MYB90* and *MYB75*:

- Identification of the *cis*-acting elements of the promoter regions of *MYB90* and *MYB75* required for senescence specific expression.
- Distinguishing where and when *MYB90* and *MYB75* are transcribed.

2 Materials and Methods

2.1 Materials

The wild type COL-0 and the MYB90 knockout, IM28 (SALK-093731) seed stock was available at Warwick HRI. MYB75 RNAi seed was purchased from Arabidopsis Genomic RNAi Knockout Line Analysis (AGRIKOLA).

2.2 Plant Growth Experiments

2.2.1 Growth Room Conditions

Plants were grown in a Weiss chamber at controlled conditions (16-hour day/ 8h night photoperiod at 22°C and light intensity 250 $\mu\text{mol}/\text{sec}/\text{m}^2$, humidity 70%, CO₂ 350ppm).

2.2.2 Plant Growth

The appropriate seed was suspended in 0.01% agarose and stratification was carried out at 4°C for 4 days. FPL7 (70x70x80mm) were filled with compost (6:1:1 ratio of Levingtons F2 compost: sand: fine grade vermiculite) and saturated with water and placed on felt covered trays. Approximately 5 individual seeds were pipetted in a small circle at the centre of the pots. The trays were covered with cling film and then placed in the growth chamber. After approximately 5-7 days the cling film and the excess seedlings were removed leaving one seedling per pot.

2.2.3 Leaf Tagging

The seventh rosette leaf to emerge was tagged with cotton between 20-25 days after sowing.

2.2.4 Glass House Conditions

Plants were grown in glass house with a 16h light period at 21°C during March when the average sunshine hours was 5.4 (Standard deviation 3.10) and the average total

solar radiation 9.63 (Standard deviation 4.89). In low light conditions there was supplemental lighting and the average light intensity was of 150 $\mu\text{mol}/\text{sec}/\text{m}^2$ at 11am.

2.2.5 Low Nitrogen High Glucose Agar Plates

Seed was sterilised in 5% bleach for 10min and washed in sterilised water. The seed was suspended in melted sterilised 0.7% low melting agarose and approximately ten seeds were pipetted on to the low nitrogen high glucose agar plates. The agar plates: 30ml per petri dish, 0.675g/L NH_4NO_3 free Murashige and Skoog basic salt (Sigma M2909), 2% (w/v) glucose and 1% agar. The plates were stored in the dark at 4 °C for three days and then placed vertically in the growth cabinet. The whole plants were harvested at 25 days after sowing and frozen in liquid nitrogen. The material was stored at -80 °C.

2.3 Gene Expression Studies

2.3.1 RNA Isolation

Total leaf RNA was isolated using the Invitrogen TRIzol reagent. 5mg of leaf tissue was ground under liquid nitrogen and then homogenised with 500 μl TRIzol. Another 500 μl of TRIzol was added and mixed by gently pipetting up and down. The samples were incubated at room temperature for 10min and then 250 μl of chloroform was added and mixed by turning the closed microfuge tube upside down for 15sec. The samples were then incubated at room temperature for 2min. The samples were centrifuged for 10min at 9501.8xg for at 4 °C. The aqueous phase was transferred to a new sterile microfuge tube and washed with 500 μl isopropanol at room temperature. The samples were incubated for 1-2hrs at -20 °C and then centrifuged at 9502xg for 10min at 4 °C. The pellet was washed with 1ml 75% ethanol and centrifuged for at 9502xg for 15min at 4 °C. The ethanol was decanted and the pellet was allowed to dry for 2min at room temperature. The pellet was resuspended in 40 μl sterile RNAase free H_2O and stored at -80 °C.

2.3.2 RNA Cleanup

The isolated RNA was cleaned using QIAgen Rneasy Total RNA cleanup kit, following the manufacturers method.

2.3.3 RNA Quantification

RNA was quantified using a Thermo Scientific Nanodrop™ 1000 full spectrum UV.VIS spectrophotometer. The spectrophotometer was cleaned using 70% ethanol. 1 µl sterile H₂O was pipetted onto the measurement pedestal and a blank measurement was initiated. Then 1 µl RNA was quantified as ng/µl and the purity determined from the 260nm /280nm absorbance ratio.

2.3.4 Determination of RNA Quality

The RNA quality was determined based on the RNA fragment size using Aligent 2100 Bioanalyser and the RNA 6000 Nano Lab Chip with the RNA 6000 standard size ladder, according to the manufacturers method.

2.3.5 Gene Expression Analysis by Real Time PCR

2.3.5.1 DNase Treatment

The RNA was DNase treated to remove any DNA contamination before cDNA synthesis. 5µg RNA was DNase treated using Ambion TURBO DNA-free™ following the manufacturer method, to remove residual DNA.

2.3.5.2 First Strand cDNA Synthesis

First strand cDNA was generated from 1µg DNase treated RNA using the Invitrogen Superscript™ First-Strand Synthesis System for RT-PCR with non specific hexamers and oligo d(T)₁₂₋₁₈ primers according to manufacturers instructions.

2.3.5.3 Real Time PCR

Five serial dilutions of 1 in 4 of standard cDNA were made for the PCR amplification. Each reaction consisted of 7.5µl Applied Biosystems SYBR® Green PCR Mastermix,

0.75µl 10µM forward primer, 0.75µl 10µM reverse primer, 5µl sterile water and 1µl template cDNA.

Name	Primer Sequence
icy MYB90F	5'-AAACCAAGAAGCTGATGCGATTG-3'
icy MYB90R	5'-TCAAACAGACTCCAAAGTTGCTC-3'
icy SAG12F	5'-AGCCAAAGCCAAACTAAAATGTCTG-3'
icy SAG12R	5'-TGATAGGGGTCACAGCTCCT-3'
icy MYB75F	5'-AGAGAGACATTACGCCCATTG-3'
icy MYB75R	5'-CATTGAGATGGTTGCAGTCG-3'
icy CHSF	5'-CGTGTTGAGCGAGTATGGAA-3'
icy CHSR	5'-GGTCCGAAACCAACAAGAC-3'
icy TUBF	5'-TGGCAAGATGAGCACAAAAG-3'
icy TUBR	5'-AGACCTCGGGGAGCTATG-3'

Table 2: A list of primers used in real time PCR for *MYB90*, *MYB75*, *SAG12*, *CHS* and *TUB*.

There were three replicate reactions for each template. The reactions were pipetted into wells of a MicroAmpTM optical 384 well reaction plate, which was then sealed with a MicroAmpTM optical adhesive film. The sample plate was spun down for 1min and then run on the Applied Biosystems ABI 7900HT Real Time PCR machine and the data obtained. The following protocol was used:

Stage 1; 50 °C for 2min, stage 2; DNA was denatured at 95°C for 2min, stage 3; 40 cycles of 95°C for 15sec and 60 °C for 30sec and stage 4; melt curve of 95°C for 15sec and 60 °C (+1°C, up to 95°C) for 30sec.

The Ct value for each gene was standardised to the internal control, Tubulin and the relative quantity was calculated from the standards.

2.3.6 Reverse Transcription PCR

Using Ready-To-GoTM RT-PCR beads (Amersham pharmacia biotech), each reaction consisted of 1µg DNase treated RNA, 0.5µg pd(T)₁₂₋₁₈ primer, 1µl 10µM gene specific forward primer and 1µl 10µM gene specific reverse primer, and DEPC-treated water to

a final volume of 50 μ l. The RT-PCR was carried out according to the manufacturers instructions.

2.3.7 Microarray Gene Expression Analysis

2.3.7.1 mRNA Amplification

1.5 μ g RNA was amplified using MessageAmpTM II aRNA amplification kit by the one step amplification following the manufacturers method.

2.3.7.2 Labelling aRNA

5 μ g of antisense RNA (aRNA) was labelled with Cy3- or Cy5-dCTP. The aRNA was pipetted into a sterile Rnase free 0.2ml microfuge tube with 0.5 μ l RNase Out and 0.75 μ l random nanomers (2 μ g/ μ l) and nuclease free water for a total volume of 10.5 μ l. The samples were incubated at 70°C for 10min in a thermocycler and then put on ice. 8 μ l of a prepared mastermix (4 μ l 5x superscript II first strand buffer (Invitrogen), 2 μ l 0.1M DTT (Invitrogen), 1 μ l dNTP mix (10mM dATP, 10mM dGTP, 10mM dTTP, 2mM dCTP), 1 μ l superscript II reverse transcriptase (Invitrogen)) was added. 1.5 μ l of 25nmol Cy3- or Cy5-dCTP (GE Healthcare PA53021 [Cy3-dCTP] PA55021 [Cy5-dCTP]) was added to the samples and mixed by pipetting up and down. The samples were spun down by briefly centrifuging the tubes. The PCR tubes were put in black boxes to protect them from light and minimise loss of fluorescence. The samples were then incubated at 42°C for 2.5hrs. 2 μ l 2.5M NaOH was added to each labelled cDNA sample, which were then incubated at 37°C for 15min. 10 μ l 2M MOPS was added and the samples were placed on ice.

2.3.7.3 Purification of Labelled cDNA

The labelled cDNA samples were purified using the QIAgen QiaQuick PCR Purification columns kit according to the manufacturers protocol. The purified sample was eluted from the column with two 30 μ l aliquots of buffer EB for a total volume of 60 μ l.

2.3.7.4 Preparation of Labelled cDNA for Hybridisations

The cDNA was then quantified using the nanodrop spectrophotometer at 532nm (Cy3) and 635nm (Cy5). 35 pmol Cy3 labelled cDNA was combined with a 35pmol aliquot of the appropriate Cy5 labelled cDNA in a 0.2ml microfuge tube. The samples were then freeze dried.

2.3.7.4 Microarray Prehybridisation

CATMA arrays were placed in Coplin jars containing prehybridisation buffer (5XSSC, 0.1%SDS, 1%BSA) prewarmed to 42°C. They were left to incubate at 42°C for 60min. The slides were then removed from the Coplin jars and washed by dipping them into sterile H₂O five times, followed by isopropanol. The slides were then left to air dry.

2.3.7.5 Microarray Hybridisation

The freeze dried labelled samples were resuspended in 50µl of Hybridisation buffer (25% formamide, 5xSSC, 0.1%SDS, 0.5mg ml⁻¹ Yeast tRNA). The samples were denatured by heating to 95°C for 5mins and then centrifuged at 12279xg for 1min. The CATMA array was placed in a hybridisation chamber. The denatured sample was applied by pipetting small drops down the centre of the CATMA array. A coverslip (Sigma Aldridge) was placed over the slide allowing the sample to spread across the surface of the array. The cover of the hybridisation chamber was placed over the top of the slide. The hybridisation chambers containing the arrays were placed in a hybridisation container, which is a plastic sealable container containing 1cm sterile H₂O, a PCR block to balance the hybridisation chamber on and a layer of tissue. The hybridisation container was wrapped in foil and then incubated at 42°C for 16-20hrs.

2.3.7.6 Microarray Post-Hybridisation Washes

The slides were washed three times to remove any non-hybridised probe. All the wash steps were carried out using a plastic black box with a fitted lid and a plate shaker. The

coverslips were carefully removed from the CATMA arrays by submerging them in Wash Solution 1 (2xSSC, 0.1%SDS), preheated to 42°C. The arrays were incubated in wash solution 1 for 5min. The arrays were then incubated in Wash Solution 2 (0.1xSSC, 0.1%SDS) for 10min. The arrays were then washed three times in Wash Solution 3 (0.1xSSC) for 1min each time. Lastly the arrays were briefly submerged in isopropanol. The arrays were transferred to 50ml falcon tubes (barcode end down) and dried by centrifugation at 2000g for 2min.

2.3.7.7 Microarray Data Analysis

The microarray slides were scanned for Cy3 (523nm) and Cy5 (635nm) using an Affymetix 428TM array scanner. The ImageneTM software (Biodiscovery) was used to place a grid onto the array image to identify and quantify the spots.

2.4 Anthocyanin and Flavonoid Analysis

2.4.1 Anthocyanin and Flavonoid Extractions

Anthocyanins were extracted using 1% HCl/methanol by grinding approximately 0.25g leaf sample under liquid nitrogen and mixing with 1.25ml 1%HCl/methanol. The samples were incubated overnight at 4°C on a rotary mixer. 0.5ml chloroform was added and mixed, followed mixing with 2.5ml water. The samples were then centrifuged at 1115.9xg for 15min and the aqueous phase was transferred to an microfuge tube and stored in the dark at 4°C as described by (Kubasek *et al*, 1992).

2.4.1.1 UV-VIS Spectroscopy

The absorbance of the anthocyanin extract was measured at 530nm and the background measurement at 657nm at 1cm path length. Subtracting the background measurement from the anthocyanin measurement and dividing by the weight of the plant material calculated the relative total anthocyanin content per mg of plant tissue.

2.4.1.2 HPLC Analysis of Anthocyanin/Flavonoid Extracts

Individual anthocyanins and flavonoids were separated using a HPLC with reverse phase column and UV-VIS detection as described by Tohge *et al.* (2005). HPLC was carried out using a the column LichroCART[®] 250-4, Lichrospher[®] 100 RP-18 (5 μ m) at a flow rate of 0.5ml/min with the elution gradient with solvent A [CH₃CN-H₂O-TFA (10:90:0.1)] and solvent B [CH₃CN-H₂O-TFA (90:10:0.1)] and the following elution profile (0min 100%A, 40min 60%A, 40.1min 100%B, 45min 100%B, 45.1min 100%A, 52min 100%A) using linear gradients between time points. DAD was used for detection of the UV-Vis absorption of flavonoids at 320nm and anthocyanins at 520nm.

2.5 Chlorophyll Fluorescence Measurement

Chlorophyll fluorescence was measured for single leaves of whole rosettes using a cf Imager (Technologica Ltd). Plants were placed inside the cf imager and the FluorImager 2 Program v1.101 was used to turn on the camera and focus the image of the plant. The aperture of the image was adjusted using the gamma bar and deleting high and low cuts in the background. The area of the image of interest was isolated and the image was saved. The appropriate protocol was then selected and run.

Step	Delay	Action	Cycles	PPFD ($\mu\text{mol m}^{-2} \text{s}^{-1}$)	Fluorescence Measurements
1	1s	change actinic		0	
2	5min	actinic pulse	1	6259	✓
3	1s	change actinic		50	
4	4min	actinic pulse	1	6259	✓
5	1s	change actinic		100	
6	4min	actinic pulse	1	6259	✓
7	1s	change actinic		200	
8	4min	actinic pulse	1	6259	✓
9	1s	change actinic		450	
10	4min	actinic pulse	1	6259	✓
11	1s	change actinic		600	
12	4min	actinic pulse	1	6259	✓
13	1s	change actinic		1000	
14	4min	actinic pulse	1	6259	✓
15	1s	change actinic		1500	
16	4min	actinic pulse	1	6259	✓
17	1s	change actinic		2000	
18	4min	actinic pulse	1	6259	✓

Table 3: Chlorophyll Fluorescence Light Curve Protocol 1. The chlorophyll fluorescence was first measured in dark- adapted material and then during a pulse of saturating light. Then in light adapted material and then during a pulse of saturating light. The plant material was light-adapted to increasing light intensities.

Step	Delay	Action	Cycles	PPFD ($\mu\text{mol m}^{-2} \text{s}^{-1}$)	Fluorescence Measurement
1	1s	change actinic		0	
2	5min	actinic pulse	1	6259	✓
3	1s	change actinic		50	
4	3min	actinic pulse	1	6259	✓
5	1s	change actinic		100	
6	3min	actinic pulse	1	6259	✓
7	1s	change actinic		150	
8	3min	actinic pulse	1	6259	✓
9	1s	change actinic		250	
10	3min	actinic pulse	1	6259	✓
11	1s	change actinic		500	
12	3min	actinic pulse	1	6259	✓
13	1s	change actinic		750	
14	3min	actinic pulse	1	6259	✓
15	1s	change actinic		1500	
16	3min	actinic pulse	1	6259	✓

Table 4: Chlorophyll Fluorescence Light Curve Protocol 2. The chlorophyll fluorescence was first measured in dark- adapted material and then during a pulse of saturating light. Then in light adapted material and then during a pulse of saturating light. The plant material was light-adapted to increasing light intensities.

Step	Delay	Action	Cycles	PPFD ($\mu\text{mol m}^{-2} \text{s}^{-1}$)	Fluorescence Measurement
1	1s	change actinic		0	
2	5min	actinic pulse	1	6259	✓

Table 5: Chlorophyll Fluorescence Dark Adaption Protocol. The chlorophyll fluorescence was measured upon the application of a saturating pulse in dark-adapted.

2.6 Total Chlorophyll and Protein Analysis

2.6.1 Total Chlorophyll and Protein Extraction

One frozen leaf was ground under liquid nitrogen in a sterile microfuge tube. 0.5ml of LE buffer (50mM lithium phosphate pH7.2, 1mM monoiodoacetic acid, 120mM β -mercaptoethanol, 5% glycerol, 1mM PMSF, 10 μ M E64) and 50 μ l LiDS (lithium dodecyl sulfate) was added. The samples were then boiled in a water bath for 45sec. The samples were centrifuged for 20min and the supernatant was transferred to a new tube. The samples were protected from the light by placing them in a black box with a fitted lid.

2.6.1.1 Total Chlorophyll Content Measurement

100 μ l of the extract was added to 900 μ l 80% acetone and mixed by vortexing. The samples were protected from the light in black boxes and incubated for 1hr at -20°C . The samples were centrifuged for 3min. The absorbance of the total chlorophyll extract was measured at 646nm and 663nm at 1cm path length.

Subtracting the background measurement from the chlorophyll measurement and using these values in the equations below calculated the total chlorophyll content.

$$\text{Chlorophyll a} = (13.19 \cdot \text{Abs}_{663\text{nm}}) - (2.57 \cdot \text{Abs}_{646\text{nm}})$$

$$\text{Chlorophyll b} = (22.1 \cdot \text{Abs}_{646\text{nm}}) - (5.26 \cdot \text{Abs}_{663\text{nm}})$$

Dividing by the weight of the plant material calculated the total chlorophyll content per mg of plant tissue.

2.6.1.2 Total Protein Content Measurement

The total protein content was measured in 25µl of the extract using the BIO-RAD RC DC Protein Assay Kit II, according to the manufacturers protocol. The assay is a modification of Lowry protocol (Lowry *et al.*, 1951).

2.7 GATEWAY CLONING

Gateway Cloning: The gateway cloning of *MYB90*, *MYB75* promoters fused to GUS: GFP reporter gene was carried out using available pDONR entry vector and the standard Invitrogen Gateway™ Technology based on the bacteriophage lambda site specific recombination system.

2.7.1 Entry Clones

2.7.1.1 PCR Amplification of MYB90 and MYB75 Promoters and MYB90 Promoter Deletions

The *MYB90* and *MYB75* promoters and the *MYB90* promoter deletions were amplified from genomic DNA using Novagen KOD (high fidelity taq) and gene specific primers containing attB site sequence. The forward primer included four guanine residues at the 5' end, the attB1 site (ACAAGTTTGTACAAAAA-AGCAGGCT) and 18-25bp of gene specific sequence. The reverse primer contained four guanine residue at the 5' end, the attB2 site sequence (ACCACTTTGTACAAGAAAGCTGGGT) and 18-25bp of gene specific sequence. The sequence of the primers are shown in table 6.

A 25µl reaction was carried out using the KOD Hotstart DNA polymerase KIT (Novagen): 1X KOD buffer, 1X KOD dNTPs, 1.5mM MgSO₄, 0.2µM of each primer, 1 unit KOD DNA polymerase, 50ng template DNA and made up to a total volume of 25µl with sterile H₂O. On a thermocycler the following protocol was used: DNA was denatured at 94°C for 2min, followed by 25 cycles of 15sec at 94°C, 30sec at 58 °C and 2min at 72 °C. This was followed by a hold of 5min at 72 °C and cooled for 2min at 4 °C.

Primer	Promoter Specific Sequence
MYB90 Promoter	
MYB90 attB1	5'-attB1-CCCACGAAATCTAATTTAACCTGCAAT-3'
MYB90 attB2	5'-attB2-CAATAGGGGGTTATTGTGGCTTC-3'
MYB75 Promoter	
MYB75 attB1	5'-attB1-TCCCAAACATGATGTACAAGTATTAATGAAC-3'
MYB75 attB2	5'-attB2-CGGAACAAAGATAGATACGTAAAA-3'
MYB90 Promoter Deletions	
MYB90 PD1 attB1	5'-attB1-CTCCCTTTCATCTGCCAATCT-3'
MYB90 PD2 attB1	5'- attB1-CCACTTCAAGCAGGCTAAGCGA-3'
MYB90 PD3 attB1	5'- attB1-CCGAGGCTTCTTCGTCCACTGA-3'
MYB90 PD4 attB1	5'- attB1-CCGGAACACCCATCTCAACAAGA-3'
MYB90 PD5 attB1	5'- attB1-CCTGATTGGTCTCAGAGGGTTCA-3'
MYB90 PD6 attB1	5'- attB1-CCCTGGAAAAGGTGCTATGAACT-3'
MYB90 attB2	5'- attB2-CAATAGGGGGTTATTGTGGCTTC-3'

Table 6: List of Primers for Gateway Cloning of *MYB90* and *MYB75* promoters, and MYB90 promoter deletions. The primers include attB sites (attB1 site: ACAAGTTTGT-ACAAAAAAGCAGGCT and attB2 site: ACCACTTTGTACAAGAAAGCTGGGT) and gene specific sequences.

2.7.1.2 PCR Purification

The PCR products were purified using the Qiagen PCR purification kit according to the manufacturers protocol.

2.7.1.3 BP Recombination Reaction

The following components were mixed for the BP recombination reaction; 100fmol attB PCR product, 300ng of the entry clone pDONRTM 221 (Invitrogen), 4µl 5X BP Clonase Reaction Buffer (Invitrogen) and TE Buffer pH 8 made up to a total volume of 16µl. A negative control without an entry clone and a positive control containing 100ng pEXP7tet were compiled. The BP ClonaseTM enzyme mix (Invitrogen) was thawed on ice and added to the samples to a final concentration of 1X. The samples were incubated overnight at 25°C. 2µl Proteinase K was added to each tube and then the samples were incubated at 37°C for 10min.

2.7.1.4 Identification of Entry Clones

1µl recombination products were transformed into 15µl EC100TM (Cambio) Electrocompetent *E.coli* cells by electroporation. 450µl room temperature S.O.C medium (Invitrogen) was added to the transformed cells and incubated at 37°C for 2hrs whilst shaking at 200rpm. Volumes of 20µl and 100µl were spread on LB plates (10g tryptone, 5g yeast extract, 10g NaCl, 10g agar, H₂O upto 1litre) containing kanamycin (50µg/ml) and incubated at 37°C overnight. Minipreparations were performed on a selection of colonies to collect entry clone DNA and sequence checked using attB primers and plasmid DNA as a template.

2.7.2 Expression Clones

2.7.2.1 LR Recombination Reaction

The following components were mixed for the LR recombination reaction; 300ng entry clone, 300ng pBGWSF7 vector (expression clone) (Karimi *et al.*, 2002) 4µl 5X LR Clonase Reaction Buffer (Invitrogen) and TE buffer pH8 to reach a total volume of 16µl. A negative control without an entry clone and a positive control containing 100ng pEXP7tet (Invitrogen) were compiled. The LR ClonaseTM (Invitrogen) was thawed on ice and then 4µl was added to the samples. The samples were incubated overnight at 25°C. 2µl Proteinase K was added to each tube and then the samples were incubated at 37°C for 10min. The LR recombination products were transformed into EC100TM electro-competent cells and the expression clones were identified the same way as the entry clones except using 100µg/mg spectinomycin. Mini preparation were performed to isolate expression clone DNA (section 2.8.1) and then sequenced (section 2.8.1.2).

2.7.3 Transformation of Expression Clones into *Arabidopsis* COL-0

2.7.3.1 Transformation of Expression Clones into *Agrobacterium*

The expression clones were transformed into electrocompetent GV3101 by electroporation and then spread on LB plates containing spectinomycin, gentamycin and rifampicin and incubated at 25 °C for 48hours.

2.7.3.2 Floral Dipping

The colonies selected for resistance to gentamycin, spectinomycin and rifampicin were picked and used to inoculate 10ml LB spectinomycin-gentamycin medium that was incubated and shaken at 25 °C and 200rpm for 48hours. 3ml of the culture was used to inoculate 500ml of LB spectinomycin-gentamycin medium that was then incubated and shaken at 25 °C for 24 hours. The culture was centrifuged at 4640xg for 15min, the pellet was re-suspended in 1 litre of 5% sucrose solution. 500µl/L silwet L-77 was added before use in floral dipping experiments.

The expression clones were transformed into COL0 by floral dipping. The flowers of 24 plants were dipped into the appropriate *Agrobacterium* culture for 2-3sec each. They were then covered with cling film to maintain the humidity for 24hours. The plants were allowed to develop in the glasshouse and seed was collected.

2.7.3.3 Selection of Homozygous Lines

The t0 seed from the plants transformed with the promoter constructs were sown onto moist compost in the green house and covered with cling film to maintain the humidity for four to five days. The seedlings were selected for BASTA resistance by spraying with BASTA (100µg/µl) a total of three times at one-day intervals. Resistant seedlings were transferred into separate pots for seed collection. Homozygous lines were selected by the T3 generation.

2.8 Plasmid DNA Isolation from *Escherichia coli* (*E.coli*) clones

2.8.1 Mini Preparations

Plasmid DNA was isolated from 5ml cultures grown in LB kanamycin using the Qiagen Qiaprep Spin Miniprep kit according to the manufacturers instructions.

2.8.1.1 Glycerol Stocks

Glycerol stocks were made by mixing 500µl culture with 500µl sterile 50 glycerol. They were snap frozen in liquid nitrogen and stored at –80°C.

2.8.1.2 Sequencing

The plasmid DNA was sequenced using AB Applied Biosystems Big Dye Terminator v3.1 Cycle Sequencing kit. A 10 μ l reaction consisted of 300ng of plasmid DNA mixed with 0.3 μ l 10 μ M primer, 2 μ l Big dye and 1 μ l sequencing buffer. Using a thermal cycler the protocol consisted of 25 cycles of 96°C for 1min followed by 50°C for 5sec and then 60°C for 4min. The appropriate attB primers were used for sequencing plasmid DNA and primers were designed for internal sequences. The primers used for internal sequencing of the constructs are shown in Table 7

Construct	Primer	Primer Sequence
MYB90 Promoter	MYB90 INT1 F	5'-TCGGTCTGGATGATTATCTATA-3'
	MYB90 INT1 R	5'-TGACACATTCCCAACAACAA-3'
	MYB90 INT2 F	5'-GGCTATGTGTTTCATGCTTGG-3'
	MYB90 INT2 R	5'-GCCATTTGCCTTCTCCATAC-3'
	MYB90 INT3 F	5'-GCACGTTATGGTTATGTTGC-3'
	MYB90 INT3 R	5'-CTTTTGCCTTTGGTGGTG-3'
	MYB90 INT4 F	5'-CACCACCAAAGGCAAAAGT-3'
	MYB90 INT4 R	5'-AAATCGCTTAGCCTGCTTGA-3'
	MYB90 INT5 F	5'-TAGATTGCCTGGTCGGAT-3'
	MYB90 INT5 R	5'-TAACTTCTGGCTGCCCGT-3'
MYB75 Promoter	MYB75 INT2 F	5'-CCCAACACATAACCCACGAA-3'
	MYB75 INT2 R	5'-AGACAATGAGCCCTCTACGC-3'
	MYB75 INT3 F	5'-TCTAATCGGCACTACTAACT-3'
	MYB75 INT3 R	5'-TTTTCTTACCATTTTACCAGTTT-3'
Both	gfp	5'-GAACCTTCAGGGTCAGCTTGC-3'

Table 7: List of the primers used in the sequencing of MYB90 and MYB75 promoter GUS fusions, and MYB90 promoter deletions GUS fusions. Several primers were designed to span the promoter for internal (INT) sequencing. The gfp primer was designed to sequence the vector and promoter.

2.9 Analysis of Transgenic Plants Containing Promoter:GUS Fusions

2.9.1 Histochemical Staining

Senescent leaves and floral tissue was harvested from the plants carrying the promoter constructs and put in a compartmentalised plate. 2ml of GUS staining solution (50mM Na phosphate buffer, 1mM Xgluc, 0.1% Triton X-100, 4mM potassium ferricyanide, 100 μ g/ml chloroamphenicol) was added to each compartment to cover the plant material. The solution was then vacuum infiltrated for 2x 3min. The plates were sealed with parafilm and then incubated at 37°C overnight. The stained plant material was de-stained in two changes of 70% ethanol for 24hours and then stored in 50% glycerol.

2.9.2 Quantification of GUS Activity

Approximately 100mg frozen leaf tissue was homogenised with 500µl lysis buffer (50mM Na Phosphate buffer pH7, 10mM EDTA, 0.1% sodium lauryl sarcosinate, 0.1% triton X-100, 10mM β-mercaptoethanol). The samples were centrifuged at full speed for 15min and the supernatant transferred to a sterile eppendorf. 10µl of the supernatant and a water control were added to 440µl aliquots of the lysis buffer and mixed by pipetting. The samples were incubated at 37°C in a water bath. The reaction was started by the addition of 50µl 10mM MUG (4-methylumbelliferyl β-D-glucuronide hydrate (SIGMA), in sodium phosphate buffer) at 30 sec intervals and incubated in the water bath. The reaction was stopped after 15, 30 and 60min intervals by removing 100µl of the reaction mix and adding it to 2.9ml 0.2M Na₂CO₃. The Hitachi F-2000 Fluorescence spectrophotometer measured fluorescence of 1ml samples at excitation wavelength 365nm and emission wave length 455nm and was zeroed and standardised using MU standards at 10 and 100nM. Measurements of eight different MU (4-methylumbelliferone) standards ranging from 0-400µM were used to quantify the MU of the samples. The total protein content of the extracts was measured (section 2.6.1.2).

2.10 DNA Isolation

2.10.1 REExtract-N-Amp

DNA was extracted from leaf tissue using REExtract-N-AmpTM Plant PCR kit (Sigma), according to the manufacturers instructions. The PCR reaction consisted of 4µl extract, 1x REExtract-N-Amp PCR reaction mix, 0.4µM forward primer, 0.4µM reverse primer, made up to a total of 20µl with sterile Milli-Q grade water. The PCR 94°C for 2min, to denature DNA, followed by 35 cycles of 94°C for 15sec, 60 °C for 30sec, 70 °C for 1min per kbp and then the final extension at 70 °C for 10min.

2.10.2 Primers

Primer Name	Primer Sequence
Agri 51	5' CAA CCA CGT CTT CAA AGC AA 3'
Agri 56	5' CTG GGG TAC CGA ATT CCT C 3'
Agri 64	5' CTT GCG CTG CAG TTA TCA TC 3'
Agri 69	5' AGG CGT CTC GCA TAT CTC AT 3'

Table 8: Primers used for PCR amplification and sequencing of the GST sequence in plants containing RNAi construct.

2.11 Statistical Analysis

2.11.1 Student t-test

The student t-test was used to determine if the means of two normally distributed samples of equal variance are equal.

$$t = \frac{X_1 - X_2}{S_{X1X2} \cdot \sqrt{\frac{2}{n}}}$$

S_{X1X2} is the pooled standard deviation.

$$S_{X1X2} = \sqrt{\frac{S^2_{X1} + S^2_{X2}}{2}}$$

The degrees of freedom is $2n-2$ where n = number of participants of each group

2.11.2 Standard error

$$\text{Standard error} = \text{SE} = \frac{\text{STDEV}}{\sqrt{n}}$$

$$\text{STDEV} = \sqrt{\frac{n \sum x^2 - (\sum x)^2}{n(n-1)}} = \text{Standard deviation}$$

3 The Role of MYB90 During Leaf Development

3.1 Introduction

The transcription factor *MYB90* was previously shown to be involved in the regulation of the flavonoid pathway by Borevitz *et al* (2000), who inserted viral enhancer sequences adjacent to *MYB75* transcription factor gene in transgenic plants. The over expression of *MYB75* massively increased activation of phenylpropanoid biosynthetic genes during plant development, such as *chalcone synthase (CHS)*, *dihydroflavonol reductase (DFR)*, *glutathione S-transferase (GST)* and *phenylalanine ammonia-lyase (PAL)* and there was increased anthocyanin accumulation in the whole plant. Borevitz *et al.*, (2000) tested the over-expression of the homologous *MYB90* protein using a 35 S promoter:cDNA fusion in transgenic plants, which resulted in increases accumulation of anthocyanins visible by the purple pigmentation of the stem and leaves.

In previous work the knockout mutant of *MYB90*, IM28, was shown by a gene expression study, to have reduced expression of certain flavonoid pathway genes during senescence. To further investigate this the effect of the loss of *MYB90* on known senescence parameters was examined in more detail during development. These parameters include gene expression changes and chlorophyll and protein content of the leaf and photosynthetic activity.

3.2 Plant Growth Experiments

The WT and *MYB90* knockout mutant, IM28 were grown under controlled conditions (as detailed in methods). Two technical replicates of five pooled leaves were harvested at days 22, 30, 32, 34, 35, 36, 37, 38, 39, 40, 41 and 42 after sowing for RNA isolation.

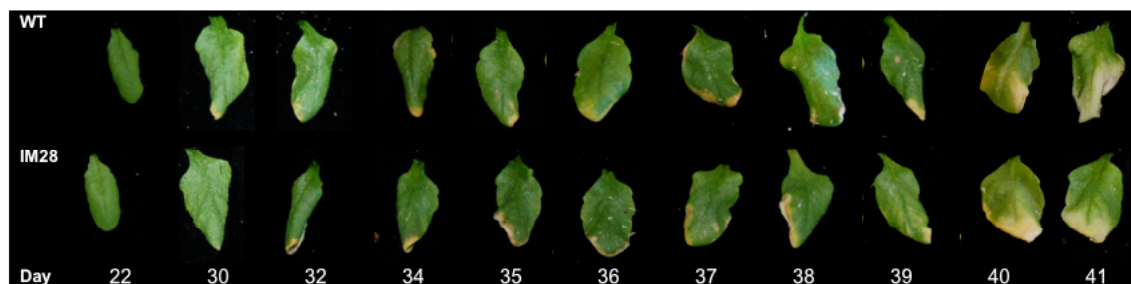


Fig 3.1: WT and IM28 Leaf 7 Development

The WT and IM28 were grown under controlled conditions in 16h light. The seventh rosette leaf was harvested at days 22, 30, 32, 34, 35, 36, 37, 38, 39, 40 and 41 after sowing.

Leaf seven was green in appearance in both the WT and IM28 following twenty two days after sowing (Fig 3.1). By day 30 the seventh leaf had fully expanded, was green in appearance and had yellowing at the tip, indicating the start of chlorophyll breakdown. The leaf remained mainly green in appearance with increased yellowing of the tips until days 40 and 41 when the majority of chlorophyll breakdown had occurred in both WT and IM28. At these late time points leaf 7 was mostly yellow in appearance.

The visual comparison of WT and IM28 leaf 7 during development showed that there appeared to be no obvious visible phenotype in the absence of *MYB90* (Fig 3.1).

During this experiment several parameters including total chlorophyll and protein content and the performance of the photosynthetic apparatus were measured. Six replicates were used for chlorophyll fluorescence and total chlorophyll and total protein content measurements.

3.2.1 Chlorophyll Measurements

The total chlorophyll content of leaf seven from WT and IM28 during development was measured and the results are shown in Figure 3.2A. The total chlorophyll content in the WT was highest in mature green leaves at day 30 and did not decrease significantly until days 40 and 41. IM28 had a variable chlorophyll content similar to the WT except at day 22 after sowing when it was higher and at day 37 when it was significantly lower. However, the data for chlorophyll levels was not significantly lower even when

senescence was obviously occurring in the leaves. These data were probably too variable to be very reliable.

3.2.2 Chlorophyll a/b ratio

The change in chlorophyll a/b ratio during the development of leaf seven in both WT and IM28 was calculated (Fig 3.2B). In both WT and IM28 the chlorophyll a content was approximately 2 fold higher than chlorophyll b in the mature green leaf. During the later time points when the chlorophyll content decreased (Fig 3.2A), the ratio of chlorophyll a/b decreased. Indicating that during senescence chlorophyll a was metabolised earlier in the senescence process than chlorophyll b in both plants.

3.2.3 Protein Measurements

The total protein content is a useful parameter of leaf development because during senescence protein is metabolised and transferred to growing regions of the plant. The reduction of total protein content is an indication of the senescence process in action. The total protein content of six replicates of leaf seven was quantified through out development for WT and IM28 (Fig 3.2C).

The total protein content did not change much from day 30 to 39 after sowing in both WT and IM28. The content decreases between day 39 and 40 in both WT and mutant.

Interestingly there was again a difference between the IM28 mutant and the WT at day 22 where IM28 had more protein and at day 37 where IM28 had less protein than the WT, which reflects the chlorophyll amounts shown in Fig 3.2 A. It is not clear why there is also a difference at day 30 in the protein levels.

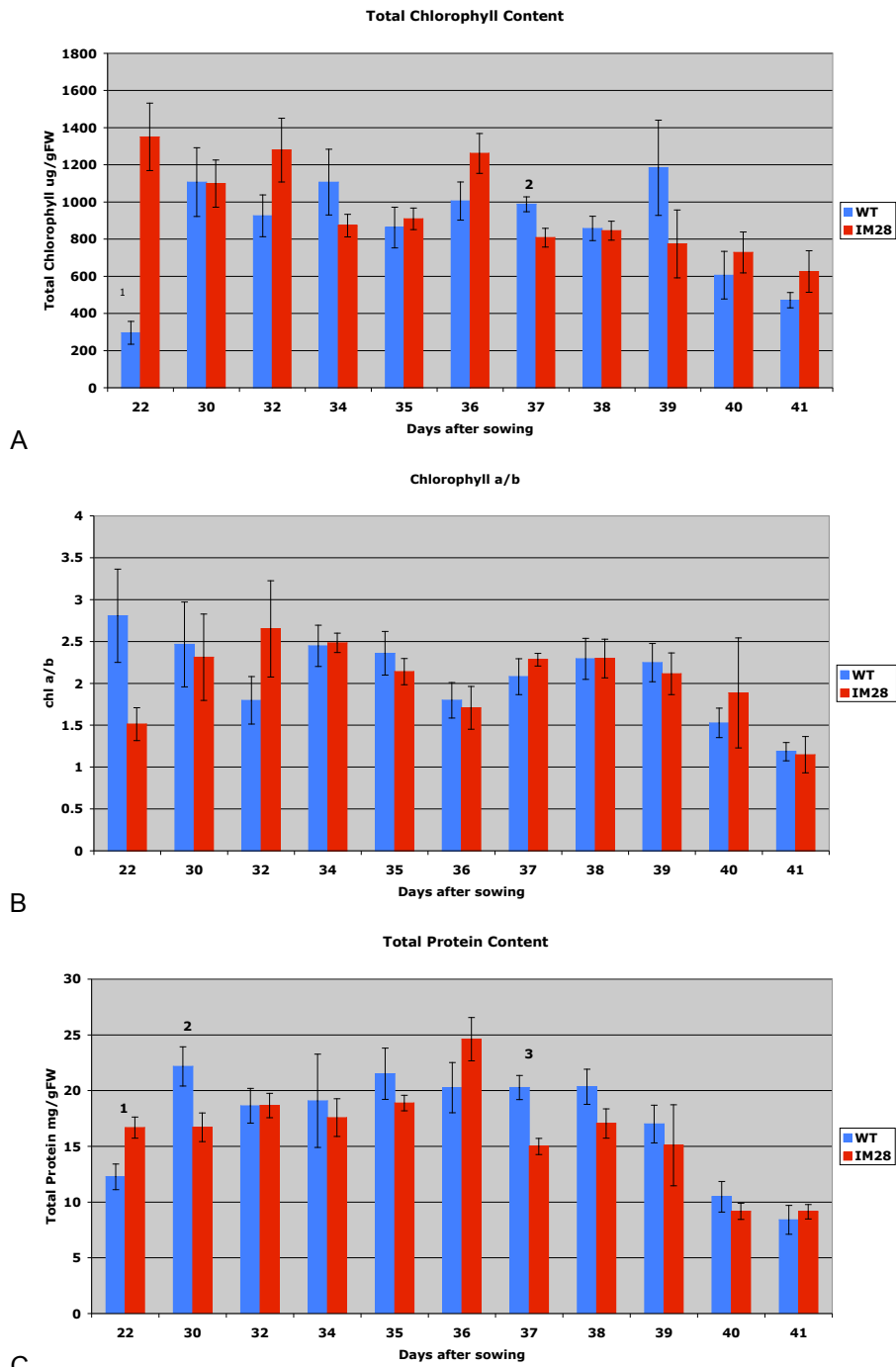


Fig 3.2: The role of *MYB90* during development and senescence was investigated in the seventh rosette leaf of WT and IM28 grown in 16h light. (A) The total chlorophyll content, (B) the chlorophyll a/b ratio and (C) the total protein content of six replicates of leaf 7 was measured at 11 time points during development, daily from 34 days after sowing. Results are presented as mean (n=6) \pm SE. (A) There were significant differences in total chlorophyll content between WT and IM28 at (1) day 22, $P=0.001$ and (2) day 37, $P=0.02$. (C) There were significant differences in protein content between WT and IM28 at (1) day 22 $P=0.013$, (2) day 30 $P=0.03$ and (3) day 37, $P=0.002$.

3.2.4 Chlorophyll Fluorescence Analysis

Another useful parameter to measure physiological change is the performance of the photosynthetic apparatus during development. A reduction in performance can indicate the level of stress of the leaf. Chlorophyll fluorescence was measured to investigate the photosynthetic performance of leaf seven throughout development of WT and IM28 plants. The plants were subjected to a light curve (section 2.5, table 3) of increasing light intensity and the different parameters of photosynthesis were assessed.

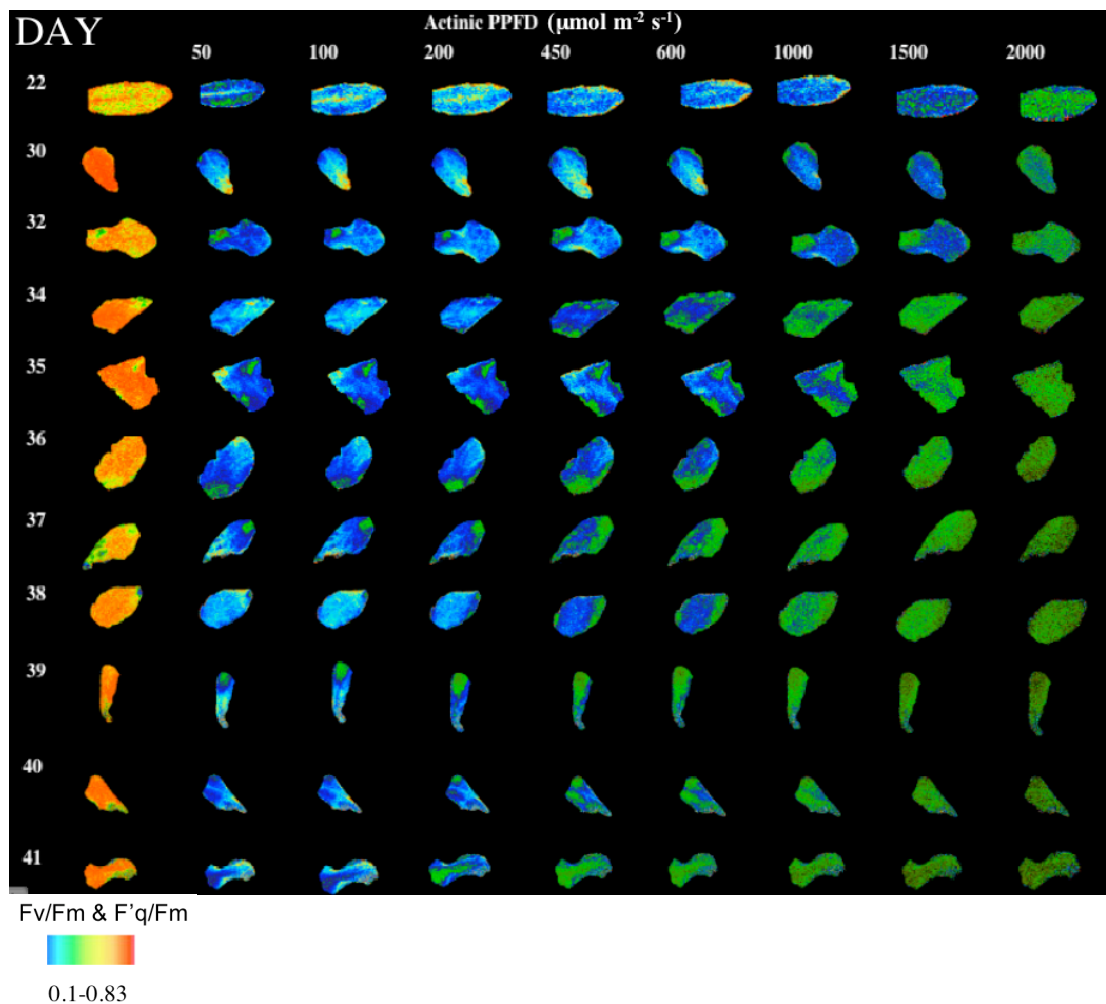


Fig 3.3: Chlorophyll Fluorescence Images of WT Leaf 7 During Development.

The chlorophyll fluorescence images of WT leaf seven during development. The role of *MYB90* during development and senescence was investigated in the seventh rosette leaf of WT grown in 16h light. The chlorophyll fluorescence of six replicates of leaf 7 on days 22, 30, 32 and daily from 34 to 41 was measured over a light curve of increasing light intensity. The images at 0 μmol m⁻² s⁻¹ represent the maximum PS2 efficiency (Fv/Fm) and images at 50 to 2000 μmol m⁻² s⁻¹ represent the operating PS2 efficiency (F'q/Fm).

Figures 3.3 and 3.4 show examples of the WT and IM28 chlorophyll fluorescence images during a light curve at different time points during development. The images after 0 actinic photosynthetic photon flux density (PPFD $\mu\text{mol m}^{-2} \text{s}^{-1}$) represents the maximum PS2 efficiency (F_v/F_m). The F_v/F_m of a healthy leaf is approximately 0.8 and this is seen as an orange colour. During the time course the colour of leaf seven ranged between orange and yellow in both WT and IM28 at 0 $\mu\text{mol m}^{-2} \text{s}^{-1}$. In the later time points there were patches on the leaves, generally at the edge, where the colour was blue and green. This indicates that the F_v/F_m had decreased in these patches.

The images from 50 to 2000 $\mu\text{mol m}^{-2} \text{s}^{-1}$ indicate the operating PSII efficiency (F'_q/F_m). As the F'_q/F_m decreased the colour changed to yellow, blue and then to green. The images of both WT and IM28 indicated that leaf seven maintained a higher F_v/F_m and F'_q/F_m at 22 days after sowing. During the time course the chlorophyll fluorescence images showed a decreasing F'_q/F_m in both WT and IM28 as the leaf aged. The green colouration occurred earlier and earlier in the light curve (Fig 3.3 and 3.4). There was no obvious difference visible between WT and IM28. The different parameters that may be calculated from the chlorophyll fluorescence measurements include the maximum PS2 efficiency, the operating PS2 efficiency, the photochemical quenching, non-photochemical quenching and the linear electron transport rate.

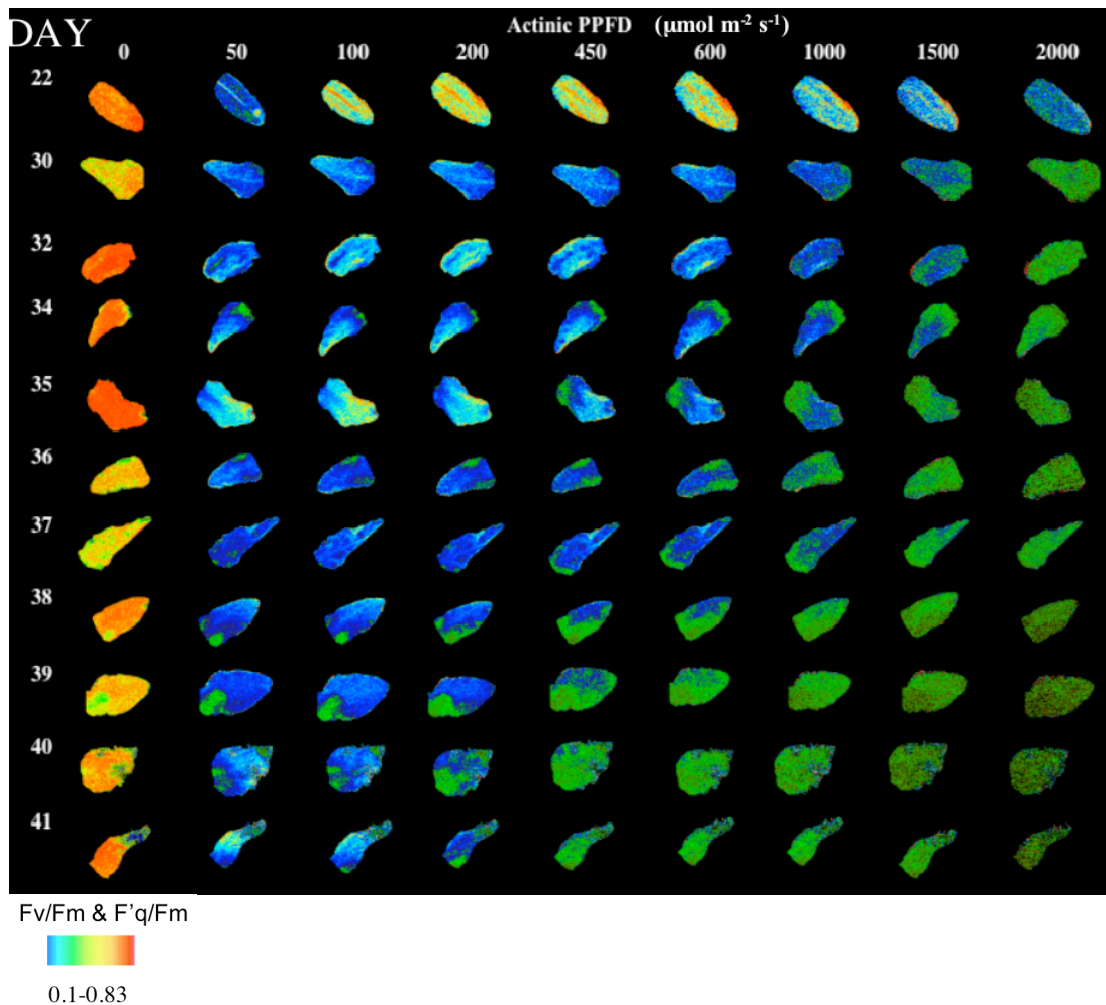


Fig 3.4: Chlorophyll Fluorescence Images of IM28 Leaf 7 During Development

The chlorophyll fluorescence images of IM28 leaf seven during development. The role of *MYB90* during development and senescence was investigated in the seventh rosette leaf of IM28 grown in 16h light. The chlorophyll fluorescence of six replicates of leaf 7 on days 22, 30, 32 and daily from 34 to 41 was measured over a light curve of increasing light intensity. The images at 0 $\mu\text{mol m}^{-2} \text{s}^{-1}$ represent the maximum PS2 efficiency (F_v/F_m) and images at 50 to 2000 $\mu\text{mol m}^{-2} \text{s}^{-1}$ represent the operating PS2 efficiency (F'_q/F_m). The

5.2.3.1 The Maximum PS2 Efficiency

The mean maximum PS2 efficiency (F_v/F_m) that was calculated by measuring the chlorophyll fluorescence after dark-adaption followed by a saturating light pulse is shown in Figure 3.5. The maximum F_v/F_m value is approximately 0.8 for healthy plants and lower values indicate that damage has occurred to the reaction centres.

After 22 days the maximum PS2 efficiency (F_v/F_m) had not reached the maximum of fully developed leaves for both WT and IM28, and the WT level was lower than IM28. The F_v/F_m increased in the mature plants and remained steady for the WT plants even

into full senescence. The WT and IM28 had similar Fv/Fm during development except at day 36 when IM28 had a significantly lower Fv/Fm. IM28 also showed a dip at day 41 but the data was very variable at this time point and this was not significant.

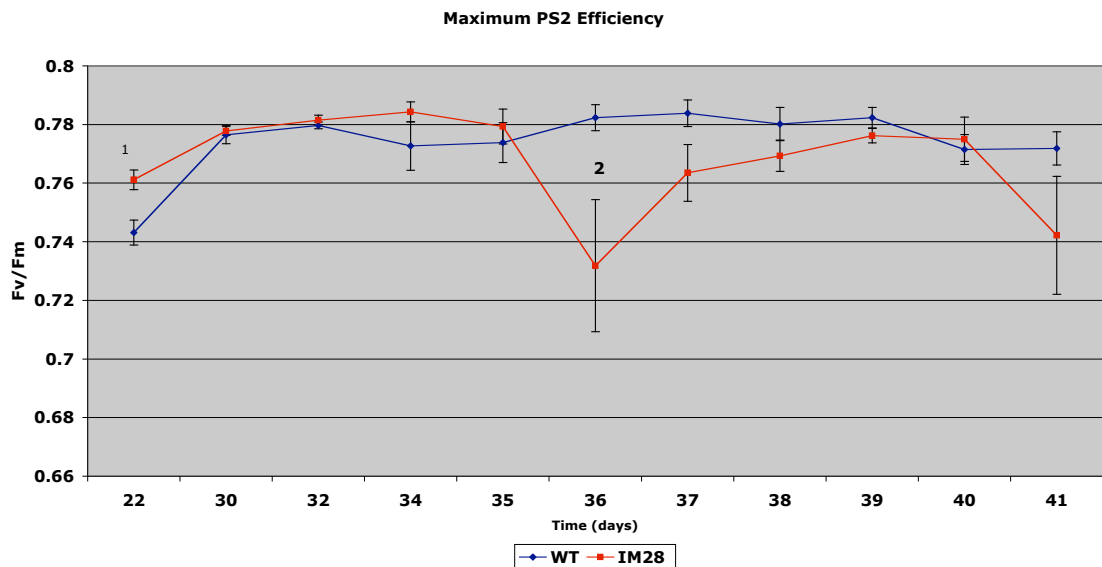


Fig 3.5: The maximum PS2 efficiency (Fv/Fm) during development.

The role of *MYB90* during development and senescence was investigated in the seventh rosette leaf of WT and IM28 grown in 16h light. The chlorophyll fluorescence of six replicates of leaf 7 on days 22, 30, 32, and daily from 34 to 41 was measured after dark adaption. Results are presented as mean (n=6) \pm SE. There was a significant difference between WT and IM28 at (1) day 22 $P = 0.007$ and (2) day 36 $P = 0.052$.

The chlorophyll fluorescence measurements were used to investigate in more detail the parameters at days 22, 36 and 41, during a light curve of increasing light intensity.

5.3.2.2 PS2 Operating Efficiency

The operating PS2 efficiency is a measurement of the PS2 efficiency that actually occurs. During the light curve of increasing light intensity the operating efficiency gradually decreased in both WT and IM28 at all the time points (Fig 3.6 A&B), which indicates that the proportion of light absorbed by chlorophyll used to drive photochemistry decreased due to the increasing damage that occurred to the reaction centres.

Both the WT and IM28 had the highest $F'q/F'm$ at day 22 which decreased during development with the lowest at the last time point, day 41. However after 32

days IM28 had an $F'q/F'm$ similar to day 36 (Fig 3.6 B). This indicates that at day 32 there was reduced proportion of absorbed light energy used in photochemistry in IM28.

5.3.2.3 Photochemical Quenching (PQ)

PQ is an indication of the fraction of reaction centres that are open and shows the efficiency of photochemistry to reduce the excitation energy. The higher the level of fluorescence measured, the lower the photochemical quenching.

Following dark adaption there was no photochemical quenching to reduce the fluorescence level because all the reaction centres are closed from a saturating light pulse and there was a delay in the activation of carbon fixing enzymes because they are light activated. This is the reason why the PQ dropped from 0 to 50 actinic PPFD and then slightly increased and stabilised from 50-150 actinic PPFD.

The WT had the highest PQ on day 22 and it decreased through development as expected (Fig 3.6C). The lowest PQ was on day 41. IM28 also had the highest PQ on day 22 and the lowest on day 41 (Fig 3.6 D). However, again there was a difference at the time points 32 and 36 between WT and IM28. For WT at day 32 the PQ was higher than at day 36, while IM28 had a higher or equal PQ at day 36 than day 32. This is presumably due to a greater decline in PQ between days 22 and 32 in IM28 (Fig 3.6 D) and indicates that at day 32 there was less excitation energy used in photochemical reactions and therefore reduced photosynthesis. This may be due to a reduction in electron acceptors and closed reaction centres.

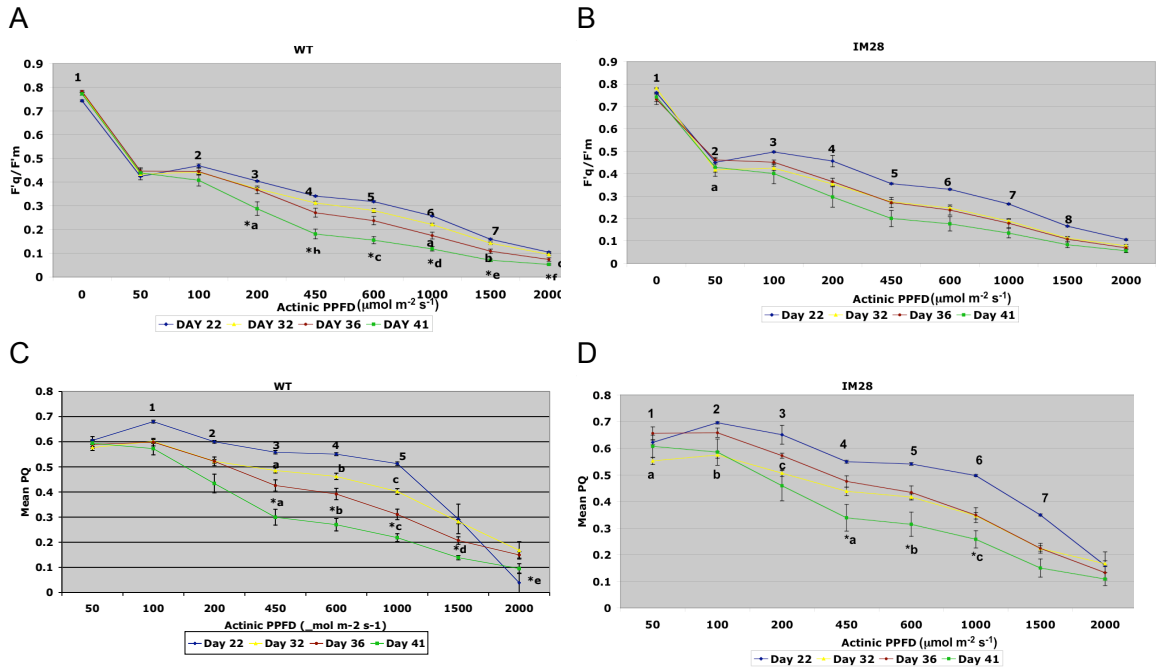


Fig 3.6: The Operating PS2 Efficiency and Photochemical Quenching

The photosynthetic parameters, (A & B) operating PS2 efficiency ($F'q/F'm$), (C & D) photochemical quenching (PQ) were measured during development and senescence in the seventh rosette leaf of (A & C) WT and (B & D) IM28 grown in 16h light. The results represent an average of six replicates of leaf 7 on days 22, 32, 36 and 41 measured over a light curve of increasing light intensity.

(A) There were significant differences in $F'q/F'm$ for WT between the time points: Day 22 and 32 shown by (1) $P=0.0007$, (2) $P=0.02$, (3) $P=0.0007$, (4) $P=0.0029$, (5) $P=0.0019$, (6) $P=0.00025$ and (7) $P=0.02$. Days 32 and 36: (a) $P=0.013$, (b) $P=0.01$ and (c) $P=0.023$. Day 36 and 41 shown by (*a) $P=0.036$, (*b) $P=0.0086$, (*c) $P=0.005$, (*d) $P=0.008$, (*e) $P=0.0047$ and (*f) $P=0.026$. (B) There were eight significant differences in $F'q/F'm$ between day 22 and 32 for IM28, (1) $P < 10^{-4}$, (2) $P=0.026$, (3) $P=0.0038$, (4) $P < 10^{-5}$, (5) $P < 10^{-6}$, (6) $P < 10^{-5}$, (7) $P < 10^{-5}$ and (8) $P=0.0017$. There was one significant difference in $F'q/F'm$ between days 32 and 36 (a) $P=0.012$. (C) There were significant differences in PQ in WT leaf 7 between the time points: day 22 and 32 (1) $P < 10^{-5}$, (2) $P < 10^{-6}$, (3) $P=0.0001$, (4) $P < 10^{-5}$, (5) $P < 10^{-6}$, days 32 and 36 (a) $P=0.03$, (b) $P=0.02$, (c) $P=0.003$ and (d) $P=0.001$ and days 36 and 41 (*a) $P=0.008$, (*b) $P=0.004$, (*c) $P=0.0054$, (*d) $P=0.0025$ and (*e) $P=0.04$. (D) There were significant differences in PQ in IM28 leaf 7 between the time points: Days 22 and 32: (1) $P=0.001$, (2) $P < 10^{-6}$, (3) $P=0.003$, (4) $P < 10^{-5}$, (5) $P < 10^{-6}$, (6) $P < 10^{-7}$ and (7) $P < 10^{-7}$. Days 32 and 36; (a) $P=0.003$, (b) $P=0.002$, (c) $P=0.0017$. Days 36 and 41: (*a) $P=0.03$, (*b) $P=0.04$.

5.3.2.4 Non-Photochemical Quenching (NPQ)

NPQ reduces the level of fluorescence by de-excitation of excess excitation energy via thermal dissipation processes. Excess excitation energy can occur during high light intensities, when the photochemical reactions cannot use all the energy or when photochemical quenching decreases due to the closure of reaction centres.

The earliest time point, day 22 had the lowest NPQ following 0 to 600 PPFD and then at higher light levels NPQ increased to a level higher than the later time points in both WT and IM28 (Fig 3.7 A&B). This suggests that the older leaves have another mechanism in place to protect the photosystems from damage caused by excess excitation energy. The NPQ gradient increased in later time points in lower PPFD because the PQ (Fig 3.6 C&D) had decreased due to reaction centres closing. This suggests that there may have been photoinhibition damage to the reaction centres in the more senescent leaves that results in a form of NPQ.

The NPQ of IM28 was found to be higher at day 32 and was similar to day 36 (Fig 3.7 B). This indicates that there was excess excitation energy at day 32, possibly due to photoinhibition of PS2 and the NPQ increased to reduce the stress on PS2.

5.3.2.5 Linear Electron Transport Rate (J)

The linear electron transport rate was highest at day 22 and then decreased as the leaf developed with the lowest at day 41 in both WT and IM28 (Fig 3.7 C&D). There was significant decline in J between the time points for WT. However the linear electron transport rate for IM28 on day 32 was low and similar to day 36 (Fig 3.7 D). There were no significant differences in IM28 between the time point 32, 36 and 41 because the results were quite variable.

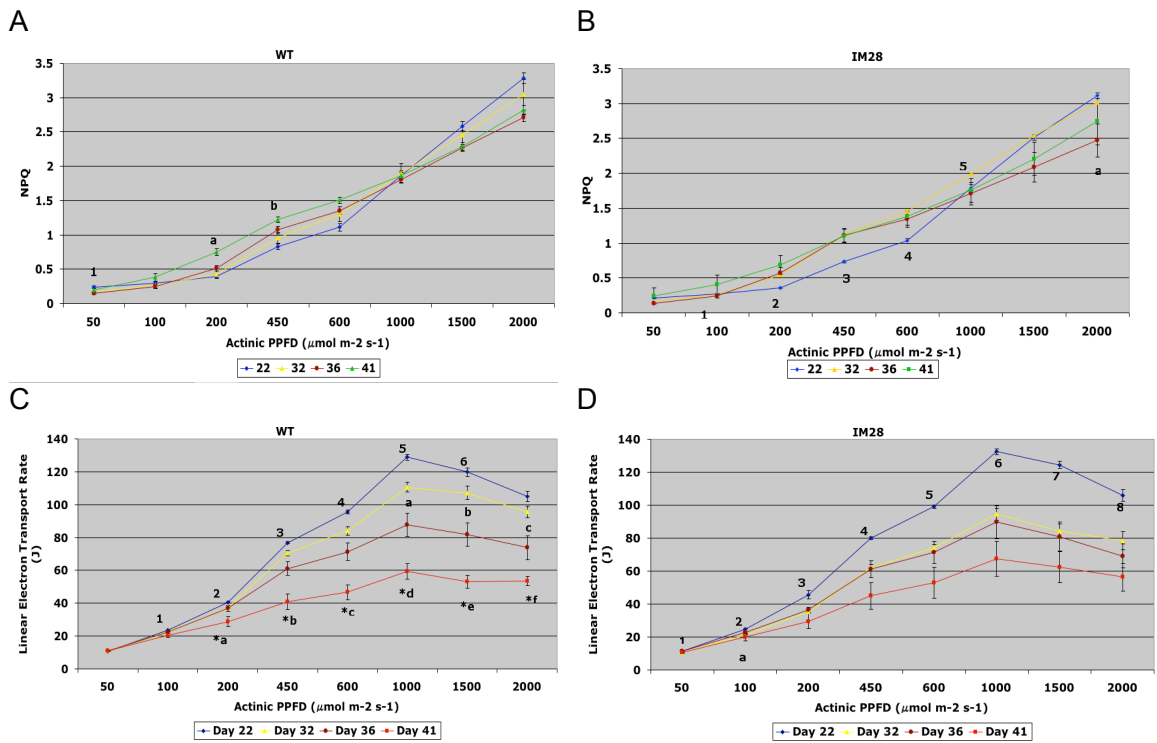


Fig 3.7: Non-photochemical Quenching and Linear Electron Transport Rate

The photosynthetic parameters, (A & B) non-photochemical quenching (NPQ) and (C & D) linear electron transport rate (J) were measured during development and senescence in the seventh rosette leaf of (A & C) WT and (B & D) IM28 grown in 16h light. The results represent an average of six replicates of leaf 7 on days 22, 32, 36 and 41 measured over a light curve of increasing light intensity.

(E) There were significant differences in NPQ in WT leaf 7 between the time points: 22 and 32; (1) $P=0.01$, 36 and 41; (a) $P=0.004$ and (b) $P=0.042$. (F) There were significant differences in NPQ in IM28 leaf 7 between the time points: 22 and 32; (1) $P=0.0008$, (2) $P=0.0001$, (3) $P<10^{-5}$, (4) $P<10^{-5}$, (5) $P=0.0056$. and 32 and 36; (a) $P=0.049$. (G) There was significant differences in J in WT leaf 7 between the time points: day 22 and 32; (1) $P=0.023$, (2) $P=0.0007$. (3) $P=0.003$, (4) $P=0.002$, (5) $P=0.0002$ and (6) $P=0.025$. Day 32 and 36; (a) $P=0.013$, (b) $P=0.01$ and (c) $P=0.023$. Day 36 and 41; (*a) $P=0.036$, (*b) $P=0.008$, (*c) $P=0.0054$ (*d) $P=0.007$ (*e) $P=0.005$ and (*f) $P=0.026$. (H) There was significant differences in J between day 22 and 32 in IM28; (1) $P<10^{-4}$, (2) $P=0.0038$, (3) $P<10^{-5}$, (4) $P<10^{-6}$, (5) $P<10^{-5}$, (6) $P<10^{-5}$ and (7) $P=0.0017$ and day 32 and 36; (a) $P=0.014$.

3.2.3.6 Chlorophyll Fluorescence Analysis at 32 and 36 Days After Sowing

The chlorophyll fluorescence parameters indicated that there was a difference in photosynthetic performance of WT and IM28 at 32 and 36 days after sowing (Fig 3.5, 3.6 & 3.7). To analyse this in more detail the photosynthetic performance of the WT was compared to IM28 at these time points (Fig 3.8 and 3.9).

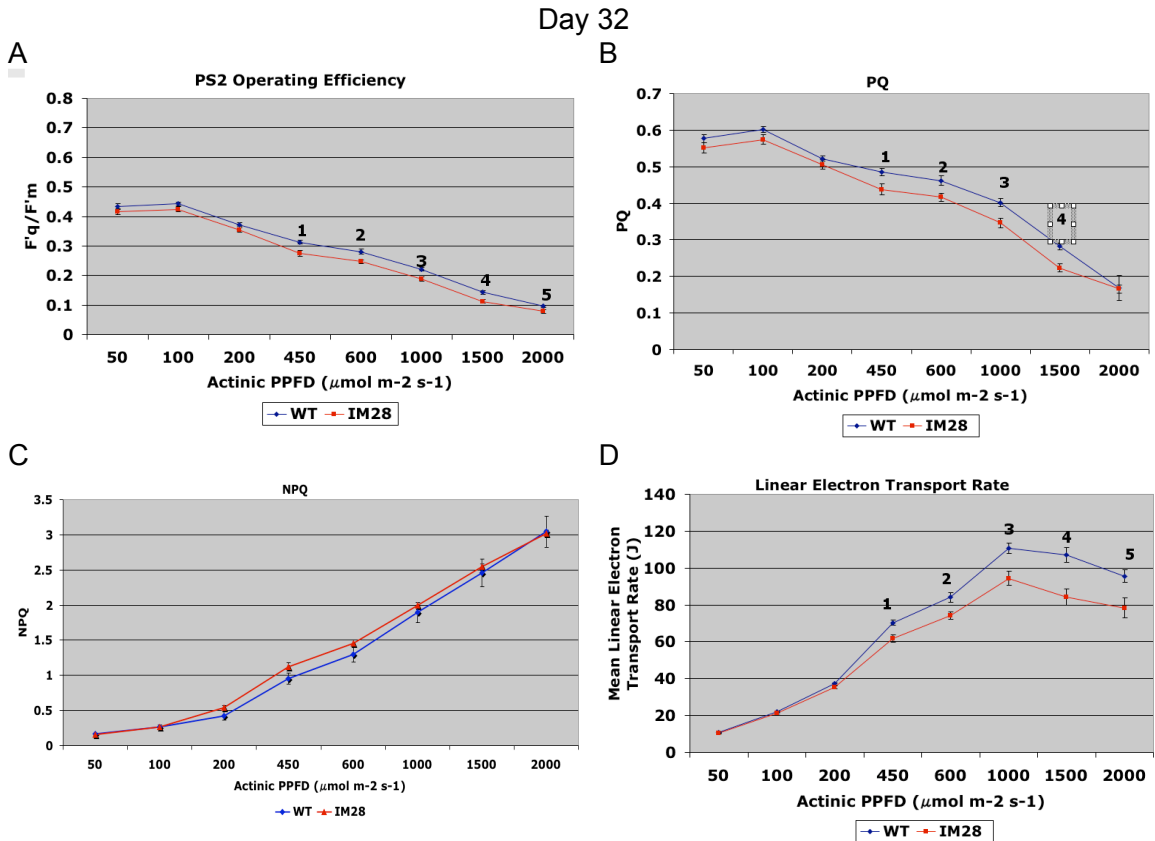


Fig 3.8: The Photosynthetic Apparatus Performance in WT and IM28 32 days after sowing.

The analysis of (A) the operating PS2 efficiency ($F'q/F'm$), (B) the photochemical quenching (PQ), (C) the non-photochemical quenching (NPQ) and (D) the linear electron transport rate (J). The role of MYB90 during development and senescence was investigated in the seventh rosette leaf of WT and IM28 grown in 16h light. The chlorophyll fluorescence of six replicates of leaf 7 on day 32 was measured for WT and IM28. Results are presented as mean ($n=6$) \pm SE. Significant difference between WT and IM28: (A) in $F'q/F'm$ 1: $P=0.007$, 2: $P=0.01$, 3: $P=0.0058$, 4: $P=0.003$ and 5: $P=0.024$, (B) in PQ 1: $P=0.028$, 2: $P=0.02$, 3: $P=0.008$ and 4: $P=0.001$ and (D) in J 1: $P=0.007$, 2: $P=0.012$, 3: $P=0.005$, 4: $P=0.003$ and 4: $P=0.024$.

The WT had a higher PS2 operating efficiency (Fig 3.8A) than IM28 at 32 days after sowing, this was due to lower photochemical quenching in IM28 (Fig 3.8B). A lower PQ indicates that less of the excitation energy was used in photochemical reactions and this may be due to the closure of reaction centres. The low linear electron transport

rate of IM28 (Fig 3.8D) also suggested that a higher proportion of IM28 reaction centres were closed. The NPQ of IM28 was not significantly different from the WT.

IM28 had a low maximum PS2 efficiency at 36 days after sowing, however this did not reduce the operating PS2 efficiency (Fig 3.9 A) compared to the WT. The maximum PS2 efficiency is linked to the NPQ, a low F_v/F_m indicates that there was some photoinhibition of the reaction centres and this usually is reflected in the increase of NPQ. However in IM28 NPQ (Fig 3.9C) was not significantly different from the WT. This appears to be because at day 36 IM28 had higher PQ than the WT (Fig 3.9B) and therefore photochemistry was more efficient. There was no difference between WT and IM28 linear electron transport rate (Fig 3.9D) and this is because both lines had similar operating PS2 efficiencies and PQ.

Day 36

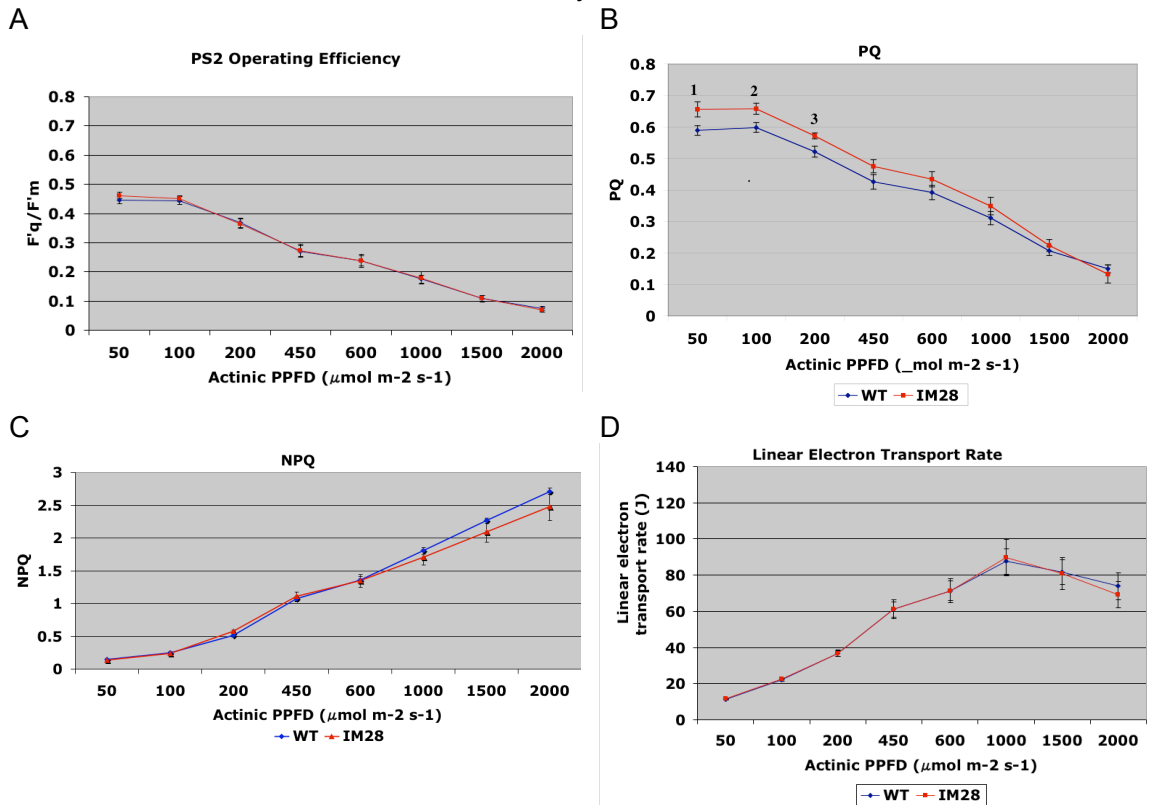


Fig 3.9: The Photosynthetic Apparatus Performance of WT and IM28 36 days after sowing.

The analysis of (A) the operating PS2 efficiency ($F'q/F'm$), (B) the photochemical quenching (PQ), (C) the non-photochemical quenching (NPQ) and (D) the linear electron transport rate (J). The role of MYB90 during development and senescence was investigated in the seventh rosette leaf of WT and IM28 grown in 16h light. The chlorophyll fluorescence of six replicates of leaf 7 on day 32 was measured for WT and IM28. Results are presented as mean ($n=6$) \pm SE

There were significant difference between WT and IM28 PQ (B), 1:P=0.04, 2: P= 0.027 and 3: P=0.029.

3.3 Gene Expression Analysis

A time course microarray experiment was carried out to identify differentially expressed genes between WT and the *MYB90* knock out, IM28. The time course consisted of 11 time points during development to allow an in depth analysis of the role of *MYB90* on gene expression over time. The gene specific sequence tag microarrays from CATMA (a Complete Arabidopsis Transcriptome MicroArray) were hybridised with WT and IM28 cDNA from the same time point. There were two biological replicates and four technical replicates from each time point. The array data represents the ratio of IM28/WT at each time point during development. The raw array data was normalised using Genespring by normalisation per chip to the 50th percentile, per spot divided by the control channel and per gene normalised to the median. Genespring was used to filter out genes that were flagged absent and to identify genes that were differentially expressed in IM28 at one or more time points by removing genes normalised between 0.66 and 1.5 in all the time points and selecting genes that were normalised 'over 1.5 or less 0.6' and test p-value up to 0.05 using the Benjamini & Hochberg false discovery rate (Benjamini & Hochberg, 1995), in at least one out of all the time points. There were 2861 genes identified as differentially expressed in IM28 compared to WT.

The software TMEV (Saeed *et al.*, 2003) was used to analyse the differentially expressed genes, they were displayed as K-means gene clusters. Genes with significantly different ratio at least one time point were analysed and 25 different gene clusters were identified (Fig 3.10).

3.3.1 Analysis of Cluster 1

MYB90 was found in a cluster containing 11 other genes. This cluster showed differential expression of genes that had reduced expression in IM28 late in development. There was increased expression of these genes on days 35 and 37 in IM28 (Fig 3.11).

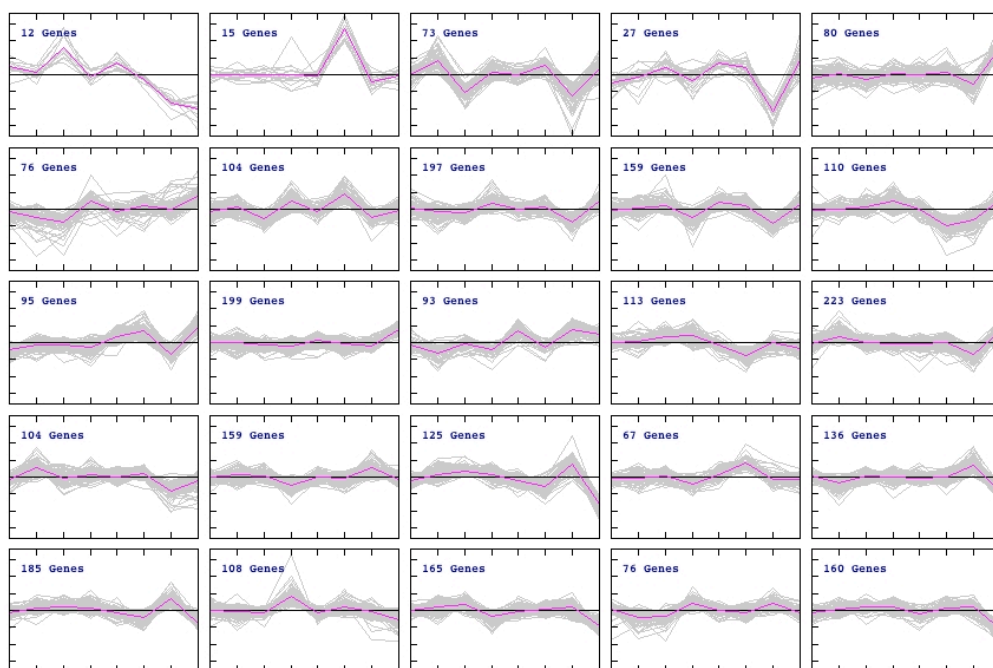


Fig 3.10: Clustering of Genes That Were Differentially Expressed During Development.

The expression data from the time course experiment was normalised and the IM28/WT ratios were determined. The data was filtered to remove genes not differentially expressed at any time point. The data was subjected to K-Means Gene Clustering, with Euclidean Distance (using TMEV software). The clusters contained groups of genes with similar mean pattern of IM28/WT ratios independent of different magnitude of fold changes. The IM28/WT (\log_2) ratios displayed on the y-axis and the days after sowing on the x-axis. The cluster analysis showed at least 25 clusters. *MYB90*, *MYB75* and some flavonoid and anthocyanin biosynthesis genes were found in the first cluster.

The twelve genes found in cluster 1 (Fig 3.11) included *MYB90* and *MYB75*. IM28 is a knockout of *MYB90* so there should be no expression, the increased expression level at 35 and 37 days after sowing is probably due to high sequence similarity between *MYB90* and another *MYB* gene, for example *MYB75* resulting in cross hybridisation to the *MYB90* spot on the array. The other genes found in this cluster belong to branches of the flavonoid and anthocyanin biosynthesis pathway such as *dihydroflavonol 4-reductase (DFR)*, *leucoanthocyanidin dioxygenase (LDOX)*, *flavonoid 3'-hydroxylase (F3'H)*, *chalcone synthase (CHS)*, *flavonone 3-hydroxylase (F3H)*, *chalcone flavanone isomerase*, *glutathione S-transferase (GST)* and *flavonone glycosyltransferase*.

These results indicate that during senescence *MYB90* regulates key genes of most of the different branches of the pathway. There were three genes from the flavonoid pathway *CHS*, *CHFI* and *F3H*, one from the flavonol pathway *F3'H*, two from the leucoanthocyanidin pathway *DFR* and *LDOX*, and one from the quercetin pathway *F3H*. However there were no genes found in cluster 1 that belong to the phenylpropanoid synthesis pathway such as *PAL*.

3.3.1.1 Cluster 1 Promoter Analysis

In order to investigate potential upstream activator sequences that might account for the expression of this group of genes the promoter sequences of the set of genes found in cluster1 were analysed using the web-based programme Athena (<http://www.bioinformatics2.wsu.edu/cgi-bin/Athena/>) (O'Connor *et al.*, 2005) to find over represented promoter motifs that potentially could be the binding site of *MYB90* (Fig 3.12). One common motif significantly over represented between all the promoters of the cluster 1 genes was the CACGT motif. The CACGT motif is also known as the G-box, which is usually found upstream of light regulated genes (Menkens & Cashmore, 1994). There were other motifs found similar to the G-box; the GBOXLERBCS found in *CFI*, the GBF1/2/3 G-box that is the binding site of bZIP proteins (de Vetten & Ferl, 1995), induced by ABA and was found in *DFR*. The TGA1 box, a G-box like element found in *LDOX* (Schindler *et al.*, 1992). The G-box is the binding site of the HY5 bZIP transcription factor that was shown to be involved in light regulation of anthocyanin biosynthesis genes (Shin *et al.*, 2007).

Another enriched promoter motif found in the cluster1 gene promoters was the ABRE-like motif (Shinozaki & Yamaguchi-Shinozak, 2000) which has similarity to the G-box. This motif was found in all the gene promoters of cluster1 except *GST* and *coronatine responsive tyrosine aminotransferase*. Genes that contain ABRE motifs in the promoter region are usually responsive to stress and ABA.

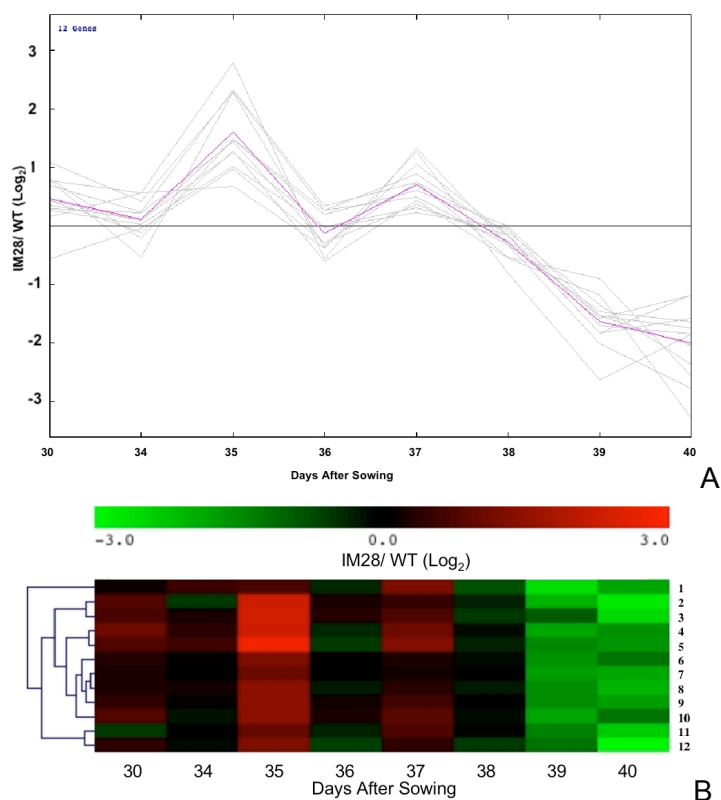


Fig 3.11: Analysis of Cluster 1

(A) The expression data from the time course experiment was normalised and the IM28/WT ratios were determined. The data was subjected to K-Means Gene Clustering, with Euclidean Distance (using TMEV software). The clusters contained groups of genes with similar mean pattern of IM28.WT ratios independent of different magnitude of fold changes. The cluster analysis showed *MYB90*, *MYB75* and some flavonoid and anthocyanin biosynthesis genes to be in this cluster.

(B) The normalised expression data from genes found in cluster 1 during the time course were subjected to hierarchical tree clustering (using TMEV software) with euclidean distance and average linkage. Red indicates high IM28/WT ratio and green indicates low IM28/WT ratio. There were 12 different genes found in this cluster, (1) At4g15210 *Beta-amylase* (*BMV1*), (2) At5g42800 *Dihydroflavonol 4-reductase* (*DFR*), (3) At4g22880 *Leucoanthocyanidin dioxygenase* (*LDOX*), (4) At5g07990 *Flavonoid 3'-hydroxylase* (*F3'H*), (5) At5g13930 *Chalcone synthase*, (6) At1g56650 *MYB75*, (7) At1g66390 *MYB90*, (8) At3g51240 *Flavonone 3-hydroxylase* (*F3H*), (9) At5g05270 *Chalcone flavanone isomerase*, (10) At5g17220 *Glutathione S-transferase* (*GST*), (11) At4g23600 *Coronatine-responsive tyrosine aminotransferase*, (12) At5g54060 *Glycosyltransferase*.

There were two motifs found to be involved in the expression of anthocyanin biosynthesis genes, both are MYB binding site motifs. The MYB binding site motif, an element found in anthocyanin biosynthesis genes that had flower specific activity, was found in *MYB75*, *F3'H*, *CHS* and *DFR* (Sablowski *et al.*, 1994). The AtMYC2 BS in

RD22 motif was found in *MYB90*, *F3H*, *F3'H*, *CHS* and *GST*. There were several other different MYB binding site motifs with roles in responses to stress, the MYB1AT motif was found in all the promoters.

All the promoters contained the W-box motif, which is the binding site for WRKY transcription factors that are generally found to be involved in stress response (Yu et al., 2000).

P-value	Name	#P	#S	Select	P-value	Name	#P	#S	Select
#P = Number of promoters with TF sites					#S = Number of predicted TF sites				
Enriched TF sites									
$< 10^{-3}$	<input type="checkbox"/> <u>ABRE-like binding site motif</u>	9	17	<input type="checkbox"/>	$< 10^{-6}$	<input type="checkbox"/> <u>CACGTGMOTIF</u>	11	34	<input type="checkbox"/>
Non-enriched TF sites									
<input checked="" type="checkbox"/> 0.0849	<input type="checkbox"/> <u>ABFs binding site motif</u>	2	2	<input type="checkbox"/>	<input checked="" type="checkbox"/> 0.1576	<input type="checkbox"/> <u>ABRE binding site motif</u>	2	2	<input type="checkbox"/>
<input checked="" type="checkbox"/> 0.3275	<input type="checkbox"/> <u>ABREATRD22</u>	1	1	<input type="checkbox"/>	<input checked="" type="checkbox"/> 0.0197	<input type="checkbox"/> <u>ACE promoter motif</u>	1	1	<input type="checkbox"/>
<input checked="" type="checkbox"/> 0.1719	<input type="checkbox"/> <u>ACGTABREMOTIFA2OSEM</u>	4	7	<input type="checkbox"/>	<input checked="" type="checkbox"/> 0.4321	<input type="checkbox"/> <u>ARF binding site motif</u>	6	7	<input type="checkbox"/>
<input checked="" type="checkbox"/> 0.6258	<input type="checkbox"/> <u>ATHB2 binding site motif</u>	2	4	<input type="checkbox"/>	<input checked="" type="checkbox"/> 0.8821	<input type="checkbox"/> <u>AtMYB2 BS in RD22</u>	1	2	<input type="checkbox"/>
<input checked="" type="checkbox"/> 0.4259	<input type="checkbox"/> <u>AtMYC2 BS in RD22</u>	6	9	<input type="checkbox"/>	<input checked="" type="checkbox"/> 0.8140	<input type="checkbox"/> <u>BoxII promoter motif</u>	5	7	<input type="checkbox"/>
<input checked="" type="checkbox"/> 0.1603	<input type="checkbox"/> <u>CARGCW8GAT</u>	10	40	<input type="checkbox"/>	<input checked="" type="checkbox"/> 0.6503	<input type="checkbox"/> <u>CCA1 binding site motif</u>	4	4	<input type="checkbox"/>
<input checked="" type="checkbox"/> 0.6906	<input type="checkbox"/> <u>DRE core motif</u>	3	4	<input type="checkbox"/>	<input checked="" type="checkbox"/> 0.4172	<input type="checkbox"/> <u>GADOWNAT</u>	2	3	<input type="checkbox"/>
<input checked="" type="checkbox"/> 0.0962	<input type="checkbox"/> <u>GAREAT</u>	10	15	<input type="checkbox"/>	<input checked="" type="checkbox"/> 0.2113	<input type="checkbox"/> <u>GBF1/2/3 BS in ADH1</u>	1	2	<input type="checkbox"/>
<input checked="" type="checkbox"/> 0.3306	<input type="checkbox"/> <u>GBOXLERBCS</u>	1	1	<input type="checkbox"/>	<input checked="" type="checkbox"/> 0.5460	<input type="checkbox"/> <u>Gap-box Motif</u>	2	2	<input type="checkbox"/>
<input checked="" type="checkbox"/> 0.7286	<input type="checkbox"/> <u>lbox promoter motif</u>	5	11	<input type="checkbox"/>	<input checked="" type="checkbox"/> 0.1018	<input type="checkbox"/> <u>L1-box promoter motif</u>	5	6	<input type="checkbox"/>
<input checked="" type="checkbox"/> 0.8285	<input type="checkbox"/> <u>LEAFYATAG</u>	1	1	<input type="checkbox"/>	<input checked="" type="checkbox"/> 0.0015	<input type="checkbox"/> <u>MRE motif in CHS</u>	1	1	<input type="checkbox"/>
<input checked="" type="checkbox"/> 0.4474	<input type="checkbox"/> <u>MYB binding site promoter</u>	5	7	<input type="checkbox"/>	<input checked="" type="checkbox"/> 0.6356	<input type="checkbox"/> <u>MYB1 binding site motif</u>	1	2	<input type="checkbox"/>
<input checked="" type="checkbox"/> 0.0727	<input type="checkbox"/> <u>MYB1AT</u>	12	31	<input type="checkbox"/>	<input checked="" type="checkbox"/> 0.2924	<input type="checkbox"/> <u>MYB1LEPR</u>	4	4	<input type="checkbox"/>
<input checked="" type="checkbox"/> 0.8582	<input type="checkbox"/> <u>MYB2AT</u>	3	5	<input type="checkbox"/>	<input checked="" type="checkbox"/> 0.6193	<input type="checkbox"/> <u>MYB3 binding site motif</u>	1	1	<input type="checkbox"/>
<input checked="" type="checkbox"/> 0.1460	<input type="checkbox"/> <u>MYB4 binding site motif</u>	11	32	<input type="checkbox"/>	<input checked="" type="checkbox"/> 0.4259	<input type="checkbox"/> <u>MYCATERD1</u>	6	9	<input type="checkbox"/>
<input checked="" type="checkbox"/> 0.5490	<input type="checkbox"/> <u>RAV1-B binding site motif</u>	2	2	<input type="checkbox"/>	<input checked="" type="checkbox"/> 0.5003	<input type="checkbox"/> <u>RY-repeat promoter motif</u>	1	2	<input type="checkbox"/>
<input checked="" type="checkbox"/> 0.6013	<input type="checkbox"/> <u>SV40 core promoter motif</u>	3	4	<input type="checkbox"/>	<input checked="" type="checkbox"/> 0.4332	<input type="checkbox"/> <u>T-box promoter motif</u>	8	10	<input type="checkbox"/>
<input checked="" type="checkbox"/> 0.2932	<input type="checkbox"/> <u>TATA-box Motif</u>	11	62	<input type="checkbox"/>	<input checked="" type="checkbox"/> 0.4365	<input type="checkbox"/> <u>TELO-box promoter motif</u>	2	2	<input type="checkbox"/>

Fig 3.12: Promoter Analysis of Cluster 1 Gene Promoters

Motif search in cluster1 gene promoters (2500bp upstream) using the web based Athena programme (O'Connor et al., 2005). The table displays the different promoter motifs, the P-value (calculated using hypergeometric distribution of the enrichment of the transcription factor sites found in the promoter sequences), the number of promoters with the transcription factor sites (TF) and the number of predicted TF sites. The enriched TF motifs in cluster1 gene promoters were ABRE-like binding motif and CACGT motif. #P= Number of promoters with TF sites. #S= Number of predicted TF sites.

3.3.2 Analysis of Other Differentially Expressed Anthocyanin Biosynthesis Genes

The cluster analysis showed that in cluster1 there were key genes of different branches of the flavonoid and anthocyanin biosynthesis pathway that are potentially regulated by *MYB90* during senescence. Other genes involved in anthocyanin, flavonoid, flavonol

and quercetin biosynthesis were identified using the AraCyc pathway viewer tool in The Arabidopsis Information Resource (TAIR, www.arabidopsis.org).

The majority of the other genes found in the pathway were not differentially expressed, however there were a few that were. These include *cinnamic acid 4-hydroxylase (C4H)* (At2g30490) involved in phenylpropanoid synthesis. This was found in cluster 22 (Fig 3.13 C). The genes in this cluster had differential expression at 36 days after sowing where IM28 showed an increased level of expression compared to WT. There was a *Plastocyanin like domain* gene (At5g20230) involved in flavonol synthesis, found to be differentially expressed in IM28 and was found to be in cluster 11 (Fig 3.13A). The genes in this cluster had increased expression levels in IM28 at 38 and 40 days after sowing. There was a *UDP-glucosyl transferase* (At4g3410) found in cluster 21 (Fig 3.13B) that was involved in quercetin synthesis. Genes found in this cluster had a higher expression level in IM28 than WT at 39 days after sowing.

Buchanan-Wollaston *et al.*, (2005) identified a potential alternative anthocyanin and flavonoid biosynthesis pathway during dark induced senescence. Four of these genes were differentially expressed in IM28, with lower expression at day 39. These included an alternative *F3H* (At5g24530) found in cluster 3, an alternative LDOX (At3g55970) and *flavonol synthase (FLS)* (At2g38240) found in cluster 4 and *FLS* (At5g05600) found in cluster 16.

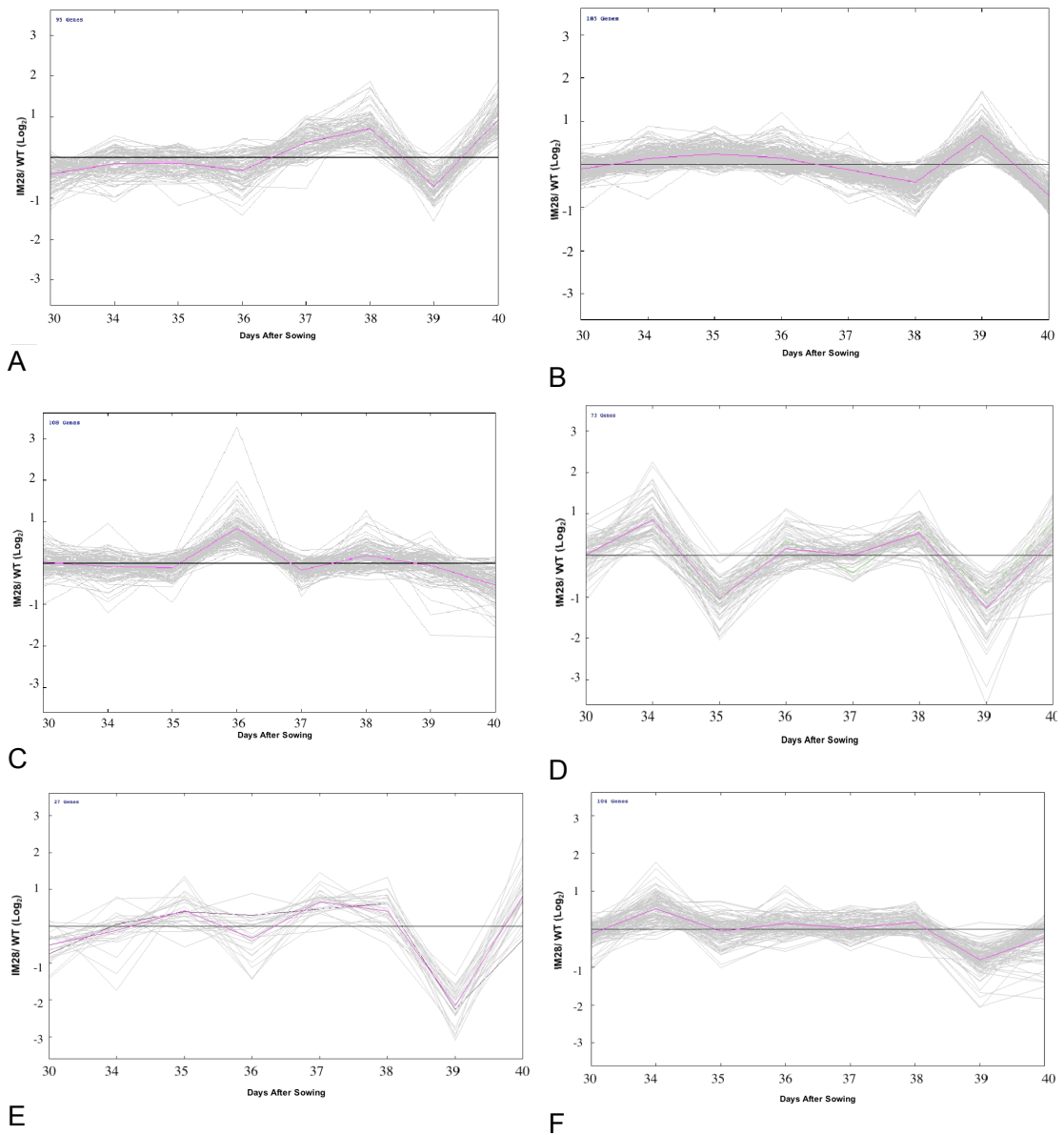


Fig 3.13: Analysis of Differentially Expressed Anthocyanin Biosynthesis Genes.

Differentially expressed anthocyanin biosynthesis genes during development. The IM28/WT ratio data from the time course experiment was normalised and the relative expression levels were determined. The data was subjected to K-Means Gene Clustering, with Euclidean Distance (using TMEV software). The clusters contained groups of genes with similar mean pattern of IM28/WT ratios independent of different magnitude of fold changes. The cluster analysis showed some flavonoid and anthocyanin biosynthesis genes to be in these clusters. *Plastocyanin like domain* gene (At5g20230) was in cluster 11 (A), *UDP-glucosyl transferase* (At4g3410) was in cluster 22 and *cinnamic acid 4-hydroxylase (C4H)* (At2g30490) was in cluster 22. (D) *flavanone 3-hydroxylase* in cluster 3 (At5g24530), (E) *LDOX* (At3g55970 and *flavanol synthase* (At2g38240) in cluster 4 and (F) *flavanol synthase* (At5g05600) in cluster 16.

3.3.3 Analysis of Cluster 2

The cluster analysis showed a group of fifteen genes that are more highly expressed in IM28 than WT at 38 days after sowing shown in figure 3.14. These genes appear to have roles in protein metabolism, response to stress, signal transduction, transport and unknown processes.

3.3.3.1 Promoter Analysis of Cluster 2 Genes

The regulation of the set of genes found in cluster 2 is of interest. The promoters of these genes were analysed for over represented promoter motifs using the Athena software (O'Connor *et al.*, 2005) (Fig 3.15). The transcription factor binding sites, T-box, ARF binding site, MYC2 BS in RD22, MYCATERD1 and MYB binding site were found to be significantly enriched in the promoter sequences. The T-box was first found in the promoter of the *GAPB* gene, which is a nuclear gene that produces a subunit of a protein located in the chloroplast (Chan *et al.*, 2001). The T-box motif is involved in light regulation and is present in all the promoters of cluster 2 genes, which indicates that they may be regulated by light. The MYC BS in RD22 and the MYCATERD1 motif sequences and binding sites overlap and they were found in all the promoters except for thionin.

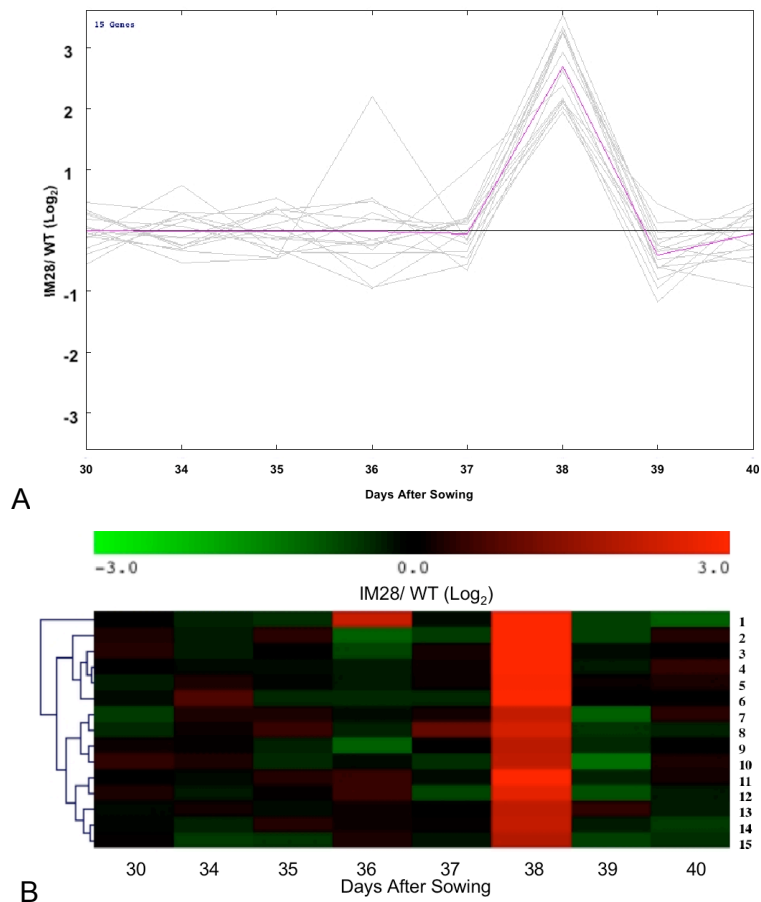


Fig 3.14: Analysis of Cluster 2 Genes.

The expression data from the time course experiment was normalised and the relative IM28/ WT ratios were determined. (A) The data was subjected to K-Means Gene Clustering, with Euclidean Distance (using TMEV software). The clusters contained groups of genes with similar mean pattern of IM28/WT ratios independent of different magnitude of fold changes. (B) Hierarchical Tree of cluster 2. The normalised expression data from genes found in cluster 1 during the time course were subjected to hierarchical tree clustering (using TMEV software) with euclidean distance and average linkage. Red indicates high IM28/WT ratio and green indicates low IM28/WT ratio. The genes found in the cluster were (1) developmental protein *SEPALLATA2* At3g02310, (2) *lipid transfer protein 6 (LTP6)* At3g08770, (3) *MLP-like protein 168 (MLP168)* At1g35310, (4) *thionin (THI2.1)* At1g72260, (5) *subtilase* At5g51750, (6) *trypsin and protease inhibitor* At1g72290, (7) *zinc finger (AN1-like)* (At3g28210), (8) *mitogen-activated protein kinase kinase kinase 18 (MAPKKK18)* At1g05100, (9) *pollen Oleo 1 allergen and extensin* At1g28290, (10) unknown At5g22580, (11) *cytochrome P450* At5g44620, (12) unknown At1g11850, (13) *hydroxyproline-rich glycoprotein* At2g34870, (14) unknown At1g20180 and (15) *hydrolase alpha/beta fold protein* At5g39220.

P-value	Name	#P	#S	Select	P-value	Name	#P	#S	Select
#P = Number of promoters with TF sites					#S = Number of predicted TF sites				
⊖ Enriched TF sites									
■ < 10 ⁻³	ARF binding site motif	13	21	<input type="checkbox"/>	■ < 10 ⁻⁴	AtMYC2 BS in RD22	14	29	<input type="checkbox"/>
■ < 10 ⁻³	MYB binding site promoter	12	23	<input type="checkbox"/>	■ < 10 ⁻⁴	MYCATERD1	14	29	<input type="checkbox"/>
■ < 10 ⁻³	T-box promoter motif	15	39	<input type="checkbox"/>					

Fig 3.15: Promoter Analysis of Cluster 2 Gene Promoters.

Promoter motif analysis of the promoters of cluster2 genes using the web based Athena programme (O'Connor et al., 2005). The promoter sequences 2500bp upstream of the genes. The table displays the different promoter motifs, the P-value (calculated using hypergeometric distribution of the enrichment of the transcription factor sites found in the promoter sequences), the number of promoters with the transcription factor sites (TF) and the number of predicted TF sites. #P= Number of promoters with TF sites. #S= Number of predicted TF sites. There were significantly enriched transcription factor binding sites found in the promoters, the T-box, ARF binding site, MYC2 BS in RD22, MYCATERD1 and MYB binding site.

3.3.4 Analysis of Clusters Containing *TT8*

In a previous study the bHLH factor *TT8* was regulated by the interaction of the WD40 protein *TTG1* with *TT8* and a MYB protein, *MYB75* on the promoter of *TT8* (Nesi et al., 2001, Baudry et al., 2006). This array experiment indicates that it may also be regulated by *MYB90* during late development or another gene whose expression was altered by the absence of *MYB90* (for example *MYB75*) because it was differentially expressed in IM28, the *MYB90* knockout, shown in figure 3.16. The expression of *TT8* was lower in IM28 than WT in the later time points between days 38 and 40 after sowing.

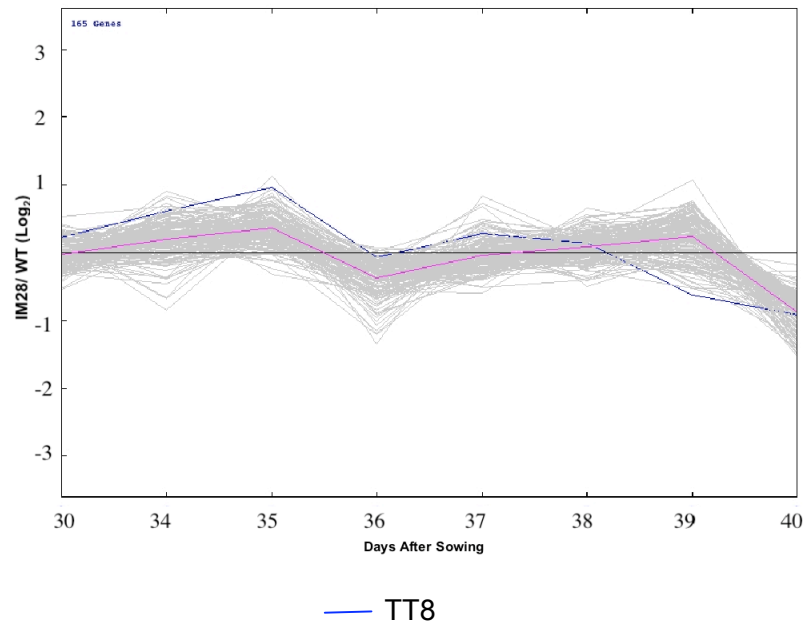


Fig 3.16: Analysis of *TT8*

Gene expression profiles of WT and IM28 in cluster 23 that contained *TT8*. The expression data from the time course experiment was normalised IM28/WT ratios were determined. The data was subjected to K-Means Gene Clustering, with Euclidean Distance (using TMEV software). The cluster contained a group of genes with similar mean pattern of IM28/WT ratios independent of different magnitude of fold changes.

3.3.4.1 Analysis of Gene Ontologies (GOs)

TT8 was found in a cluster of 165 genes. The analysis of Gene Ontologies (GOs) using a web based tool Gostat (Beissbarth & Speed, 2004) indicated that a significant proportion of the genes had a molecular function GO for the catalysis of the unwinding of a DNA or RNA duplex (GO: 0004386) and interacting with RNA molecule (GO: 0003723) (Table 9).

This set of genes was found to have a significant over representation of enzyme activity, such as NTPase activity (GO:0017111), catalysis of the hydrolysis (GO:0016462, GO:0016817 and GO:0016818). Hydrolysis reactions breakdown polymers, which indicated that some macromolecule breakdown may be reduced in IM28 compared to the WT after 38 days from sowing. There was also a significant number of genes involved in protein ubiquitinylation (GO:0016567).

Gene Ontology (GO)	Genes	No. of genes	P-Value
GO:0004386	atrx, emb3011, chr4, mee29, at2g40700	5	0.000353
GO:0003724	emb3011, mee29	2	0.00153
GO:0003723	at2g33440, gr-rbp3, at5g60170, at5g25060, atfip1, at3g55340, apum	7	0.00189
GO:0017111	at5g46070, at1g59820, at1g67120, at3g06670, emb1047, mee29, at2g40700	7	0.00368
GO:0016567	ask19, at2g45920, at1g60190	3	0.0042
GO:0016462	at5g46070, at1g59820, at1g67120, at3g06670, emb1047, mee29, at2g40700	7	0.00468
GO:0016818	at5g46070, at1g59820, at1g67120, at3g06670, emb1047, mee29, at2g40700	7	0.00477
GO:0016887	at159820, at1g67120, at3g06670, emb1047, mee29, at2g40700	6	0.00512

Table 9: The set of genes that clustered with TT8 in cluster 23 were analysed to find the significant Gene Ontologies (GOs) using web based tool Gostat (Beissbarth & Speed, 2004) (<http://gostat.wehi.edu.au/cgi-bin/goStat2.pl>). The significantly overrepresented GOs were displayed in a table with the list of genes and P-values.

3.3.4.2 Promoter Analysis

The promoter sequences of the genes found to cluster with *TT8* were analysed to find common promoter motifs that may regulate transcriptional activity. They were analysed using Athena (O'Connor *et al.*, 2005). Twenty- seven different promoter motifs were identified (Fig 3.17). A large number of the promoters contained the W-box motif, which is the binding site for WRKY transcription factors (Yu *et al.*, 2001). This indicates that this cluster of genes may be involved in response to stress. They may also be regulated by light because the I-box, CACGTG and T-box motifs were identified (Giuliano *et al.*, 1998, Menkens & Cashmore, 1994 and Chan *et al.*, 2001). There were several different MYB binding site motifs, including MYB1AT, MYB2AT, MYB4 binding site and the MYB binding site.














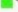













P-value	Name	#P	#S	Select	P-value	Name	#P	#S	Select
#P = Number of promoters with TF sites					#S = Number of predicted TF sites				
Enriched TF sites									
	<input checked="" type="checkbox"/> ABFs binding site motif	18	21	<input type="checkbox"/>		<input checked="" type="checkbox"/> ABRE binding site motif	21	24	<input type="checkbox"/>
	<input checked="" type="checkbox"/> ABRE-like binding site motif	65	121	<input type="checkbox"/>		<input checked="" type="checkbox"/> ACGTABREMOTIFA2OSEM	49	75	<input type="checkbox"/>
	<input checked="" type="checkbox"/> ARF binding site motif	121	194	<input type="checkbox"/>		<input checked="" type="checkbox"/> BoxII promoter motif	109	173	<input type="checkbox"/>
	<input checked="" type="checkbox"/> CACGTGMOTIF	52	140	<input type="checkbox"/>		<input checked="" type="checkbox"/> CARGCW8GAT	127	564	<input type="checkbox"/>
	<input checked="" type="checkbox"/> DRE core motif	64	100	<input type="checkbox"/>		<input checked="" type="checkbox"/> DREB1A/CBF3	28	39	<input type="checkbox"/>
	<input checked="" type="checkbox"/> GAREAT	119	230	<input type="checkbox"/>		<input checked="" type="checkbox"/> GBF1/2/3 BS in ADH1	10	22	<input type="checkbox"/>
	<input checked="" type="checkbox"/> GBOXLERBCS	15	18	<input type="checkbox"/>		<input checked="" type="checkbox"/> GCC-box promoter motif	28	35	<input type="checkbox"/>
	<input checked="" type="checkbox"/> Hexamer promoter motif	44	57	<input type="checkbox"/>		<input checked="" type="checkbox"/> Ibox promoter motif	103	162	<input type="checkbox"/>
	<input checked="" type="checkbox"/> MYB binding site promoter	76	115	<input type="checkbox"/>		<input checked="" type="checkbox"/> MYB1AT	156	636	<input type="checkbox"/>
	<input checked="" type="checkbox"/> MYB2AT	80	123	<input type="checkbox"/>		<input checked="" type="checkbox"/> MYB4 binding site motif	146	434	<input type="checkbox"/>
	<input checked="" type="checkbox"/> RAV1-B binding site motif	49	57	<input type="checkbox"/>		<input checked="" type="checkbox"/> SV40 core promoter motif	61	80	<input type="checkbox"/>
	<input checked="" type="checkbox"/> T-box promoter motif	124	237	<input type="checkbox"/>		<input checked="" type="checkbox"/> TATA-box Motif	150	641	<input type="checkbox"/>
	<input checked="" type="checkbox"/> TELO-box promoter motif	32	41	<input type="checkbox"/>		<input checked="" type="checkbox"/> UPRMOTIFIIAT	17	20	<input type="checkbox"/>
	<input checked="" type="checkbox"/> W-box promoter motif	139	331	<input type="checkbox"/>					

Fig 3.17: Promoter motif analysis of the promoters of cluster genes from Fig 3.18B using the web based Athena programme (O'Connor et al., 2005). The promoter sequences 2500bp upstream of the genes. There were 27 enriched transcription factor binding sites found in the promoters. The table displays the different promoter motifs, the P-value (calculated using hypergeometric distribution of the enrichment of the transcription factor sites found in the promoter sequences), the number of promoters with the transcription factor sites (TF) and the number of predicted TF sites. #P= Number of promoters with TF sites. #S= Number of predicted TF sites.

3.3.5 Analysis of Differentially Expressed MYB Genes in the *MYB90* Knockout

There were eleven different MYB transcription factors differentially expressed in the absence of *MYB90*, including *MYB90* and *MYB75* (Fig 3.18). *MYB90* and *MYB75* expression levels were lower in IM28 than WT during senescence, from days 38 to 40 after sowing. During these time points the MYB genes, *MYB* (At1g15720), *MYB* (At5g08520), *MYB30* (At3g28910), *MYB* (At5g41020), *GLK2* (At5g44190), *MYB91* (At2g37630) expression levels were lower in IM28 at day 38 and 40 and higher at day 39 compared to the WT. *MYB15* and *MYB50* were higher at day 38. *MYB51* expression levels declined in IM28 at days 39 and 40. *MYB15* expression declined at

day 39 and then increased to higher levels in IM28. *MYB29* had lower expression levels at day 38 which then increased to higher levels than the WT at day 40.

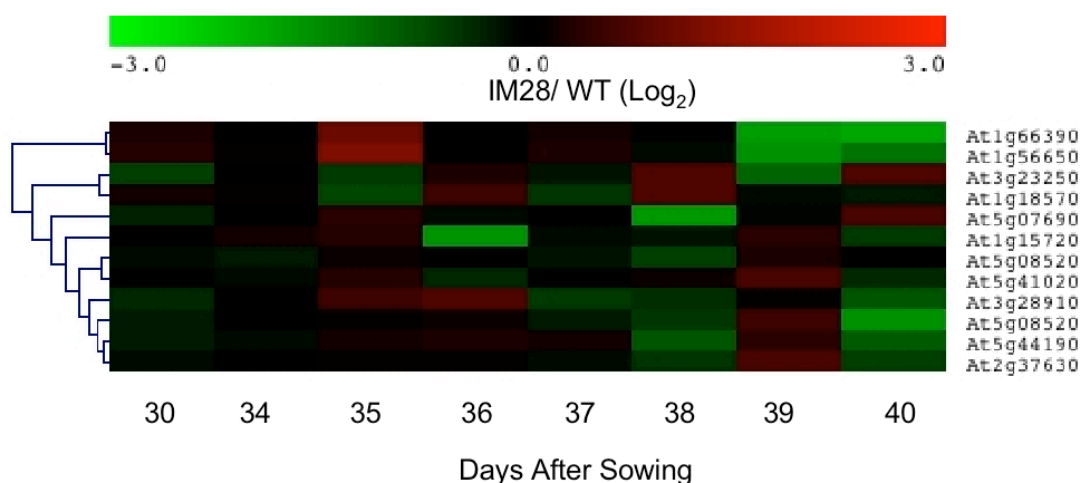


Fig 3.18: Analysis of MYB Genes Differentially Expressed in IM28

Hierarchical Tree of cluster 2. The normalised expression data from MYB genes during the time course were subjected to hierarchical tree clustering (using TMEV software) with euclidean distance and average linkage. Red indicates high IM28/WT ratio and green indicates low IM28/WT ratio. The MYB genes found were *MYB90* (At1g66390), *MYB75* (At1g56650), *MYB15* (At3g23250), *MYB51* (At1g18570), *MYB29* (At5g07690), *MYB* (At1g15720), *MYB* (At5g08520), *MYB* (At5g41020), *MYB30* (At3g28910), *GLK2* (At5g44190), *MYB91* (At2g37630).

3.3.6 Real Time PCR Analysis to Check Microarray Results

The gene expression of *MYB90*, *MYB75*, *CHS* and *SAG12* in WT and IM28 was analysed by real time PCR to compare with the microarray results, shown in figure 3.19.

3.3.6.1 *MYB90*

There was undetectable or very low expression of *MYB90* in the WT from 22-38 days following sowing. The expression began to increase from day 38 to 39 with the highest on day 41 (Fig 3.19 A). As expected IM28 (*MYB90* KO) showed no increased levels of *MYB90* mRNA.

3.3.6.2 MYB75

The expression of *MYB75* in WT was very variable during development (Fig 3.19 B). Replicate one had high expression at 22, 36, 37 and 41 days following sowing. Expression of *MYB75* in IM28 was very low throughout development compared to WT, which indicates that *MYB90* may be a positive regulator of *MYB75*.

3.3.6.3 Chalcone synthase

There was very low expression of *CHS* from 22 to 37 days following sowing in the WT. Expression levels increased from day 38 with highest expression at day 41 (Fig 3.19 C). This pattern of expression during development was similar to the expression of *MYB90* (Fig 3.19 A). There was reduced expression of *CHS* in IM28 compared to WT at the later stages of development, indicating that *MYB90* had a role regulating this gene, at least during senescence.

3.3.6.4 SAG12

SAG12 is a reliable marker of senescence and was previously shown to be expressed late in senescence process (Lohman *et al.*, 1994). There was no or very low *SAG12* expression from 22 to 38 days after sowing in WT, expression then increased at day 39 and was highest at days 40 and 41 (Fig 3.19 D). This indicates that the increased expression of *MYB90* and *CHS* was associated with senescence. IM28 had similar *SAG12* expression to WT indicating little effect on the senescence process itself by the mutation.

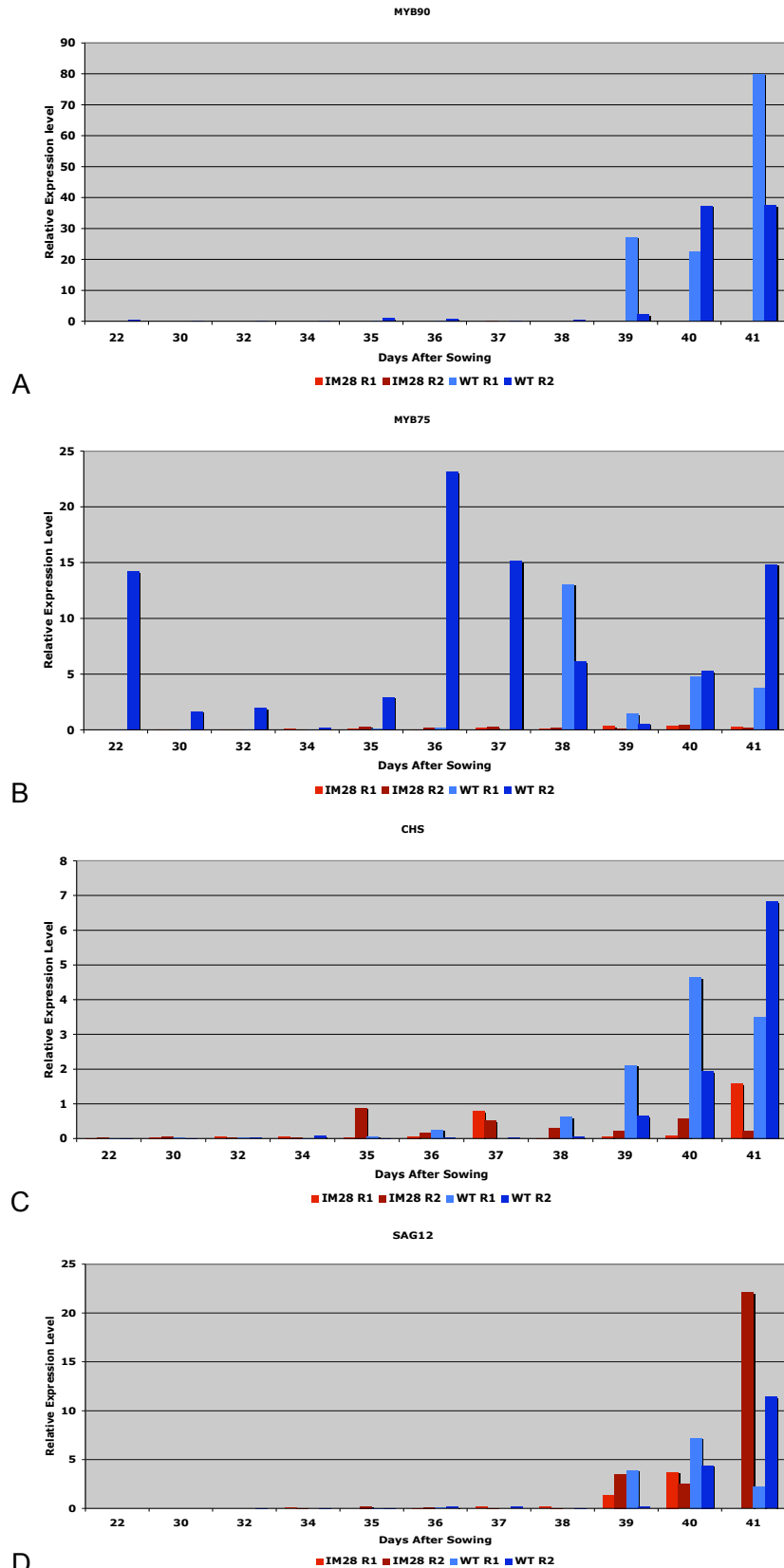


Fig 3.19: The Relative Expression of (A) *MYB90*, (B) *MYB75*, (C) *CHS* and (D) *SAG12* in the Seventh Rosette of WT and IM28 During Development. Gene expression level was estimated using Real Time PCR and standardised against Tubulin expression.

3.4 Analysis of Anthocyanin Biosynthesis During Leaf Development.

Changes in anthocyanin during senescence have not been previously investigated in detail in Arabidopsis leaves. Therefore it was of interest to determine the changes in both total anthocyanin content and the individual components throughout the development of the leaf. Also, in the microarray experiment IM28 was shown to have reduced expression of certain anthocyanin biosynthesis pathway genes (Fig 3.11), which might be expected to be seen by a reduction or change in the products of the anthocyanin pathway in the mutant.

3.4.1 Anthocyanin Biosynthesis Plant Growth Experiment

The eighth rosette leaf of COL-0 and IM28 was tagged with cotton and was harvested from ten replicates at 24, 27, 30, 33, 36, 39 and 42 days after sowing for anthocyanin and flavonoid extractions. Leaf material was pooled and frozen rapidly in liquid nitrogen and then stored at -80°C

3.4.2 Total Anthocyanin Measurements

The total anthocyanin content was measured in the 8th leaf of IM28 and WT during the course of development. The results showed that both IM28 and WT had the highest total anthocyanin content at 42 days after sowing (Fig 3.20), with no significant difference seen between the two lines. The anthocyanin content increased significantly in both lines after 36 days from sowing ($P=0.02$).

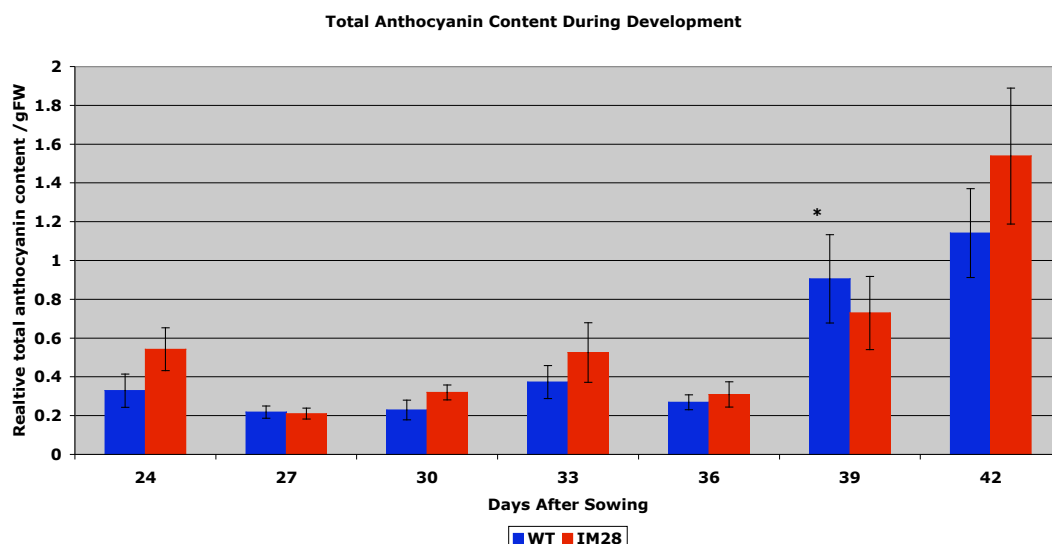


Fig 3.20: Analysis of the Total Anthocyanin Content During Development of Leaf 8

The measurement of total anthocyanins in the MYB90 knockout mutant (IM28) and WT during development. Results are presented as mean (n=10) /gFW \pm SE.

There was a significant difference in the WT between the time points (*) 36 and 39, $P=0.02$

3.4.3 Anthocyanin Composition During Development

The representation of different anthocyanin components at different stages during senescence has not been previously investigated. Anthocyanins were extracted from five replicates of leaf 8 from WT and IM28, and the anthocyanin profile analysed by HPLC DAD detection (Fig 3.21& 3.22).

In the WT at the early stages of leaf development from 24 to 30 days after sowing, a single anthocyanin peak was detected, a₁(Fig 3.21). This peak continued to be the highest peak throughout development. Several new peaks were observed at day 33 and the size of the peaks had increased. Day 36 after sowing had a similar profile. Following that a significant increase of around 100 fold in the height and number of the anthocyanin peaks was observed for WT at day 39. By day 42 the level of anthocyanins had decreased dramatically. This is different from the total anthocyanin measurements (Fig 3.20), which suggests that there may be another compound measured at 530nm.

COL 0

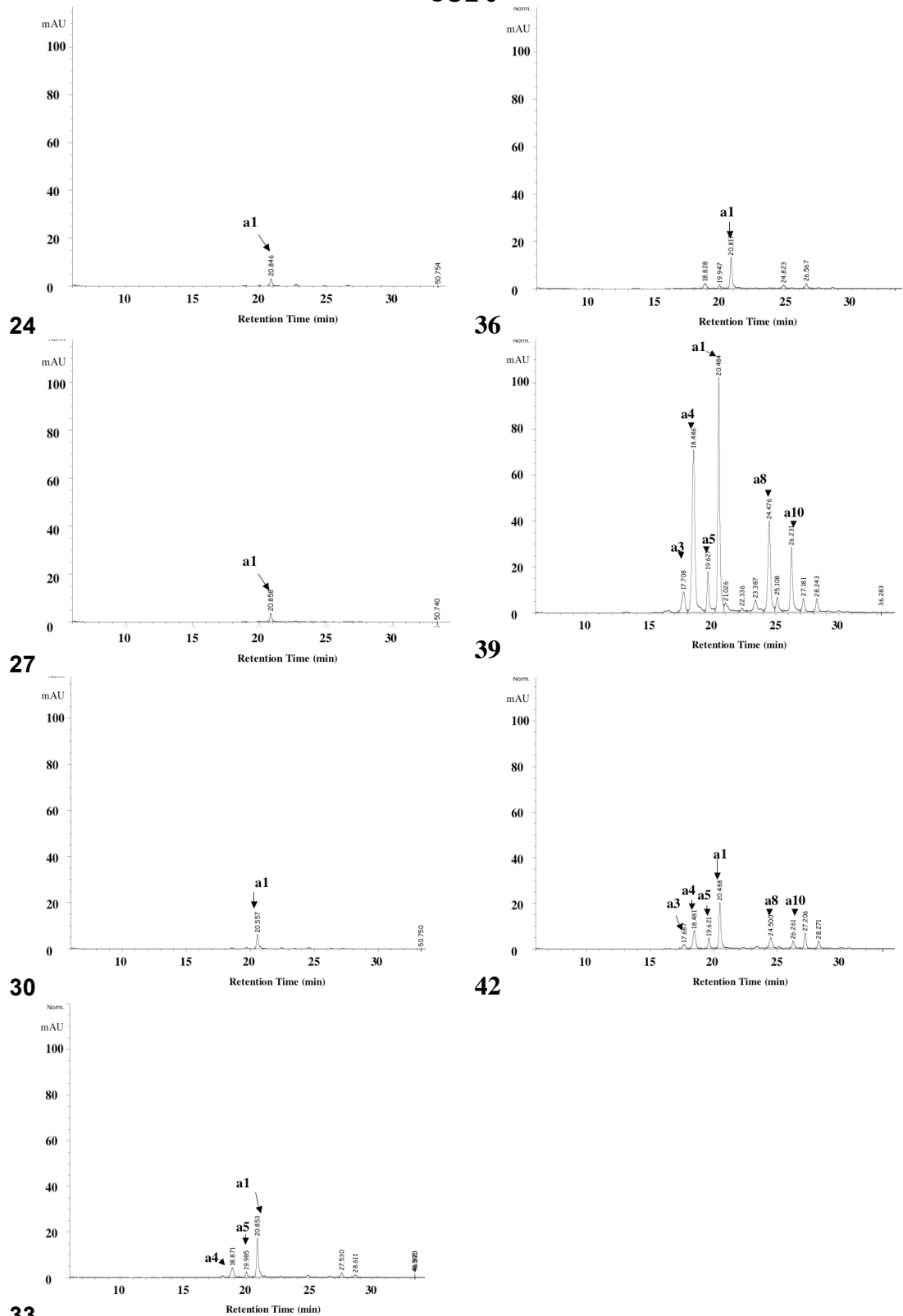


Fig 3.21: Anthocyanins in leaf 8 from WT during development, days 24, 27, 30, 33, 36, 39 and 42. Each trace is from one of five replicates and represents a good example from the five. The arrows indicate the main anthocyanin components.

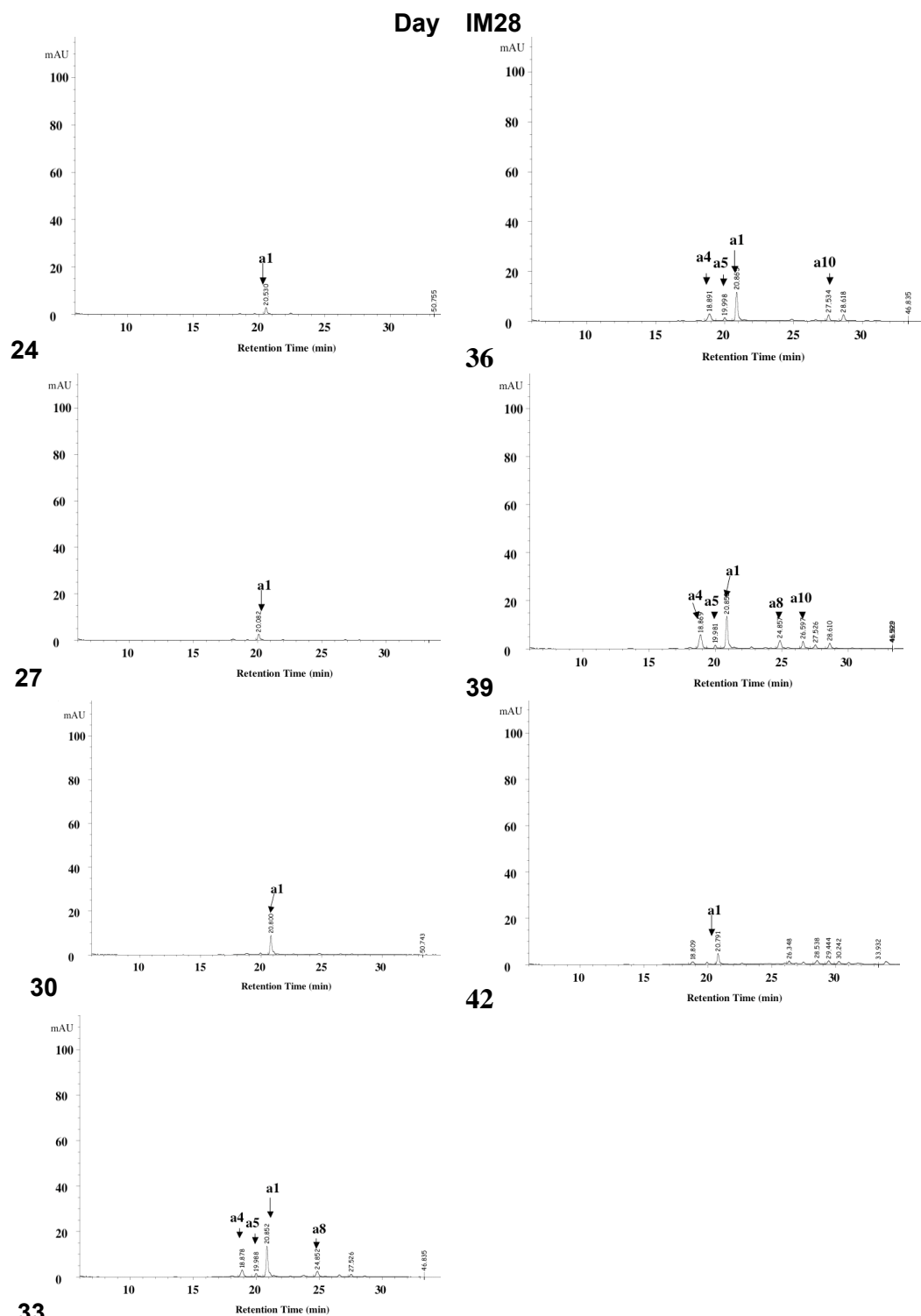


Fig 3.22: Anthocyanins in leaf 8 from IM28 during development. Each trace is from one of five replicates and represents a good example from the five. The arrows indicate the main anthocyanin components.

Throughout development IM28 had a similar anthocyanin profile to WT (Fig 3.21 & 3.22), except at day 39, where the levels of anthocyanins were significantly less in the mutant than in the control. This is an indication that between day 36 and 39 there may

be a key stage of development when there is a requirement for increased biosynthesis of anthocyanins. The regulation of anthocyanin biosynthesis at this stage required expression of *MYB90*.

3.4.3 Quantitative Analysis of the Anthocyanin Composition.

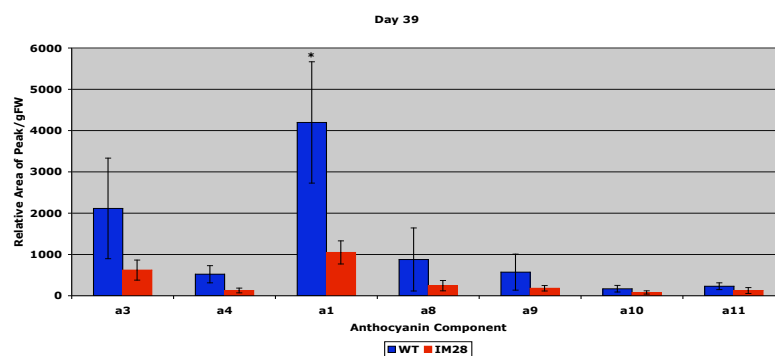
The anthocyanins measurements showed, not only that the number of anthocyanins produced increased in later stages of development, but also that the proportion of each was different at the different time points. Each anthocyanin assay was carried out on five replicates of single leaf extracts per time point. To obtain an overall view of the average anthocyanin content at each time point, the area under the peaks were measured and the average amount of each component was calculated (Fig 3.23A-B).

At day 39 IM28 had significantly lower level of peak a1 than WT (Fig 3.23A). At day 42 (Fig 3.23 B) there was no significant difference between IM28 and COL 0 for any of the anthocyanin peaks. The highest anthocyanin peak for WT and IM28 at any development stage was a1.

3.5 Analysis of the Flavonoid Biosynthesis During Leaf Development

The effect of the knockout of *MYB90* in IM28 on the flavonoid biosynthesis was investigated by analysing the flavonoid content and composition of IM28 and WT during leaf development.

A



B

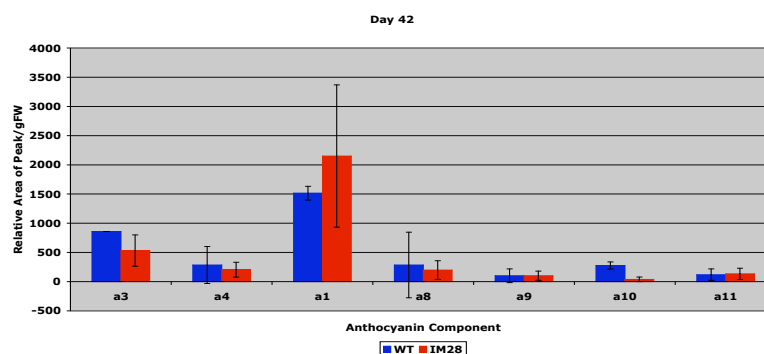


Fig 3.23: Quantitative Analysis of the Anthocyanin Composition.

An average anthocyanin content of time points day 39 (A) and 42 (B), the area under the peaks was measured and the average of each component was calculated, presented as mean \pm SE. (A) There was a significant difference between WT and IM28 a1 content $P=0.05$

3.5.1 Flavonoid Composition of WT and IM28

Flavonoids were extracted from five replicates of leaf 8 and the components analysed by HPLC DAD detection (Fig 3.24 and 3.25). Throughout development, IM28 had a similar flavonoid profile to WT with only one prominent peak f1 (Fig 3.24) and many smaller peaks. The number of different flavonoid peaks increased gradually from day 30 to later stages. The only obvious difference between IM28 and WT was at day 39 where the peaks appeared to be about half the size in IM28 as in WT.

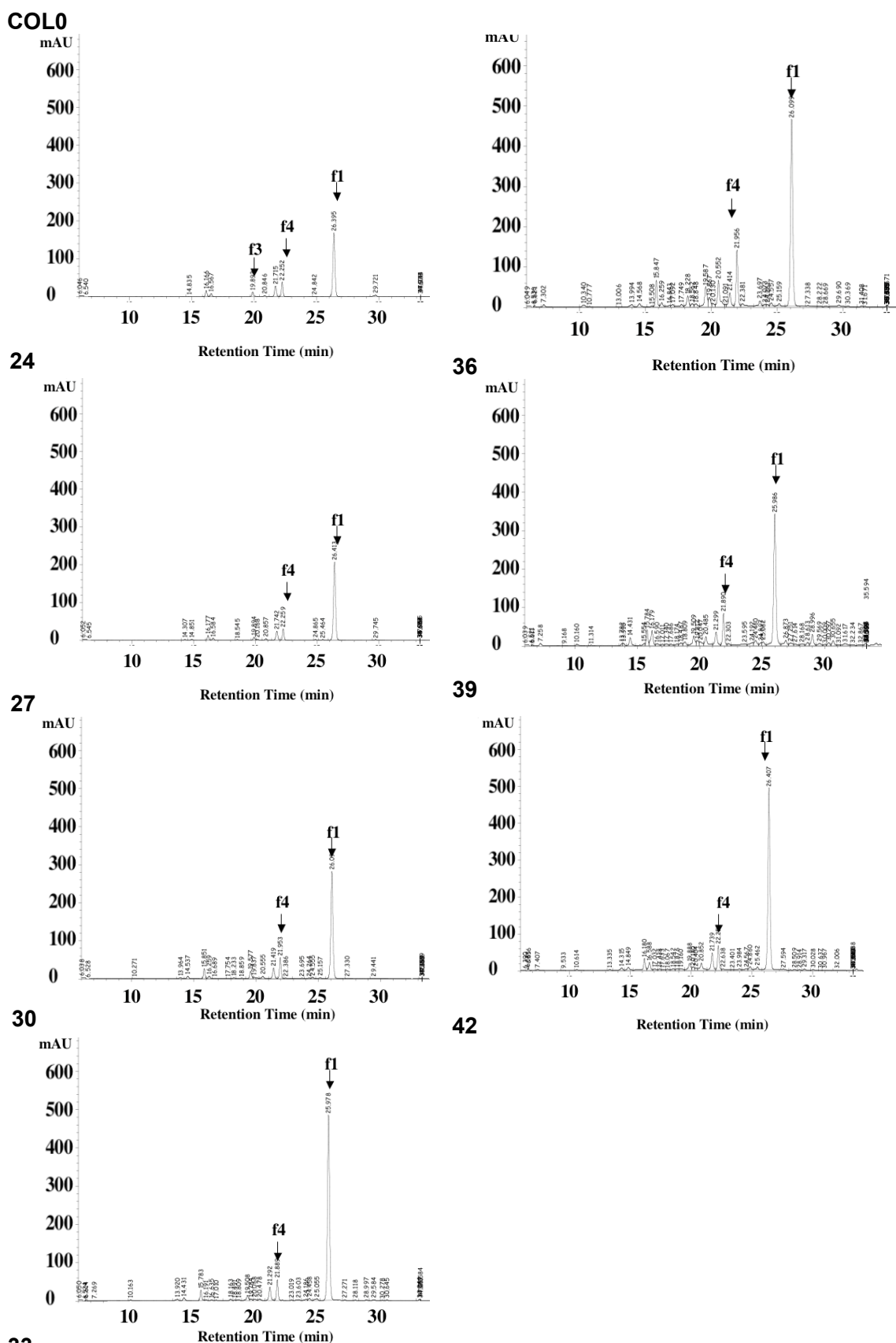


Fig 3.24: Flavonoids in leaf 8 from WT during development. Each trace is from one of the five replicates and represents a good example from the five. The arrows indicate the main flavonoid components.

3.5.2 Total Flavonoid Content Measurement

The total flavonoid content was calculated by measuring the total area of the peaks from the flavonoid profiles (Fig 3.26). This showed that in contrast to the anthocyanin data, flavonoid levels were high in young leaves, dropped slightly and then increased again as leaves aged. This implied a differential regulation between flavonoid and anthocyanin synthesis early in development. In IM28 the flavonoid content followed the same pattern as the WT until day 36 where there was higher level of flavonoids in the mutant and than on day 39 there was reduced flavonoid level in IM28. This correlated with the anthocyanin data and may indicate that *MYB90* is important for flavonoid synthesis at this development stage. The flavonoid level was restored to WT by day 42.

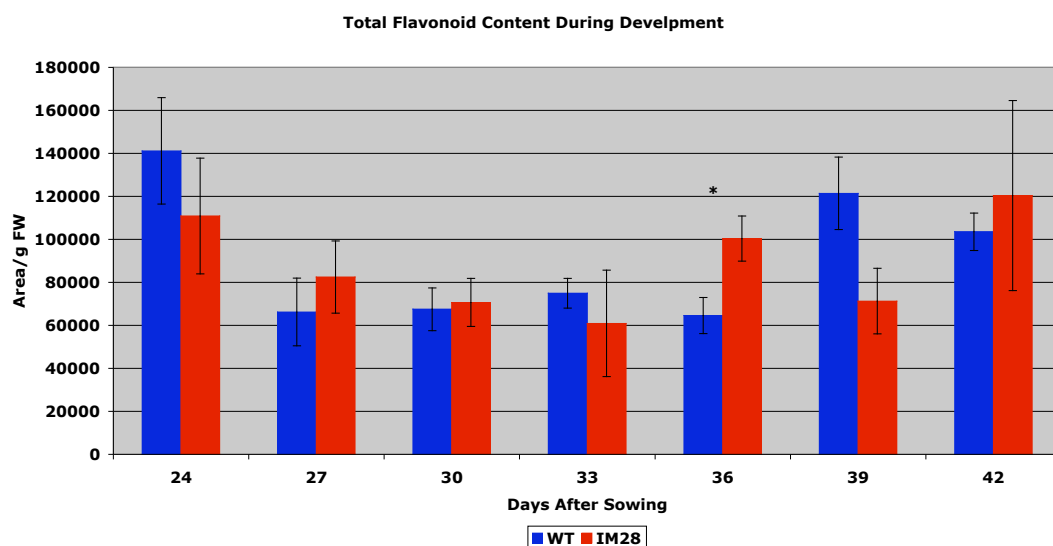


Fig 3.26: Total Flavonoid Content in the Eighth Rosette Leaf From WT and IM28.

The analysis of total flavonoids by separation of flavonoids by HPLC DAD detection in *MYB90* knockout mutant (IM28) and WT during development. Results are presented as mean (n=5) total area of peaks/gFW \pm SE.

There was a significant difference between WT and IM28 at day 36, $P=0.017$.

3.6 Conclusions

In this chapter the effect of the absence of *MYB90* during development was investigated by comparing the phenotype of the *MYB90* knockout with the WT. Chlorophyll content, protein content, photosynthesis parameters, gene expression and anthocyanin biosynthesis were assessed.

3.6.1 Total Chlorophyll and Protein Levels During Development

There appeared to be no visible difference in the phenotype of the seventh rosette leaf in the *MYB90* knockout mutant, IM28, when compared to the WT during development and senescence. In both lines there was a decline in chlorophyll content from day 39 to day 41 after sowing. The protein content also greatly decreased from day 39 to 41 after sowing. The chlorophyll and protein content was lower in the WT at day 22 compared to IM28, which may be due to the development of the leaf. Both chlorophyll and protein levels were lower in IM28 at day 37 than in the WT which may indicate the early onset of senescence in the mutant.

3.6.2 Photosynthetic Performance

During early senescence photo-oxidative protection has been seen to help maintain chloroplast function (Munné-Bosch & Peñuelas, 2003) and in senescent Aspen leaves the photosynthetic performance is maintained until late stages of senescence, when there was a loss of 80% of chlorophyll (Keskitalo *et al.*, 2005). Similarly in this study the Fv/Fm was maintained during senescence in the WT until a late stage. However, analysis of photosynthetic performance did indicate some differences between the WT and IM28. The maximum PS2 efficiency (Fv/Fm) was lower in the WT at day 22, which was also reflected in the chlorophyll and protein content. Also at day 36, IM28 had a lower Fv/Fm compared to the WT, which may also be reflected by a consequent chlorophyll and protein difference seen at day 37. Bjorkman & Demming (1987) observed an inverse correlation between Fv/Fm levels and photoinhibition and so the conclusion can be made that IM28 plants at day 36 were exposed to more stress than

the WT plants leading to some damage in the reaction centres, resulting in photoinhibition. This occurs when the light levels are near to saturating the photosynthesis machinery (Barr *et al.*, 1975, Debus *et al.*, 1988) and results in the modification of the D1 protein bound to PS2 and the destabilisation of a D1 bound electron acceptor, semiquinone Q_B , which results in the formation of Q_A^- (Ohada *et al.*, 1990). The intrinsic fluorescence levels increase and there is a reduction in the rate of electron flow. There is a reduced maximum fluorescence caused by the dissociation of PS2 reaction centre from the antenna complexes (Schuster *et al.*, 1986). This indicates that there was not sufficient protection in the absence of *MYB90* against photoinhibition. Non-photochemical quenching mechanisms involve the Mehler peroxidase reaction producing electron flow from PSII to PSI without net oxygen gain (Asada, 1999) and produces a proton gradient needed for the xanthophyll cycle, which reduces excess excitation in response to fluctuations in irradiance and short durations of high light stress (Li *et al.*, 2002). Other protective mechanisms include antioxidants such as α -tocopherol and ascorbate (Munné-Bosch & Peñuelas, 2003, Müller-Moulé *et al.*, 2002) and pigments to absorb light energy such as β -carotene (Munné-Bosch & Peñuelas, 2003) and anthocyanins (Field *et al.*, 2002, Hoch *et al.*, 2001, Liakopoulos *et al.*, 2006).

Further analysis of other photosynthetic parameters including PSII operating efficiency ($F'q/F'm$), photochemical quenching (PQ), non-photochemical quenching (NPQ) and linear electron transport rate at day 36 showed that IM28 had a higher PQ than the WT. This suggests that at day 36 in IM28 there was a higher proportion of light absorbed by chlorophyll associated with PSII that was utilised in photochemistry, this compensated for the reduced F_v/F_m , which resulted in WT level of $F'q/F'm$ and electron transport.

Measurements of other photosynthetic parameters in the WT indicated a gradual decline in photosynthetic performance as the seventh rosette leaf aged. However in IM28 at day 32 these parameters were low and comparable to day 36 in IM28. This indicates that there was some stress on PS2 reaction centres at day 32 due

to an imbalance of light capture and utilisation and there was recovery by day 34. Comparison of the parameters at day 32 in WT and IM28 showed that the $F'q/F'm$, PQ and linear electron transport rate were lower in IM28. This indicates that there was a reduction in the available electron acceptors and a closure of reaction centres, which reduced the linear electron transport rate and the proportion of light absorbed used in photochemistry due to reduced carbon metabolism (Maxwell & Johnson, 2000).

3.6.3 Gene Expression During Development

Gene expression studies during development of the seventh rosette leaf in WT and IM28 showed a cluster of genes that had reduced expression in IM28 during senescence. In this cluster there were several key anthocyanin and flavonoid biosynthesis genes suggesting that the anthocyanin biosynthesis pathway was regulated by *MYB90* during senescence. *MYB75* was also found in this cluster, which suggests that *MYB90* is an upstream regulator of *MYB75* during senescence. A *beta-amylase* (*BMV1* At4g15210) was found in this cluster and sugar has previously been reported to induce anthocyanin biosynthesis accumulation and a mutant that had decreased β -amylase expression had reduced sugar induced anthocyanin levels (Mita *et al.*, 1997a,b). *MYB90* is induced by low nitrogen and high glucose levels and *MYB75* was found to be required for sucrose induced anthocyanin biosynthesis (Pourtau *et al.*, 2005, Teng *et al.*, 2005). These results suggest that *MYB90* may have a role in sugar response during senescence.

The genes in this cluster were found to be enriched for CACGTG and ABRE-like promoter motifs. The CACGTG motif is also known as the Gbox and the ABRE-like motif is similar to the Gbox. These motifs are regulated by light, stress and abscisic acid (Menkens & Cashmore, 1994, Shinozaki & Yamaguchi-Shinozak, 2000). There were also several MYB binding site motifs found in the promoters of these genes.

The absence of *MYB90* had a knock on effect to downstream genes. Nesi *et al.*, (2001) and Baudry *et al.*, (2005), previously reported *TT8* to be regulated by *MYB75* and the expression level of *TT8* was reduced in IM28 compared to the WT

from day 38 to day 41, during senescence. TT8 is a bHLH transcription factor that regulates anthocyanin biosynthesis by forming a transcriptional complex, consisting of a WD40 protein, *TTG1*, and the MYB transcription factors MYB90 and MYB75 (Koes *et al.*, 2005, Ramsey *et al.*, 2003, Zimmermann *et al.*, 2004, Zhang *et al.*, 2003, Baudry *et al.*, 2004, Baudry *et al.*, 2006 & Nesi *et al.*, 2001). Reduced expression of *MYB90*, *MYB75* and *TT8* may reduce the activity of the transcription factor complex and resulting in reduced transcriptional activation of anthocyanin biosynthesis genes in IM28.

There was a cluster of genes that were highly up-regulated in IM28 compared to the WT at day 38 after sowing. These genes had roles in response to stress, signal transduction, transport and protein metabolism.

3.6.4 Anthocyanin Biosynthesis During Development

Anthocyanin accumulation is associated with senescence (Hoch *et al.*, 2001, Keskitalo *et al.*, 2005). Anthocyanins provide protection against photo-oxidative damage by absorbing light when leaves are more susceptible to photoinhibition (Hoch *et al.*, 2001) and potentially as antioxidants (Yokozawa *et al.*, 1998, Shao *et al.*, 2007). The reduction of light absorbed by chlorophyll would reduce the requirement for the dissipation of heat energy by activity of the xanthophyll-cycle, which would be stretched under stressful conditions (Hendrickson *et al.*, 2004, Liakopoulos *et al.*, 2006). *MYB90* and *MYB75* were shown to be involved in the regulation of anthocyanin and flavonoid biosynthesis by Borevitz *et al.*, (2000). Transgenic plants that over expressed *MYB90* or *MYB75* had a massive induction of anthocyanin and flavonoid biosynthesis (Borevitz *et al.* 2000, Tohge *et al.*, 2005). The gene expression studies indicated that reduced anthocyanin biosynthesis might be expected during senescence in IM28 since significantly reduced expression of key genes such as *DFR*, *CHS* etc. is seen in the mutant. However, anthocyanin measurements showed that anthocyanin levels did increase during senescence in IM28. These results suggest an alternative pathway for anthocyanin and flavonol biosynthesis, which does not depend on *MYB90* or *MYB75*. A

possibility for this was seen in a study by Buchanan-Wollaston *et al.*, (2005), who identified an alternative pathway during dark-induced senescence. However the gene expression data did not show the alternative anthocyanin biosynthesis genes to have increased expression in the *MYB90* knockout compared to the WT, it was in fact the opposite.

Analysis of the anthocyanin profiles showed that the level and number of anthocyanin components increased during development in both the WT and IM28. There was one main anthocyanin component, a1, in all the time points. This anthocyanin is likely to be cyanidin 3-O-[2"-O-6"-O-(sinapoyl) xylosyl] 6"-O-(p-O-(glucosyl)—p-coumaroyl glucoside] 5-O-(6"-O-malonyl)glucoside. Tohge *et al.*, 2005 found this cyanidin derivative to account for 74% of the anthocyanin content in WT *Arabidopsis*. The anthocyanin profiles showed that there was a significant difference in the anthocyanin content between WT and IM28 at day 39. The WT had higher anthocyanin levels, with a significant difference in the main anthocyanin component, a1. The level of anthocyanins decreased in the WT from day 39 to day 42. This change was not observed in the total anthocyanin content, which indicates that there may have been another compound in the extract that had the same absorbance as anthocyanins, such as carotenoids. Lazcona *et al.*, (2001) had difficulty measuring anthocyanin levels in transgenic carrots because of the high carotenoids levels. In senescing Aspen leaves carotenoids were degraded at a slow rate and there was an accumulation of carotenoids derivatives (Keskitalo *et al.*, 2005).

3.6.5 Flavonoid Biosynthesis During Development

The flavonoid content was high in the early time points in both WT and *MYB90* knockout and dropped slightly and then increased during late development. At day 36 the *MYB90* knockout had significantly higher flavonoid content than the WT. The flavonoid profiles showed one main flavonoid component, f1 present in all the extracts. This flavonoid component was likely to be kaempferol dirhamnoside (Tohge *et al.*, 2005, Veit & Pauli, 1999). The level and number of flavonoid components increased

during development of the WT. At day 39 there appeared to be a reduced level of the flavonoid components in IM28 compared to the WT. These results indicated that the flavonoid biosynthesis was separated from anthocyanin biosynthesis during early development and there may be an alternative gene and pathway regulating flavonoid biosynthesis in the *MYB90* knockout.

3.6.6 Other Potential MYB Transcription Factors Involved in Anthocyanin Biosynthesis.

The increased anthocyanin content and increased number of anthocyanin components during senescence in IM28 plants showed that there was an increased level of anthocyanin biosynthesis. This suggested that there was another gene compensating for the absence of *MYB90* expression. This was likely to be a MYB gene because they have been shown to be required for anthocyanin biosynthesis in many species (Goff *et al.*, 1992, Davies and Schwinn, 2003, Quattrocchio *et al.*, 1999). Transgenic plants over-expressing *MYB113* and *MYB114* had TTG1 and bHLH dependent accumulation of anthocyanins, similar to that seen previously in plants over-expressing *MYB75* (Gonzalez *et al.*, 2008). There were several differentially expressed MYB genes in the *MYB90* knockout plants. *MYB15* and *MYB51* had increased level of expression at days 38 and 40, and a group of MYB genes including *MYB29*, *MYB30*, *GLK2* and *MYB90* had increased expression at day 39 in IM28 compared to the WT. One or more of these genes may have been responsible for the increased anthocyanin biosynthesis.

3.7 Summary

In summary, data presented in this chapter shows that the *MYB90* gene has a role in controlling anthocyanin synthesis during senescence. The physiological effects of the knockout mutant are clearly measurable at specific stages of development and the mutation also has an effect on gene expression and anthocyanin levels that reflect function of *MYB90* in controlling anthocyanin biosynthesis genes such as *DFR* and *CHS*. However, data show that *MYB90* is not essential for anthocyanin biosynthesis during senescence.

4 The Role of *MYB90* During Plant Stress Responses

4.1 Introduction

In the previous chapter the absence of *MYB90* was shown to decrease the expression of genes involved in anthocyanin and flavonoid biosynthesis during senescence resulting in reduced anthocyanin levels at one time point and altered physiological parameters. As discussed in the introduction, increased expression of *MYB90* and accumulation of anthocyanins during different stresses has been shown previously. Anthocyanins provide protection against photo-oxidative damage during stress, particularly high light levels.

The hypothesis to be tested in this chapter is that *MYB90* is required for the synthesis of anthocyanins in the response to stress. Further investigation into the role of *MYB90* was carried out, by comparing the effects of high light on growth, phenotype and photosystem II parameters in IM28, and WT (COL-0). In addition the total anthocyanin content and the individual anthocyanins and flavonoid components were measured and compared in the two plant lines following light stress treatments.

4.2 High Light Stress

4.2.1 High Light Plant Growth Experiments

The effect of a high light ($830\mu\text{mol}/\text{sec}/\text{m}^2$) stress on the growth and phenotype of WT plants was initially investigated and compared with the effects on the *MYB90* mutant IM28. Plants were grown in glass house with a 16h light period at 21°C . WT and IM28 were grown in compost in the glass house during March when the light intensity was $150\mu\text{mol}/\text{sec}/\text{m}^2$. Eight plants of COL-0 and IM28 aged 49 days after sowing were placed under a sodium lamp and exposed to high light ($830\mu\text{mol}/\text{sec}/\text{m}^2$) for 72hours.

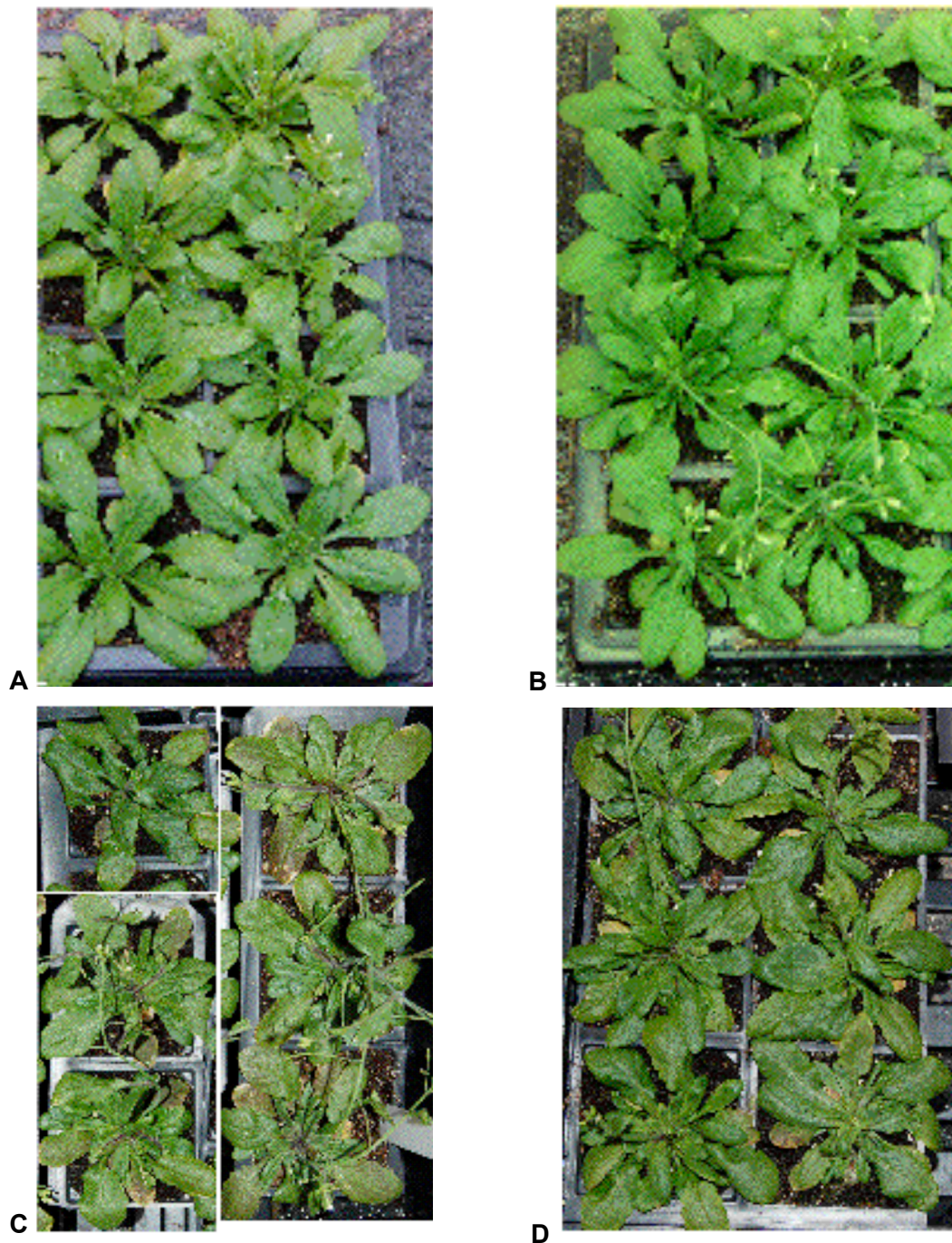


Fig 4.1: WT and IM28 High Light Plant Growth Experiment.

WT and IM28 plants after 72 hours of high light stress under a sodium lamp. (A) untreated WT, (B) untreated IM28, (C) WT light stressed and (D) IM28 light stressed. The untreated WT and IM28 appeared green and healthy. Following 72 hours of high light exposure the WT plants were smaller than the untreated plants and had yellowing at the edge of leaves and purple pigmentation. IM28 plants exposed to 72h high light were smaller than the untreated mutant plants. The larger leaves were mostly green and the older leaves were yellow/green with some purple pigmentation.

After this treatment both the WT and IM28 showed an altered phenotype, their growth over the period of time had been altered and the rosettes of both lines were smaller compared to the untreated plants (light levels approximately 150 $\mu\text{mol}/\text{sec}/\text{m}^2$) (Fig 5.1 A-D). Also the WT rosettes following high light appeared to be smaller than IM28 rosettes (Fig 4.1 C & D).

The colour of the rosettes also showed some differences following treatment and with both WT and IM28 displayed yellowing of the tips of leaves. The WT also had purple pigmentation of the leaves and stems (Fig 4.1).

4.2.2 The Role of MYB90 in Anthocyanin Biosynthesis During High Light Exposure

Whole rosettes of glasshouse grown WT and IM28 were harvested following 72h exposure to high light. Total anthocyanins were extracted for analysis as described in the methods.

4.2.2.1 Total Anthocyanin Content Measurement

The anthocyanin assay was carried out on extracts of whole rosette harvested after 72hr high light treatment. The light stressed WT exhibited an approximately 40 fold increase in anthocyanin content compared to the untreated plants, whereas light stressed IM28 showed an approximately 15 fold increase in anthocyanin content. There was a significantly lower total anthocyanin content in IM28 compared to WT after 72 hours of high light at (Fig 4.2). The controls contained similar anthocyanin levels and these were significantly lower than the levels measured in the stressed plants from both the mutant and the WT. The significant difference between IM28 and WT light stressed plants shows that *MYB90* was required for the normal response of WT to the high light stress. However, IM28 stressed plants did have a significantly higher anthocyanin content than the untreated IM28 controls which shows there must be an alternative pathway for anthocyanin biosynthesis that does not require *MYB90* expression.

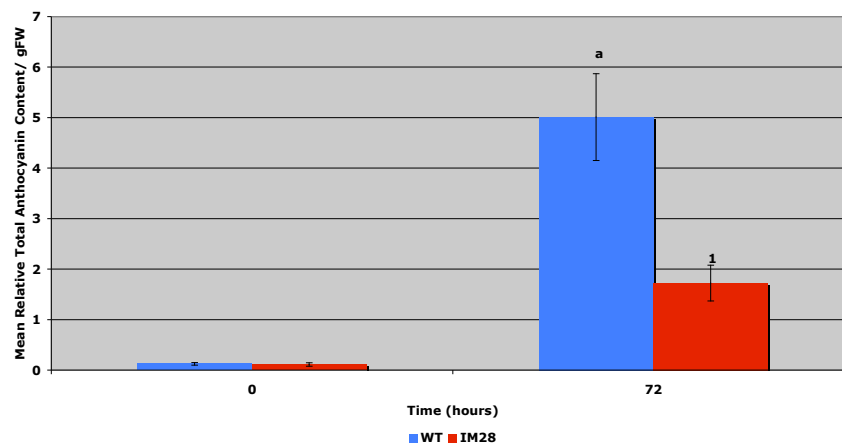


Fig 4.2: Total Anthocyanin Measurement

The analysis of total anthocyanins of eight whole rosette replicates from glasshouse grown IM28 and WT harvested after 72hours of high light stress. Results are presented as mean (n=8) \pm SE. High light treated WT showed significantly higher anthocyanin levels compared to untreated control (a, $P=0.0007$) and treated WT showed significantly more anthocyanin than the treated mutant (1, $P= 0.006$).

4.2.2.2 Anthocyanin Profiles

To investigate the reduced anthocyanin levels in more detail, profiles of individual anthocyanin composition in IM28 and WT were obtained by HPLC separation of the total anthocyanin extracts. Figure 4.3 and 4.4 shows typical profiles for one of the replicates of WT and IM28 with and without the high light treatment. Figure 4.4 shows the average results for all five replicates for each treatment.

The IM28 untreated plants showed a similar anthocyanin profile to the WT untreated plants (Fig 4.3 A and C). The high light stressed WT (Fig 4.3B) had four large prominent peaks (a1, a4, a8 & a10), while IM28 had one prominent anthocyanin peak (a1) (Fig 4.3 D) and three smaller peaks (a4, a8 & a10). Therefore, the difference between the total anthocyanin content in IM28 and WT light stressed plants (Fig 4.2) may be due to the reduced accumulation of these three specific anthocyanins in IM28 (Fig 4.3D).

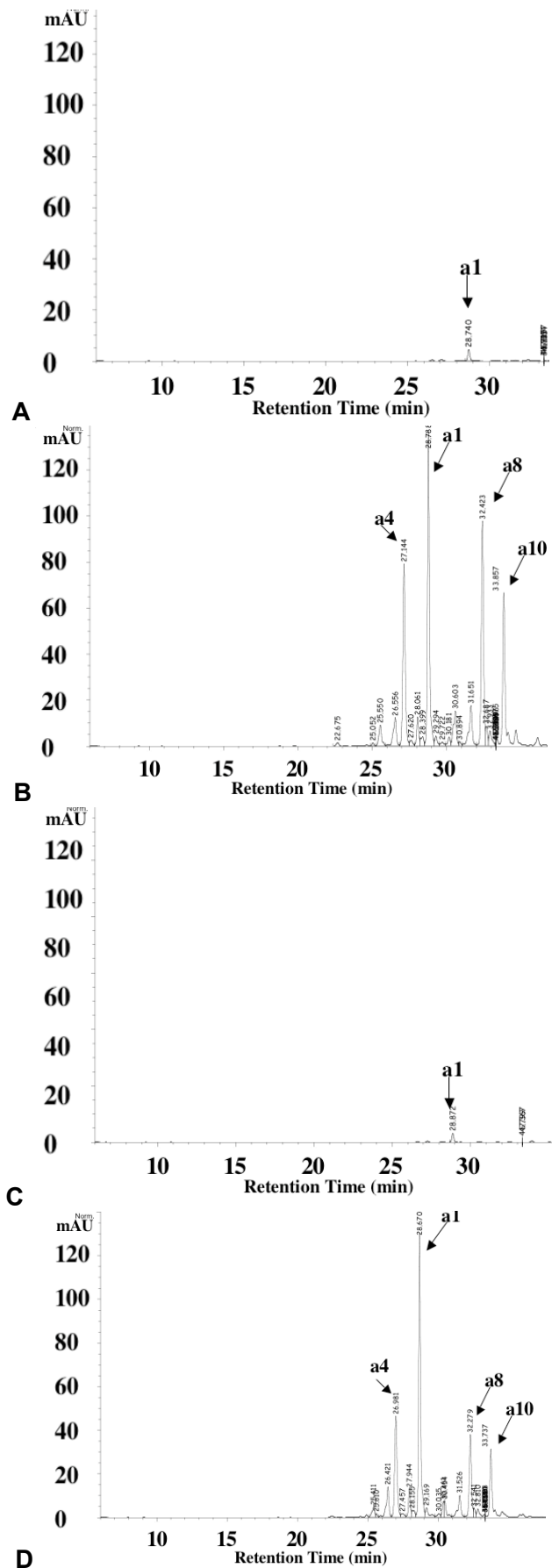


Fig 4.3: Anthocyanin Profiles of WT and IM28 Following High Light Exposure

Anthocyanin profiles of WT and IM28 untreated or following 72h high light treatment. (A) WT untreated and (B) WT high light treated. (C) IM28 untreated and (D) IM28 high light treated.

Arrows indicate the main anthocyanin peaks in IM28 and WT following light stress. This figure shows typical profiles from the five replicates analysed. The arrows indicate the main

4.2.2.3 Quantification of the Anthocyanin Components

The separation of the anthocyanin components showed an increase in the anthocyanins produced after high light stress in both WT and IM28 (Fig 4.3). Each anthocyanin assay was carried out on five replicates of whole rosettes and the areas under the ten main peaks were calculated.

The untreated WT rosettes had one major anthocyanin component (a1) (Fig 4.4). Interestingly IM28 untreated rosettes had a higher level of four of the anthocyanin components. After light stress, both WT and IM28 were shown to have increased anthocyanin content with many more components (Fig 4.5). However, WT had much higher anthocyanin content than IM28 and the four main peaks, anthocyanin components a1, a4, a8 and a10 were significantly higher compared to the same components in IM28.

The results of the high light stress experiment clearly show that *MYB90* was required for the normal response of WT to the stress. In the *MYB90* knockout mutant there were significantly lower levels of the four main anthocyanin components. However there must be some compensation for the absence of *MYB90* in IM28 since the anthocyanin content in IM28 does increase following high light treatment (Fig 4.5).

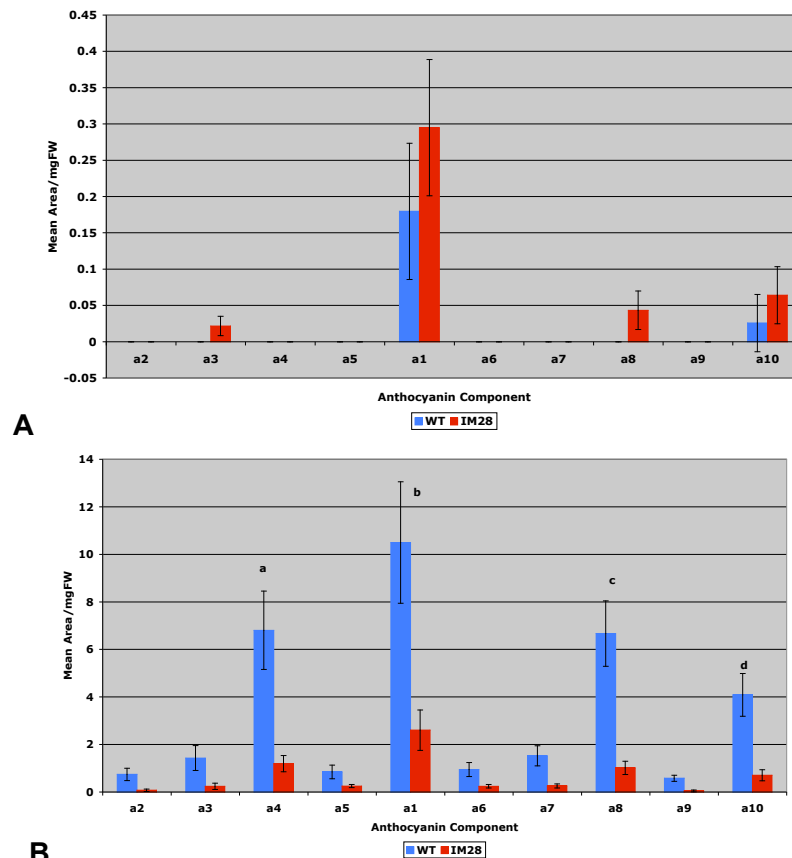


Fig 4.4: Quantification of Anthocyanin Components in Untreated and High Light Treated WT and IM28.

The average of each anthocyanin component was calculated from five replicate anthocyanin profiles of (A) untreated controls and (B) high light treated WT and IM28 rosettes. The area under the anthocyanin peaks were measured and presented as mean $n=5 \pm SE$. (B) There were significant differences between high light treated WT and high light treated IM28 (a) $P=0.025$, (b) $P=0.033$, (c) $P=0.0134$ and (d) $P=0.0178$

4.2.3 Role of MYB90 in Flavonoid Biosynthesis During High Light Exposure

The regulation of flavonoid biosynthesis during high light exposure was of interest because flavonoids protect against photo-oxidative damage and the flavonoid biosynthesis pathway shares some of genes involved in anthocyanin biosynthesis. In the previous chapter these genes were observed to have reduced expression in IM28 during senescence (Chapter 3; Fig 3.11) and the regulation of flavonoid biosynthesis appeared to be separated from anthocyanin biosynthesis during early stages of development (Chapter 3; Fig 3.26).

4.2.3.1 Quantification of the Total Flavonoid Content

The total flavonoid content in the rosettes of the treated and untreated WT and IM28 plants was calculated by measuring the total area of the peaks from the flavonoid profiles (Fig 4.5). The flavonoid content in WT significantly increased following high light stress but there was no significant difference between the treated and untreated IM28 plants and between the high light treated WT and high light treated IM28 plants.

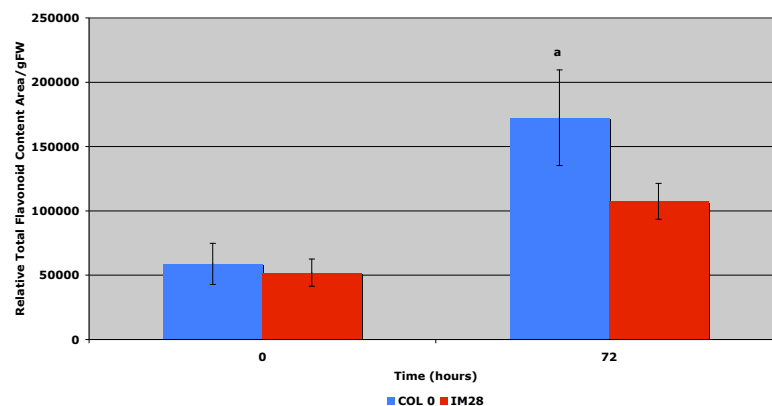


Fig 4.5: Quantification of the Total Flavonoid Content During High Light Exposure

The analysis of total flavonoids WT and IM28 rosettes after 72 hours of high light stress. The average total flavonoid content was calculated from five replicate flavonoid profiles. The area under the flavonoid peaks were measured and results are presented as mean (n=5) total area of peaks/gFW \pm SE. There was a significant difference between untreated and high light treated WT (a) $P = 0.042$.

4.3 High Light Time Course

The initial high light treatment experiment in section 4.1, showed that *MYB90* is required for the normal stress response in WT. To investigate the stress response in more detail using more time points, the experiment was repeated several times but unfortunately the outcome was seriously affected by the time of year. Variables in light levels and day length made it difficult to repeat. Plants grown in the summer were not so affected by the high light treatment. Eventually the effect of high light stress was tested again using WT and IM28 Arabidopsis grown in a shaded environment and treated to a series of high light treatments to assess the effect of the duration of stress

on photosynthesis, anthocyanin and flavonoid biosynthesis and gene expression at different time points.

4.3.1 High Light Time Course Plant Growth Experiment

WT and IM28 were grown in FPL7 pots (70x70x80mm) filled with compost in the glass house under shading at the light intensity of approximately 80 $\mu\text{mol}/\text{sec}/\text{m}^2$. Eight plants of WT and IM28 aged 61 days after sowing were placed under a sodium lamp and exposed to high light (830 $\mu\text{mol}/\text{sec}/\text{m}^2$) treated for 4, 8, 48 and 72 hours.

4.3.2 Chlorophyll Fluorescence Measurements

One physiological parameter that was assessed during the high light time course was chlorophyll fluorescence, since this is a useful tool to study the effects of environmental stresses on photosynthetic performance in leaves (Björkman & Demmig, 1987). The maximum efficiency of Photosystem 2 (PS2) was measured in rosettes of high light treated and untreated WT and IM28, by measuring the chlorophyll fluorescence after dark-adaption (section 2.5, table 5) when all the reaction centres are open. The maximum possible F_v/F_m for healthy leaves is 0.8 and lower levels indicate that a proportion of PS2 reaction centres are damaged.

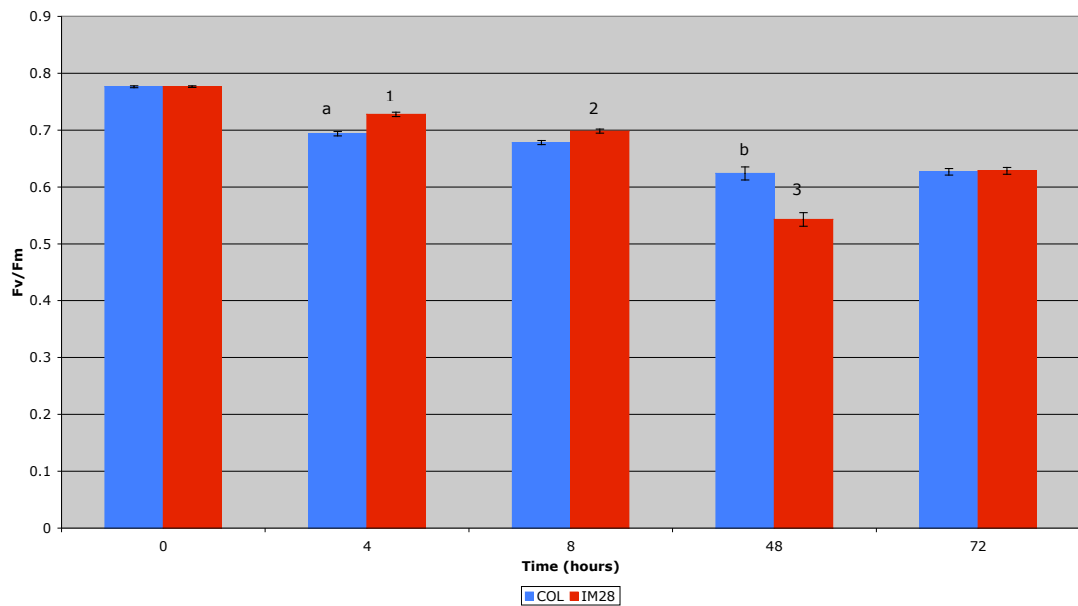
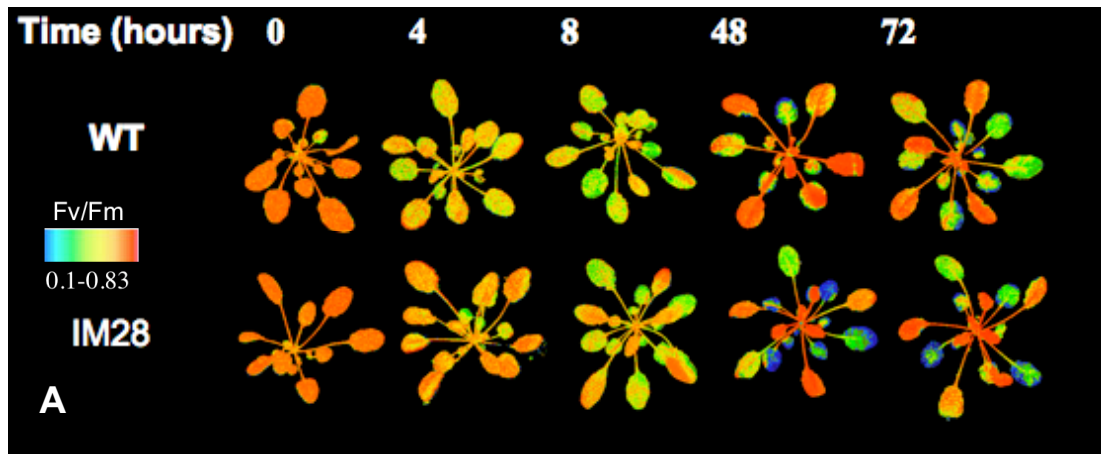


Fig 4.6: The Effect of High Light Exposure Times on the Maximum PS2 Efficiency (Fv/Fm)

The analysis of photosystem 2 efficiency of IM28 and WT by measuring the chlorophyll fluorescence at dark-adapted value after 0, 4, 8, 48 and 72hours of light stress. Fv/Fm fluorescence image (A), orange (high Fv/Fm) to blue (low Fv/Fm). (B) Results presented as mean (n=6) \pm SE. There were significant differences between WT and IM28 following 4, 8 and 48hr high light exposure at (1) $P < 0.001$, (2) $P = 0.003$ and (3) $P < 0.001$.

There were significant differences between WT time points 0 and 4hr (a) $P = 0.000003$, 8 and 48hr (b) $P = 0.0041$.

The Fv/Fm fluorescence images of WT and IM28 rosettes treated to high light stress (Fig 4.6A) show that different leaves have different PS2 efficiencies, this was clearly seen after 48 hours for IM28, the younger leaves of the rosette had high PS2 efficiency

shown by orange colour whereas the older leaves had a low PS2 efficiency shown by blue colour. There were differences between the leaves of WT rosette after 48 hours, but in general the older leaves of the WT appeared to have a higher PS2 (Fv/Fm) than IM28, represented by the orange/yellow in WT compared with green/blue colour in IM28. After 72 hours the WT and IM28 plants appeared more similar.

The different Fv/Fm values of different aged leaves within a rosette seen after 48 and 72hour high light treatment did not occur so obviously in the 4 and 8hour treatments. Following 4 and 8 hour high light all the leaves in a rosette showed decreased photosynthetic performance as shown by the yellow colour. After 48 and 72 hours, the Fv/Fm had decreased further in the older leaves, however the younger leaves appeared to show an increase in Fv/Fm closer to that of the healthy leaf. This suggests that there was recovery of younger leaves of the rosette.

The mean photosystem 2 efficiency (Fv/Fm) was quantified by measuring the chlorophyll fluorescence of six replicate rosettes of WT and IM28 (Fig 4.6 B). The untreated WT had an Fv/Fm of 0.77 close to the maximum efficiency, after 4 and 8 hours of high light stress the Fv/Fm significantly decreased. After 48-hour treatment there was a further significant decrease in Fv/Fm, which remained at the same level after 72h. This indicates that the photosystem 2 efficiency had stabilised after 48+ hour treatment of high light stress in the WT. The changes in Fv/Fm are linked to changes in non-photochemical quenching, specifically the photoinhibition quenching that occurs due to damage to reaction centres. This is a slow acting and slow relaxing process. Therefore the changes in Fv/Fm during the time course (Fig 4.7 B) are due to the level of photoinhibition.

At the time point 0, before any stress treatment, IM28 had a similar Fv/Fm to WT. After 4 and 8-hour high light stress there was significant decrease compared to the untreated IM28 rosettes. Interestingly, the 4 and 8-hour treated IM28 had a significantly higher Fv/Fm than WT but after 48 hours there was a sharp drop that results in levels significantly lower than WT. After 72-hour treatment the Fv/Fm of IM28

had increased back to WT level. This indicates that there was eventual recovery of PS 2 efficiency in IM28 due to a factor compensating for the loss of *MYB90* expression.

4.3.3 Role of MYB90 in Anthocyanin Biosynthesis During Different High Light Exposure Times

4.3.3.1 Total Anthocyanin Content Measurement after Different High Light Exposure Times

The effect of the knockout of *MYB90* in IM28 on the anthocyanin and flavonoid biosynthesis during high light stress was investigated again in this time course experiment. The anthocyanin and flavonoid profiles of IM28 and WT were measured.

Anthocyanin assays were carried out on 6 replicate rosette extracts from WT and IM28 plants treated to a series of high light treatments (Fig 4.7 A, B). There was a significant increase in anthocyanin content in WT after 8 hours of light stress, but no significant differences were seen between the IM28 treatments (Fig 4.7 B). However after 48 hours (Fig 4.8 A) there was a significant increase in anthocyanin content in both plant lines compared to 0, 4 and 8-hour treatments. There was approximately a 106-fold increase for WT and a 134 fold increase for IM28 but most interestingly the WT had a significantly higher content than IM28. After 72 hours the total anthocyanin content had significantly increased from the 48-hour treatment in both lines and IM28 had a similar content to the WT.

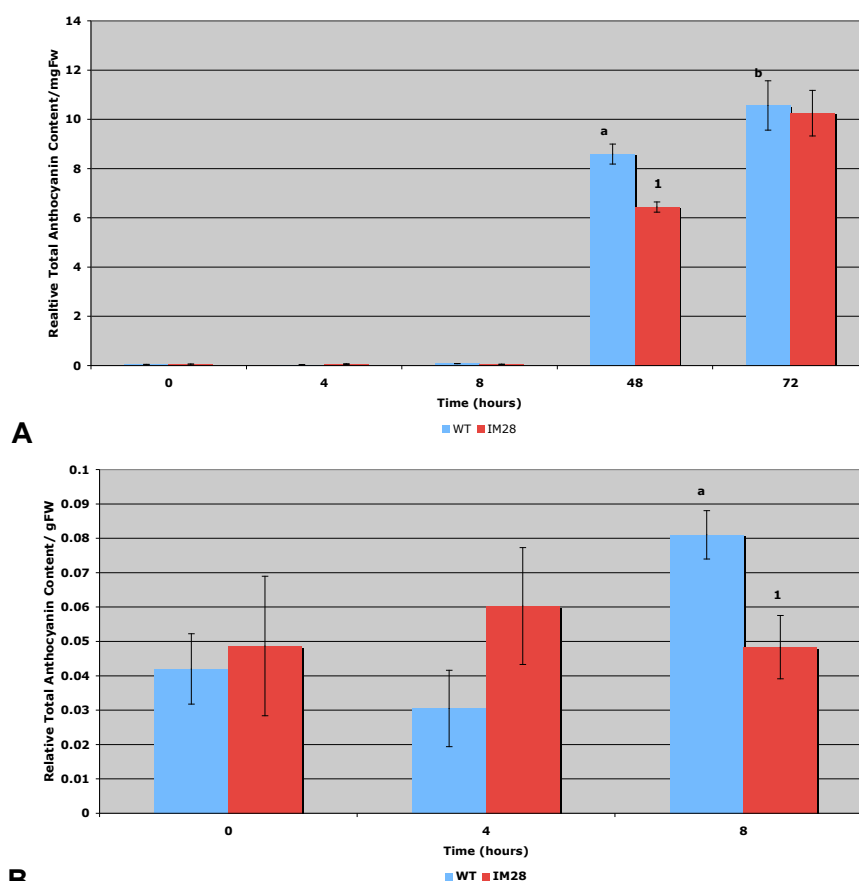


Fig 4.7: Total Anthocyanin Content Measurements

The analysis of total anthocyanins of six rosette replicates by UV-Vis spectroscopy of IM28 and WT after 0, 4, 8, 48 and 72 hours of high light stress (A) and 0, 4 and 8 hour high light (B). Results presented as mean ($n=6$) \pm SE. (A) There was a significant difference between WT and IM28 following 48h high light exposure (1) $P=0.004$. There were significant differences between WT time points 8 and 48h (a) $P=0.00003$ and 48 and 72h (b) $P=0.006$. (B) There was a significant difference between WT and IM28 following 8hr high light exposure (1) $P=0.02$. There was a significant difference between WT time points 4 and 8hr (a) $P=0.0079$.

The changes in total anthocyanin content (Fig 4.7) may account for the changes in PS2 efficiency (Fig 4.6) since anthocyanin may be acting as a screen to protect the reaction centres from photo-oxidative damage. This is indicated by the results obtained after 48 and 72-hour high light treatment. In the WT, the anthocyanin content had significantly increased at 48 hours and the PSII efficiency had stabilised by 72 hours. The WT had a significantly higher anthocyanin content after 48-hour treatment compared to IM28,

which was reflected in a higher PS 2 efficiency at this time point. The anthocyanin content of IM28 had reached WT levels after 72 hours and this was reflected again in the PS 2 efficiency. The PSII efficiency decreased rapidly in WT and IM28 following the 4 and 8-hour treatments but this can be explained by the total anthocyanin content not altering significantly from the untreated samples, therefore there was no protective screen at these early time points.

4.3.3.2 Anthocyanin Profiles after Different High Light Exposure Times

In the previous section 4.2.2.2 measurements of the anthocyanin profiles showed a difference between the anthocyanin composition of high light treated WT and IM28. The total anthocyanin measurements in the second experiment (Fig 4.7) indicated that the duration of high light exposure affected anthocyanin accumulation in IM28. This was investigated in detail by analysing the anthocyanin profiles of IM28 and WT following different times of treatment. This was to determine if the duration of the exposure to high light affects the anthocyanin composition. Fig 4.8 shows typical profiles for one of five replicates of WT and IM28 at the different high light treatments.

The WT and IM28 samples had similar anthocyanin profiles after 0, 4 and 8-hour high light treatment showing very low traces of anthocyanins with one to two main peaks (Fig 4.8 A, B, C, F, G, H). After 48-hour treatment the levels of different anthocyanins significantly increased and the WT has a higher content than IM28 (Fig 4.8 D & I). Twenty-nine different anthocyanin peaks were detected after 48-hour high light treatment. After 72 hours the levels of each anthocyanin detected increased, in the WT and in IM28 with levels in both lines being much more similar to each other than those seen at 48h (Fig 4.8 E & J).

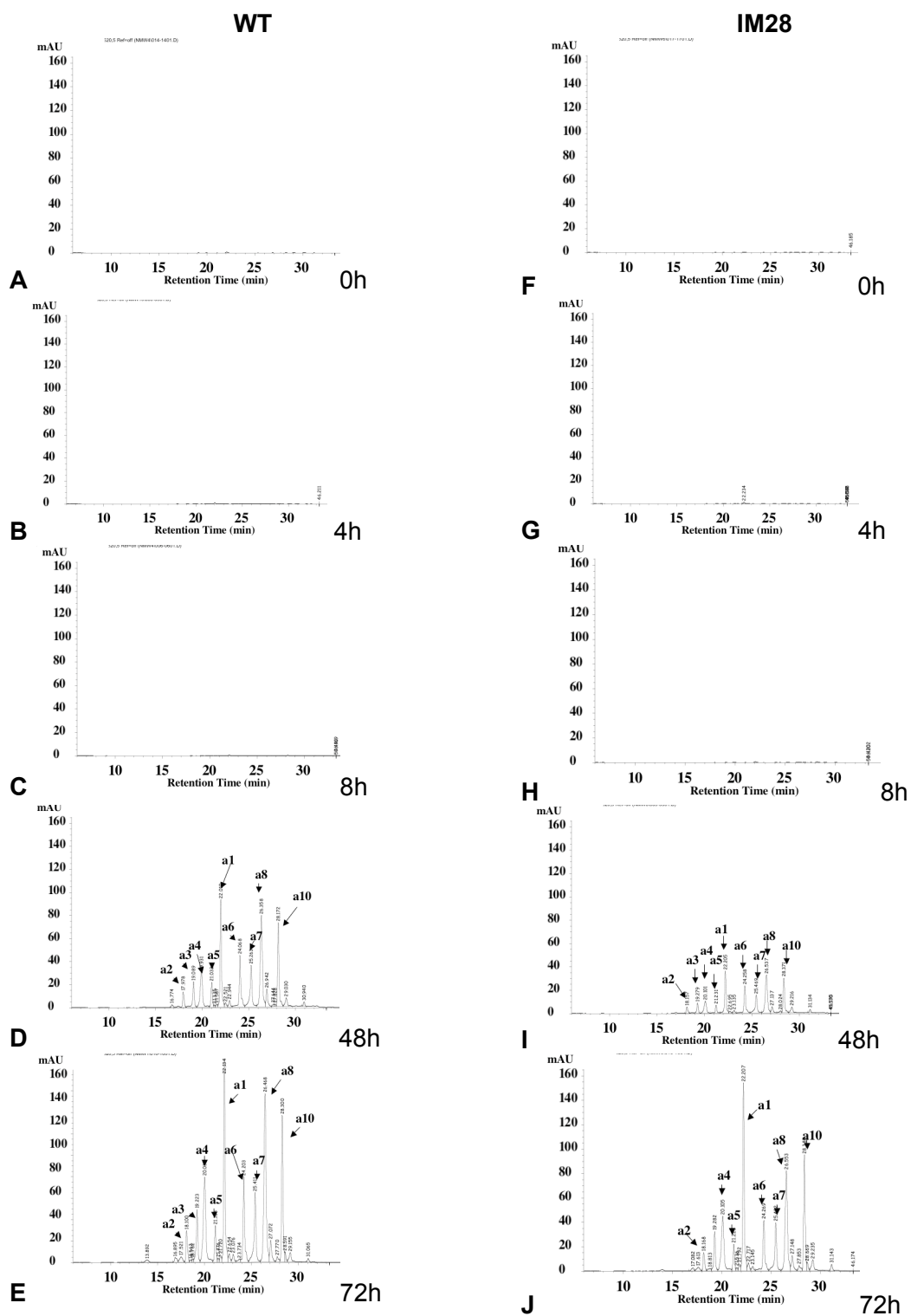


Fig 4.8: Effect of High Light Exposure Duration on Anthocyanin Profiles of WT and IM28

Anthocyanin profiles after 0, 4, 8, 48, and 72 hours of high light treatment from WT (A-E) and IM28 (F-J). Each trace is from one of six replicates and represents a good example from the six. The arrows indicate the main anthocyanin components.

4.3.3.3 Quantification of Anthocyanin Components After 48 and 72h High Light Exposure

The ten main anthocyanin peaks from the traces were quantified using 6 replicates (Fig 4.9). This showed a significant difference in the level of certain anthocyanins between the WT and IM28 following 48h high light. The anthocyanin components a4, a7 and a8 were significantly higher in WT than IM28. After 72h the WT had significantly higher levels of a4 and a8.

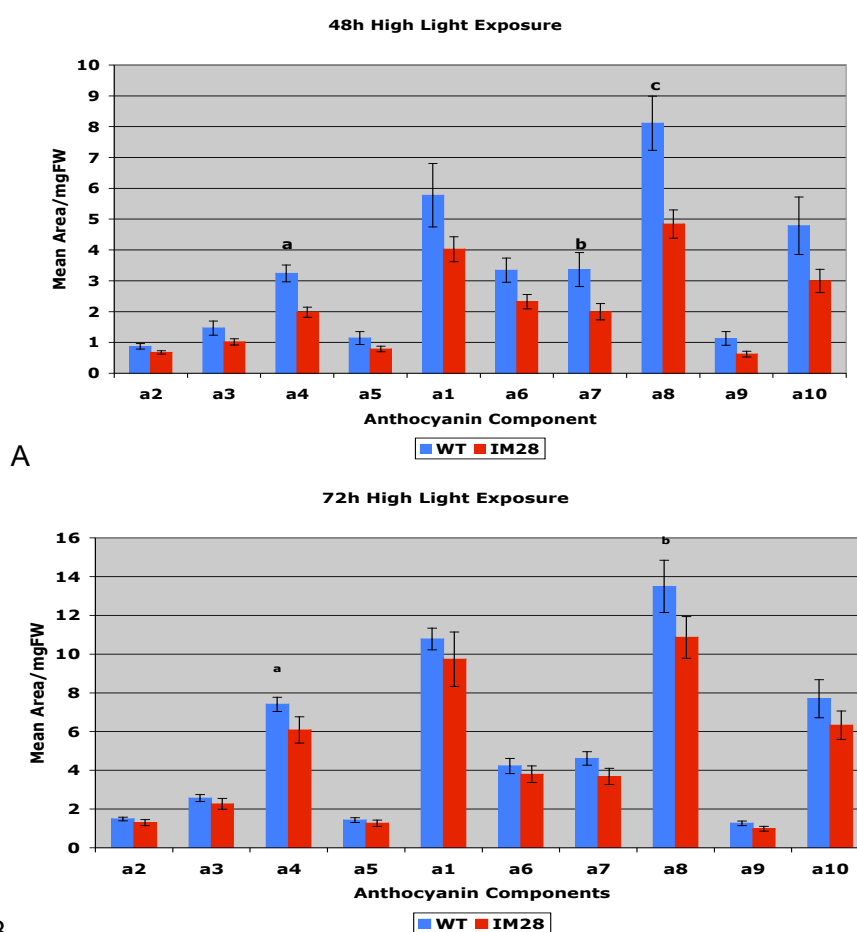


Fig 4.9: Quantification of Anthocyanin Components Following 48 and 72h High Light Exposure

The average of each anthocyanin component was calculated from five replicate anthocyanin profiles for WT and IM28 following (A) 48h and (B) 72h high light exposure. The area under the peaks was measured and the average of each component was calculated, presented as mean \pm SE. (A) There were significant differences between WT and IM28 after 48h treatments (a) $P = 0.002$, (b) $P = 0.042$ and (c) $P = 0.009$. (B) There were significant differences between the WT and IM28 after 72h treatments (a) $P = 0.002$ and (b) $P = 0.002$.

4.3.4 Role of MYB90 in Flavonoid Biosynthesis During Different High Light Exposure High Light Exposure Times

4.3.3.1 Flavonoid Profiles After Different High Light Exposure Times

The potential effect of the loss of *MYB90* in IM28 on specific flavonoids was investigated by comparing the flavonoid profiles of IM28 and WT during the series of high light treatments (Fig 4.10). One main flavonoid peak (f1) was present in all the flavonoid extracts at all time points (Fig 4.10). The number of different flavonoids detected greatly increased after 48 hours and there were 12 main peaks, including the peak described earlier. There were no noticeable differences between the profiles of IM28 and WT after 48 and 72 hours but the scale at 48h indicated lower levels of all in the IM28 mutant.

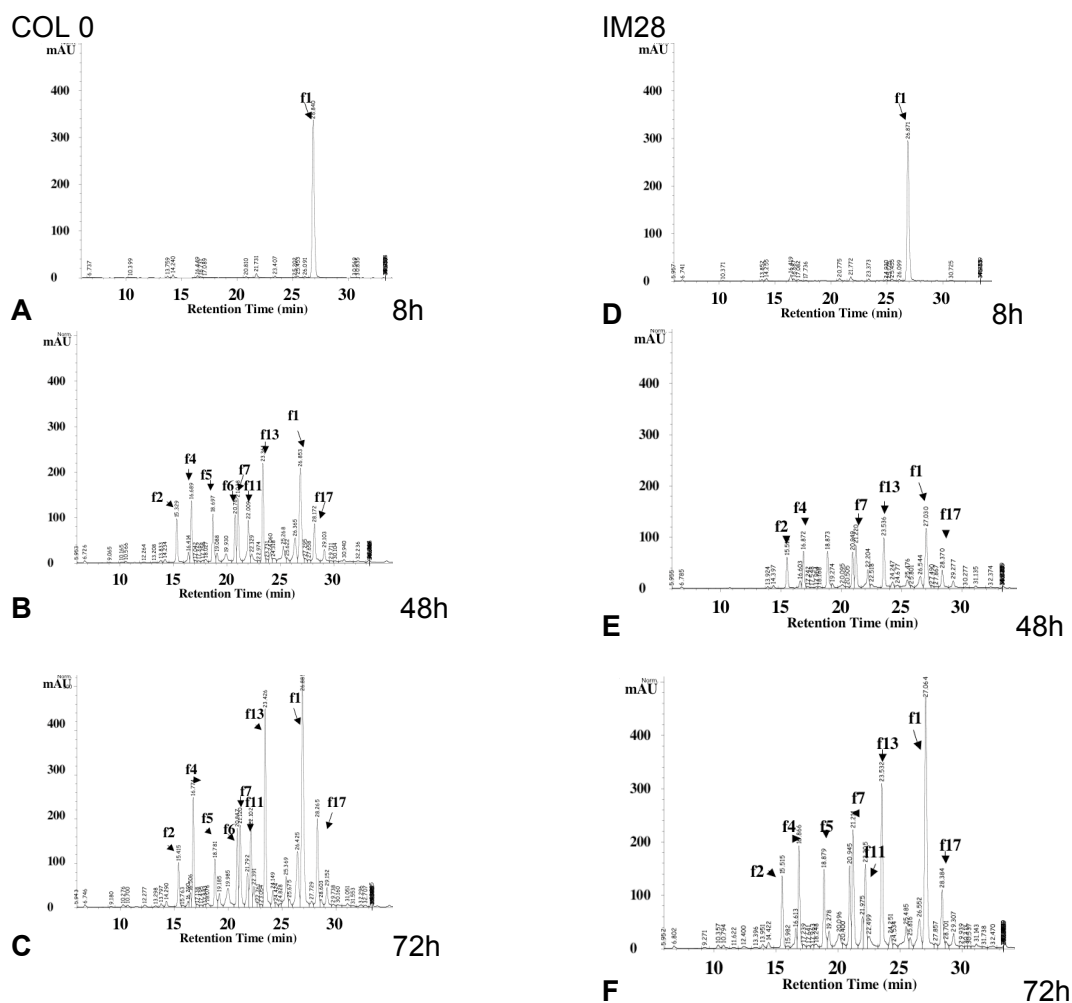


Fig 4.10: Effect of High Light Exposure Duration on Flavonoid Profiles of WT and IM28.

Flavonoid profiles after 8, 48, and 72 hours of high light treatment from WT (A-C) and IM28 (D-F). Each trace is from one of six replicates and represents a good example from the six. The arrows indicate the main flavonoid components.

4.3.4.2 Quantification of Total Flavonoid Content After Different High Light Exposure Times

In the preliminary high light treatment experiment there was a significant increase in total flavonoid content after high light treatment (Fig 4.5). The total flavonoid content and the flavonoid profiles of WT and IM28 treated to a series of different high light treatments was investigated because part of the anthocyanin biosynthesis pathway is the shared with the flavonoid biosynthesis pathway and the duration of high light exposure affected anthocyanin accumulation in WT and IM28 (Fig 4.7).

The total flavonoid content was quantified from traces similar to those shown in Fig 4.10. There were no significant changes in the total flavonoid content between 0, 4 and 8-hour extracts and between IM28 and WT (Fig 4.11). However flavonoid content greatly increased after 48 hours. By 72 hours of high light both the WT and IM28 content increased and levels in IM28 were similar to those in the WT.

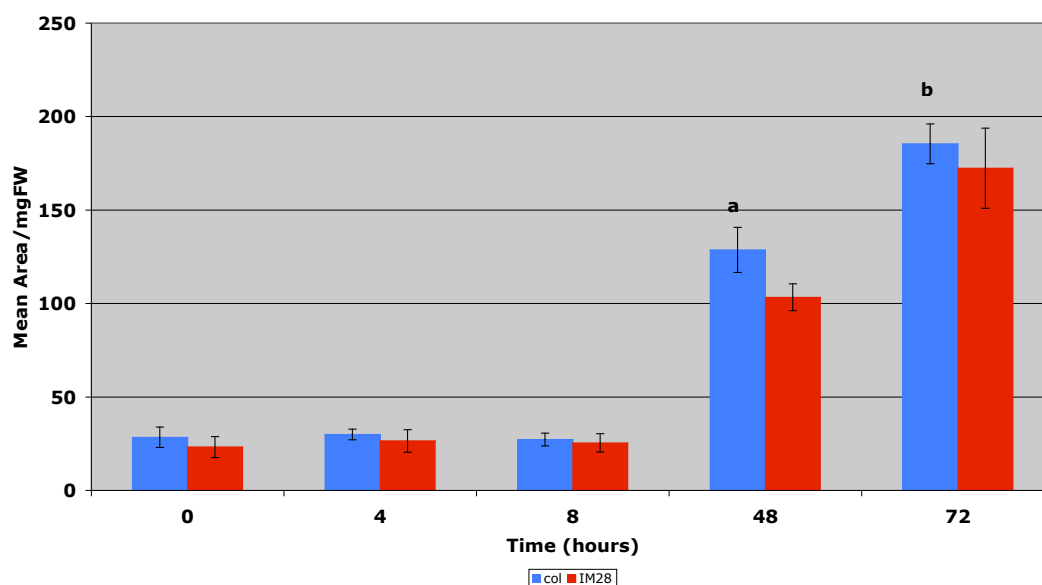


Fig 4.11: Quantification of the Total Flavonoid Content Following Different High Light Exposure Times.

The analysis of total flavonoid content of IM28 and WT after 0, 4, 8, 48 and 72 hours of light stress. Results presented as mean (n=6) \pm SE. There were significant differences in the WT between the time points (a) 8-48hr $P=0.0006$ and (b) 48-72hr $P=0.006$.

4.3.4.3 Quantification of Flavonoid Components Following 48 and 72 h High Light Exposure

The data from the flavonoid traces after 48h and 72h were quantified using six replicates and this is shown in Fig 4.12. Eighty-two different flavonoid peaks were detected after the 48h and 72h high light treatment in both WT and IM28. After 48 h there were significant differences between WT and IM28, the WT had higher level of three different flavonoids components f13, f15 and f16. After 72h the level of the

different flavonoids increased from 48h in both lines and there was no significant difference between the two lines (Fig 4.12 B).

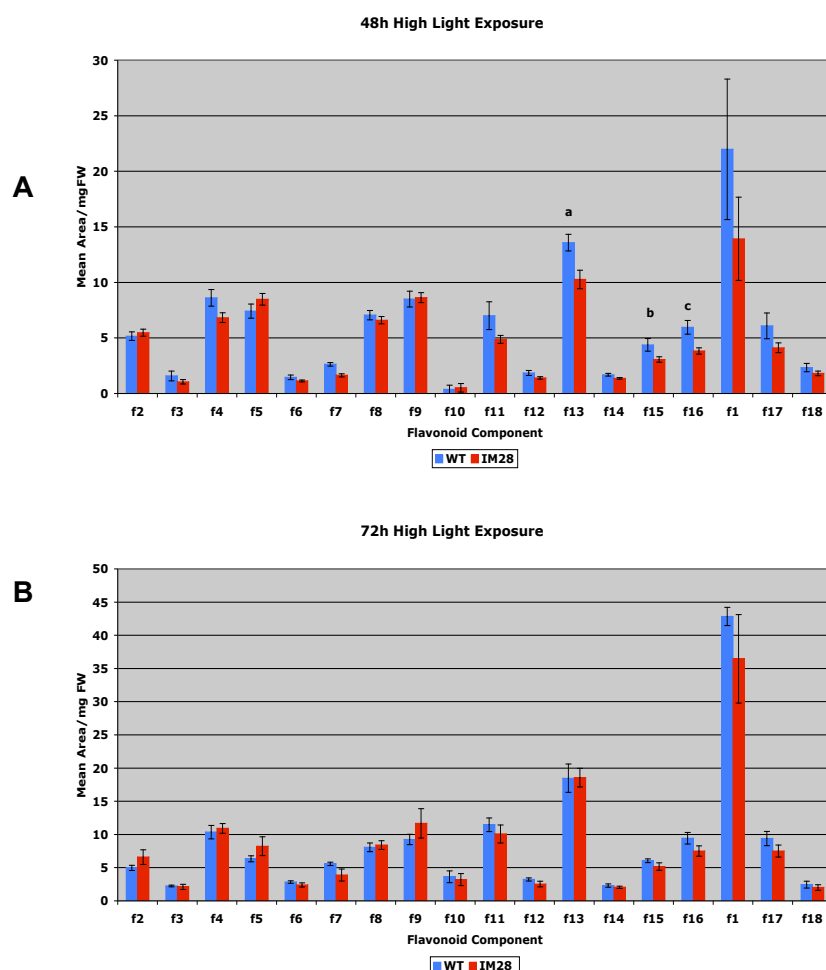


Fig 4.12: Quantification of Flavonoid Components Following 48 and 72h High Light Exposure

The average of each flavonoid component was calculated from five replicate flavonoid profiles for WT and IM28 following (A) 48h and (B) 72h high light exposure. The area under the peaks was measured and the average of each component was calculated, presented as mean=6 ± SE. (A) There were significant differences between the WT and IM28 following 48h high light exposure (a) $P=0.017$, (b) $P=0.048$, (c) $P=0.009$.

4.3.4.4 Analysis of the Main Flavonoid Component f1 Following Different High Light Exposure Times

There was one main flavonoid component (f1) present in all the extracts (Fig 4.10 & 4.12) the level and the fraction that this peak contributes to the total flavonoid composition were compared in all the time points in both IM28 and WT (Fig 4.13 A&B).

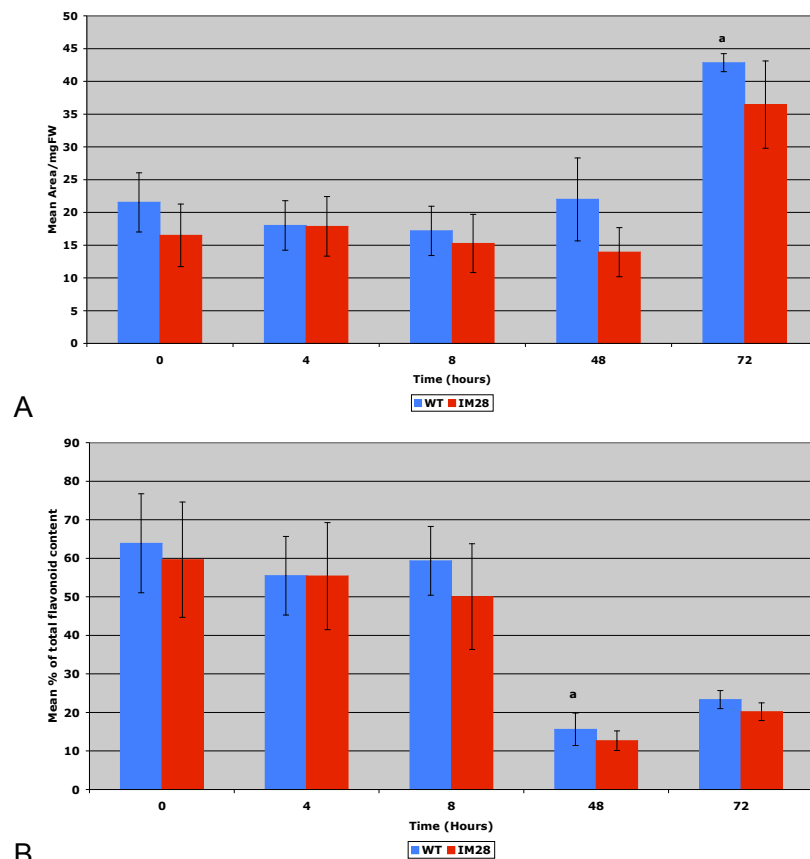


Fig 4.13: Analysis of the Main Flavonoid Component, F1 Following Different High Light Exposure Times

(A) The total flavonoid content of the flavonoid component f1 in 0, 4, 8, 48 and 72hour high light treated WT and IM28 plants. The area under the main flavonoid peak (f1) in six replicates was measured and the average was calculated. There was significant difference in the WT between time (a) 48- 72h $P=0.004$.

(B) The percentage f1 contributes toward the total flavonoid content of WT and IM28 following 0, 4, 8, 48 and 72hour high exposure, presented as mean \pm SE. There was a significant difference in the WT between the time points (a) 8-48h $P=0.0098$.

Following 4, 8 and 48h high light treatment there was no significant change in the amount of f1 in both WT and IM28 compared to the 0h, untreated plants (Fig 4.14 A). The fraction of f1 in the total flavonoid content was approximately 60% following 0, 4, and 8h high light in both WT and IM28 (Fig 4.13B). This rapidly dropped to approximately 12-15% after 48h. This indicated that the increase in total flavonoid

content at 48h is due to the production of more different flavonoids rather than the increased level of this particular flavonoid, which may indicate that components of the flavonoid pathway are regulated separately. After 72 hours the level of f1 greatly increased (Fig 4.13 A) and the fraction of f1 in the total flavonoid content increased to approximately 20-23% in both WT and IM28 (Fig 4.13 B).

4.5 Conclusions

The role of *MYB90* during high light stress response was studied in this chapter and the differences in phenotype, anthocyanin biosynthesis and photosynthesis parameters have been characterised. High light stimulates anthocyanin accumulation in maize (Chalker-Scott, 1999).

The initial experiment of 72 hour high light treatment showed that the WT had a different visible phenotype to the *MYB90* knockout, IM28. In the treated WT there was more purple pigmentation of the leaves and the rosette appeared smaller than the treated IM28 plants (Fig 4.1). IM28 had mostly green leaves and the older leaves had increased yellowing of the leaves and some purple pigmentation. In both lines the untreated plants were larger and the leaves green in appearance.

Anthocyanins have a role in protection against excessive light induced photo-oxidative damage during stress by acting as a screen that absorbs light and reduces the level of excess excitation energy. The anthocyanin content was measured in IM28 and WT to find out if *MYB90* had a role in the regulation of anthocyanin biosynthesis during high light stress. The total anthocyanin measurements indicated an increased anthocyanin content following high light treatment compared to the untreated plants in both the WT and IM28. However, high light treated WT had a higher anthocyanin content than treated IM28, which suggests that *MYB90* expression is required for the normal response of WT to the high light stress.

The separation of anthocyanin components by HPLC indicated that the number of anthocyanins produced increased following exposure to high light in both the WT

and IM28. However IM28 had lower levels of the anthocyanin components than the WT after high light treatment.

The high light treatment was investigated in more detail over a range of treatment times of 0, 4, 8, 48 and 72h, in the whole rosettes of WT and IM28. In this experiment the effect of the high light stress on photosynthetic performance was also analysed. In the WT the maximum PS2 efficiency (Fv/Fm) steadily declined from healthy levels after 4, 8 and 48 hours high light treatment. This indicates an increase in the level of photoinhibition of the reaction centres. The levels following 72hour treatment were comparable to that of the 48h treatment. The IM28 plants treated to 4 and 8h high light had higher Fv/Fm than the WT, which indicates that the IM28 plants had less photoinhibition and were healthier and potentially more resistant to high light stress. Following 48h treatment the IM28 plants had a much lower Fv/Fm than the WT indicating the plants were more susceptible to a more extensive stress. The Fv/Fm of IM28 increased to WT levels following 72h high light treatment. These results suggested that the absence of *MYB90* affected the plants ability to cope with the 48h hour high light treatment and by 72h there was recovery of the plants' to WT ability to cope with the stress. The fluorescence images of 48h high light treated WT and IM28 indicate that the photosynthetic performance of different aged leaves was different in the two lines. The smaller younger leaves near the centre of the rosette had higher Fv/Fm levels than the older leaves in both lines and this may indicate a higher level of protective mechanisms in the younger leaves to manage the increased light intensity. However the older leaves in IM28 showed relatively more stress than those in WT. In the future, the effect of high light stress on individual leaves in mutant and WT could be investigated, which may show clearer differences and potentially an age dependent effect.

The total anthocyanin content was measured in the rosettes of WT and IM28 following the high light treatments. There were low levels of anthocyanins in both WT and IM28 in the untreated plants and in the plants treated with 4 and 8h high light.

There was a sharp increase in anthocyanin content following 48h treatment and a further increase after 72h, in both lines but the increase in anthocyanin levels in IM28 plants after 48h treatment increased at a significantly lower level than that in the WT plants. Following 72h treatment the anthocyanin content increased to WT levels in IM28 plants. The anthocyanin profiles showed that following 48h and 72h treatments there was an increase in the number and level of anthocyanin components in both WT and IM28 plants. The WT had significantly high levels of certain anthocyanin components than IM28 plants after 48h treatment. In a previous study transgenic plants that over-expressed *MYB75* showed increased accumulation of three cyanidin derivative anthocyanin components, these included a cyanidin derivative with 4 glycosides and 3 acyl moieties attached and a cyanidin derivative that was a desinapoylated version of the first (Tohge *et al.*, 2005, Bloor & Abrahams, 2002).

The results show that both Fv/Fm and anthocyanin levels are significantly reduced in the *MYB90* mutant IM28, following the 48h high light treatment. This shows the importance of *MYB90* in the synthesis of anthocyanin, which has an important role in protecting the photosynthetic apparatus, most likely by absorbing light at the same wavelength as chlorophyll *b*, reducing excess light and reducing the excitation energy and thus reducing photoinhibition of the reaction centres (Smillie & Hetherington, 1999, Niell & Gould, 1999). The photo-protective role of anthocyanins was previously reported during high light intensity and suboptimal temperatures where they provided protection of photosynthetic apparatus and reduced the need for antioxidants (Pietrini *et al.*, 2002). Also, in red senescing leaves of red-osier dogwood recovered from high light stress, whereas yellow leaves were damaged (Field *et al.*, 2001). There may be some compensation for the absence of *MYB90* in the knockout, possibly by a closely related MYB gene, because the anthocyanin content does increase in IM28 after 48h high light exposure. After 72h high light exposure the anthocyanin content and Fv/Fm had increased further and was at WT levels. *MYB75* may compensate for the absence of *MYB90* expression and has been shown to be important in light regulation of anthocyanin biosynthesis (Cominelli *et al.*, 2007). Also, anthocyanins accumulated in

transgenic seedlings over-expressing *MYB113* and *MYB114*, which shows that there are a number of MYB genes that can potentially induce anthocyanin biosynthesis in *Arabidopsis* (Gonzalez *et al.*, 2008).

The flavonoid content sharply increased after 48h high light treatment and a further significant increase was seen after 72h treatment. The total flavonoid levels in IM28 were similar to those of the WT. The flavonoid profiles of WT and IM28 following the different high light treatments showed that the number and level of flavonoid components increased after 48 and 72h treatment. These profiles indicated that there is selective production of different flavonoid components. The flavonoid profiles showed a high level of one flavonoid component in all the different high light treatments and in the untreated plants. This component was most likely a kaempferol dirhamnoside (Veit & Pauli, 1999). In the untreated plants and plants exposed to 4 and 8h high light this flavonoid represented approximately 60% of the total flavonoid content. Following 48h and 72h high light exposure the proportion of this compound dropped to approximately 20% of the total flavonoid content, due to synthesis of many additional flavonoid components. Tohge *et al.*, 2005, found that in transgenic plants that had over expression of MYB75, kaempferol dirhamnoside biosynthesis was repressed and quercetin glycosides accumulated. In the high light experiment, the increased flavonoid content following 48h and 72h high light exposure may be accounted for by the accumulation of quercetin glycosides.

After 72h high light, levels of f1 increased, this shows that biosynthesis of f1 was under different control to the biosynthesis of other flavonoid components. Increased biosynthesis of f1 was induced late in the stress, while all the other components were induced earlier, following 48h stress.

4.5 Summary

In summary, results described in this chapter show that *MYB90* plays an important role in during high light stress by protecting leaves against photo-oxidative damage. The increased susceptibility to high light stress in the knock out mutant was associated with

decreased anthocyanin and flavonoid content. Eventually there was compensation for the absence of *MYB90* expression in the mutant and the anthocyanin and photosynthetic performance levels increased back to wild type levels.

5 Functional Analysis of MYB75

5.1 Introduction

The role of a closely related MYB gene, *MYB75* in high light stress response was investigated to compare with the role of *MYB90*. *MYB75* was previously shown to be involved in the regulation of the flavonoid pathway by Borevitz *et al.*, 2000, who showed that constitutive over expression of the gene increased the production of anthocyanins, seen by the purple pigmentation of the leaves, stem and flowers. The expression of *MYB75* was found to be up-regulated during senescence in WT plants (Buchanan-Wollaston *et al.*, 2005) and in chapter 3 gene expression analysis of the *MYB90* mutant showed that *MYB75* was downstream of *MYB90* during senescence. Previously *MYB75* has been found to be required for sucrose specific induction of anthocyanins and in the response to different stresses (Teng *et al.*, 2005, Lillo *et al.*, 2008, Borevitz *et al.*, 2000, Vanderauwera *et al.*, 2005, Scheible *et al.*, 2004). The potential role of *MYB75* in the regulation of anthocyanin biosynthesis was investigated in using transgenic plants expressing RNAi of *MYB75* during high light stress.

5.2 MYB75 RNAi

MYB75 RNAi seed was obtained from the collection generated by the AGRIKOLA project and homozygous lines at T3 generation were selected and checked for *MYB75* expression by reverse transcription (Fig 5.1) and that the plants contained the construct by sequencing.

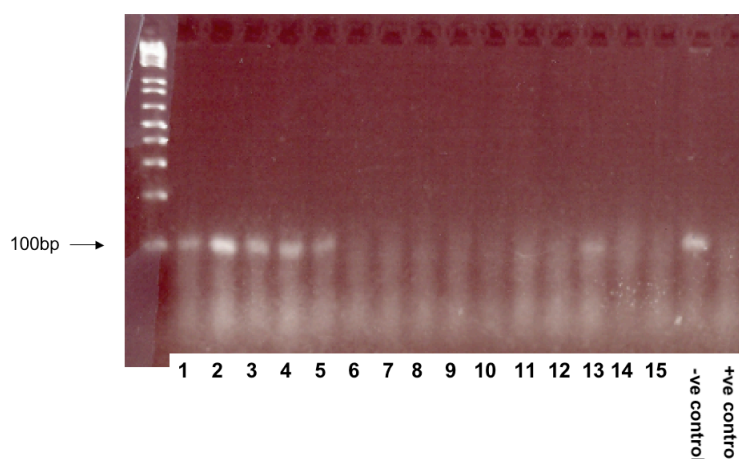


Fig 5.1: Selecting homozygous MYB75 RNAi Lines

Homozygous *MYB75* RNAi lines were selected at the T3 generation and then checked for *MYB75* expression by RT PCR using *MYB75* primers. A plant lines that had no detectable *MYB75* expression were selected for further investigation into the role of *MYB75*.

5.3 The Role of *MYB75* During High Light Exposure.

The effect of the *MYB75* knockout on photosynthetic performance and anthocyanin biosynthesis was analysed in *MYB75* RNAi and WT plants. WT and *MYB75* RNAi were grown in FPL7 pots filled with compost in the glass-house under shading at light intensity of $80 \mu\text{mol}/\text{sec}/\text{m}^2$. Eight plants of WT and *MYB75* RNAi before bolting, aged 61 days after sowing were placed under a sodium lamp and exposed to high light ($830 \mu\text{mol}/\text{sec}/\text{m}^2$) for 48 hours.

5.3.1 Chlorophyll Fluorescence Measurements

Chlorophyll fluorescence was measured to compare the photosynthetic performance of the untreated and high light treated WT and *MYB75* RNAi plants as described in Methods (section 2.5, table 4). The plants were subjected to a light curve of increasing light intensity, and the chlorophyll fluorescence measurements from the light curve were used to analyse the different parameters of photosynthesis.

The fluorescence images of the WT and *MYB75* RNAi untreated rosettes and following high light exposure illustrate the PSII performance (Fig 5.2). The images of the rosettes at 0 PPFD represent the maximum PSII efficiency (F_v/F_m) when all the

reaction centres are open. The highest Fv/Fm value of a healthy leaf is 0.8 and this was represented by a dark orange colour. Figure 5.2 shows that the untreated WT and *MYB75* RNAi rosettes had the highest high Fv/Fm. Following the high light exposure both the WT and *MYB75* RNAi rosettes were an orange/yellow colour, indicating that the treatment caused damage to PS2 reaction centres.

The images between 50 and 1500 PPFD ($\mu\text{mol m}^{-2} \text{s}^{-1}$) represent the chlorophyll fluorescence of operating PS2 reaction centres. Following the light curve treatment the untreated WT and *MYB75* RNAi plants appeared to have lower PS2 efficiency compared to the 48h light treated rosettes. The untreated rosettes leaves were mostly blue between 50 and 150 PPFD, ($\mu\text{mol m}^{-2} \text{s}^{-1}$) with increasing green colouration of the leaves during the light curve. WT and *MYB75* RNAi rosettes from the 48h high light treatment had higher PSII efficiency shown by the orange colouration of some rosette leaves and there was little green colouration until 1500 PPFD. These results indicate that the plants that had been exposed to high light were more resistant to the increasing light intensities that they were subjected to during the light curve than the untreated plants.

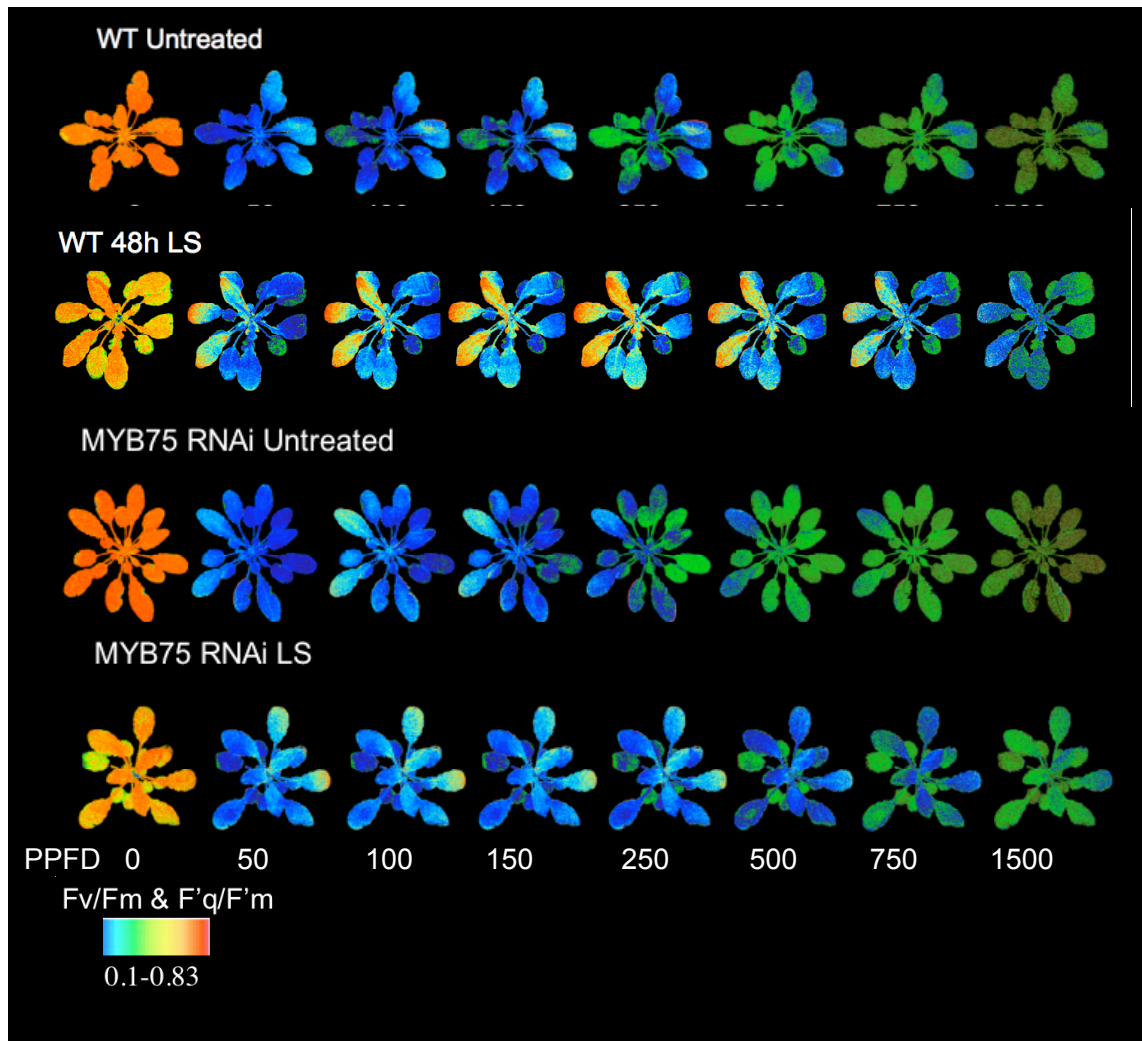


Fig 5.2: Maximum and Operating PS2 Efficiency Images Following 48h High Light Exposure

The analysis of maximum (following 0 PPFD) and operating (50-1500 PPFD) PS2 efficiency (Fv/Fm and F'q/F'm) of *MYB75* RNAi and WT following high light exposure (LS) by measuring the Chlorophyll fluorescence during a light curve.

5.3.1.1 Maximum PSII Efficiency

The mean maximum PS2 efficiency (Fv/Fm) was calculated by measuring the chlorophyll fluorescence after dark-adaption followed by a saturating light pulse. The maximum Fv/Fm value is approximately 0.8 for healthy plants, and both WT and *MYB75* RNAi had a high Fv/Fm at 0h, when they had not been light stressed (Fig 5.3). Following 48h high light stress, the Fv/Fm values of both the WT and *MYB75* RNAi Fv/Fm values had significantly declined ($P=0.0001$), which may indicate there is damage to the reaction centres. The WT had a slightly higher Fv/Fm than *MYB75* RNAi following 48h of high light, but this was not significant.

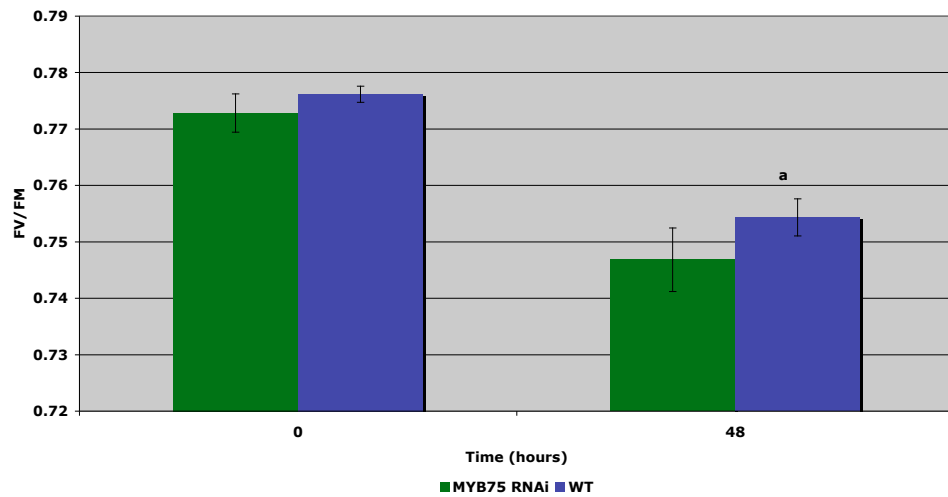


Fig 5.3: Maximum PS2 Efficiency (Fv/Fm) of WT and IM28 Plants Following High Light Exposure

The analysis of the maximum PS2 efficiency (Fv/Fm) of six rosette replicates by measuring the chlorophyll fluorescence the dark-adapted value of WT and *MYB75* RNAi after 0 and 48 hours of high light stress. Results are presented as mean (n=6) \pm SE.

There was a significant difference between untreated WT and the WT following 48h high light exposure (a) $P=0.0001$.

5.3.1.2 Operating PS2 Efficiency

The mean operating PS2 efficiency ($F'q/F'm$) was calculated by measuring the chlorophyll fluorescence of WT and *MYB75* RNAi during a light curve of increasing light intensity (Fig 5.4A). This parameter is a measurement of the PS2 efficiency that actually occurred. The operating efficiency sharply dropped between 0 and 50 actinic PPFD ($\mu\text{mol m}^{-2} \text{s}^{-1}$) for both lines, untreated and treated with high light. This was due to a delay in light activated fluorescence quenching involving carbon-fixing enzymes. The $F'q/F'm$ stabilised from 50 to 150 actinic PPFD ($\mu\text{mol m}^{-2} \text{s}^{-1}$), this indicated that the fluorescence quenching mechanisms could cope with the de-excitation of excitation energy from the absorbed light. Following the light pulses of 150-1500 actinic PPFD ($\mu\text{mol m}^{-2} \text{s}^{-1}$) the $F'q/F'm$ of untreated plants rapidly dropped and was much lower than that of the high light treated plants indicating that the untreated plants of both lines were more sensitive to high light intensities. This was likely to be because the high light treated plants had already activated protective mechanisms. In both the untreated and

high light treated plants the WT had a higher $F'q/F'm$ than *MYB75* RNAi from 150-1500 actinic PPFD. This suggests that the reduced levels of *MYB75* expression may make the plants more sensitive to the increased light intensities.

5.3.1.3 Photochemical Quenching

The chlorophyll fluorescence measurements were used to calculate the efficiency of photochemistry, also known as photochemical quenching (PQ) (Fig 5.4B). This assay indicates the fraction of the reaction centres that are open and therefore the efficiency of photochemistry resulting in a reduction of excitation energy. The higher the level of fluorescence, the lower the photochemical quenching. There was no photochemical quenching to reduce the fluorescence level following dark adaption because all the reaction centres are closed from a saturating light pulse and the carbon fixing enzymes are light activated. This is the reason why the PQ dropped from 0 to 50 actinic PPFD ($\mu\text{mol m}^{-2} \text{s}^{-1}$) and then slightly increased and stabilised from 50-150 actinic PPFD ($\mu\text{mol m}^{-2} \text{s}^{-1}$). The PQ rapidly dropped from 150-1500 actinic PPFD in the untreated plants and was much lower than in the high light treated plants. *MYB75* RNAi had lower PQ values than WT before and after high light. This related to the operating PSII efficiency (Fig 5.4A), suggesting that following 48h high light both lines had developed a protective mechanism to allow the photosynthetic apparatus to cope with higher light intensities but in the *MYB75* RNAi line, in the absence of *MYB75*, this was less successful.

5.3.1.4 Non-photochemical Quenching

The chlorophyll fluorescence measurements were also used to calculate the non-photochemical fluorescence quenching (NPQ). NPQ reduced excess excitation energy by thermal dissipation processes and thereby reducing the fluorescence level. The NPQ value rapidly increased as the actinic PPFD ($\mu\text{mol m}^{-2} \text{s}^{-1}$) increased in the light curve in both WT and *MYB75* RNAi untreated plants (Fig 5.4C). This suggests that the plants required increased down regulation by NPQ to cope with increased light

intensity and therefore increased levels of excitation energy. The high light treated plants NPQ levels increased slowly following 0 to 150 actinic PPFD and then rapidly increased following 150-1500 actinic PPFD ($\mu\text{mol m}^{-2} \text{s}^{-1}$). This suggests that both lines were able to cope with the light intensities 0-150 PPFD ($\mu\text{mol m}^{-2} \text{s}^{-1}$) but needed increasing levels of NPQ as the light intensity increased. *MYB75* RNAi untreated and high light treated plants had reduced levels of NPQ compared to the WT. This indicates that there was not sufficient protection against the light exposure.

5.3.1.5 Linear Electron Transport Rate

The linear electron transport rate was calculated from the chlorophyll fluorescence measurements of untreated and high light treated WT and *MYB75* RNAi as described in methods (Fig 5.4D). In the untreated and high light treated plants, linear electron transport rate increased in parallel as the light intensity increased from 0 to 150 PPFD. From this point the two treatments separated, in the high light treated plants the linear electron transport rate continued to increase rapidly and in the untreated plants the rate increased much less.

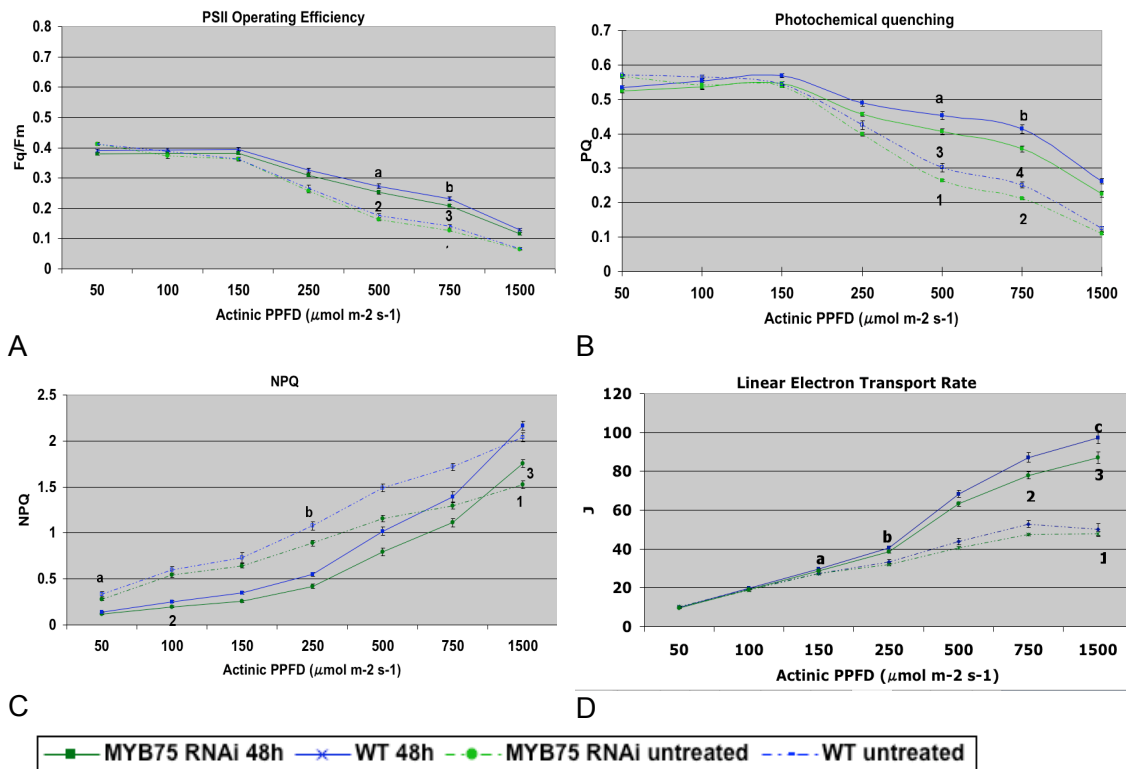


Fig 5.4: Measurements of Photosynthetic Parameters Following High Light Exposure

The analysis of the (A) operating PS2 efficiency ($F'q/F'm$), (B) photochemical quenching (PQ), (C) non-photochemical quenching (NPQ) and (D) linear electron transport rate (J) of six rosette replicates of WT and *MYB75* RNAi after 0 and 48 hours of high light stress by measuring the chlorophyll fluorescence at different light intensities. Results are presented as mean ($n=6$) \pm SE. (A) There were significant differences between untreated WT and the WT following high light exposure at (a) 500 PPFD $P=0.000002$ and (b) 750 PPFD $P=0.0000005$.

There was a significant difference between the untreated WT and the untreated *MYB75* RNAi plants at (1) 750 PPFD $P=0.027$. There were significant differences between WT and *MYB75* RNAi following high light exposure at (2) 500 PPFD $P=0.042$ and (3) 750 PPFD $P=0.012$.

(B) There were significant differences in the untreated WT and high light treated WT at (a) 500 PPFD $P=0.0000038$ and (b) 750 PPFD $P=0.0000012$. There were significant differences between the untreated WT and untreated *MYB75* RNAi at (1) 500 PPFD $P=0.025$ and (2) 750 PPFD $P=0.0046$ and the high light treated WT and high light treated *MYB75* RNAi at (3) 500 PPFD $P=0.011$ and (4) 750 PPFD $P=0.003$. (C) There were significant differences between the untreated and high light treated WT at (a) 50 PPFD $P=0.00037$ and (b) 250 PPFD $P=0.000014$. There were significant differences between the untreated WT and untreated *MYB75* RNAi plants at (1) 1500 PPFD $P=0.000016$ and the high light treated WT and high light treated *MYB75* RNAi at (2) 100 PPFD $P=0.0017$ and (3) 1500 PPFD $P=0.000085$. (D) There were significant differences between untreated and high light treated WT at (a) 150 PPFD $P=0.0053$, (b) 250 PPFD $P=0.00057$ and (c) 1500 PPFD $P=0.0000006$.

There were significant differences between the untreated WT and untreated *MYB75* RNAi plants at (1) 1500 PPFD $P=0.045$ and the high light treated WT and high light treated *MYB75* RNAi plants at (2) 750 PPFD $P=0.0014$ and (3) 1500 PPFD $P=0.035$.

5.3.2 Role of *MYB75* in Anthocyanin Biosynthesis During High Light Exposure

5.3.2.1 Total Anthocyanin Content Measurements

The effect of the reduced levels of *MYB75* in the knockout *MYB75* RNAi plants on the anthocyanin during high light stress was investigated. The total anthocyanin content was extracted and measured, as described in Methods (section 2.4).

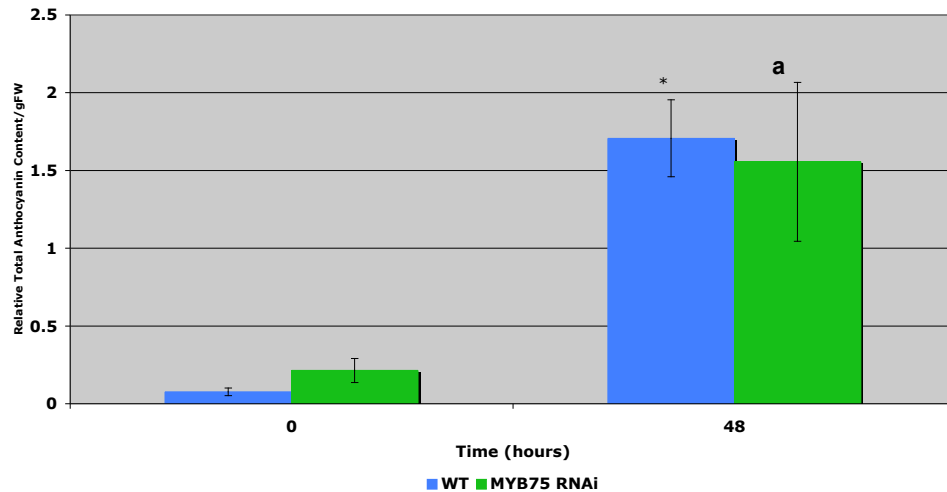


Fig 5.5: Total Anthocyanin Content Measurement

The analysis of total anthocyanins of eight rosette replicates by UV-Vis spectroscopy of WT and *MYB75* RNAi after 0 and 48 hours of high light stress. Results are presented as mean ($n=6$) \pm SE. There was a significant difference between the untreated and high light treated WT (*) $P=0.00123$ and the untreated and high light treated *MYB75* RNAi plants (a) $P=0.046$.

Anthocyanin assays were carried out on 6 replicate rosette extracts from WT and *MYB75* RNAi following 0 and 48 hour high light treatments. Following 48h high light there was a significant increase in total anthocyanin content in both WT and *MYB75* RNAi compared to the untreated plants (Fig 5.5). Interestingly, the untreated *MYB75* RNAi appeared to have a higher anthocyanin content than the WT indicating that the reduced levels of *MYB75* may alter the normal production of anthocyanins during growth.

5.3.2.2 Anthocyanin Profiles

Separating different anthocyanins by HPLC and analysing the profiles investigated the specific effect of the knockout of *MYB75* in *MYB75* RNAi on the anthocyanin biosynthesis during high light stress.

Both WT and *MYB75* RNAi had an increase in the level and number of anthocyanins following 48h light stress compared to the 0h, untreated profiles (Fig 5.6 B&D). The WT had thirty different anthocyanins and *MYB75* RNAi had twenty-six different anthocyanin peaks in total. They had similar profiles with four main anthocyanin peaks, a1, a4, a8 and a10. However the untreated *MYB75* RNAi profile was different to the WT (Fig 5.6 A&C). The WT had one main anthocyanin peak, a1 and *MYB75* RNAi had three main peaks, a1, a8 and a10 and the levels of the anthocyanin peaks were higher.

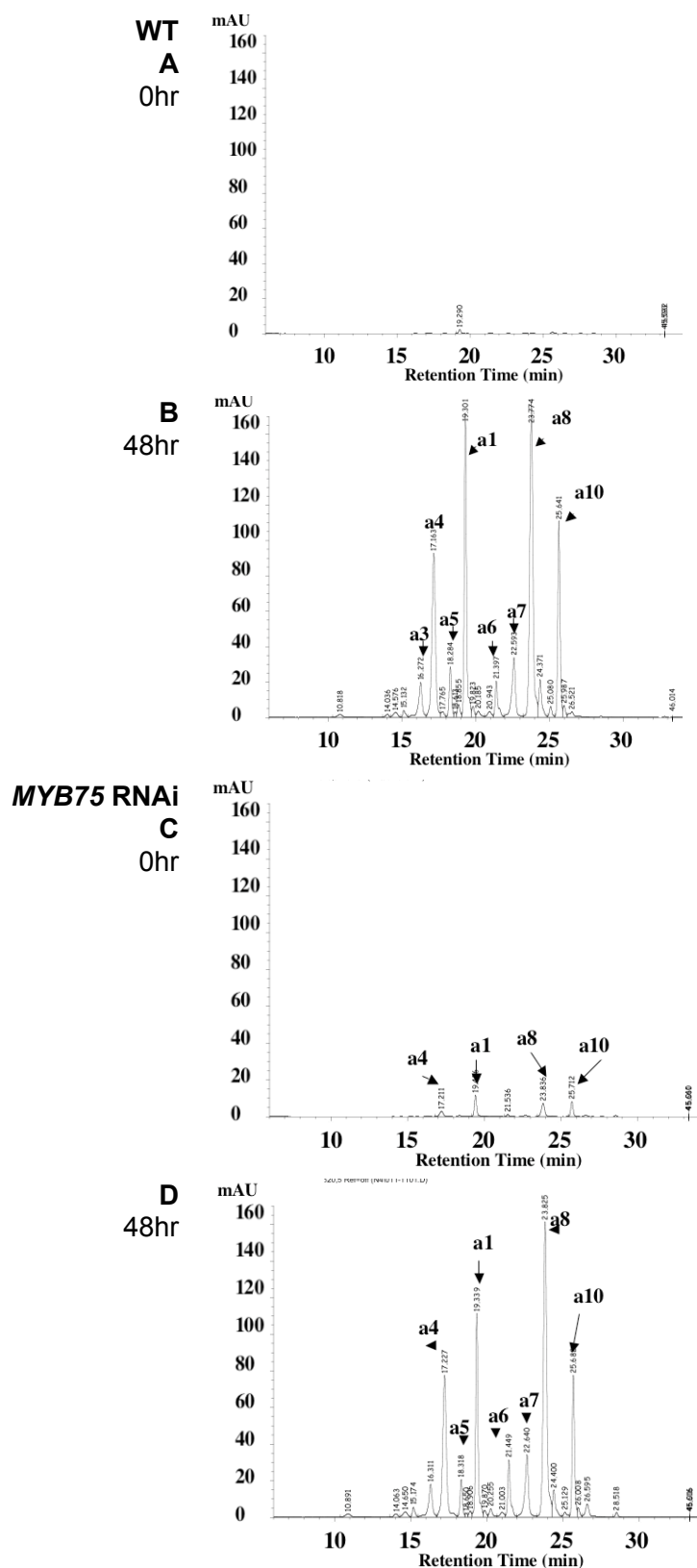


Fig 5.6: Anthocyanin Profiles of WT and MYB75 RNAi Following High Light Exposure

Anthocyanin profile after 0 and 48 hours of high light treatment from WT (A-B) and MYB75 RNAi (C-D). Each trace is from one of six replicates and represents a good example from the six. The arrows indicate the main anthocyanin components.

5.3.2.3 Quantification of Anthocyanin Components

The data from the ten main anthocyanin components were quantified and are shown in Fig 5.7. Both the untreated WT and *MYB75* RNAi had five of the main anthocyanin components. These peaks appeared to be at a higher level in *MYB75* RNAi than in WT, but data were not significant. This suggests that the absence of *MYB75* in *MYB75* RNAi had altered the normal regulation of the anthocyanin biosynthesis and increased the level and number of different anthocyanins compared to the WT.

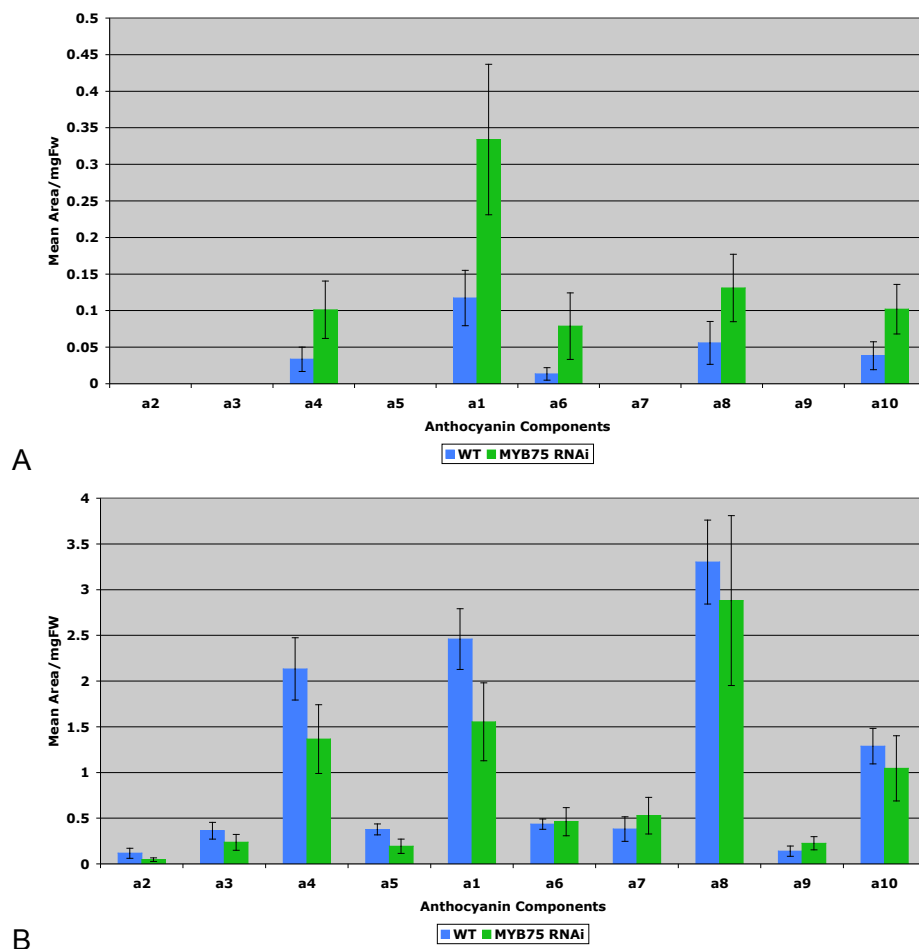


Fig 5.7: Quantification of Anthocyanin Components in Untreated and 48h High Light Treated WT and *MYB75* RNAi.

The average of each anthocyanin component was calculated from five replicate anthocyanin profiles for (A) untreated and (B) 48h high light treated WT and *MYB75* RNAi. The area under the peaks was measured and the average of each component was calculated, presented as mean=5 \pm SE.

Following 48h high light exposure the number and level of the different anthocyanins had increased in both WT and *MYB75* RNAi compared to the untreated plants (Fig 5.7B). There were four main anthocyanin components in both WT and *MYB75* RNAi a4, a1, a8 and a10 that were at a higher level than the other anthocyanins. These peaks were also seen in the untreated profiles (Fig 5.7B) but the most prominent anthocyanin component had changed from number a1 to a8. This indicates that the regulation of the biosynthesis of individual anthocyanins was differentially regulated in the response to high light. Again there was no significant difference between the WT and *MYB75* RNAi, which indicates that *MYB75* may have no role in synthesis of anthocyanins following high light stress.

5.3.3 Role of *MYB75* in Flavonoid Biosynthesis During High Light Exposure

5.3.3.1 Flavonoid Profiles

The potential effect of the loss of *MYB75* in *MYB75* RNAi on specific flavonoids was investigated by comparing the flavonoid profiles of *MYB75* RNAi and WT following 48 hours of high light treatment or no treatment (Fig 5.8).

As shown in chapter 4, the flavonoid profile of the untreated WT showed one main peak (Fig 5.8 A). The untreated *MYB75* RNAi had a similar profile but had higher level of the flavonoids (Fig 5.8 C). Following 48h high light the WT had an increased number and levels of flavonoids compared to the untreated profiles. It had one main peak and five other prominent peaks (Fig 5.8 B). *MYB75* RNAi had a similar profile following light stress but the flavonoid peaks were possibly at a lower level (Fig 5.8 D).

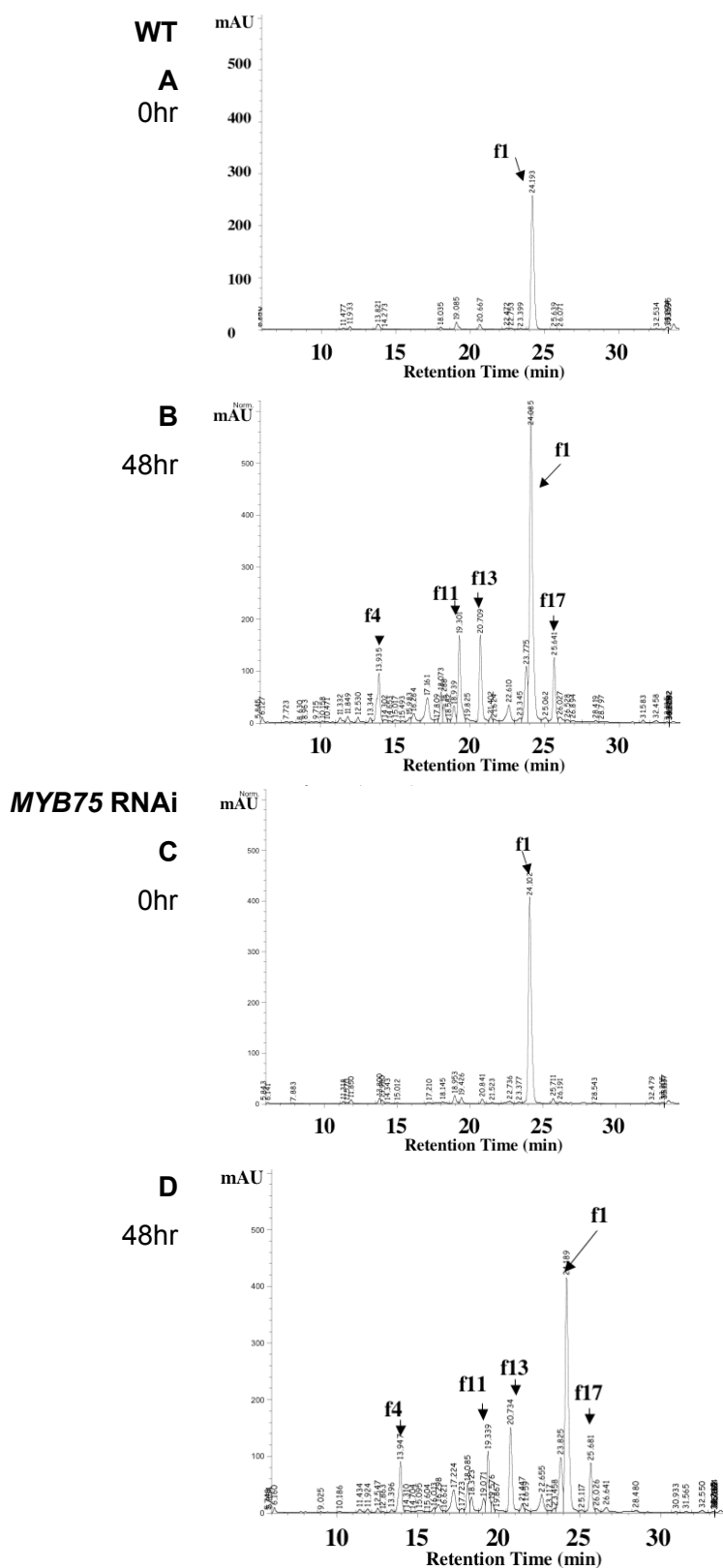


Fig 5.8: Flavonoid Profiles of WT and *MYB75* RNAi Following High Light Exposure

Flavonoid profile after 0 and 48 hours of high light treatment from WT (A-B) and *MYB75* RNAi (C-D). Each trace is from one of six replicates and represents a good example from the six. The arrows indicate the main flavonoid components.

5.3.3.2 Quantification of Total Flavonoid Content

The data from the 6 replicate flavonoid traces were quantified to find the total flavonoid content in WT and *MYB75* RNAi following 0 and 48h high light (Fig 5.9).

After 48h high light treatment there was a significant increase in total flavonoid content compared to the untreated plants. However the untreated WT had a significantly lower flavonoid content than *MYB75* RNAi. It appears that the absence of *MYB75* in *MYB75* RNAi may alter the normal regulation of the flavonoid pathway, since there were increased flavonoid levels in a healthy plant and the response to high light was possibly reduced.

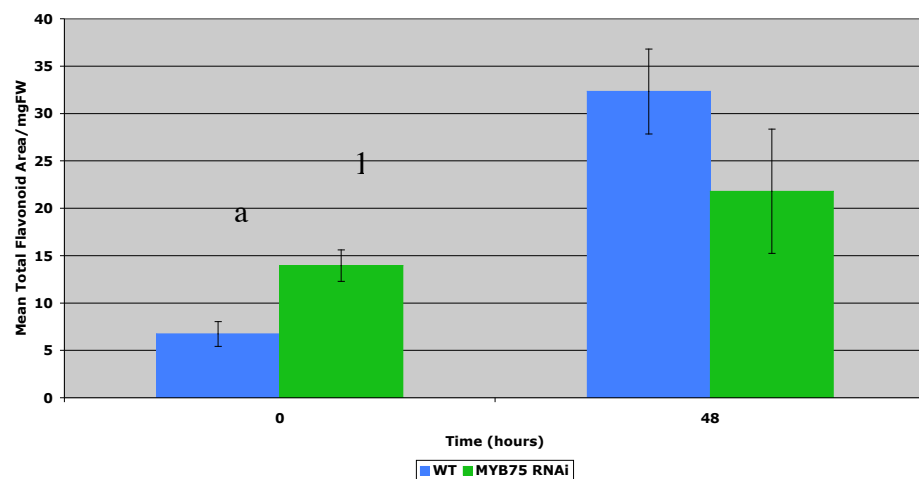


Fig 5.9: Quantification of the Total Flavonoid Content of WT and *MYB75* RNAi Plants Following High Light Exposure

The analysis of total flavonoid content of WT and *MYB75* RNAi after 0 and 48 hours of high light stress. Results are presented as mean ($n=6$) \pm SE.

There was a significant difference between the untreated and high light treated WT plants (a) $P=0.0017$. Also, there was a significant difference between untreated WT and *MYB75* RNAi plants (1) $P=0.05$.

5.4 Conclusions

The role of *MYB75* during a high light stress response was studied in this chapter and the differences in phenotype, anthocyanin biosynthesis and photosynthesis parameters in a RNAi knockout compared to the WT have been characterised.

The maximum PS2 efficiency (F_v/F_m) was closer to healthy levels (0.8) in the untreated WT and *MYB75* RNAi plants and decreased following 48 hours high light treatment. These results suggest that there was some photoinhibition of the high light treated plants. However, the untreated plants from both lines had a lower photosynthetic performance than the plants subjected to 48 hours of high light. This was indicated by the low operating PS2 efficiency (F'_q/F'_m), photochemical quenching (PQ) and linear electron transport levels, and the higher non-photochemical quenching (NPQ) levels. The low PQ and linear electron transport rate indicated that the reaction centres were closed due to a reduction in the available electron acceptors and there was therefore reduced photochemistry. The increased NPQ levels implied that there was an excess excitation energy that needed to be dissipated as heat. NPQ under normal conditions dissipates 45-64% absorbed light energy and during stress this increases to 75-92% (Flexas & Medrano, 2002). During light stress NPQ is not sufficient for reducing excitation energy (Golan *et al.*, 2005). These results suggest that the plants exposed to high light had developed a protection mechanism. The plants grown in the shade were more vulnerable to the increasing light intensity of the chlorophyll fluorescence light curve protocol (Chapter 2, table 4).

The untreated and high light treated *MYB75* RNAi had lower levels of all the above photosynthetic parameters compared to the equivalent WT plants. This indicates that the absence of *MYB75* expression reduced the plants photosynthetic performance. Also, there were reduced NPQ levels in *MYB75* RNAi plants', which indicates that the plants were not releasing excess excitation energy as heat. This would increase the damage caused to reaction centres.

MYB75 has been reported to regulate anthocyanin and flavonoid biosynthesis, particularly during high light treatment (Borevitz *et al.*, 2000, Cominelli *et al.*, 2007). The *MYB75* RNAi plants have undetectable levels of *MYB75* expression and were therefore expected to have reduced anthocyanin and flavonoid levels compared to the WT. The total anthocyanin content was measured in the untreated and 48h high light treated WT and *MYB75* RNAi plants. There was a significant increase in total anthocyanin content following high light exposure of WT plants. Levels in the *MYB75* RNAi plants also increased but were too variable to show significance. Therefore there was no significant difference in anthocyanin levels between the *MYB75* RNAi line and the wild type. This may indicate a different role for this gene than that found for *MYB90* as described in the previous chapters.

Interestingly, there was a significantly higher flavonoid content in untreated *MYB75* RNAi plants than the untreated WT plants. This suggests that the absence of *MYB75* resulted in an increased flavonoid biosynthesis rather than the expected reduction.

Tohge *et al.*, 2005 found that over expression of *MYB75* increased the accumulation of specific anthocyanins and flavonoid components, such as cyanidin and quercetin, and there was repression of the flavonol F1. The effect of the absence of *MYB75* expression was investigated further by analysing the anthocyanin profiles of the anthocyanin extracts. These indicated that the untreated *MYB75* RNAi plants had a higher content of some anthocyanin components than the untreated WT plants. Following 48h high light treatment there was an increase in the number and level of anthocyanin components in both the WT and *MYB75* RNAi but again no significant differences were seen between the two lines.

These results suggested that the higher photosynthetic performance of high light treated plants compared to the untreated plants might be due to the difference in anthocyanin and flavonoid levels. The increased anthocyanin and flavonoid content of WT and *MYB75* RNAi plants following high light treatment might have acted as a

screen that absorbed excess light and reduced the level of excitation energy and increased the photosynthetic performance of the plants. There have been reports of anthocyanin protecting against photo-oxidative stress during high light stress (Field *et al.*, 2001, Smillie & Hetherington, 1999, Krol *et al.*, 1995).

MYB75 RNAi untreated and 48h high light treated plants had a lower photosynthetic performance than WT plants. However, since there was no significant difference in the anthocyanin levels in *MYB75* RNAi compared to WT plants, this shows that *MYB75* RNAi plants had reduced protection against photo-oxidation which was not associated with anthocyanin and flavonoid biosynthesis. Other photoprotective mechanisms include other pigments such as carotenoids (Munné-Bosch & Peñuelas, 2003) and in grape, olive and oak leaves physical barriers such as trichomes, which are more effective at absorbing light and reducing light stress than anthocyanins (Karabourniotis *et al.*, 1992, Karabourniotis & Bomman, 1999, Liakopoulus *et al.*, 2006).

5.5 Summary

In summary, the data shows that anthocyanin and flavonoids accumulation are associated with resistance to high light stress, presumably by absorbing light and reducing excitation energy. *MYB75* expression was required for increased resistance to high light stress, but this was not associated with anthocyanin levels. This suggests that there are other protective mechanisms affected by *MYB75* expression during high light stress.

6 Analysis of *MYB90* & *MYB75* Expression Using a Reporter Gene

6.1 Introduction

In previous chapters, results have shown that the absence of *MYB90* in plants during senescence altered the photosynthetic performance, gene expression and anthocyanin and flavonoid biosynthesis. Also high light treatment affected the photosynthetic performance and anthocyanin biosynthesis of the *MYB90* knockout mutant IM28 and the *MYB75* knockdown mutant *MYB75* RNAi. The expression patterns of *MYB90* and *MYB75* were investigated further by fusing their promoters to the GUS.GFP reporter gene and transforming them into *Arabidopsis* (Karimi *et al.*, 2002). This allowed the quantification and visualisation of expression patterns of each. The GUS reporter gene activity was visualised in the whole plant and quantified in the rosette leaves during development and stress. This was used to determine the timing, level and cell type for *MYB90* and *MYB75* expression.

6.2 Gateway Cloning of *MYB90* and *MYB75* Promoters

The promoters (Fig 6.1) were amplified from BAC DNA using primers containing the attB sites (Chapter 2, section 2.7.1.1) using high fidelity KOD DNA polymerase. The PCR products were purified and gel electrophoresis used to ensure that the correct size fragment had been amplified for the promoters. The promoter fragments are approximately 2kb (Fig 6.1)

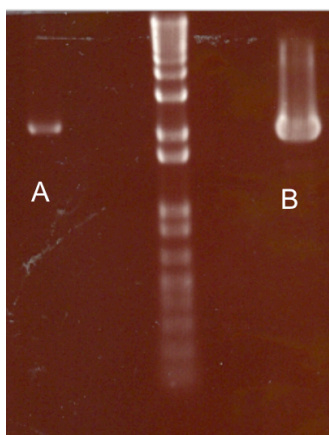


Fig 6.1: *MYB90* and *MYB75* Promoter Fragments

The *MYB75* (A) and *MYB90* (B) promoter fragment were approximately 2kbp. They were amplified from BAC DNA using primers containing attB sites. Following PCR clean up the insert was sequenced to confirm that the promoters had been cloned with no sequence changes.

The PCR products were used in the BP recombination reaction. The BP recombination reaction and transformation into electro-competent cells were carried out as described

in Methods and the cells grown on LB plates containing kanamycin. Figure 6.2 shows the expected result.

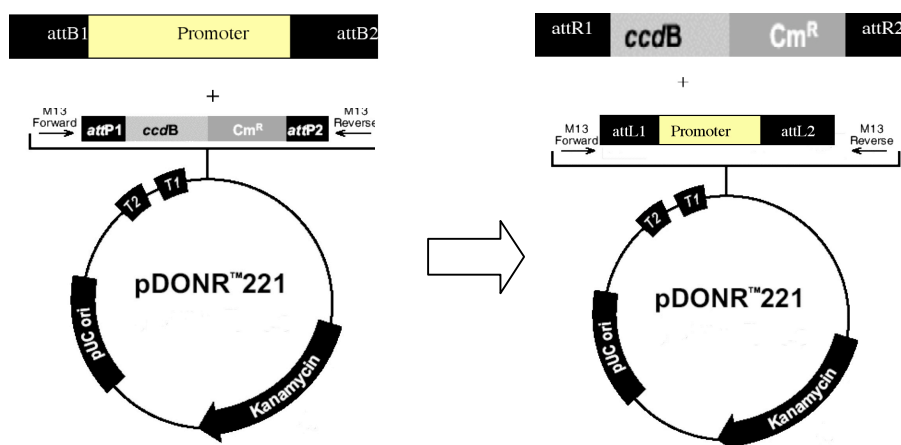


Fig 6.2: Gateway BP Recombination Reaction

Gateway cloning BP Recombination Reaction: PCR fragments containing attB sites were amplified from BAC DNA using gene specific primers and attB sites. Recombination between the attB sites of the promoter and the attP sites of the CmR-ccdB cassette of the pDONR 221 vector created the entry clone that has kanamycin resistance and attL sites flanking the promoter.

The promoter inserts were sequenced to confirm that the correct promoters had been cloned with no sequence changes. Several primers spanning the promoters were used in the sequencing reaction, the sequencing was successful and confirmed the constructs to be used in the LR reaction. The LR reaction (Fig 6.3) was performed as described in the methods section and, following transformation into electro-competent cells and growth on LB spectinomycin plates selective for the pHGWS7 vector, the plant transformation constructs were selected.

Sequencing using specific primers that span the vector and the insert was used to ensure that the promoter was inserted into the vector. Suitable promoter GUS fusions were transformed into GV3101 *Agrobacterium* as described in the methods. The promoter GUS fusions were transformed into COL-0 by floral dipping. T0 seed was sown and selected for BASTA resistance. Twenty four BASTA resistant lines for each promoter construct were selected and homozygous lines containing *MYB90* and

MYB75 promoter GUS fusions identified. Analysis of GUS expression was carried out with three individual transformants for each construct.

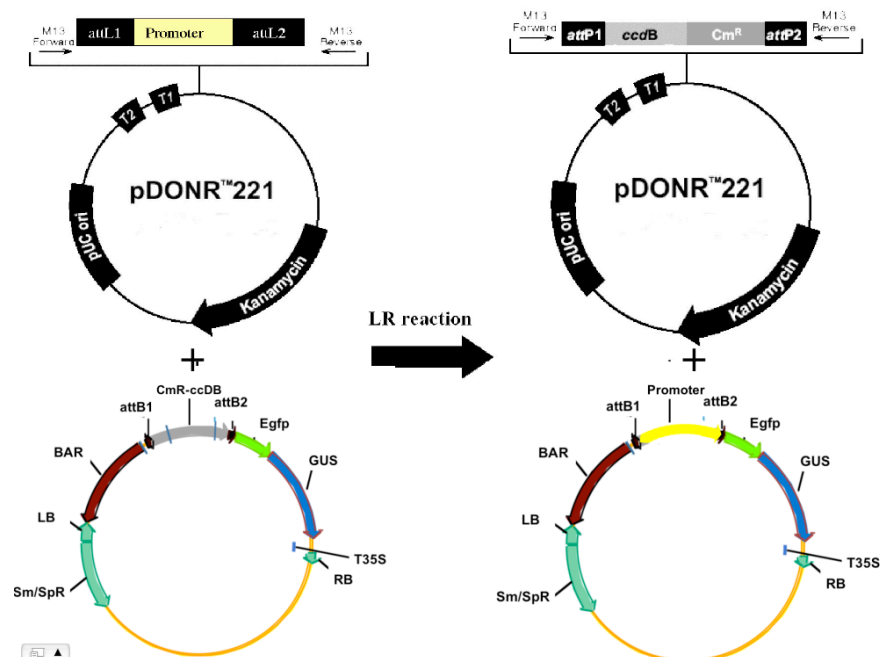


Fig 6.3: Gateway LR Recombination Reaction

Recombination between the attR sites of the destination vector (pBGWFS7) and the attL sites of the entry clone (pDONR 221) generated the expression clones. The final promoter GUS fusions plasmids contain the promoters, GUS: GFP and Basta resistance.

6.3 *MYB90* Promoter GUS Fusion Plant Growth Experiments

6.3.1 Analysis of GUS Activity During Senescence

Three individual *MYB90* promoter: GUS fusions transformants were grown in the glass house. The GUS activity was visualised by histochemical staining of senescent transgenic plants containing the *MYB90* promoter GUS fusions (Fig 6.4). Blue staining represents the GUS activity but this was rarely visible in the *MYB90* promoter lines. A small amount of blue staining was found in the veins of some senescent leaves as shown in Figure 6.4A-C.

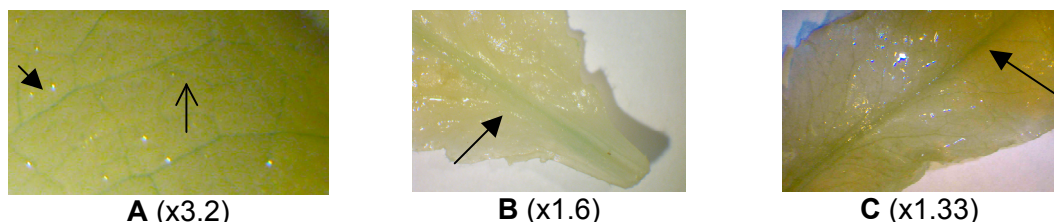


Fig 6.4: Histochemical Staining of Transgenic Plants Containing the *MYB90* Promoter GUS

Fusions During Senescence.

Blue staining represented positive GUS activity.

Three individual *MYB90* promoter constructs transformants were stained for GUS activity during senescence. There was staining in the veins of senescent leaves, including the primary vein (B-C) and the secondary (filled in arrow) (A) and tertiary veins (open arrow) (A).

The average GUS activity was quantified during the later stages of development in whole rosettes from senescing plants containing *MYB90* promoter GUS fusions (3 lines) (Fig 6.5). The rosette leaves were harvested from transgenic plants containing the *MYB90* promoter GUS fusion at three time points during late development. At the first time point the largest rosette leaves were mainly green in appearance while some of the older leaves had some yellowing of the leaves. This indicated that senescence was occurring. At the second time point the rosette leaves were green and yellow in appearance and at the last time points the rosette leaves appeared stressed and were mostly yellow (Fig 6.5B). The GUS activity increased during development and there was significant difference between the time points in the *MYB90* line.

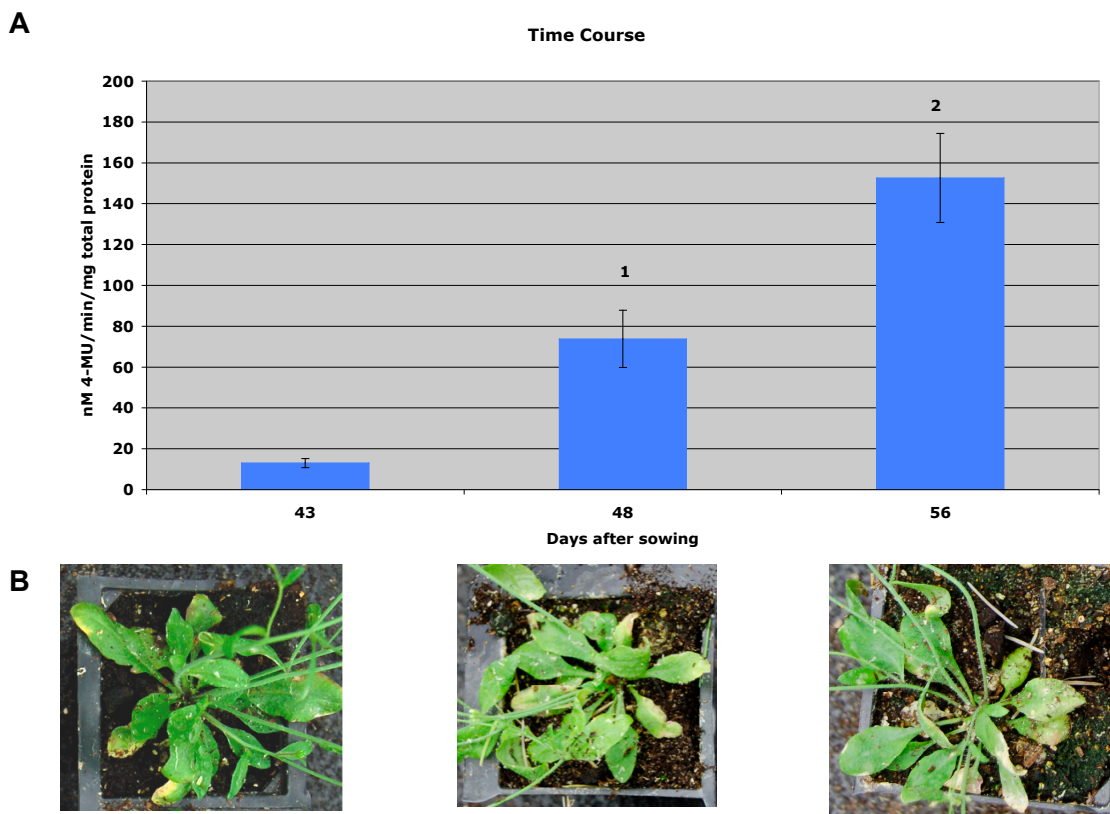


Fig 6.5: The Quantification GUS Activity in *MYB90* Promoter GUS Fusions During Development.

(A) The quantification of GUS activity in the leaves of six rosettes from the *MYB90* promoter GUS fusion at three time points. There was significant difference between the time points (1) 43 AND 48 Days after sowing $P = 0.00046$ and (2) 48 and 56 days after sowing $P = 0.0049$.

(B) Photographs of plants at the three time points.

6.3.2 Analysis of GUS Activity During Low Nitrogen High Glucose Stress.

Previous studies have indicated that anthocyanins are produced during stress and *MYB90* expression was found to be associated with the accumulation of anthocyanins during low N and high glucose stress (Pourtau *et al.*, 2005).

The transgenic plants carrying *MYB90* promoter constructs were grown under low N high glucose conditions in 16h days. Under these conditions, GUS staining was clearly visible in the veins of the *MYB90* promoter GUS fusions plants (Fig 6.6). The staining was concentrated around the vascular system (Fig 6.6 B-C) and appeared to spread into the neighbouring mesophyll cells (Fig 6.6 B). There were some instances where GUS activity appeared to be in cells close to the veins, possibly the companion cells (Fig 6.6C). In the leaves there was staining at the hydathodes (Fig 6.6D), which

are close to the end of the vascular system at the edge of the leaves. There was staining of pollen shown in figure 6.6E.

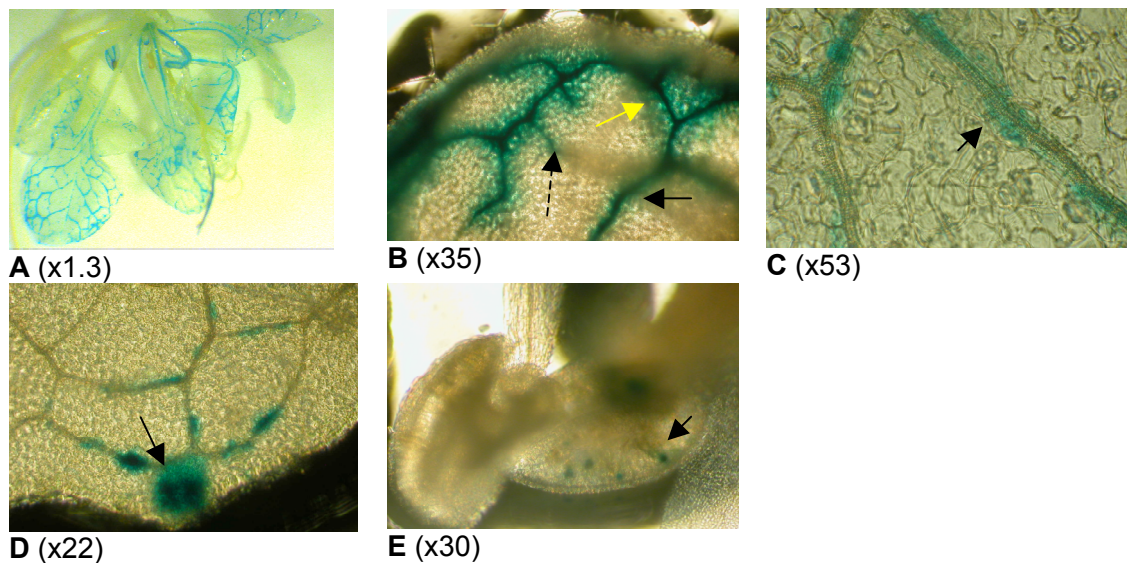


Fig 6.6: Effects of Low N High Glucose Stress on Transgenic Plants Carrying *MYB90*

Promoter GUS Fusions.

Histochemical staining transgenic plants carrying *MYB90* promoter GUS fusions. (A-D) The vascular system of the rosette leaves, (B) such as the secondary veins (filled in arrow), (B) in the tertiary veins (dashed arrow). (B) In the mesophyll cells neighbouring the veins (yellow arrow), (C) around the veins in leaves, (D) hydathodes and (E) young developing pollen.

6.4 MYB75 Promoter Construct Growth Experiments

6.4.1 Analysis of GUS Activity During Senescence

The GUS activity was visualised by histochemical staining of three different senescent transgenic plants containing *MYB75* promoter GUS fusions (Fig 6.7). Blue staining represented the GUS activity. GUS activity was seen in the mesophyll cells (Fig 6.7C-D) on the edge of senescent rosette leaves where chlorophyll breakdown was occurring (Fig 6.7B) and in the veins of the leaf (Fig 6.7A and E). There was GUS staining in the floral tissue, specifically the petals, stigma and stamen (Fig 6.7 F-H).

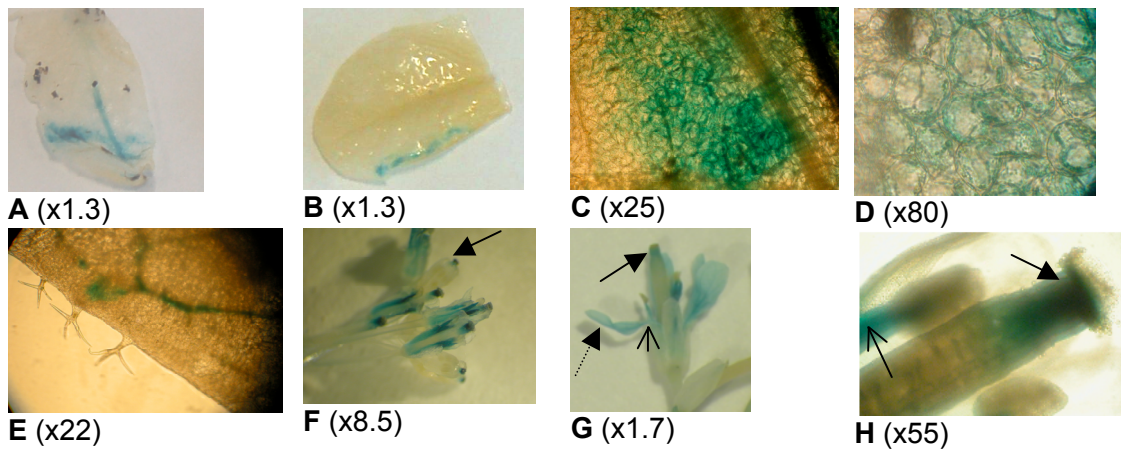


Fig 6.7: Histochemical Staining of Transgenic Plants Containing *MYB75* Promoter GUS

Fusions During Senescence.

Blue staining represented positive GUS activity.

There was staining in senescent rosette leaves (A-B), mesophyll cells (C-D), the leaf veins (E), the stamen (open arrow), stigma papillae (filled in arrow) and petals (dashed line arrow) (F-H).

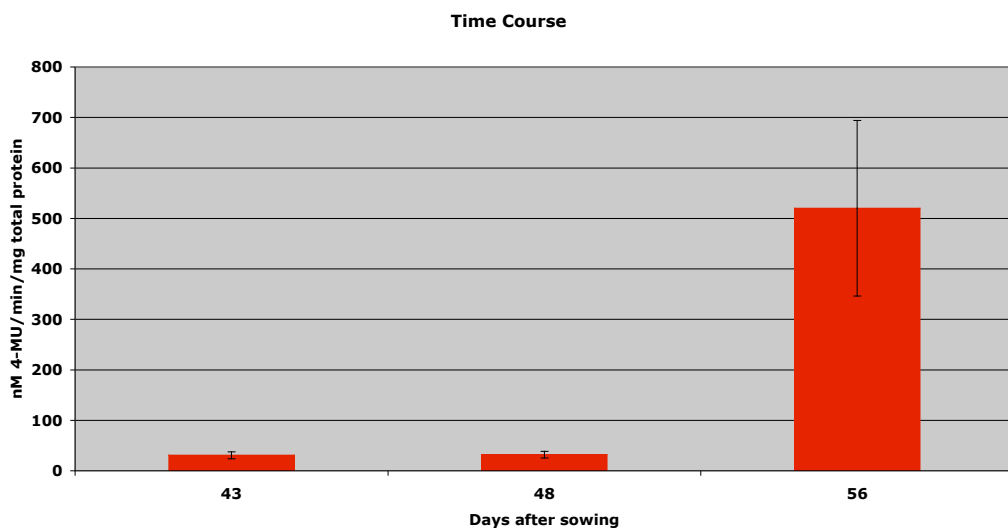


Fig 6.8: The Quantification GUS Activity in *MYB75* Promoter GUS Fusions During Development.

The quantification of GUS activity in the leaves of two rosettes from each of the three *MYB75* promoter lines at three time points. There was a significant difference between 48 and 56 days after sowing (1) $P = 0.01$.

The GUS activity of transgenic plants carrying three different *MYB75* promoter GUS fusions were quantified in whole rosettes at three different time points during late

development (Fig 6.8). The activity was low at the first two time points and then significantly increased in the last time point ($P= 0.01$). These results indicate that *MYB75* was up-regulated during senescence as has been shown previously in microarray experiments.

6.4.2 Analysis of GUS Activity During Low Nitrogen High Glucose Stress

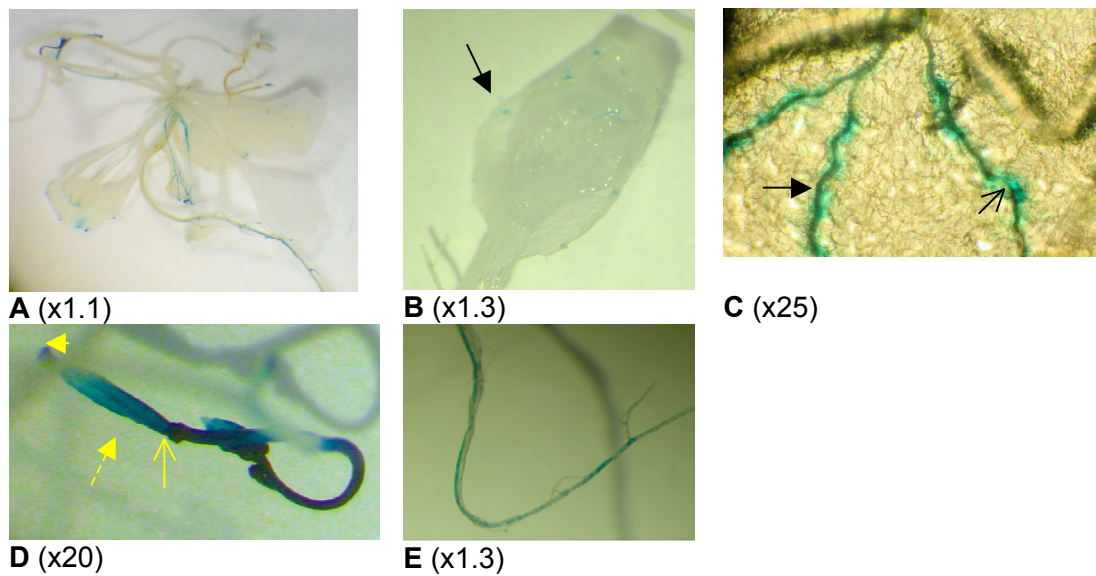


Fig 6.9: Effects of Low N High Glucose Stress on Transgenic Plants Carrying *MYB75*

Promoter GUS Fusions.

Histochemical staining transgenic plants carrying *MYB75* promoter GUS fusion. (A): in the hydathodes of leaves (B), the veins of leaves (filled in arrow) and around the veins (open arrow) (C). In the floral tissue such as the stigma papillae (filled in arrow), the ovary (dashed arrow) and the peduncle (open arrow) (D). There was blue staining of the roots (E).

Three different transgenic plant lines carrying *MYB75* promoter GUS fusions were grown in low N high glucose conditions for 16h days and then stained for GUS expression. In the leaves there was staining at the hydathodes (Fig 6.9 B), which are close to the end of the vascular system at the edge of the leaves and along the outside of the veins of the rosette leaves (Fig 6.9 C). There was staining in the roots (Fig 6.9E). The strongest visible staining was in the floral tissue such as the stigma papillae, the ovary and the peduncle below the floral tissue (Fig 6.9D).

6.4.3 Analysis of GUS Activity During High Light Exposure

Following high light stress there was no visible GUS staining of the *MYB90* promoter line. However there was GUS expression in of the *MYB75* promoter lines in the primary veins of younger rosette leaves (Fig 6.10B-E), the hydathodes of the older leaves (Fig 6.10G) and the top of the roots (Fig 6.10 I). The expression in the light stressed plants was in younger leaves and none was seen in the floral tissue. These locations were different to those seen in the low N high glucose stressed plants (Fig 6.9).

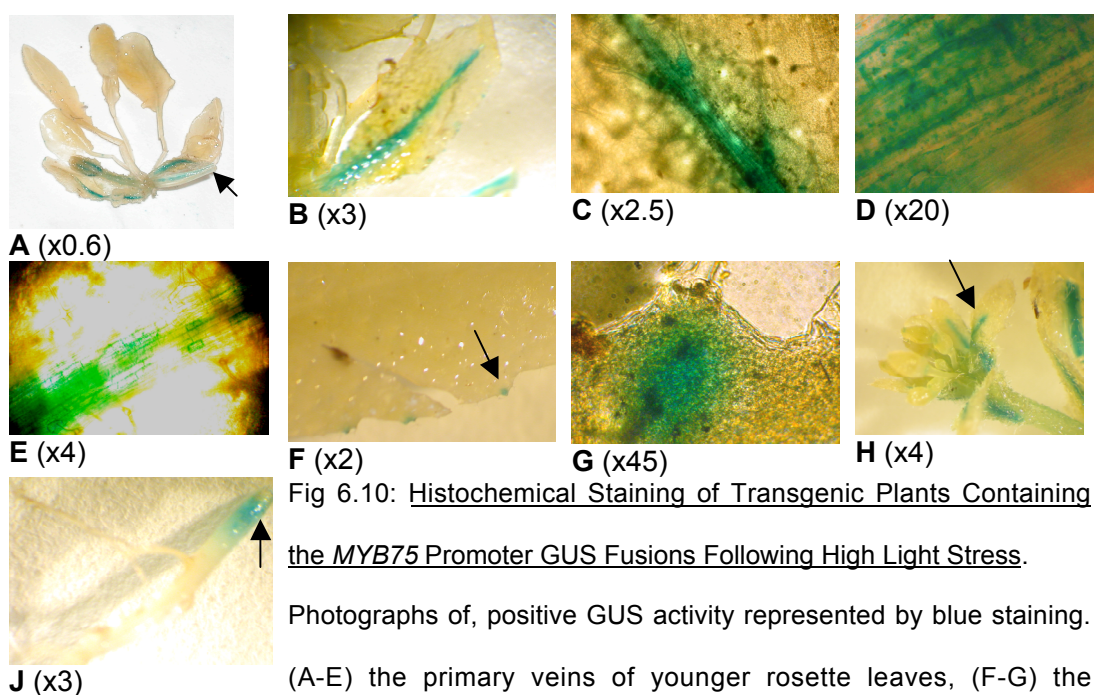


Fig 6.10: Histochemical Staining of Transgenic Plants Containing the *MYB75* Promoter GUS Fusions Following High Light Stress.

Photographs of, positive GUS activity represented by blue staining. (A-E) the primary veins of younger rosette leaves, (F-G) the hydathodes of older leaves, (H) the primary vein of sepals and (J) the top of the primary root.

6.5 Promoter Analysis

The *MYB90* and *MYB75* promoter sequences were analysed to identify potential transcription factor binding sites that may have a role in the differential transcriptional activation of the genes. The Athena web-based programme was used for this (O'Connor *et al.*, 2005). The programme identified several promoter motifs some of which were common to both gene promoters (Table 10 & Fig 6.11).

6.5.1 The promoter motifs shared by both promoters:

Both genes were shown in previous studies to regulate anthocyanin biosynthesis. The MYC2 BS in RD22 motif was found in both promoters and is known to positively regulate phenylpropanoid biosynthesis (Abe *et al.*, 1997). The motif is responsive to wounding, JA signalling pathway and ABA.

The promoters contained motifs that indicated that they are regulated by light and stress. The I-box and T-box motifs are involved in light regulation (Guiliano *et al.*, 1998, Chan *et al.*, 2001). The T-box was first found in the promoter of the GAPB gene, which is a nuclear gene that produces a subunit of a protein located in the chloroplast (Chan *et al.*, 2001).

Both genes may also have a role in response to stress because their promoters contained the W-box motif, which is the binding site for WRKY transcription factors (Yu *et al.*, 2000).

6.5.2 MYB90:

There were some promoter motifs that were identified only in the *MYB90* promoter. These included the CACGTG motif, also known as the G-box found upstream of light regulated genes such as the anthocyanin biosynthesis genes (Menkens & Cashmore, 1994, Shin *et al.*, 2007). This indicates that *MYB90* may be regulated by some factors that regulate the anthocyanin biosynthesis as might be expected. The ABRE –like motif, which has similarity to the G-box and known to be involved in the response to stress such as dehydration and low temperature (Shinozaki & Yamaguchi-Shinozaki, 2000). There is also a MYB2AT motif, which is a binding site for MYB transcription factor and a SV40- enhancer motif that has a role in enhancing transcriptional activity (Beaudoin & Rothstein, 1997).

The *MYB90* promoter sequence was further analysed using the web-based programme called Promomer. There were several significant promoter motifs (Table 10), these include Box P that was found upstream of the *PAL* gene and was involved in light mediated transcriptional activation (Logemann *et al.*, 1995). The I-box mentioned

earlier was also found by Promomer. The MEJARELELOX motif indicates that *MYB90* may be regulated in response to methyl jasmonate. An interesting motif found in the analysis of *MYB90* promoter was the COREOS motif, previously found in three antioxidant defence genes in rice (Tsukamoto *et al.*, 2005). Anthocyanins have antioxidant properties and this indicated that the regulation of anthocyanins biosynthesis by *MYB90* might have a role in antioxidant defence or at least be initiated by oxidative stress.

6.5.3 MYB75

The *MYB75* promoter contained a MYB binding site motif that has previously been shown to be flower specific and positively regulated phenylpropanoid biosynthesis genes (Sablowski *et al.*, 1994). This may indicate that *MYB75* and *MYB90* have different promoter motifs, which could differentially regulated anthocyanin biosynthesis. There was another MYB binding site, the MYB4 binding motif that has been implicated in responses to environmental stress (Chen *et al.*, 2002). The presence of the CCA1 motif indicates that the *MYB75* promoter may under circadian regulation (Wang *et al.*, 1997).

Promoter Motif	P-value	MYB75 No.	MYB90 No.
ARF binding site motif	0.4355	3	1
Box II promoter motif	0.5041	4	1
AtMYC2 BS in RD22	0.4332	1	3
I-box promoter motif	0.4637	5	3
CARGCW8AT	0.6553	10	8
GAREAT	0.6114	3	1
L1- box promoter motif	0.2918	2	1
MYB1AT	0.8038	5	2
MYCATERD1	0.4332	1	3
T-box promoter motif	0.5982	3	2
W-box promoter motif	0.6976	3	1
TATA box motif	0.8063	3	11
CCA1 binding site motif	0.3488	1	
Leafytag	0.1366	1	
MYB binding site promoter	0.3605	1	
MYB4 binding site motif	0.7431	4	
RAV1B binding site motif	0.1408	1	
ABRE-like binding site motif	0.2620		1
CACGTGMOTIF	0.1978		3
MYB2AT	0.3557		1
SV40 core promoter motif	0.2474		1
TELO box promoter motif	0.1211		1
COREOS*	0.009		4
BOX P*	0.003		3
MEJARELELOX*	0.005		3

Table 10: Web-Based Motif Analysis of MYB90 and MYB75 Promoters.

Motif search in *MYB90* and *MYB75* promoters (2000bp upstream) using the web based Athena programme (O'Connor *et al.*, 2005). The table displays the different promoter motifs, the P-value (calculated using hypergeometric distribution of the enrichment of the transcription factor sites found in the promoter sequences), the number of promoters with the transcription factor sites.

*Motif search using the web based Promomer programme (http://bar.utoronto.ca/ntools/cgi-bin/BAR_Promomer.cgi).



- | | |
|-------------------------------|--------------------------------|
| 1- MYC2 BS in RD22/ MYCATERD1 | 12- TATA |
| 2- ABRE-like and CACGTG motif | 13- MYC2 BS in RD22/ MYCATERD1 |
| 3- W-box | 14- CARGCW8GAT |
| 4- I-box | 15- TATA |
| 5- I-box | 16- ARF |
| 6- MYC2 BS in RD22/ MYCATERD1 | 17- MYB1AT |
| 7- GAREAT | 18- SV40 Core |
| 8- T-box | 19- TATA |
| 9- TATA | 20- L1- Box |
| 10-TATA | 21- TATA |
| 11- I-box | 22- MYB1AT |

MYB90 PROMOTER



- | | | |
|---------------------------|-----------------------|---------------|
| 1- W-box | 12- TATA | 23- MYB1AT |
| 2- MYB1AT | 13- TATA | 24- TATA |
| 3- TATA | 14- GAREAT | 25- CARGCW8AT |
| 4- TATA | 15- MYB4 and MYB1LEPR | 26- TATA |
| 5- CACGTG motif | 16- TATA | 27- MYB1AT |
| 6- MYB4 and | 17- TATA | 28- MYB4 |
| 7- MYB binding site motif | 18- GAREAT | 29- MYB4 |
| 8- MYB1AT | 19- W- box | 30- TATA |
| 9- MYB4 | 20- ABRE like | 31- DRE |
| 10- MYB4 | 21- MYB1AT | 32- L1-box |
| 11- GAREAT | 22- TATA | 33- MYB2AT |

MYB75 PROMOTER

Fig 6.11: *MYB90* and *MYB75* Promoter Motif Maps

Picture representing the location of promoter motifs 2000bp upstream *MYB90* (A) and *MYB75* (B) gene using the web based Athena programme (O'Connor *et al.*, 2005). The different motifs are represented by a coloured line and are numbered. The blue boxes represent potential CpG islands.

6.6 *MYB90* Promoter Deletions GUS Fusion Plant Growth Experiments

The promoter of *MYB90* was further analysed to determine the role of different cis elements in the transcriptional activation during senescence and following stress. A range of *MYB90* promoter deletion fragments were cloned and fused to the GUS.GFP reporter gene (Fig 6.12). Quantification of reporter gene expression in transgenic plants was used to determine the cis elements required for expression of *MYB90*.

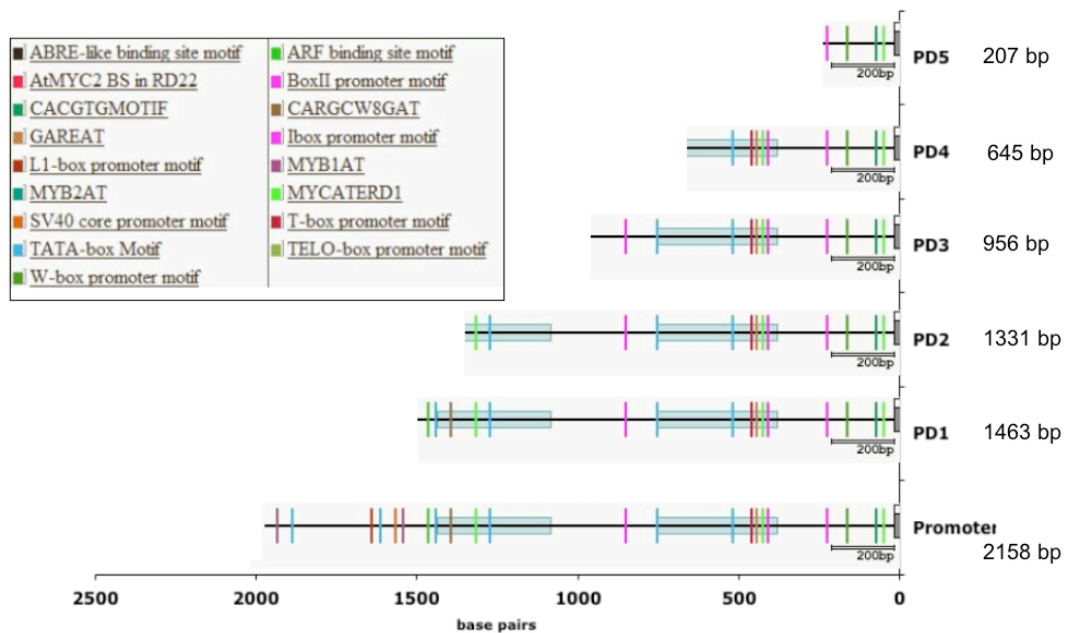


Fig 6.12: *MYB90* Promoter Deletion: GUS Fusions

The promoter deletion fragments of the *MYB90* promoter fused to the GUS.GFP reporter gene were designed to vary in size and span the promoter. Different coloured lines, shown in the legend, represent the transcription factor binding sites. The blue boxes represent the CpG islands. The GUS activity in each promoter deletion construct was analysed during senescence and stress.

GUS activity was quantified in the rosette leaves of transgenic plants carrying the *MYB90* promoter deletion fragment constructs at the mature green stage, senescent stage and following high light and low N high glucose stress, shown in Figure 6.13.

The highest GUS activity found was during senescence and following low N high glucose stress. The full-length promoter had the highest activity and the promoter motif

analysis indicated that the transcriptional activity may be enhanced by the SV40 core motif, which is the most obvious difference between the full length and PD1 constructs. The full-length promoter had significantly higher GUS activity during senescence than the promoter constructs 1 to 4, but interestingly, expression in PD5 was restored to full-length levels (Fig 6.13).

The full-length promoter had significantly higher activity following low N high glucose stress than the promoter deletion constructs 2 to 4. The smallest promoter deletion construct number 5 (PD5) had significantly higher activity than promoter deletion constructs 2 and 3. This indicates that there may be a motif involved in negative regulation of *MYB90* promoter. This motif is present in promoter deletion construct 1,2 3, and 4 but remains in PD4 implicating the sequence –956 to –645 of the promoter. PD5 contained the promoter motifs MYC2 BS in RD22 and CACGTG motif, which both have roles in regulation of anthocyanin biosynthesis. PD5 also contained W-box and ABRE-like motifs that are involved in stress response.

The full length promoter activity was low in mature green and high light stressed plants. The promoter deletion fragment PD5 had the highest activity during light stress and PD5 and PD4 had the highest activity in mature green plants.

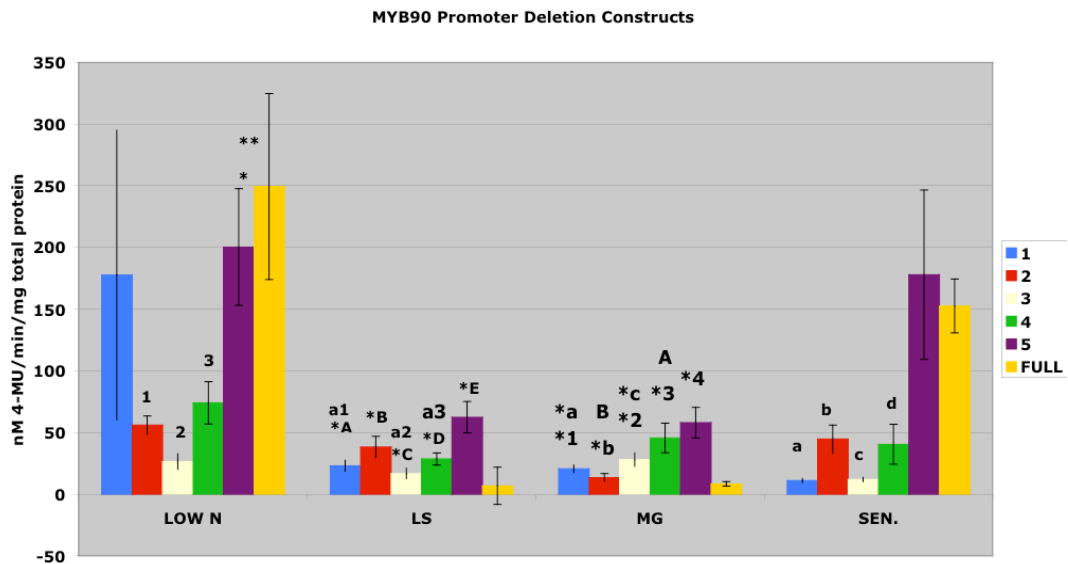


Fig 6.13: Quantification GUS Activity in Transgenic Plants Containing *MYB90* Promoter Deletion Constructs.

The quantification of GUS activity in the leaves of six rosettes from the *MYB90* Promoter deletion constructs 1-5 and the full length *MYB90* promoter in mature green (MG) and senescent (SEN) plants and following high light (LS) and low N high glucose stress (low N). Following low N high glucose the *MYB90* promoter had significant difference to the promoter deletion constructs PD2 (1) $P=0.001$, PD3 (2) $P=0.0001$ and PD4 (3) $P=0.005$. There was also a significant difference between the promoter construct 5 and the promoter constructs 2 and 3, (*) $P=0.0006$ and (**) $P=0.0029$. During senescence (SEN) the *MYB90* promoter had significant difference to the promoter constructs PD1 (a) $P>10^{-6}$, PD2 (b) $P=0.0002$, PD3 (c) $P>10^{-6}$ and PD4 (d) $P=0.0063$. There were significant differences in mature green (MG) plants between the full length promoter and promoter constructs PD1 (*1) $P=0.0056$, PD3 (*2) $P=0.013$, PD4 (*3) $P=0.025$ and PD5 (*4) $P=0.0026$, between the promoter construct 5 and the PD 1 (*a) $P=0.015$, PD2 (*b) $P=0.0058$ and PD3 (*c) $P=0.051$, between the PD4 and PD2 (A) $P=0.027$ and between PD3 and PD2 (B) $P=0.044$. Following high light treatment (LS) there were significant differences between the full length promoter and the promoter deletion constructs PD1 (*A) $P=0.012$, PD2 (*B) $P=0.013$, PD3 (*C) $P=0.056$, PD4 (*D) $P=0.0024$ and PD5 (*E) $P=0.007$ and between the promoter deletion construct PD5 and the promoter deletion constructs PD1 (a1) $P=0.016$, PD3 (a2) $P=0.015$ and PD4 (a3) $P=0.046$.

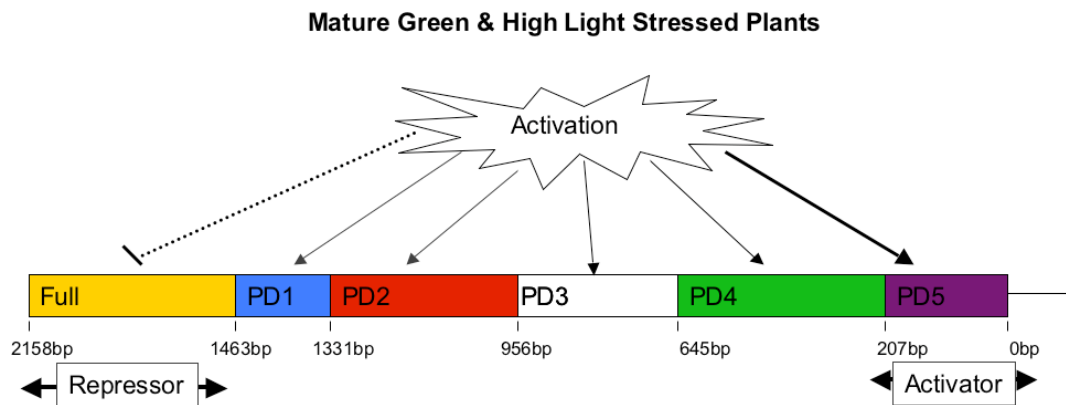
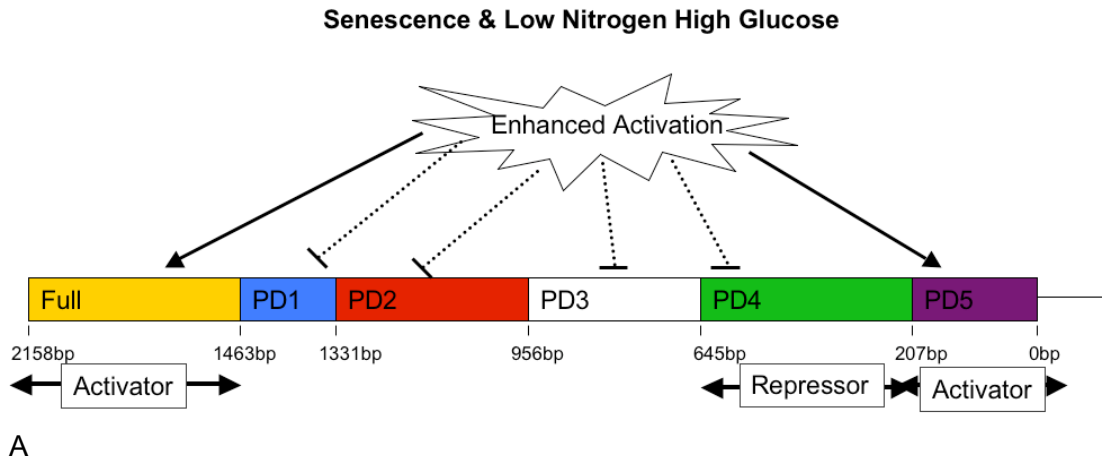


Fig 6.14: Cartoon representation of *MYB90* promoter activity in (A) senescent, low nitrogen high glucose treated, (B) mature green and high light stressed plants. (A) There is a motif for enhanced activity during senescence and low Nitrogen and high glucose treatment in the region 1463- 2158bp and there was repression of activity in PD4 from 207-645bp. (B) The thickness of the arrows represent the promoter activity in mature green and high light treated plants. The highest activity was in PD5, 0-207bp. The lowest activity was in the full length promoter, region 1463-2158bp.

Figure 6.14 shows a cartoon representation of the *MYB90* promoter activity in senescent, low nitrogen high glucose treated, mature green and high light treated plants. The activity of the promoter deletion GUS: fusions showed that activation of the promoter requires the region 207-0bp. This promoter fragment contains the I-box and CACGTG promoter motifs involved in light activation (Guiliano *et al.*, 1998, Menkens & Casmore, 1994), the Wbox and ABRE-like motifs involved in stress response (Yu *et al.*, 2000, Shinozaki & Yamaguchi-Shinozaki, 2000) and the MYC2 BS, MYCATERD1 and

CACGTG promoter motifs involved in phenylpropanoid biosynthesis (Abe *et al.*, 1997, Menkens & Cashmore, 1994). The senescence and low nitrogen high glucose enhanced promoter activity required the region 2158-1463bp and there was repression of activity at 207-645bp. The enhanced activation region had a SV40 promoter motif, which may be the motif required for senescence and low nitrogen high glucose specific enhanced activity (Beaudoin & Rothstein, 1997). There is no obvious motif found in the PD4 sequence that could be responsible for the repression of promoter activity.

6.7 Conclusions

In this chapter the activity of the *MYB90* and *MYB75* promoters were visualised and quantified during senescence, high light and low nitrogen- high glucose stress to analyse the temporal, spatial and level of expression. The promoter sequences were analysed to narrow down the promoter motifs responsible for senescence and stress specific enhanced expression and tested in a promoter deleting experiment.

6.7.1 MYB90

During senescence GUS staining was rarely visible, which suggests that there was a tight timing issue. GUS activity was observed in the vascular tissue of senescent leaves. The levels of GUS activity increased during late senescence.

MYB90 has been shown to be involved in the regulation of anthocyanin biosynthesis in the response to low nitrogen conditions (Pourtau *et al.*, 2005, Lea *et al.*, 2007). GUS activity was highly visible following low N high glucose treatment around the vascular tissue; possibly in the companion or bundle sheath cells. There was staining of the hydathodes and young pollen. *MYB90* was found to be involved in the regulation of anthocyanin biosynthesis and previous chapters have shown the role of *MYB90* anthocyanin biosynthesis during senescence and stress. Localisation of anthocyanin biosynthesis to cells close to vascular tissue may protect the cells essential for transportation of nutrients from the senescing or stressed leaves to other

regions of the plant, such as the flowers or younger and more photosynthetically active leaves.

In a previous chapter, *MYB90* expression was found to be required for a normal WT response to high light stress. However, following 48h high light treatment there was no detectable GUS activity seen in the transgenic plants. This may be due to different factors affecting anthocyanin biosynthesis. Anthocyanin biosynthesis is regulated by a combination of factors such as light intensity, temperature and age (Keskitalo *et al.*, 2005). The plants may not have been stressed enough for the induction of *MYB90* promoter activity.

Analysis of a series of *MYB90* promoter deletion: GUS fusions indicated that there was a senescence and low nitrogen high glucose specific enhanced activation region in the promoter. The SV-40 enhancer motif may be a critical element for this enhanced activity of the promoter. The SV40 enhancer motif was identified in simian virus 40 (SV40) and has been shown to have enhancer activity in mammalian cells and in algae cells (Ondek *et al.*, 1987, Neuhaus *et al.*, 1984). There are three segments to the SV40 enhancer and each of these segments can act as an enhancer in multiple copies. The segments also have different cell specificity and can differ the specificity in different combinations (Schirm *et al.*, 1987, Ondek *et al.*, 1987). The SV40 core enhancer sequence was identified in the *MYB90* promoter and is present in the region 258-1462bp. Also, there is a SV40 octamer enhancer sequence in the region 1463-1331bp. These two sequences may potentially be the senescence and low nitrogen high glucose activation element.

There is a repressor region 645-207bp that reduced *MYB90* promoter activity during senescence and low nitrogen high glucose treatment. It is not clear which motif is responsible for the repressor activity.

6.7.2 *MYB75*

During senescence of transgenic plants containing the *MYB75* promoter GUS fusions, GUS activity increased during senescence and there was visible GUS activity in

senescent leaves; in or around the vascular tissue of leaves and in leaf mesophyll cells. There was activity in floral tissue; in the petals, stamen and stigma papillae. *MYB75* regulates anthocyanin biosynthesis and the localisation to the primary vein again may be for the protection of nutrient transport out of the senescent leaf. The localisation to floral tissue may be to ensure efficient and successful reproduction.

MYB75 has been shown in a previous chapter to affect the plants resistance to high light and has also been shown to be important in the light induction of anthocyanin biosynthesis (Cominelli *et al.*, 2008). There was visible GUS activity following 48h high light treatment in the primary vein of young leaves, but only in the hydathodes of older leaves. This indicated that *MYB75* may be involved in selective protection of younger leaves. There was GUS activity in the primary vein of sepals of young floral tissue, probably for protection of the development of the flowers and reproduction. In roots activity was only at the top of the root/ base of the stem below the rosette leaves presumably because the rest of the root system is protected from the high light exposure by compost.

Following low nitrogen high glucose stress there was GUS activity in and/or around the vascular tissue of all the leaves, in the floral tissue such as in the stigma papillae and the peduncle and the whole root system. The expression pattern in low nitrogen high glucose conditions may be due to the distribution of glucose in the plant that is taken up from the medium. These results suggest that the *MYB75* promoter may be regulated differently during different stresses in different tissues.

Analysis of the *MYB75* promoter sequence found several promoter motifs that may be important for regulation of the promoter. These included a MYB binding site, a W-box and the CCA1 motif. In a previous chapter *MYB75* expression was regulated by *MYB90* during senescence and the MYB binding site may be the required binding site of *MYB90*.

Both *MYB90* and *MYB75* promoter activity was localised to vascular tissue during senescence and stress. In high light stressed leaves and during wounding H₂O₂ has

been shown to accumulate in vascular tissue (Orozco-Cárdenas *et al.*, 2001, Fryer *et al.*, 2003). During high light stress the activity of a peroxidase gene (*APX2*) has been shown to be localised in the photosynthetically active bundle sheath cells that surround the phloem and xylem in the vascular tissue (Fryer *et al.*, 2003). *MYB90* and *MYB75* activation of anthocyanin biosynthesis around the vascular tissue, possibly in bundle sheath cells, may reduce photo-oxidative stress and anthocyanins may potentially act as antioxidants to reduce ROS and ensure efficient nutrient recovery (Field *et al.*, 2001, Yokozawa *et al.*, 1998).

6.8 Summary

In summary, the *MYB90* promoter had the highest activity during senescence and low nitrogen high glucose treatment. GUS expression was mainly localised around the vascular system in leaves, indicating a role in efficient nutrient transport during senescence and stress. The promoter had a repressor element that reduced the promoter activity and an activation element that enhanced promoter activity during senescence and low nitrogen and high glucose stress.

MYB75 promoter activity was induced during senescence, high light stress and low nitrogen high glucose treatment but with different tissue specificity. There was activity in leaves and floral tissue, which shows that *MYB75* is differentially regulated compared to *MYB90*.

7 General Discussion

Senescence in leaves is frequently associated with anthocyanin accumulation (Hoch *et al.*, 2001) and this may increase the efficiency of nutrient recycling from the senescing leaf to other parts of the plant (Field *et al.*, 2001). Anthocyanins are generally thought to provide photoprotection by reducing the light available to chlorophyll and therefore reducing the level excitation energy (Krol *et al.*, 1995, Pietrini & Massacci, 1999, Smillie & Hetherington, 1999). Two senescence enhanced MYB transcription factors, *MYB90* and *MYB75* had been previously found to be involved in anthocyanin biosynthesis in *Arabidopsis* (Borevitz *et al.*, 2000). The purpose of this study was to determine the role of these two genes during senescence and stress.

7.1.1 MYB90 Regulates Anthocyanin Biosynthesis During Senescence

Work presented in this thesis has shown that *MYB90* has an important regulatory role in anthocyanin biosynthesis during senescence. *MYB90* is an upstream regulator of *MYB75*, regulates transcriptional activation of anthocyanin biosynthesis genes, and has downstream effect on *TT8* expression during senescence. In the absence of *MYB90* expression, there was a reduction in the photosynthetic performance, at different time points during development. This may indicate that altered anthocyanin levels reduce the photoprotection resulting in increased stress and damage to the photosystems. However, some anthocyanin synthesis did occur, this indicates that there are other regulatory genes involved.

There are other genes that have a role in regulation of anthocyanin biosynthesis and these may partly compensate for the absence of *MYB90* expression. These genes may include other MYB transcription factors, for example over-expression of *MYB113* and *MYB114* showed increases anthocyanin accumulation similar to that seen following over-expression of *MYB75* (Gonzalez *et al.*, 2008, Borevitz *et al.*, 2000). Other genes that regulate anthocyanin biosynthesis include *PIF3* and *HY5* (Shin *et al.*, 2007).

Other modes of regulation of anthocyanin biosynthesis may involve post-transcriptional or post-translational regulation. In *petunia* the reduction of *CHS* expression or the increase of *FLS* expression repressed anthocyanin biosynthesis (Satio *et al.*, 2006). In transgenic *petunia* over-expressing *CHS*, *F3H* or *DFR* was observed to occasionally repress anthocyanin biosynthesis by post-transcriptional gene silencing (van Blokland *et al.*, 1994, van der Krol *et al.*, 1990 and Napoli *et al.*, 1990). In dark grown cell cultures of *Daucous carota* L. UV irradiation increased the activity of enzymes involved in the phenylpropanoid pathway and enzymes of the flavonoid and anthocyanin biosynthesis pathways in an ordered sequential co-ordinated induction resulting in enhanced anthocyanin accumulation (Glaeûgen *et al.*, 1998). Alterations of mRNA levels mediated the de novo synthesis of the key enzyme proteins involved in anthocyanin biosynthesis in carrot (Glaeûgen *et al.*, 1998).

7.1.2 MYB90 and MYB75 Have a Role in Photo-oxidative Protection During High Light Stress

Anthocyanin have been reported to increase resistance to high light stress (Field *et al.*, 2001). In this experiment anthocyanin accumulation was also associated with increased photosynthetic performance during prolonged high light stress. During shorter duration of light stress the NPQ mechanisms depending on the xanthophyll cycle provide photooxidative protection by dissipating excess energy (Li *et al.*, 2002). During normal light conditions NPQ dissipates 45-64% of absorbed light energy and during stress this increases to 75-92% (Flexas & Medrano, 2002). However NPQ is not sufficient protection during prolonged high light stress and other protective mechanisms are required (Golan *et al.*, 2005). The increased accumulation of anthocyanins helps to reduce excitation pressure on PS2 by absorbing light energy. *MYB90* was important in the response to high light stress, and shown to regulate anthocyanin biosynthesis. The low photosynthetic performance was seen more clearly in older leaves, indicating a leaf age dependent response. Reduced anthocyanin levels were seen in the *MYB90* knock out mutant following light stress but there was

compensation by another gene since levels of both anthocyanin and flavonoids eventually became the same as the wild type during high light stress. This may be a MYB gene as discussed earlier. *MYB75* expression was regulated by *MYB90* during senescence but may be under different regulation during light stress. Cominelli *et al.*, (2008) found *MYB75* expression preceded *MYB90* expression in response to light. Another gene that induced anthocyanin accumulation during high light stress was a zinc finger (*RHL41*); over-expression of this gene resulted in increased resistance to high light stress and increased anthocyanin accumulation, probably by inducing an enhanced stress response (Asakolida *et al.*, 2000).

Data reported in this thesis shows that *MYB75* also has a role in resistance to high light stress, and transgenic *MYB75* RNAi knockout plants showed reduced photosynthetic performance. However, the absence of *MYB75* expression did not effect anthocyanin accumulation, which was presumably compensated for by another gene. This may show that *MYB75* is associated with other protective mechanisms.

7.1.3 Regulation of *MYB90* and *MYB75* Promoter Activity

Increased *MYB90* expression accompanied by anthocyanin accumulation were previously been seen in low nitrogen and low nitrogen high glucose conditions (Pourtau *et al.*, 2005, Lea *et al.*, 2007). The experiments described here, with the *MYB90* promoter GUS fusions showed that activity was highly induced by low nitrogen high glucose treatment and also in senescent leaves. GUS expression from the *MYB90* promoter was mostly localised to vascular tissue with some activity in the hydathodes and mesophyll cells.

The experiments with the *MYB75* promoter GUS fusions showed that expression of this gene was also localised to vascular tissue, mesophyll cells and floral tissue.

The localisation of *MYB90* and *MYB75* promoter activity at the vascular tissue may be to maintain efficient nutrient recovery. During stress there are increased levels

of H₂O₂ in vascular tissue (Fryer *et al.*, 2003). Anthocyanins may have a role as antioxidants scavenging reactive oxygen species (Yokozawa *et al.*, 1999). An antioxidant enzyme APX2 associated with photosynthetically active bundle sheath cells is expressed around vascular tissue during light stress (Fryer *et al.*, 2003). The bundle sheath cells form 15% of chloroplast containing cells in an Arabidopsis leaf (Kinsman & Pyke, 1998) so anthocyanins biosynthesis in these cells may have a role in protecting the photosynthetic apparatus from excess excitation energy and maintaining cell viability while nutrient mobilisation takes place..

7.1.4 Identification of Potential Promoter Motifs Regulating MYB90

Deletion analysis of the *MYB90* promoter indicated the presence of both an activator and a repressor region. The repressor region reduced the *MYB90* promoter activity during senescence and low N high glucose activity. There have been a few negative regulators of anthocyanin biosynthesis in Arabidopsis reported previously. The gene *ICX1* was found to have a role in repressing anthocyanin biosynthesis in numerous conditions including light (Wade *et al.*, 2003). Other regulators include *COP*, *DET* and *FUS* proteins that were identified by mutant studies (Misera *et al.*, 1994, Hardtke & Deng, 2000). Recently a R3-MYB protein, MYBL2 has been identified and has been shown to bind to the TT8 protein and suppress the expression of *DFR*, also the *MYBL2* knockout mutant had enhanced accumulation of anthocyanins (Matsui *et al.*, 2008, Dubos *et al.*, 2008). Also, an Arabidopsis MYB transcription factor MYB60, has been shown to repress anthocyanin biosynthesis in lettuce (Park *et al.*, 2008). The activator region was responsible for enhanced *MYB90* promoter activity during senescence and low N high glucose activity and contains an SV40 enhancer motif that has been shown to enhance promoter activity and have cell type specific activity (Ondek *et al.*, 1987, Schirm *et al.*, 1987).

There was some difficulty in repeating the high light stress experiments and the expression of *MYB90* in transgenic plants containing *MYB90* promoter: GUS fusions

was difficult to detect in senescent leaves following high light stress. These difficulties may have occurred due to the variability of the environmental conditions in the glasshouse. The regulation of anthocyanin synthesis has been shown to depend on variables such as development stage and previous light exposure (Rabino & Mancinelli, 1986, Mita *et al.*, 1997, Lillo *et al.*, 2008, Hoch *et al.*, 2001). In senescing Aspen anthocyanins were continuously metabolised and new anthocyanin biosynthesis depended on environmental conditions (Keskitalo *et al.*, 2005).

7.2 Summary

MYB90 is important for anthocyanin accumulation during senescence and is an upstream regulator of *MYB75* during senescence. Both *MYB90* and *MYB75* are important during high light stress but other factors can partly compensate for their absence. The expression of *MYB90* is mostly localised to vascular tissue during senescence and high light stress, which indicates a role in protection of nutrient recovery. There are both activator and repressor regions that regulates *MYB90* promoter activity which adds another level of complexity to the regulation of anthocyanin biosynthesis.

7.3 Future Work

In the future, the role of *MYB90* may be further investigated using a double knockout mutant of *MYB90* and *MYB75*. Analysis of gene expression and anthocyanin biosynthesis in a *MYB90* and *MYB75* double knockout line would perhaps provide further insight into their roles in regulating anthocyanin biosynthesis during senescence and stress. Elucidation of the regulation of *MYB90* transcriptional activation would require the identification of potential transcriptional regulators that may have roles in activating and repressing induction of *MYB90* by yeast1- hybrid assay.

The role of *MYB90* in the response to high light stress may be further analysed by gene expression studies in the *MYB90* knockout mutant to identify the gene compensating for the absence of *MYB90* expression. Also there was indication of a

leaf age-dependent response by *MYB90*, which may be further investigated in individual leaves.

8 BIBLIOGRAPHY

- Abe, H., Yamaguchi-Shinozaki, K., Urao, T., Iwasaki, T., Hosokawa, D., Shinozaki, K.** (1997). Role of Arabidopsis MYC and MYB homologs in drought- and abscisic acid-regulated gene expression. *Plant Cell* 9:1859-1868.
- Abrahams, S., Lee, E., Walker, A.R., Tanner, G.J., Larkin, P.J. & Ashton, A.R.** (2003). The Arabidopsis TDS4 gene encodes leucoanthocyanidin dioxygenase (LDOX) and is essential for proanthocyanidin synthesis and vacuole development. *The Plant Journal* 35: 624-636.
- Aharoni, A., De Vos, C.H., Wein, M., Sun, Z., Greco, R., Kroon, A., Mol, J.N. & O'Connell, A.P.** (2001). The strawberry FaMYB1 transcription factor suppresses anthocyanin and flavonol accumulation in transgenic tobacco. *Plant Journal* 28: 319-332
- Ali, M., Jensen, C.R., Mogensen, V.O., Anderson, M.N., Henson, I.E.** (1999). Root signalling and osmotic adjustments during intermittent soil drying sustain grain yield of field grown wheat. *Field Crops Research* 62: 35-52.
- Allan, D., Billah, M.M., Finean, J.B. & Michell, R.H.,** (1976). Release of diacylglycerol-enriched vesicles from erythrocytes with increased intracellular $[Ca^{2+}]$. *Nature* 261: 58-60.
- Asada, K.** (1999). The water-water cycle in chloroplasts: scavenging of active oxygens and dissipation of excess photons. *Annual Review Plant Physiology and Plant Molecular Biology* 50: 601–639.
- Austin, J.R., 2nd Frost, E., Vidi, P.A., Kessler, F., Staehelin, L.A.** (2006). Plastoglobules are lipoprotein subcompartments of the chloroplast that are permanently coupled to thylakoid membranes and contain biosynthetic enzymes. *The Plant Cell* 18: 1693–1703.
- Bachmann, A., Fernández-López, J., Ginsburg, S., Thomas, H., Bouwkamp, J.C., Solomos, T. and Matile P.** (1994). Stay green mutant genotypes of *Phaseolus vulgaris* L: chloroplast proteins and chlorophyll catabolites during foliar senescence. *New Phytologist* 126: 593-600.
- Baker, N.R., Oxborough, K., Lawso, T. & Morison, J.I.L.** (2001). High resolution imaging of photosynthetic activities of tissues, cells and chloroplasts in leaves. *Journal of Experimental Botany* 52: 1-7.
- Barbagallo, R.P., Oxborough, K., Pallet, K.E. & Baker, N.R.** (2003). Rapid, non-invasive screening for perturbations of metabolism and plant growth using chlorophyll fluorescence imaging. *Plant Physiology* 132: 485-493.

- Barber, R.F., and Thompson, J.E.** (1980). Senescence-dependent increase in the permeability of liposomes prepared from bean cotyledon membranes. *Journal of Experimental Botany* 31: 1305–1313.
- Barber, R.F., and Thompson, J.E.** (1983). Neutral lipids rigidify unsaturated acyl chains in senescing membranes. *Journal of Experimental Botany* 34 268–276.
- Barr, R., Crane, F.C., & Giaquinta, R.T.** (1975). Dichlorophenylurea-insensitive reduction of silicomolybdic acid by chloroplast photosystem II. *Plant Physiology* 55: 460-462.
- Bate, N.J., Rothstein, S.J., and Thompson, J.E.** (1991). Expression of Nuclear and Chloroplast Photosynthesis-Specific Genes During Leaf Senescence. *Journal of Experimental Botany* 44: 801-811.
- Baudry, A., Heim, M.A., Dubreucq, B., Caboche, M., Weisshaar, B. & Lepiniec, L.** (2004). TT2, TT8 and TTG1 synergistically specify the expression of BANYLUS and proanthocyanidins biosynthesis in *Arabidopsis thaliana*. *The Plant Cell* 39, 366-380.
- Baudry, A., Caboche, M. & Lepiniec L.** (2006). TT8 controls its own expression in a feedback regulation involving TTG1 and homologous MYB and bHLH factors, allowing a strong and cell specific accumulation of flavonoids in *Arabidopsis thaliana*. *The Plant Journal* 46: 768-779.
- Beaudoin, N. & Rothstein, S.J.** (1997). Developmental regulation of two tomato lipoxygenase promoters in transgenic tobacco and tomato. *Plant Molecular Biology* 33:835-846
- Beissbarth T. and Speed T.P.** (2004). GOstat: find statistically overrepresented Gene Ontologies within a group of genes. *Bioinformatics* 6: 1464-1465
- Benjamini, B. & Hochberg, Y.** (1995). Controlling the false discovery rate: a practical and powerful approach to multiple testing. *Journal of the Royal Statistical Society B.* 57: 289-300.
- Bhattachara, P.K., Pappelis, A.J., Lee, S.C., BeMiller, J.N., Karagiannis, C.S.** (1996). Nuclear (DNA, RNA, histone and non-histone protein) and nucleolar changes during growth and senescence of may apple leaves. *Mechanisms of Ageing & Development* 92: 83–99.
- Binns, A.N.** (1994). Cytokinin accumulation and action: biochemical, genetic, and molecular approaches. *Annual Review Plant Physiology Plant Molecular Biology* 45: 173-196.
- Björkman, O., & Demmig, B.** (1987). Photon yield of O₂ evolution and chlorophyll fluorescence characteristics at 77 K among vascular plants of diverse origins. *Planta* 170: 489–504.
- Bleeker and Patterson** (1997). Last exit: senescence, abscission, and meristem arrest in

- Arabidopsis. *Plant Cell* 9: 1169-1179.
- van Blokland, R., van der Geest, N., Mol, J.N.M. & Kooter, J.M.** (1994). Transgene mediated suppression of chalcone synthase expression in *Petunia hybrida* results from an increase in RNA turnover. *Plant Journal* 6: 861-877.
- Bloor, S.J. & Abrahams, S.** (2002). The structure of the major anthocyanin in *Arabidopsis thaliana*. *Phytochemistry* 59: 343-346.
- Borevitz, J. O., Xia, Y., Bount, J., Dixon, R.A. & Lamb, C.** (2000). Activation tagging identifies a conserved MYB regulator of phenylpropanoid biosynthesis. *The Plant Cell* 12: 2383-2393.
- Borochoy, A., Halevy, A.H. and Shinitzky, M.,** (1982). Senescence and the fluidity of rose petal membranes: Relationship to phospholipids metabolism. *Plant Physiology* 69: 296-299.
- Boyer, P.D.** (1998). ATP synthase—past and future. *Biochimica et Biophysica Acta* 1365: 3–9.
- Brenner, W.G., Romanov, G.A., Kollmer, I., Burkle L. & Schmulling, T.** (2005). Immediate-early and delayed cytokinin response genes of *Arabidopsis thaliana* identified by genome-wide expression profiling reveal novel cytokinin-senesitive processes and suggest cytokinin action through transcriptional cascades. *The Plant Journal* 44: 314-333.
- Brouquisse, R., Masclaux, C., Feller, U. and Raymond, P.** (2001). Protein hydrolysis and nitrogen remobilisation in plant life and senescence. In: Lea PJ, Moro-Gaudry J-F, eds. *Plant nitrogen*. Berlin: Springer-Verlag, 275-293.
- Brown, J.H., Lynch, D.V. and Thompson, J.E.** (1987). Molecular species specificity of phospholipids breakdown in microsomal membranes of senescing carnation flowers. *Plant Physiology* 85: 679-683.
- Brown, J.H., Paliyath, G. and Thompson, J.E.,** (1991). *Plant Physiology: A treatise* Vol. X. academic press, 227-275.
- Buchanan-Wollaston, V.** (1997). The molecular biology of leaf senescence. *Journal of Experimental Botany* 48, 181–199.
- Buchanan, B., Gruissem, W., Jones, R.L.,** (2000). *Biochemistry and molecular biology of Plants*. John Wiley and sons Ltd.
- Buchanan-Wollaston, V., Earl, S., Harrison, E., Mathas, E., Navabpour, S., Page, T., Pink, D.** (2003). The molecular analysis of leaf senescence- a genomics approach. *Plant Biotechnology Journal* 1: 3-22.

- Buchanan-Wollaston, V., Page, T., Harrison, E., Breeze, E., Lim, O.P., Nam, H.G., Lin, J., Wu, S., Swizinski, J., Ishizaki, J., and Leaver, C.,** (2005). Comparative transcriptome analysis reveals significant differences in gene expression and signalling pathways between developmental and dark/starvation-induced senescence in Arabidopsis. *The Plant Journal* 42: 567-586.
- Burbulis, I.E. & Winkel Shirley, B.** (1999). Interactions among enzymes of the Arabidopsis flavonoid biosynthetic pathway. *PNAS* 96: 12929-12934.
- Causin, H.F., Jauregui, R.N. & Barneiz, A.J.** (2006). The effect of light spectral quality on leaf senescence and oxidative stress in wheat. *Plant Science* 171, 24-33.
- Chalker-Scott, L.,** (1999). Environmental significance of anthocyanins in plant stress responses. *Photochemistry and Photobiology* 70: 1-9.
- Chan, C.S., Guo, L. & Shih, MC.** (2001). Promoter analysis of the nuclear gene encoding the chloroplast glyceraldehyde-3-phosphate dehydrogenase B subunit of Arabidopsis thaliana. *Plant Molecular Biology* 46: 131-141.
- Chang, D-Y., Miksche, J.P. & Dhillon, S.S.** (1985). DNA changes involving repeated sequences in senescing soybean (Glycine max) cotyledon nuclei. *Physiologia Plantarum* 64: 409-417.
- Charlton, W.L., Johnson, B., Graham, I.A., and Baker, A.** (2005). Non-coordinate expression of peroxisome biogenesis, β -oxidation and glyoxylate cycle genes in mature Arabidopsis plants. *Plant Cell Reports* 23: 647-653.
- Chen, W., Provart, N., Glazebrook, J., Katagiri, F., Chang, HS., Eulgem, T., Mauch, F., Luan, S., Zou, G., Whitham, S., Budworth, P.R., Tao, Y., Xie, Z., Chen, X., Lam, S., Kreps, J., Harper, J., Si-Ammour, A., Mauch-Mani, B., Heinlein, M., Kobayashi, K., Hohn, T., Dangl, J., Wang, X. and Zhu, T.** (2002). Expression profile matrix of Arabidopsis transcription factor gene suggests their putative functions in the response to environmental stresses. *The Plant Cell* 14: 559-574.
- Chiba, A., Ishida, H., Nishizawa, N.K., Makino, A., & Mae, T.** (2003). Exclusion of Ribulose-5-bisphosphate carboxylase/oxygenase from chloroplasts by specific bodies in naturally senescing leaves of wheat. *Plant Cell Physiology* 44: 914-921.

- Chung, B.C., Lee, S.Y., Oh, S.A., Rhew, T.H., Nam, H.G. and Lee C.H.** (1997). The promoter activity of sen1, a senescence associated gene of Arabidopsis is repressed by sugars. *Journal Plant Physiology* 151, 339–345.
- Clements J. & Atkins C.** (2001). Characterisation of a non abscission mutant in *Lupinus angustifolius*. Genetic and structural aspects. *American Journal of Botany* 88: 31-42.
- Clouse, S.D.** (2002) Brassinosteroids. Plant counterparts to animal steroid hormones? *Vitamines & Hormones* 65: 195-223.
- Cominelli, E., Gusmaroli, G., Allegra, D., Galbiati, M., Wade, H.K., Jenkins, G.I. & Tonelli, C.** (2007). Expression analysis of anthocyanin regulatory genes in response to different light qualities in Arabidopsis thaliana. *Journal of Plant Physiology* 165: 886-894.
- Corpas, F.J., de la Colina, C., Sánchez-Rasero, F., del Río, L.A.,** (1997). A role for leaf peroxisomes in the catabolism of purines. *Journal Plant Physiology* 151: 246–250.
- Dai, N., Schaffer, A., Petreikov, M., Shahak, Y., Giller, Y., Ratner, K., Levine, A. & Granot, D.,** (1999). Overexpression of Arabidopsis hexokinase in tomato plants inhibits growth, reduces photosynthesis, and induces rapid senescence. *The Plant Cell* 11: 1253-1276.
- Davies, K. M. & Schwinn, K.E.** (2003). Transcriptional regulation of secondary metabolism. *Functional Plant Biology* 30: 913-925.
- Davies, S.J. & Millar, A.J.** (2001). Watching the hands of the Arabidopsis biological clock. *Genome Biology* 2: 1008.1-1008.4.
- Debus, R.J., Barry, A., Sithole, I., Babcock, G.T. & McIntosh, L.** (1988). Directed mutagenesis indicates that donor to P680+ in the photosystem II is tyrosine-161 of the D1 polypeptide. *Biochemistry* 27: 9071-9074.
- Deikman, J. and Hammer, P.** (1995). Induction of anthocyanin accumulation by cytokinins in Arabidopsis thaliana. *Plant Physiology* 108: 47-57.
- Diaz, C., Saliba-Colombani, V., Loudet, O., Belluomo, P., Moreau, L., Daniel-Vedele, F., Morot-Gaudry, J-F. & Daubresse, C.M.** (2006) Leaf Yellowing and anthocyanin accumulation are two genetically independent strategies in response to nitrogen limitation in Arabidopsis thaliana. *Plant and Cell Physiology* 47: 74-83.
- Doelling, J.H., Walker, J.M., Friedman, E.M., Thompson, A.R., Vierstra, R.D.** (2002). The APG8/12-activating Enzyme APG7 Is Required for Proper Nutrient Recycling and Senescence in Arabidopsis thaliana. *Journal of Biological Chemistry* 277: 33105-33114

- Doke, N., Miura, Y., Sanchez, L., Kawakita, K.,** (1994), Involvement of superoxide in signal transduction: Response to attack by pathogens, physical and chemical shocks, UV irradiation. In *Causes of Photo-oxidative stress and amelioration of defense systems in plants* (eds C.H. Foyer and P. Mullineaux), 177-198. CRC Press, Boca, FL, USA.
- Duan, K., Yi, K., Huang, H., Wu, W. & Wu, P.** (2008). Characterisation of a sub-family of Arabidopsis genes with the SPX domain reveals their diverse functions in plant tolerance to phosphorus starvation. *The Plant Journal* doi: 10.1111/j.1365-313X.2008.03460.x
- Dubos, C., Le Gourrierec, J., Baudry, A., Huep, G., Lanet, E., Debeaujon, I., Routaboul, J.M., Alboresi, A., Weisshaar, B., Lepiniec, L.,** (2008). MYBL2 is a new flavonoid biosynthesis regulator in Arabidopsis thaliana. *Plant Journal* 55: 940-953.
- Duxbury C.L., Legge R.L., Paliyath G., Barber R.F. and Thompson J.E.** (1991b). Alterations in membrane protein conformation in response to senescence- related changes. *Phytochemistry* 30: 63-68.
- Duxbury C.L., Legge R.L., Paliyath G. and Thompson J.E.** (1991a). Lipid breakdown in smooth microsomal membranes from bean cotyledons alters membrane proteins and induces proteolysis. *Journal of Experimental Botany* 42: 103-112.
- Espinoza, C., Medina, C., Somerville, S. & Arce-Johnson, P.** (2007). Senescence-associated genes induced during compatible viral interactions with grapevine and Arabidopsis. *Journal of Experimental Botany* 58: 3197-3212.
- Evans, P. T. & Malmberg. R.L.** (1989). Do polyamines have roles in plant development? *Annual Review Plant Physiology and Plant Molecular Biology* 40: 235-269.
- Field, T.S., Lee, D.W., & Kolbrook, M.** (2001). Why Leaves Turn Red in Autumn. The Role of Anthocyanins in Senescing Leaves of Red-Osier Dogwood. *Plant Physiology* 127: 566–574.
- Feller U. and Fisher A.** (1994). Nitrogen metabolism in senescing leaves. *Critical Reviews in Plant Sciences* 13: 241-273.
- Ferré-D'Amaré, A.R., Pognonec, P., Roeder, R.G., & Burley, S.K.** (1994). Structure and function of the b/HLH/Z domain of USF. *The EMBO Journal* 13, 180-189.
- Flexas, J. & Medrano, H.** (2002). Energy dissipation in C3 plants under drought. *Functional Plant Biology* 29: 1209–1215.
- Foyer CH. & Noctor G.** (2005), Oxidant and antioxidant signalling in plants: a re-evaluation of the concept of oxidative stress in physiological context. *Plant, Cell and Environment* 28: 1056-1071.

- Fryer, M.J., Andrews, J.R., Oxborough, K., Blowers, D.A., Baker, N.R.** (1998). Relationship between CO₂ assimilation, photosynthetic electron transport and active O₂ metabolism in leaves of maize in the field during periods of low temperature. *Plant Physiology* 116: 571-580.
- Galliard, T.** (1980). *The Biochemistry of Plants*, Vol. IV. Academic Press, New York, 85-114.
- Gan, S.** (2003). Mitotic and Postmitotic Senescence in Plants. 2004, available from <http://sageke.sciencemag.org/cgi/content/full/sageke:2003/38/re7>.
- Gan, S. & Amasino, R.M.** (1995). Inhibition of leaf senescence by autoregulated production of cytokinin. *Science* 270: 1986-1988.
- Geiger, D.R. & Servaites, J.C.** (1994). Diurnal Regulation of Photosynthetic Carbon Metabolism in C₃ Plants. *Annual Review Plant Physiology & Plant Molecular Biology* 45: 235–256.
- Ghanem, M.E., Albacete, A., Martínez-Andújar, C., Acosta, M., Romero-Aranda, R., Dodd, I.C., Lutts, S. & Pérez-Alfocea, F.** (2008). Hormonal changes during salinity-induced leaf senescence in tomato (*Solanum lycopersicum* L.). *Journal of Experimental Botany* 59: 3039-3050.
- Giuliano, G., Pichersky, E., Malik, V.S., Timko, M.P., Scolnik, P.A. & Cashmore, A.R.** (1988). An evolutionarily conserved protein binding sequence upstream of a plant light-regulated gene. *PNAS* 85:7089-7093.
- Glaëûgen, W.E., Rose, A., Madlung, J., Koch, W., Gleitz, J., Seitz, H.U.** (1998) Regulation of enzymes involved in anthocyanin biosynthesis in carrot cell cultures in response to treatment with ultraviolet light and fungal elicitors. *Planta* 204: 490-498.
- Goff, S.A., Cone, K.C. & Chandler, V.L.** (1992). Functional analysis of the transcriptional activator encoded by the maize B gene: evidence for a direct functional interaction between two classes of regulatory proteins". *Genes and Development* 6, 864-875.
- Golan, T., Müller-Moulé, P. & Niyogi, K.K.** (2006). Photoprotection mutants of *Arabidopsis thaliana* acclimate to high light by increasing photosynthesis and specific antioxidants. *Plant, Cell and Environment* 29: 879–887
- Gonzalez, A., Zhao, M., Leavitt, J.M. & Lloyd, A.M.** (2008). Regulation of the anthocyanin biosynthetic pathway by the TTG1/Bhlh/ Myb transcription complex in *Arabidopsis* seedlings. *The Plant Journal* 53: 814-827.

- Gould, K.S., McKelvie, J. & Markham, K.R.** (2002). Do anthocyanins function as antioxidants in leaves? Imaging of H₂O₂ in red and green leaves after mechanical injury. *Plant Cell & Environment* 25: 1261–1269
- Gounaris, K., Barber, J. & Harwood, J.L.** (1986). The thylakoid membranes of higher plant chloroplasts. *Biochemistry Journal* 237: 313-326.
- van der Graaff, E., Schwacke, R., Schneider, A., Desimone, M., Flügge, U.-I. & Kunze, R.,** (2006), Transcription analysis of Arabidopsis membrane transporters and hormone pathways during developmental and induced leaf senescence. *Plant Physiology* 141: 2, 776-792.
- Graham, I.A. and Eastmond, P.J.** (2002). Pathways of straight and branched chain fatty acid catabolism in higher plants. *Progress in Lipid Research* 41: 156–181.
- Graham I.A., Leaver, C.J. & Smith, S.M.,** (1992), Induction of Malate Synthase gene expression in senescent and detached organs of cucumber. *The Plant Cell* 4, 349-357.
- Grbic V. & Bleecker AB.** (1995). Ethylene regulates the timing of leaf senescence in Arabidopsis. *Plant Journal* 8: 595-602.
- Grossman, S. and Leshem, Y.Y.** (1978). Lowering of endogenous lipoxygenase activity in *Pisum sativum* foliage by cytokinin as related to senescence. *Physiologia Plantarum* 43: 359-362.
- Guo, Y., Cai, Z. & Gan, S.** (2004). Transcriptome of Arabidopsis leaf senescence. *Plant Cell and Environment* 27: 521–549.
- Gut, H., & Matile, P.,** (1988), Apparent induction of key enzymes of the glyoxylic acid cycle in senescent barley. *Planta* 176, 548-550.
- Haldimann, P., Fracheboud, Y. & Stamp, P.** (1995). Photosynthetic performance and resistance to photoinhibition of *Zea mays* L. Leaves grown at suboptimal temperature. *Plant, Cell and Environment* 19: 85-92.
- Hankamer, B., Barber, J. & Boekema, E.J.** (1997). Structure and membrane organisation of photosystem II in green plants. *Annual Review of Plant Physiology & Plant Molecular Biology* 48: 641-671.
- Hanaoka, H., Noda, T., Shirano, Y., Kato, T., Hayashi, H., Shibata, D., Tabata, S. & Ohsumi, Y.** (2002). Leaf senescence and starvation-induced chlorosis are accelerated by the disruption of an Arabidopsis autophagy gene. *Plant Physiology* 129: 1181–1193

- Hardtke, C.S. & Deng, X-W.** (2003). The cell biology of the COP/DET/FUS proteins. Regulating proteolysis in photomorphogenesis and beyond? *Plant Physiology* 124: 1548–1557.
- Harmer, S. L., Hognesch, J.B., Straume, M., Chang, H.S., Han, B., Zhu, T., Wang, X., Kreps J.A. & Kay S.A.** (2000). Orchestrated transcription of key pathways in *Arabidopsis* by the circadian clock. *Science* 290: 2110-2113.
- Harrison, M.A. & Allen, J.F.** (1992). Differential phosphorylation of individual LHC-II polypeptides during short term and long term acclimation to light regime in the green algae. *Biochimica et Biophysica Acta* 1141: 37-44.
- Hatier, J.H. & Gould, K.S.** (2008). Foliar anthocyanins as modulators of stress signals. *Journal of Theoretical Biology* 253: 625-627.
- Hendrickson, L., Forster, B., Furbank, R.T., Chow, W.S.** (2004). Processes contributing to photoprotection of grapevine leaves illuminated at low temperature. *Physiologia Plantarum* 121: 272–281.
- Hensel, L.L., Grbic, V., Baumgarten, D.A. and Bleecker, A.B.** (1993). Developmental and age related processes that influence the longevity and senescence of photosynthetic tissues in *Arabidopsis*. *Plant Cell* 5: 553-564.
- Herremann, R.G.** (1996). Photosynthesis research: Aspects and perspectives in. B. Andersson, H.A., Salter & J. Barber (eds.), *Frontiers of Molecular Biology. Molecular Genetics in Photosynthesis*. IRL Press. Oxford. Pp. 1-44.
- He, Y., Fukushige, H., Hildebrand, D.F. and Gan, S.** (2002). Evidence Supporting a Role of Jasmonic Acid in *Arabidopsis* Leaf Senescence. *Plant Physiology* 128: 876–884.
- He, Y., Gan, S.,** (2002). A gene encoding an acyl hydrolase is involved in leaf senescence in *Arabidopsis*. *The Plant Cell* 14: 805–815.
- Himelblau, E. & Amasino, R.M.** (2001). Nutrients mobilized from leaves of *Arabidopsis thaliana* during leaf senescence. *Journal of Plant Physiology* 158, 1317–1323.
- Hinder, B., Schellenberg, M., Rodoni, S., Ginsburg, S., Vogt, E., Martinoia, E., Matile, P., and Hörtensteiner S.** (1996). How plants dispose of chlorophyll catabolites. Directly energised uptake of tetrapyrrolic breakdown products into isolated vacuoles. *Journal of Biological Chemistry* 271: 27233-27236.
- Hoch W.A., Singaas E.L. & McCown B.H.** (2003). Resorption protection. Anthocyanins facilitate nutrient recovery in autumn by shielding leaves from potentially damaging light levels. *Plant Physiology* 133: 1296-1305.

- Hong, Y., Wang, T-W., Hudak, K.A., Schade, F., Froese, C.D., Thompson, J.E.,** (2000). An ethylene-induced cDNA encoding a lipase expressed at the onset of senescence. *PNAS USA* 97: 8717–8722.
- Hörtensteiner, S. & Feller, U.** (2002). Nitrogen metabolism and remobilisation during senescence. *Journal of Experimental Botany* 53: 927-937.
- Hörtensteiner S., Vicentinin F. & Matile P.** (1995). Chlorophyll breakdown in senescent cotyledons of rape, *Brassica napus* L: Enzymatic cleavage of pheophorbide *a in vitro*. *New Phytologist* 129: 237-246.
- Hudak, K.A. & Thompson, J.E.** (1996), Floatation of lipid-protein particles containing triacylglycerol and phospholipid from the cytosol of carnation petals. *Physiologia Plantarum* 98: 810–818.
- Hudak, K., Yao, K. & Thompson, J.E.** (1995). Release of fluorescent peroxidised lipids from membranes in senescing tissue by blebbing of lipid protein particles. *Hortscience* 30: 209-213.
- Hwang, I. and Sheen, J.** (2001). Two component circuitry in *Arabidopsis* cytokinin signal transduction. *Nature* 413: 383-389.
- Inada, N., Sakai, A. & Kuroiwa, T.** (1998). Three-dimensional analysis of the senescence program in rice (*Oryza sativa* L.) coleoptiles. *Planta* 206: 585–597.
- Ishida, H., Yoshimoto, K., Izumi, M., Reisen, D., Yano, Y., Makino, A., Ohsumi, Y., Hanson, M.R. & Mae, T.** (2008). Mobilisation of Rubisco and stromal-localised fluorescent proteins of chloroplasts to the vacuole by an *ATG* gene-dependent autophagic process. *Plant Physiology Preview* doi:10.1104/pp.108.122770.
- Jeevanandam, M. & Peterson, S.R.** (2001). Clinical role of polyamine analysis: problem and promise. *Current Opinion in Clinical Nutrition & Metabolic Care* 4: 385-390.
- Jing, H-C., Schippers, J.H.M., Hille, J. and Dijkwel, P.P.** (2005), Ethylene-induced leaf senescence depends on age-related changes and OLD genes in *Arabidopsis*. *Journal of Experimental Botany* 56: 2915–2923,
- John, I., Drake, R., Farrell, A., Cooper, W., Lee, P., Horton, P. & Grierson, D.** (1995). Delayed leaf senescence in ethylene-deficient ACCoxidase antisense tomato plants: molecular and physiological analysis. *The Plant Journal* 7: 483–490.
- Joliot, P. and Joliot, A.** (1984). Electron transfer between the two photosystems: II. Equilibrium constants. *Biochimica et Biophysica Acta* 765: 219–226.

- Jones, M.L. and Woodson, W.R.** (1997). Pollination-induced ethylene in carnation (role of stylar ethylene in corolla senescence). *Plant Physiology* 115: 205–212.
- Kappus H.** (1985), "Oxidative Stress." Academic Press, New York, 273-309.
- Karabourniotis, G. & Bornman, J.F.** (1999). Penetration of UV-A, UV-B and blue light through the leaf trichome layers of two xeromorphic plants olive and oak, measured by optical fibre microprobes. *Physiologia Plantarum* 105: 655–661.
- Karabourniotis, G., Papadopoulos, K., Papamarkou, M. & Manetas, Y.** (1992). Ultraviolet-B radiation absorbing capacity of leaf hairs. *Physiologia Plantarum* 86: 414–418.
- Karimi, M., Inze, D. & Depicker, A.** (2002). GATEWAY vectors for Agrobacterium-mediated plant transformation. *Trends in Plant Science* 7: 193-195
- Karpinski, S., Escobar, C., Karpinska, B., Creissen, G. & Mullineaux, P.M.** (1997). Photosynthetic electron transport regulates the expression of cytosolic ascorbate peroxidase genes in *Arabidopsis* during excess light stress. *The Plant Cell* 9: 627-640.
- Kaup, M.T., Froese, C.D., and Thompson, J.E.** (2002). A role for diacylglycerol acyltransferase during leaf senescence. *Plant Physiology* 129: 1616–1626.
- Kaur Sawhney, R., Shekhawat, N.S. and Galston, A.W.** (1985). Polyamine levels as related to growth, differentiation and senescence in protoplast-derived cultures of *Vigna aconitifolia* and *Avena sativa*. *Plant Growth Regulation* 3: 329-337.
- Keech, O., Pesquet, E., Ahad, A., Askne, A., Nordvall, D., Vodnala, S.M., Tuominen, H., Hurry, V., Dizengremel, P. & Gardestrom, P.** (2007). The different fates of mitochondria and chloroplasts during dark-induced senescence in *Arabidopsis* leaves. *Plant Cell and Environment* 30: 1523-1534.
- Keskitalo, J., Bergquist, G., Gardestrom, P., Jansson, S.,** (2005). A cellular time table of autumn senescence. *Plant Physiology* 139: 1635-1648.
- Kim, J., & Klionsky, D.J.** (2000). Autophagy, cytoplasm-to-vacuole targeting pathway, and pexophagy in yeast and mammalian cells. *Annual Review of Biochemistry* 69: 303–342.
- Kim, M-J., Oh, J-M., Cheon, S-H., Cheong, T-K., Lee, S-H., Choi, E-O., Lee, H.G, Park, C.S., Park, K.H.** (2001). Thermal inactivation kinetics and application of phospho- and galactolipid-degrading enzymes for evaluation of quality changes in frozen vegetables. *Journal of Agriculture and Food Chemistry* 49: 2241–2248.
- Kim, H. J., Ryu, H., Hong, S.H., Woo, H.R., Lim, P.O., Lee. I.C., Sheen, J., Nam,**

- H.G., Hwang, I.** (2006). Cytokinin-mediated control of leaf longevity by AHK3 through phosphorylation of ARR2 in Arabidopsis. *PNAS* 103: 814-819.
- Kim, J., Yi, H., Choi, G., Shin, B., Song, P-S. & Choi, G.,** (2003). Functional characterisation of Phytochrome interacting factor 3 in Phytochrome mediated light signal transduction. *The Plant Cell* 15: 2399-2407.
- Kinsman, E.A. and Pyke, K.A.** (1998). Bundle sheath cells and cell-specific plastid development in Arabidopsis Leaves. *Development* 125: 1815-1822
- Kirby, C.J. and Green, C.** (1980). Erythrocyte membrane cholesterol levels and their effects on membrane proteins. *Biochemica et Biophysica Acta* 59: 422-425.
- Koes, R., Verweij, W. and Quattrocchio, F.** (2005). Flavonoids: a colourful model for the regulation and evolution of biochemical pathways. *Trends in Plant Science* 10: 236-242.
- Kolodziejek, I., Koziol, J., Waleza, M., Mostowska, A.** (2003). Ultrastructure of mesophyll cells and pigment content in senescing leaves of maize and barley. *Journal of Plant Growth Regulation* 22: 217–227.
- Kozlowski T.T.** (1976). Water supply and leaf shedding. In 'Water deficit and plant growth. (Ed. TT Kozlowski) 191-231. (Academic Press: New York, NY).
- Krause, G. H. and Weis, E.** (1992). Chlorophyll Fluorescence and Photosynthesis: The Basics. *Annual Review in Plant Physiology & Molecular Biology* 42: 313-349.
- van der Krol, A.R., Mur, L.A., Beld, M., Mol, J.N. & Stuitje, A.R.** (1990), Flavonoid genes in petunia: addition of a limited number of gene copies may lead to a suppression of gene expression. *Plant Cell* 2: 291-299.
- Krol, M., Gray, G.R., Hurry, V.M., Öquist, G., Malek, L., Huner, N.P.A.** (1995). Low-temperature stress and photoperiod effect an increased tolerance to photoinhibition in *Pinus banksiana* seedlings. *Canadian Journal of Botany* 73: 1119–1127.
- Kubasek, W. L., Shirley, B.W., McKillop, A., Goodman, H.M., Briggs, W., and F. M. & Ausubel,** (1992). Interactions among enzymes of the Arabidopsis flavonoid biosynthetic pathway. *The Plant Cell* 4: 1229-1236.
- Landolt, R., & Matile, P.** (1990). Glyoxysome-like microbodies in senescent spinach leaves. *Plant Science* 72: 159–163.
- Landry, L.G., Chapple, C.C.S. & Last, R.L.** (1995). *Arabidopsis* mutants lacking phenolic sunscreens exhibit enhanced ultraviolet-B injury and oxidative damage. *Plant Physiology* 109: 1159-1166.

- Lawson T., Oxborough K., Morison J.I.L. and Baker N.R.** (2002). Responses of Photosynthetic electron transport in stomatal guard cells and mesophyll cells in intact leaves to light, CO₂, and humidity. *Plant Physiology* 128: 52-62
- Lazcano, C.A., Yoo, K.S., Pike, L.M.,** (2001). A method for measuring anthocyanins after removing carotenes in purple colored carrots. *Scientia Horticulturae* 90: 321-324.
- Lea, U.S. Slimestad, R., Smedvig .P., Lillo ,C.** (2007). Nitrogen deficiency enhances expression of specific MYB and bHLH transcription factors and accumulation of end products in the flavonoid pathway. *Planta* 225: 1245–53.
- Lee, R.H., Wang, C.H., Huang, L.T., and Chen, S.C.G.** (2001). Leaf senescence in rice plants: cloning and characterization of senescence up-regulated genes. *Journal of Experimental Botany* 52: 1117-1121.
- Liakopoulos, G., Nikolopoulos, D., Klouvatou, A., Vekkos, K-A., Manetas, Y. & Karabourniotis, G.** (2006). The protective role of epidermal anthocyanins and surface pubescence in young leaves of grapevine (*Vitis vinifera*). *Annals of Botany* 98: 275-265.
- Lida, A., Kazuoka, T., Torikai, S., Kikuchin, H., Oeda, K.** (2000). A zinc finger protein RHL41 mediates the light acclimatization response in *Arabidopsis*. *The Plant Journal* 24: 191-203.
- Lillo, C., Lea, U. & Ruoff, P.** (2008). Nutrient depletion as a key factor for manipulating gene expression and product formation in different branches of the flavonoid pathway. *Plant, Cell and Environment* 31: 587-601.
- Lim, P. O., Woo, H.R. & Nam, H.G.** (2003). Molecular genetics of leaf senescence in *Arabidopsis*. *Trends in Plant Science* 8 (6): 272-278
- Lin, J.-F. & Wu, S-H.** (2004). Molecular events in senescing *Arabidopsis* leaves. *The Plant Journal* 39: 612-628.
- Lin, J.N. & Kao, CH.** (1998). Effect of oxidative stress caused by hydrogen peroxide on senescence of rice leaves. *Botanical Bulletin of Academia Sinica* 39: 161-165.
- Li, X.-P., Müller-Moulé, P., Gilmore, A.M. & Niyogi, K.K.** (2002). PsbS-dependent enhancement of feedback de-excitation protects photosystem II from photoinhibition. *PNAS USA* 99, 15222–15227.
- Logemann, E., Parniske, M. & Hahlbrock, K.** (1995). Modes of expression and common structural features of the complete phenylalanine ammonia-lyase gene family in parsley. *PNAS USA* 92:5905-5909

- Lowry, O.H., Rosbrough, N.J., Farr, A.L. & Randall, R.J.,** (1951). Protein measurement with folin phenol reagent. *Journal of Biological Chemistry* 193: 265-275.
- Lynch, D.V., Sridhara, S. & Thompson, J.E.** (1985). Lipoxygenase-generated hydroperoxides account for the nonphysiological features of ethylene formation from 1-aminocyclopropane-1-carboxylic acid by microsomal membranes of carnations. *Planta* 164: 121-125.
- Lynch, D.V. and Thompson, J.E.,** (1984). Lipoxygenase- mediated production of superoxide anion in senescing plant tissue. *FEBS letters* 173: 251-254.
- Ma, S. & Bohnert, H.** (2007). Integration of *Arabidopsis thaliana* stress- related transcript profiles, promoter structures, and cell specific expression. *Genome Biology* 8: R49.1-R49.21.
- Mach, J. M., Castillo, A., Hoogstraten, R. and Greenberg, J.T.** (2001). Chlorophyll breakdown: Pheophorbide a oxygenase is a Rieske-type iron–sulfur protein, encoded by the accelerated cell death 1 gene. *PNAS. USA* 98: 771-776.
- Makrides, S. & Goldthwaite, J.** (1981). Biochemical changes during bean leaf growth, maturity and senescence. *Journal of Experimental Botany* 32: 725–735.
- Malkin, R.** (1992). Cytochrome *bc₁* and *b₆f* complexes of photosynthetic membranes. *Photosynthesis Research* 33: 121–136.
- Martin, C. & Paz-Ares, J.** (1997). MYB transcription factors in plants. *Trends in Genetics* 13: 67-73.
- Martinez, D.E., Costa, M.L., Gomez, F.M., Otegui, M.S., and Guamet, J.J.** (2008). Senescence-associated vacuoles' are involved in the degradation of chloroplast proteins in tobacco leaves. *The Plant Journal* doi: 10.1111/j.1365-313X.2008.03585.x
- Martin, W., Stoebe, B., Goremykin, V., Hansmann, S., Hasegawa, M. and Kowallik, K.V.** (1998). Gene transfer to the nucleus and the evolution of chloroplasts *Nature* 393: 162-165.
- Marty, F.** (1999). Plant vacuoles. *The Plant Cell* 11: 587–600.
- Masclaux, C., Valadier, M-H., Brugiere, N., Morot-Gaudry, J-F. and Hirel, B.** (2000). Characterisation of the sink/source transition in tobacco (*Nicotiana tabacum* L.) shoots in relation to nitrogen management and leaf senescence. *Planta* 211: 510-518.
- Masferrer A., Arró M., Manzano D., Schaller H., Fernández- Busquets X., Moncaleán P., Fernández B., Cunillera N., Boronat A. and Ferrer A.** (2002). Overexpression of *Arabidopsis thaliana* farnesyl diphosphate synthases (FPS1S) in transgenic *Arabidopsis*

- induces a cell death/senescence-like response and reduced cytokinin levels. *Plant Journal* 30, 123–132.
- Matile, P.** (1992). Chloroplast senescence. In Baker NR, Thomas H. eds. *Crop photosynthesis: spatial and temporal determinants*. Amsterdam: Elsevier, 413–440.
- Matthews, R.E.F.** (1991). Disease symptoms and effects on metabolism. In: *Plant Virology*. 3rd edn. London: Academic Press, 380–422.
- Maxwell, K. & Johnson, G.N.** (2000). Chlorophyll fluorescence- a practical guide. *Journal of Experimental Botany* 51: 659–668.
- McLaughlin, J.C. & Smith, S.M.** (1994), Metabolic regulation of glyoxylate-cycle enzyme synthesis in detached cucumber cotyledons and protoplasts. *Planta* 195, 22–28.
- McClure J.W.** (1975). Physiology and functions of flavonoids. In Harborne J.B., Mabry H., eds. *The Flavonoids*. London, UK: Chapman & Hall Ltd, 970–1055.
- McKegney, G., Yao, K., Ghosh, S., Huff, A., Mayak, S., Thompson, J.E.** (1995). The lipid composition of cytosolic particles isolated from senescing bean cotyledons. *Phytochemistry* 39: 1335–1345.
- Mehrtens, F., Kranz, H., Bednarek, P. & Weisshaar, B.** (2005). The Arabidopsis Transcription factor MYB12 is a Flavonoid- specific regulator of Phenylpropanoid Biosynthesis. *Plant Physiology* 138: 1083–1096.
- Menkens, AE. & Cashmore, AR.** (1994). Isolation and characterization of a fourth Arabidopsis thaliana G-box-binding factor, which has similarities to Fos oncoproteins. *PNAS USA* 91: 2522–2526.
- Miao, Y., Laun, T., Zimmermann, P. & Zentgraf, U.** (2004). Targets of WRKY53 transcription factor and its role during leaf senescence in Arabidopsis. *Plant Molecular Biology* 53: 853–867.
- Miller, C.O., Skoog, F., Okomura F.S., von Salta, M.H. and Strong, F.M.** (1956). Isolation, structure and synthesis of kinetin, a substance promoting cell division. *Journal of the American Chemical Society* 78: 1375–1380.
- Misera, S., Mueller, A.J., Weiland-Heidecker, U., Juergens, G.** (1994). The FUSCA genes of Arabidopsis: negative regulators of light responses. *Molecular General Genetics* 244: 242–252

- Mita, S., Hirano, H., Nakamura, K.,** (1997a). Negative regulation in the expression of sugar-inducible genes in *Arabidopsis thaliana* – a recessive mutation causing enhanced expression of a gene for β -amylase. *Plant Physiology* 114: 575-582.
- Mita, S., Murano, N., Akaike, M., Nakamura, K.,** (1997b). Mutants of *Arabidopsis thaliana* with pleiotropic effects on the expression of the gene for beta-amylase and on the accumulation of anthocyanin that are inducible by sugars. *Plant Journal* 11: 841-851.
- Mol, J., Grotewold, E. & Koes, R.** (1998). How genes paint flowers and seeds. *Trends in Plant Science* 3: 212-242.
- Moore, B., Zhou, L., Rolland, F., Hall, Q., Cheng, W.H., Liu, Y.X., Hwang, I., Jones, T. & Sheen, J.** (2003). Role of the *Arabidopsis* glucose sensor HXK1 in nutrient, light and hormone signalling. *Science* 300: 332-336.
- Moriyasu, Y. & Hillmer, S.** (2000) Autophagy and vacuole formation. In *Vacuolar Compartments* (Robinson, D.G. and Rogers, J.C., eds). Boca Raton, FL: CRC Press, 71–89.
- Morris, K., MacKerness, S.A., Page, T., John, C.F., Murphy, A.M., Carr, J.P. & Buchanan-Wollaston, V.** (2000). Salicylic acid has a role in regulating gene expression during leaf senescence." *Plant Journal* 23: 677-685.
- Müller-Moulé, P., Conklin, P.L. & Niyogi, K.K.** (2002). Ascorbate deficiency can limit violaxanthin de-epoxidase activity in vivo. *Plant Physiology* 128: 970–977.
- Müller, P., Li, X-P. & Niyogi, K.K.,** (2001). Non-photochemical quenching. A response to excess light energy. *Plant Physiology* 125: 1558-1566.
- Munné-Bosch S. & Alegre L.** (2004). Die and let live: leaf senescence contributes to plant survival under drought stress. *Functional Plant Biology* 31, 203-216
- Munné-Bosch, S. & Peñuelas, J.** (2003). Photo- and antioxidative protection during summer leaf senescence in *Pistacia lentiscus* L. grown under Mediterranean field conditions. *Annals of Botany* 92: 385-391.
- Murata, N. & Miyao, M.** (1985). Extrinsic membrane proteins in the photosynthetic oxygen-evolving complex. *Trends Biochemical Science*. 10:122-124.
- Mur, L.A., Brown, I.R., Darby, R.M., Bestwick, C.S., Bi, Y.M., Mansfield, J.W. & Draper, J.** (2000). A loss of resistance to avirulent bacterial pathogens in tobacco is associated with the attenuation of a salicylic acid-potentiated oxidative burst. *Plant Journal* 23: 609–621

- Mur, L.A.J, Bi, Y.M., Darby, R.M., Firek, S. & Draper, J.** (1997). Compromising early salicylic acid accumulation delays the hypersensitive response and increases viral dispersal during lesion establishment in TMV-infected tobacco. *Plant Journal* 12: 1113–1126
- Murre C, McCaw PS, Baltimore D.** (1989). A new DNA binding and dimerization motif in immunoglobulin enhancer binding, daughterless, MyoD, and myc proteins. *Cell* 56: 777–783.
- Napoli, C., Lemieux, C., Jorgensen, R.** (1990), Introduction of a chimeric chalcone synthase gene into *Petunia* results in reversible co-suppression of homologous genes in trans. *Plant Cell* 2: 279-289.
- Navabpour S., Morris K., Allen R., Harrison E., Mackerness SA. & Buchanan-Wollaston V.** (2003). Expression of senescence enhanced genes in response to oxidative stress. *Journal of experimental botany* 54: 2285-2292.
- Neuhaus, G., Neuhaus-Url, G., Gruss, P., Schweiger, H.G.** (1984). Enhancer-controlled expression of the simian virus 40 T-antigen in the green alga *Acetabularia*. *The EMBO Journal* 3: 2169-2172.
- Neill, S.O. & Gould, K.S.** (1999). Anthocyanins in leaves: light attenuators or antioxidants? *Functional Plant Biology* 30: 865 – 873.
- Nesi, N., Jond, C., Debeaujon, I., Caboche, M. & Lepiniec, L.** (2001). The *Arabidopsis* TT2 gene encodes an R2R3 MYB domain protein that acts as a key determinant for Proanthocyanidin accumulation in developing seed. *The Plant Cell* 13: 2099-2114.
- Niell, S. & Gould, K.S.** (1999). Optical properties of leaves in relation to anthocyanin concentration and distribution. *Canadian Journal of Botany* 77: 1777-1782.
- Nooden, L.D., Hillsberg, J.W. & Schneider, M.J.,** (1996). Induction of leaf senescence in *Arabidopsis thaliana* by long days through a light dosage effect. *Physiologia Plantarum* 96: 491-495
- Oberhuber, M., Berghold, J., Breuker, K., Hörtensteiner, S., and Kräutler, B.** (2003). Breakdown of chlorophyll: A nonenzymatic reaction accounts for the formation of the colourless ‘nonfluorescent’ chlorophyll catabolites. *PNAS* 100: 6910-6915.
- O'Connor, T.R., Dyreson, C. & Wyrick, J.J.** (2005). Athena: a resource for rapid visualization and systematic analysis of *Arabidopsis* promoter sequences. *Bioinformatics* 21: 4411–4413.
- Ogawara, T. Higashi, K. Kamada, H. and Ezura, H.** (2003). Ethylene advances the transition from vegetative growth to flowering in *Arabidopsis thaliana*. *Journal of Plant Physiology* 160 pp. 1335–1340

- Ohad, I., Adir, N., Koike, H., Kyles, D.J. & Inoue, Y.** (1990). Mechanisms of photoinhibition *in Vivo*. *The Journal of Biological Chemistry* 265: 1972-1979.
- Oh, S. A., Park, J.H., Lee, G.I., Paek, K.H., Park, S.K. & Nam, H.G.** (1997). Identification of three genetic loci controlling leaf senescence in *Arabidopsis thaliana*. *Plant Journal* 12: 527-535.
- Ondek, B., Shepard, A. & Herr, W.** (1987). Discrete elements within the SV40 enhancer region display different cell-specific enhancer activities. *The EMBO Journal* 6: 1017-1025.
- Orozco-Cárdenas, M.L., Narváez-Vásquez, J. & Ryan, C.A.** (Hydrogen peroxide acts as a second messenger for the induction of defense genes in tomato plants in response to wounding, systemin, and methyl jasmonate. *The Plant Cell* 13: 179-191.
- Otegui, M. S., Noh, Y.S., Martinez, D.E., Petroff, M.G.V., Staehelin, L.A., Amasino, R.M., Guimard, J.J.,** (2005). Senescence-associated vacuoles with intense proteolytic activity develop in leaves of *Arabidopsis* and soybean. *The Plant Journal* 41: 831-844.
- Oxborough, K.** (2004). Imaging of Chlorophyll Fluorescence: theoretical and practical aspects of an emerging technique for the monitoring of photosynthetic performance. *Journal of Experimental Botany* 55: 1195-1205.
- Paliyath, G. and Thompson, J.E.,** (1987). Calcium- Calmodulin- regulated breakdown of phospholipid by microsomal membranes from bean cotyledons. *Plant Physiology* 83: 63-68.
- Paramonova, N.V., Shevyakova, N.I., Kuznetsov, V.I.V.,** (2004). Ultrastructure of chloroplasts and their storage inclusions in the primary leaves of *Mesembryanthemum crystallinum* affected by putrescine and NaCl. *Russian Journal of Plant Physiology* 51: 86–96.
- Park, J-S., Kim, J-B., Cho, K-J., Cheon, C-I., Sung, M-K., Chung, M-G., Roh, K-H.** (2008). *Arabidopsis* R2R3-MYB transcription factor AtMYB60 functions as a transcriptional repressor of anthocyanin biosynthesis in lettuce (*Lactuca sativa*). *Plant Cell Reports* 27: 985-994
- Park, J-H., Oh, S.A., Kim, Y.H., Woo, H.R., Nam, H.G.** (1998). Differential expression of senescence-associated mRNAs during leaf senescence induced by different senescence-inducing factors in *Arabidopsis*. *Plant Molecular Biology* 37: 445–454.
- Parthier, B.** (1990). Jasmonates: hormonal regulators or stress factors in leaf senescence. *Journal of Plant Growth Regulation* 9: 445–454.
- Pastori, G.M., del Río, L.A.,** (1994). An activated-oxygen-mediated role for peroxisomes in the mechanism of senescence of pea leaves. *Planta* 193: 385–391.

- Pastori, G.M., del Río, L.A.,** (1997). Natural senescence of pea leaves: an activated oxygen-mediated function for peroxisomes. *Plant Physiology* 113: 411–418.
- Peng, M., Bi, Y-M., Zhu, T. & Rothstein, S.J.** (2007), Genome wide analysis of Arabidopsis responsive Transcriptome to nitrogen limitation and its regulation by the ubiquitin ligase gene *NLA*. *Plant Molecular Biology* 65: 775-797.
- Penninckx, I.A., Thomma, B.P., Buchala, A., Metraux, J.P. & Broekaert, W.F.** (1998). Concomitant activation of jasmonate and ethylene response pathways is required for induction of a plant defensin gene in Arabidopsis. *Plant Cell* 10: 2103–2113
- Pic, E., de la Serve, B.T., Tardieu, F. & Turc, O.** (2002), Leaf senescence induced by mild water deficit follows the same sequence of macroscopic, biochemical and molecular events at monocarpic senescence. *Plant Physiology* 128: 236-246.
- Pietrini F., Iannelli M.A. & Massacci A.,** (2002). Anthocyanin accumulation in the illuminated surface of maize leaves enhances protection from photo-inhibitory risks at low temperature, without further limitation to photosynthesis. *Plant, Cell and Environment* 25: 1251-1259.
- Pistelli, L., Nieri, B., Smith, S.M., Alpi, A., De Bellis, L.,** (1996). Glyoxylate cycle enzyme activities are induced in senescent pumpkin fruits. *Plant Science* 119: 23–29.
- Portis, A.R.** (1992). Regulation of Ribulose 1,5-Bisphosphate Carboxylase/Oxygenase Activity *Annual Review of Plant. Physiology & Plant Molecular Biology* 43: 415–437.
- Pourtau, N., Jennings, R., Pelzer, E., Pallas, J. and Wingler, A.** (2006) Effect of sugar-induced senescence on gene expression and implications for the regulation of senescence in *Arabidopsis*. *Planta* 224: 1432-2048.
- Prins, A., van Heerden, P.D.R., Olmos, E., Kunert, K.J. & Foyer, C.H.** (2008). Cysteine proteinases regulate chloroplast protein content and composition in tobacco leaves: a model for dynamic interactions with ribulose-1,5-bisphosphate carboxylase/oxygenase (Rubisco) vesicular bodies. *Journal of Experimental Botany* 59: 1935-1950.
- Procházkará D. and Wilhelmova N.** (2004). Changes in antioxidant protection in Bean cotyledons during natural and continuous irradiation accelerated senescence. *Biologia Planta* 48: 33-39
- Prochazkova, D., Sairamm, R.K., Srivastava, G.C. & Singh, D.V.,** (2001). Oxidative stress and antioxidant activity as the basis of senescence in maize leaves. *Plant Science* 161, 765-771.
- Pruzinská, A., Anders, I., Aubry, S., Schenk, N., Tapernoux-Lüthi, E., Müller, T.,**

- Krätler, B., and Hörtensteiner, S.** (2007). In vivo participation of red chlorophyll catabolites reductase in chlorophyll breakdown. *The Plant Cell* 19: 369-387.
- Pruzinská, A., Tanner, G., Aubry, S., Anders, I., Moser, S., Müller, T., Ongania, K.-H., Krätler, B., Youn, J.-Y., Liljgren, S.J., and Hörtensteiner, S.** (2005). Chlorophyll breakdown in senescent *Arabidopsis* leaves: Characterisation of chlorophyll catabolites and of chlorophyll catabolic enzymes involved in the degreening reaction. *Plant Physiology* 139: 52-63.
- Quattrocchio, F., Wing, J., van der Woude, K., Souer, E., de Vetten, N., Mol, J., & Koes, R.** (1999). Molecular analysis of the *anthocyanin2* gene of *Petunia* and its role in the evolution of flower color. *Plant Cell* 11: 1433–1444.
- Quirino, B.F., Noh, Y.-S., Himelbau, E. and Amasino, R.M.** (2000). Molecular aspects of leaf senescence. *Trends in Plant Science* 5: 278-282.
- Rabino, L., and Mancinelli A.L.** (1986). Light, Temperature, and Anthocyanin Production. *Plant Physiology* 81:922-924
- Ramsay, N.A., Walker, A.R., Mooney, M. & Gray, J.C.** (2003). Two basic-helix-loop-helix genes (*MYC-146* and *GL3*) from *Arabidopsis* can activate anthocyanin biosynthesis in a white-flowered *Matthiola incana* mutant. *Plant Molecular Biology* 52: 679-688.
- Renger, G. and Eckert, H.-J.** (1980). Studies on the structural and functional organisation of water cleavage by visible light in photosynthesis. *Bioelectrochemistry & Bioenergetics* 7: 101-124.
- Rey, P., Gillet, B., Roemer, S., Eymery, F., Massimino, J., Peltier, G., Kuntz, M.,** (2000). Over-expression of a pepper plastid lipid-associated protein in tobacco leads to changes in plastid ultrastructure and plant development upon stress. *The Plant Journal* 21: 483–494.
- Richmond, A.E. & Lang, A.** (1957). Effect of kinetin on protein content and survival of detached *Xanthium* leaves. *Science* 125: 650–651.
- del Río, L.A., Pastori, G.M., Palma, J.M., Sandalio, L.M., Sevilla, F., Corpas, F.J., Jiménez, A., López-Huertas, E. & Hernández JA.** (1998). The activated oxygen role of peroxisomes in senescence. *Plant Physiology* 116:1195–1200.
- del Río, L.A., Sandalio, L.M., Corpas, F.J., Palma, J.M. & Barroso, J.B.** (2006). Reactive Oxygen Species and Reactive Nitrogen Species in Peroxisomes. Production, Scavenging, and Role in Cell Signaling. *Plant Physiology* 141: 330-335.

- Rivero, R.M., Kojima, M., Gepstein, A., Sakakibara, H., Mittler, R., Gepstein, S. & Blumwald, E.** (2007), Delayed leaf senescence induces extreme drought tolerance in a flowering plant. *PNAS* 104: 19631–19636.
- Robatzek, S. and Somissich, I.E.** (2001). A new member of the Arabidopsis WRKY transcription factor family, AtWRKY6, is associated with both senescence- and defence-related processes. *Plant Journal* 28, 123–133.
- Robatzek, S. and Somissich, I.E.** (2002). Targets of AtWRKY6 regulation during plant senescence and pathogen defense. *Genes & Development* 16, 1139–1149.
- Rodoni, S., Mühlecker, W., Anderl, M., Kräutler, B., Moser, D., Thomas, H., Matile, P., and Hörtensteiner, S.** (1997). Chlorophyll breakdown in senescent chloroplasts. Cleavage of pheophorbide *a* in two enzymatic steps. *Plant Physiology* 115: 669-676.
- Roitsch, T.** (2000). Regulation of source/sink relations by cytokinins. *Plant Growth Regulation* 32: 359-367.
- Rolland F., Moore B. and Sheen J.** (2002). Sugar sensing and signalling in plants. *Plant Cell* 14, S185–S205.
- Rong-hual, L., Pei-pol, G., Baumz, M., Grand, S. and Ceccarelli, S.** (2006). Evaluation of Chlorophyll Content and Fluorescence Parameters as Indicators of Drought Tolerance in Barley. *Agricultural Sciences in China* 5: 751-757.
- Roulin S. & Feller U.,** (1998). Light independent degradation of Stromal proteins in intact chloroplasts isolated from *Pisum sativum* L. leaves: requirement for divalent cations. *Planta* 205: 297-304.
- Ryan, C.A.** (1990). Protease inhibitors in plants: genes for improving defenses against insects and pathogens. *Annual Review in Phytopathology* 28: 425–449.
- Sablowski, R.W.M., Moyano, E., Culianez-Macia, F.A., Schuch, W., Martin, C., Bevan, M.** (1994). A flower-specific Myb protein activates transcription of phenylpropanoid biosynthetic genes. *The EMBO Journal* 13:128-137.
- Saeed, A.I., Sharov, V., White, J., Li, J., Liang, W., Bhagabati, N., Braisted, J., Klapa, M., Currier, T., Thiagarajan, M., Sturn, A., Snuffin, M., Rezantsev, A., Popov, D., Ryltsov, A., Kostukovich, E., Borisovsky, I., Liu, Z., Vinsavich, A., Trush, V., Quackenbush, J.** (2003). TM4: a free, open-source system for microarray data management and analysis. *Biotechniques*. 34 (2):374-8.
- http://www.tigr.org/software/tm4/menu/TM4_Biotechniques_2003.pdf

- Sagasser, M., Lu, G-H., Hahlbrock, K. & Weisshaar, B. (2002).** *A. thaliana* TRANSPARENT TESTA 1 is involved in seed coat development and defines the WIP subfamily of plant zinc finger proteins. *Genes & Development* 16:138-149
- Scheible, W.R., Morcuende, R., Czechowski, T., Fritz, C., Osuna, D., Palacios-Rojas, N., Schindelasch, D., Thimm, O., Udvardi, M.K. & Stitt, M. (2004).** Genome- wide reprogramming of primary and secondary metabolism, protein synthesis, cellular growth processes, and the regulatory infrastructure of Arabidopsis in response to nitrogen. *Plant Physiology* 136: 2483-2499.
- Schindler, U., Beckmann, H. & Cashmore, A.R. (1992).** TGA1 and G-box binding factors: two distinct classes of Arabidopsis leucine zipper proteins compete for the G-box-like element. *Plant Cell* 4: 1309-1319.
- Schirm, S., Jiricny, J. & Schaffner, W. (1987).** The SV40 enhancer can be dissected into multiple segments each with a different cell type specificity. *Genes & Development* 1:65-74
- Schoenbohm, C., Martens, S., Eder, C., Forkmann, G., & Weisshaar, B. (2000).** Identification of the *Arabidopsis thaliana* flavonoid 3'-hydroxylase gene and functional expression of the encoded P450 enzyme. *Biological Chemistry* **381**: 749-753
- Schuster, G., Dewit, M., Staehelin, L.A. & Ohad, I. (1986).** Transient activation of the thylakoid photosystem II light- harvesting protein kinase system and concomitant changes in intramembrane particle size during photoinhibition of *Chlamydomonas reinhardtii*. *Journal of Cell Biology* 103: 71-80.
- Shao, L., Shu, Z., Sun, S-L., Peng, C-L., Wang, X-J. & Lin, Z-F. (2007).** Antioxidation of anthocyanins in photosynthesis under high temperature stress. *Journal of Integrative Plant Biology* 49: 1341-1351.
- Shikanai, (2007).** Cyclic electron transport around photosystem I: genetic approaches. *Annual Review in Plant Biology* 58: 199–217.
- Shin, J. Park, E. & Choi, G. (2007).** PIF3 regulates anthocyanin biosynthesis in an HY5 dependent manner with both factors directly binding anthocyanin gene promoters in Arabidopsis. *The Plant Journal* 49: 981-994.
- Shinozaki, K. and Yamaguchi-Shinozaki, K. (2000).** Molecular responses to dehydration and low temperature. *Current Opinion Plant Biology* 3: 217-223.

- Shioi, Y., Tomita, N., Tsuchiya, T. and Takamiya, K.** (1996). Conversion of chlorophyllide to pheophorbide by Mg-dechelating substrate in extracts of *Chenopodium album*. *Plant Physiology & Biochemistry* 34: 41–47.
- Shirley, B.W., Kubasek, W.L., Storz, G., Bruggemann, E., Koornneef, M., Ausubel, F.M. & Goodman, H.M.** (1995). Analysis of *Arabidopsis* mutants deficient in flavonoid biosynthesis. *The Plant Journal* 8: 659–671.
- Smalle, J. and Van Der Straeten, D.** (1997). Ethylene and vegetative development. *Plant Physiology* 100: 593–605.
- Smart, C.** (1994). Gene expression during leaf senescence. *New Phytol* 126: 419–448
- Smillie, R.M. & Hetherington, S.E.** (1999). Photoabatement by anthocyanin shields photosynthetic systems from light stress. *Photosynthetica* 36: 451–463.
- Smith, M.D., Licatalosi, D.D., and Thompson, J.E.** (2000). Co association of cytochrome f catabolites and plastid-lipid-associated protein with chloroplast lipid particles. *Plant Physiology* 124: 211–221.
- Sodmergen, Kawano S., Tano S. & Kuroiwa T.** (1991). Degradation of chloroplast DNA in second leaves of rice (*Oryza satia*) before leaf yellowing. *Protoplasma* 160: 89–98.
- Sodmergen, Kawano, S., Tano, S. & Kuroiwa T.** (1989). Preferential digestion of chloroplast nuclei (nucleoids) during senescence of the coleoptile of *Oryza satia*. *Protoplasma* 152: 65–68.
- Stressman, D., Miller, A., Spalding, M., Rodermeil, S.** (2002). Regulation of photosynthesis during *Arabidopsis* leaf development in continuous light. *Photosynthesis Research* 72: 27–37.
- Steyn, W. J., Wand, S.J.E., Holcroft, D.M. & Jacobs, G.** (2002). Anthocyanins in vegetative tissues: a proposed unified function in photoprotection. *New Phytologist* 155: 349–361.
- Suzuki, T., Sakurai, K., Ueguchi, C. and Mizuno, T.** (2001). Two types of putative nuclear factors that physically interact with histidine containing phosphotransfer (HPT) domains, signalling mediators in His-to-Asp phosphorelay, in *Arabidopsis thaliana*. *Plant Cell Physiology* 42: 37–45.
- Suzuki, T., and Shioi, Y.** (2002). Re-examination of Mg-dechelation reaction in the degradation of chlorophylls using chlorophyllin *a* as substrate. *Photosynthesis Research*. 74: 217–223.
- Takamiya, K., Tsuchiya, T. & Ohta, H.** (2000). Degradation pathway(s) of chlorophyll: What has gene cloning revealed? *Trends in Plant Science* 5: 426–43.1

- Tanaka, R., Hirashima, M.M Satoh, S., and Tanaka, A.** (2003). The *Arabidopsis*- accelerated cell death gene *ACD1* is involved in oxygenation of Pheophorbide a: Inhibition of the Pheophorbide a Oxygenase activity does not lead to the “stay green” phenotype in *Arabidopsis*. *Plant Cell Physiology* 44: 1266-1274.
- Tang, X. and Woodson, W.R.** (1996). Temporal and spatial expression of 1-aminocyclopropane-1-carboxylate oxidase mRNA following pollination of immature and mature petunia flowers. *Plant Physiology*. 112 pp. 503–511.
- Tanimoto, M., Roberts, K. and Dolan, L.** (1995). Ethylene is a positive regulator of root hair development in *Arabidopsis thaliana*. *Plant Journal* 8: 943–948
- Teng, S., Keurentjes, J., Bentsink, L., Koorneef, M. & Smeekeens, S.** (2005). Sucrose specific induction of anthocyanin biosynthesis in *Arabidopsis* requires the MYB75/PAP1 gene. *Plant Physiology* 139: 1840-1852.
- Tevini, M. & Steinmüller, D.** (1985). Composition and function of plastoglobuli. *Planta* 163: 91-96.
- Thomas, H. & Donnison, I.** (2000). Back from the brink: plant senescence and its reversibility. In: Bryant JA., Hughes S.G., Garland J.M., eds., Programmed cell death in animals and plants. Oxford: Bios, 149-162.
- Thomma, B.P.H.J., Eggermont, K., Penninckx, I.A.M.A., Mauch-Mani, B., Vogelsang, R., Cammue, B.P.A. & Broekaert, W.F.** (1998). Separate jasmonate-dependent and salicylate-dependent defense-response pathways in *Arabidopsis* are essential for resistance to distinct microbial pathogens. *PNAS USA* 95: 15107–15111
- Thompson, J., Taylor, C. & Wang, T-W.** (2000). Altered membrane lipase expression delays leaf senescence. *Biochemical Society Transactions* 28: 775–777.
- Thompson, J.E.** (1988). Senescence and Aging in Plants. Academic Press, San Diego, 51-83.
- Thornber, J. P. & Barber, J.** (1979). in Topics in Photosynthesis, Vol. 3: Photosynthesis in Relation to Model Systems (Barber, J., ed.), pp. 27-70, Elsevier, Amsterdam
- Tohge, T., Nishiyama, Y., Hirai, M.Y., Nakajima, J., Awazuhara, M., Inoue, E., Takahashi, H., Goodenowe, D., Kitayama, M., Noji, M., Yamazaki, M. & Saito, K.,** (2005). Functional genomics by integrated analysis of metabolome and transcriptome of *Arabidopsis* plants over-expressing an MYB transcription factor. *The Plant Journal* 42: 218-235.

- Tsuchiya, T., Ohta, H., Katsuya, O., Iwamatsu, A., Shimada, H., Masuda, T. and Takamiya, K.** (1999). Cloning of chlorophyllase, the key enzyme in chlorophyll degradation: Finding of a lipase motif and the induction by methyl jasmonate. *PNAS USA* 96: 15362–15367.
- Tsukamoto, S., Morita, S., Hirano, E., Yokoi, H., Masumura, T. Tanaka, K.** (2005). A novel cis-element that is responsive to oxidative stress regulates three antioxidant defense genes in rice. *Plant Physiology* 137: 317-327
- Turina, P. Samoray, D. and Graber, P.** (2003). H⁺/ATP ratio of proton transport-coupled ATP synthesis and hydrolysis catalysed by CF0F1-liposomes, *The EMBO Journal* 22: 418–426.
- Ugeuchi, C., Koizumi, H., Suzuki, T. & Mizuno, T.** (2001). Novel family of sensor histidine kinase genes in *Arabidopsis thaliana*. *Plant Cell* 14: 1751-1766.
- Vanderauwera, S., Zimmermann, P., Rombauts, S., Vandenabeele, S., Langebartels, C., Gruissem, W., Inze, D. & Breusegem, F.V.** (2005). Genome-Wide Analysis of Hydrogen Peroxide-Regulated Gene Expression in Arabidopsis Reveals a High Light-Induced Transcriptional Cluster Involved in Anthocyanin Biosynthesis. *Plant Physiology* 139: 806-821.
- Veit M. & Pauli G.F.,** (1999). Major flavonoids from *Arabidopsis thaliana* leaves. *Journal of Natural Products* 62: 1301-1303.
- de Vetten, N. & Ferl, R.J.** (1995). Characterisation of a maize G-box binding factor that is induced by hypoxia. *Plant Journal* 7: 589-601.
- Vicentini, F., Hörtensteiner, S., Schellenberg, M., Thomas, H., Matile, P.** (1995). Chlorophyll breakdown in senescent leaves: identification of the biochemical lesion in a stay-green genotype of *Festuca pratensis* Huds. *New Phytologist* 129: 247-252.
- Vonshak, A. & Richmond, A.E.** (1975). Initial stages in the onset of senescence in tobacco leaves. *Plant Physiology* 55: 786-790.
- Wade, H.K., Sohal, A.K. & Jenkins, G.I.** (2003). Arabidopsis ICX1 is a negative regulator of several pathways regulating flavonoid biosynthesis genes. *Plant Physiology* 131: 707-715.
- Walker, A. R., Davison, P.A., Bolognesi-Winfield, A.C., James, C.M., Srinivasan, N., Blundell, T.L., Esch, J.J., Marks, D. & Gray, J.C.** (1999). The TRANSPARENT TESTA GLABRA1 locus, which regulates trichome differentiation and anthocyanin biosynthesis in Arabidopsis, encodes a WD40 repeat protein. *The Plant Cell* 11: 1337-1349.

- Wang, Z-Y., Kenigsbuch, D., Sun, L., Harel, E., Ong, M.S., Tobin, E.M.** (1997). A myb-related transcription factor is involved in the phytochrome regulation of an Arabidopsis Lhcb gene. *Plant cell* 9:491-507.
- Weaver, L.M. and Amasino, R.M.**, (2001). Senescence is induced in individually darkened Arabidopsis leaves, but inhibited in whole darkened plants. *Plant Physiology* 127: 876-886.
- Weiher, H., König, M. & Gruss, P.** (1983). Multiple point mutations affecting the simian virus 40 enhancer. *Science* 219:626-631.
- Werner, T., Holst, K., Pörs, Y., Guivarc'h, A., Mustroph, A., Chriqui, D., Grimm, B. & Schmülling, T.** (2008). Cytokinin deficiency causes distinct changes of sink and source parameters in tobacco shoots and roots. *Journal of Experimental Botany* 59: 2659-2672.
- Werner, T., Motyka, V., Laucou, V., Smets, R., van Onckelen, H. & Schmülling T.**, (2003). Cytokinin-deficient transgenic *Arabidopsis* plants show multiple developmental alterations indicating opposite functions of cytokinins in the regulation of shoot and root meristem activity. *The Plant Cell* 15: 2532-2550.
- Willekens, H., Chammongpol, S., Davey, M., Schraudner, M., Langebartels, C., Van Montagu, M., Inzé, D. & Van Camp, W.** (1997). Catalase is a sink for H₂O₂ and is indispensable for stress defense in C₃ plants. *The EMBO Journal* 16: 4806-4816
- Wingler, A., Marès, M. & Pourtau, N.** (2004). Spatial patterns and metabolic regulation of photosynthetic parameters during leaf senescence. *New Phytologist* 161: 781-789.
- Wingler, A., Purdy, S., MacLean, J.A. & Pourtau, N.** (2006), The role of sugars in integrating environmental signals during the regulation of leaf senescence. *Journal of Experimental Botany* 57: 391-399.
- Wingler, A., van Schäwen, A., Leegood, R.C., Lea, P.J. and Quick, W.P.** (1998). Regulation of leaf senescence by cytokinin, sugars, and light. *Plant Physiology* 116: 329–335.
- Wisman, E., Hartmann, U., Sagasser, M., Baumann, E., Palme, K., Hahlbrock, K., Saedler, H., & Weisshaar, B.** (1998). Knock-out mutants from an En-1 mutagenized *Arabidopsis thaliana* population generate new phenylpropanoid biosynthesis phenotypes. *PNAS*. 95: 12432-12437
- Wi, S.J. & Park, K.Y.** (2002). Antisense expression of carnation Cdn encoding ACC synthase or ACC oxidase enhances polyamine content and abiotic stress tolerance in transgenic tobacco plants. *Molecules and Cells* 13: 209–222.

- Wittenhach, V.A.** (1977). Induced senescence of intact wheat seedlings and its reversibility. *Plant Physiology* 59: 1039-1042.
- Woo, H.R., Chung, K.M., Park, J-H., Oh, S.A., Ahn, T., Hong, S.H., Jang, S.K. & Nam, H.G.** (2001). ORE9, an F-Box Protein That Regulates Leaf Senescence in Arabidopsis. *The Plant Cell* 13: 1779-1790.
- Woolhouse H.W.** (1984). The biochemistry and regulation of senescence in chloroplasts. *Canadian Journal of Botany* 62: 2934-2942.
- Yamasaki H.** (1997). A function of color. *Trends in Plant Science* 2: 7–8.
- Yang, J.C., Wang, Z.Q. & Zhu, Q.S.** (2002). Carbon remobilisation and grain filling in Jarponica/Indica hybrid rice subjected to postanthesis water deficits. *Agronomy Journal* 94: 102-109
- Yang, S.H., Berberich, T., Sano, H. and Kusano, T.,** (2001). Specific association of transcripts of tbzF and tbz17, tobacco genes encoding basic region leucine zipper-type transcriptional activators, with guard cells of senescing leaves and/or flowers. *Plant Physiology* 127, 23–32
- Yao, K., Paliyath, G. & Thompson, J.E.** (1991a). Nonsedimentable microvesicles from senescing Bean cotyledons contain gel phase-forming phospholipids degradation products. *Plant Physiology* 97: 502-508.
- Yao, K., Paliyath, G., Humphrey, R.W., Hallet, F.R. & Thompson, J.E.** (1991b). Identification and characterization of nonsedimentable lipid-protein microvesicles. *PNAS* 88: 2269-2273.
- Yokozawa, T., Chen, C.P., Dong, E., Tanaka, T., Nonaka, G.I., Nishioka, I.** (1998). Study on the inhibitory effect of tannins and flavonoids against the 1,1-diphenyl-2-picrylhydrazyl radical. *Biochemical Pharmacology* 56: 213-222.
- Yoshida, S.** (2003). Molecular regulation of leaf senescence. *Current Opinion in Plant Biology* 6: 79-84.
- Yoshida S, Ito M, Nishida I, Watanabe A** (2002) Identification of a novel gene *HYS1/CPR5* that has a repressive role in the induction of leaf senescence and pathogen-defense responses in *Arabidopsis thaliana*. *Plant Journal* **29**: 427–437
- Young, A.J., Phillipa, D., Rubanb, A.V., Hortonb, P., and Frank, H.A.** (1997). The xanthophyll cycle and carotenoid-mediated dissipation of excess excitation energy in photosynthesis. *Pure & Applied Chemistry*. 69: 2125-2130.
- Young, T.E., Meeley, R.B. & Gallie, D.R.** (2004). ACC synthase expression regulates leaf performance and drought tolerance in maize. *The Plant Journal* 40, 813–825.

- Yu, D., Chen, C. & Chen, Z.** (2001). Evidence for an important role of WRKY DNA binding proteins in the regulation of NPR1 gene expression. *Plant Cell* 13: 1527-1540.
- Zacarias, L. & Reid, MS.,** (1990). Role of plants growth regulators in the senescence of *Arabidopsis thaliana* leaves. *Physiologia Plantarum* 80: 549-554.
- Zhang, F., Gonzalez, A., Zhao, M., Payne, C. & Lloyd, A.** (2003). A network of redundant bHLH proteins functions in all TTG1- dependent pathways of *Arabidopsis*. *Development* 130: 4859-4869.
- Zhang, L.F., Rui, Q., Zhang, P., Wang, X-Y. & Xu, L-L.** (2007). A novel 51-kDa fragment of the large subunit of ribulose-1,5-bisphosphate carboxylase/oxygenase formed in the stroma of chloroplasts in dark-induced senescing wheat leaves. *Physiologia Plantarum* 131: 64–71.
- Zhang N., Kallis R.P., Ewy G.R., Portis A.R.** 2002. Light modulation of Rubisco in *Arabidopsis* requires a capacity for redox regulation of larger rubisco activase isoform. *PNAS. USA* 99: 3330–3334.
- Zimmermann, I. M., Heim, M.A. & Uhrig, J.** (2004a). Comprehensive identification of *Arabidopsis thaliana* MYB transcription factors interacting with R/B-like BHLH proteins. *The Plant Journal* 40: 22-34.
- Zimmermann, P., Hirsch-Hoffmann, M., Hennig, L. & Gruissem, W.** (2004b). GENEVESTIGATOR. *Arabidopsis* Microarray Database and Analysis Toolbox. *Plant Physiology* 136: 2621-2632.
- Zubko, E., Adams, C.J., Macháèková, I., Malbeck, J., Scollan, C. and Meyer, P.** (2002). Activation tagging identifies a gene from *Petunia hybrida* responsible for the production of active cytokinins in plants. *Plant Journal* 29, 797–808.

